TECHNISCHE UNIVERSITÄT BERGAKADEMIE FREIBERG

Volcanism, Hydrothermal Processes and Biological Communities at Shallow Submarine Volcanoes of the New Ireland Fore-Arc (Papua New Guinea)

CRUISE REPORT
SONNE - 133

(BMBF FK 03G0133A)

July 10 – August 10, 1998

Manila – Kavieng – Rabaul – Suva

Peter Herzig, Mark Hannington, Peter Stoffers,
Klaus-Peter Becker, Mario Drischel, Leander Franz, Bruce Gemmell, Bernd Höppner,
Christian Horn, Kersten Horz, James Franklin, Thomas Jellineck, Ian Jonasson,
Paul Kia, Norbert Mühlhan, Sönke Nickelsen, Jeanne Percival, Mike Perfit,
Sven Petersen, Mark Schmidt, Thomas Seifert, Olaf Thiessen, Michael Türkay,
VerenaTunnicliffe, and Kyaw Winn

December 1998

Freiberg University of Mining and Technology

FREIBERG UNIVERSITY OF MINING AND TECHNOLOGY

Volcanism, Hydrothermal Processes and Biological Communities at Shallow Submarine Volcanoes of the New Ireland Fore-Arc (Papua New Guinea)

CRUISE REPORT
SONNE - 133

(BMBF FK 03G0133A)

July 10 – August 10, 1998

Manila – Kavieng – Rabaul – Suva

Peter Herzig, Mark Hannington, Peter Stoffers,
Klaus-Peter Becker, Mario Drischel, Leander Franz, Bruce Gemmell, Bernd Höppner,
Christian Horn, Kersten Horz, James Franklin, Thomas Jellineck, Ian Jonasson,
Paul Kia, Norbert Mühlhan, Sönke Nickelsen, Jeanne Percival, Mike Perfit,
Sven Petersen, Mark Schmidt, Thomas Seifert, Olaf Thiessen, Michael Türkay,
VerenaTunnicliffe, and Kyaw Winn

December 1998

Freiberg University of Mining and Technology

FREIBERG UNIVERSITY OF MINING AND TECHNOLOGY

Volcanism, Hydrothermal Processes and Biological Communities at Shallow Submarine Volcanoes of the New Ireland Fore-Arc (Papua New Guinea)

CRUISE REPORT
SONNE - 133

(BMBF FK 03G0133A)

Project Leader and Chief Scientist:
Prof. Peter M. Herzig
Institute of Mineralogy
Department of Economic Geology
Freiberg University of Mining and Technology
Brennhausgasse 14
D-09596 Freiberg, Germany

Tel. +49-3731-39-2662/2626
Fax. +49-3731-39-2610
email: herzig@mineral.tu-freiberg.de

Table of Contents

Executive Summary

Cruise SO-133 of RV Sonne conducted detailed mapping and sampling in the active tectonic zone south of Lihir Island, Papua New Guinea, between July 20 and August 3, 1998. The objectives of the cruise were to establish the extent of volcanism and hydrothermal activity associated with active extension of the old forearc crust of the New Ireland Basin in the vicinity of Lihir. The main focus of work was on several young volcanic cones discovered during SO-94 (Edison Seamount, TUBAF Seamount, and Conical Seamount) and nearby fault zones associated with the uplift of the pedestal of Lihir. Indications of epithermal-style gold-rich vein mineralization at the summit of one volcano (Conical Seamount) were confirmed during SO-133. Samples collected from the summit area include locally intense clay-silica alteration with a zonal distribution from a central clay-silica-pyrite stockwork to polymetallic (Au+Zn+Pb+As+Sb+Ag) vein mineralization at the margin. More than 1200 kg of mineralized rock was recovered, consisting of stockwork and disseminated sulfides similar to material currently being mined on the island of Lihir. The mineral assemblage includes pyrite, marcasite, sphalerite, galena, chalcopyrite, stibnite and various sulfosalts. This discovery represents a new type of seafloor mineralization and has important implications for understanding the metallogenic history of the Lihir area.

New observations were also made of the eruptive history of several of the recent volcanic cones which significantly improve the present understanding of the regional tectonic setting of Lihir. The volcanoes occur in an area of active extension where several large-scale, reactivated NW-trending strike-slip faults cut across the axis of the Lihir group (e.g., Tabar Fracture Zone). These faults are thought to be related to left-lateral rotation of the structural block of Lihir caused by transform motion between the Manus-Kilinailau trench and the Tabar Fault system. The faults have been the focal mechanism for volcanic and hydrothermal activity in the area for at least several hundred thousand years to the present. Several cones that have erupted along these structures contain mantle-derived xenoliths, suggesting that the faults penetrate deeply into the forearc crust. Mapping adjacent to New Ireland also revealed the presence of major NE-trending normal faults, parallel to the axis of Lihir, and these are the first evidence of seafloor extension in the area.

TUBAF Seamount is the most recent volcano in the area and appears to have erupted through the debris apron on the flank of Lihir. An extensive suite of new samples from TUBAF provides a detailed cross-section of the old New Ireland Basin forearc crust, as recorded in xenoliths recovered from the volcanic ash. These include a full suite of lithologies from mantle nodules (dunite, peridotite), through gabbroic material and plagiogranite, to metasedimentary rocks. Additional sampling at Edison Seamount revealed that this older volcano also contains abundant xenoliths. Both volcanoes are small pyroclastic cones, formed by highly explosive eruptions of volatile-rich, phlogopite-bearing pyroxene-phyric basalts. Distinctive peritic textures were also found in the samples from Edison, indicating eruption of the basalt into wet pelagic sediments.

Mapping and sampling of Edison Seamount has also established an important time series on the development of chemosynthetic biological communities in the region. Large beds of giant clams (calypotgena or vesicomyid) discovered in 1994 were sampled along with other fauna typically associated with sulfide-rich hydrothermal vents. A number of new fauna were also discovered at this site. The density of organisms in the clam beds on Edison Seamount is among the highest yet recorded in any seafloor environment and confirms that fluid venting from this cone is a major source of reduced gases for sulfur- and methane-oxidizing bacteria.

Biological communities were also discovered along the wall of a major structural block southeast of Edison Seamount, at the location of a strong near-bottom methane anomaly (9,000 nl/l CH_4). Bottom photography, sediment coring, and TV-grabs revealed the presence of clam and mussel beds and sediments that were charged with H_2S and CH_4. Strong indications in bottom photography for the presence of methane hydrates (white deposits on the sediments), suggest that the observed venting may be analogous to cold seeps normally associated with accretionary tectonics at subducted margins (e.g., Cascadia Margin). The presence of clams, mussels, and vestimentifera implies that large strike-slip faults in the area have likely been a major source of reduced gases throughout the recent tectonic history of the New Ireland Basin. If the presence of solid methane hydrates is confirmed, this site may be the first documented example of gas hydrates in an intra-arc setting.

1 Introduction

1.1 Previous Work

BY PETER HERZIG AND MARK HANNINGTON

During March-April 1994, detailed mapping and sampling was carried out in the active tectonic zone off Lihir Island, in the New Ireland Basin. Previously unknown areas of submarine alkaline volcanism and hydrothermal venting were discovered in the area immediately south of Lihir Island and along its northwest flank. The area of study is in the region east of mainland Papua New Guinea and northwest of New Ireland, where the islands of the Bismarck Archipelago are host to several important porphyry Cu-Au and epithermal Au deposits, including the giant Ladolam deposit on the island of Lihir (ca. 40 million oz. Au). The principal objective of the cruise was to map the seafloor in the vicinity of recently active alkaline volcanic islands in the Tabar-Feni chain and to characterize the tectonic setting of large high-level porphyry and epithermal gold deposits in the region.

Surveys carried out in the Tabar-Feni island chain during SO-94 identified at least 4 (and probably 6 or 7) previously unknown volcanic cones between 5 and 10 nautical miles south of Lihir. The immature morphology of the volcanoes and lack of sediment cover on at least one volcano indicates that volcanic activity is relatively young. This recent volcanism corresponds closely to the locations of shallow seismic epicenters and appears to be related to large-scale faults produced by regional plate rotation and extension of the old forearc crust of the New Ireland Basin. The distinctive alkaline character of the volcanic rocks is consistent with low degrees of partial melting associated with an extensional environment. Their volatile- and LIL element-rich nature and low HFSE may indicate derivation from a subduction-modified mantle wedge underlying the New Ireland Basin.

One volcano at 1450 m water depth (Edison Seamount) comprises a low pyroclastic cone about 1.5 km in diameter and 175 m high. A summit crater, about 300 m in diameter and 30 m deep was characterized by diffuse hydrothermal venting in 1994, with large areas (100-200 m across) populated by beds of giant clams (probably Calyptogena or vesicomyid). Other fauna indicative of sulfide-rich vents were also present, including crabs, snails, sulfide worms, scale worms, and limpets. Several mussels known to live with methanotrophic symbiotic bacteria were also found, suggesting the presence of both CH_4 and H_2S. The clam beds sit on a hardened crust of indurated ash, cemented by hydrothermally baked pelagic sediment. The crust contains traces of black sulfidic mud (amorphous Fe-monosulfides) and fine-grained, disseminated pyrite.

A second, much larger cone at a depth of 1050 m (Conical Seamount) is a constructional feature composed of massive vesicular lavas (ankaramite). The volcano is 2.5 km in diameter at its base and rises to a height of nearly 600 m, but lacks a well-defind summit crater. A single camera survey of the summit area revealed local Fe-staining in sediments between the lava blocks. A single large sample of the massive lava was locally intensely fractured and mineralized by disseminated sulfide. The sulfides occur as fracture-fillings, stockwork-like veins, and fine disseminations in the altered lava. Abundant low-temperature amorphous silica occupies several late fractures and cavities in the lava. Samples of the vein material consisting of abundant clays and silica contained up to 6% sulfides. Shipboard analyses of the vein material indicated bulk concentrations of 6.4 wt% Fe, 5.9-6.2 wt% S, 1.5-2.1 wt% Pb, 0.98-1.7 wt% Zn, and 0.42-0.35 wt% Cu. This material also contained 864 ppm As, 443 ppm Sb, 496 ppm Cd, 390 ppm Ag, and 17-43 ppm Au. A sample of oxidized sulfides contained 2 ppm Au.

A third pyroclastic cone, located at a depth of 1280 m (TUBAF Seamount), is about 1 km in diameter at its base and 200 m high. It was covered by a recently erupted ejecta blanket and, in contrast to other volcanoes in the vicinity, no pelagic sediment was observed covering the pyroclastic deposits. The tephra contains abundant lapilli and block-sized bombs, which appear to have been blown out of a small summit crater. Nearly all of the cm-sized and larger bombs contained mafic/ultramafic xenoliths, mantled by highly vesivular, phlogopite-bearing trachybasalt (shoshonite). The xenoliths include anorthositic gabbros, dunites, and spinel lherzolites. This highly refractory material have come from a deep sub-arc mantle source at crustal depths of more than 40-60 km. The presence of gabbro, diabase, basalt, plagiogranite, and sediments as xenoliths suggests that the TUBAF suite represents a unique cross-section of the lithospheric plate overlying the mantle which was sampled by volatile-rich basalt during its ascent to the present seafloor. Although the xenoliths may represent old mantle material, the host lavas were not mantle-derived.

Seafloor mapping northeast of Lihir revealed the existence of a fourth large, cone-shaped volcano (New World Seamount), similar to Conical Seamount. The volcanic cone is greater than 2.5 km in diamter at its base, and rises from the seafloor at 1950 m to a minimum depth of 1200 m (approximately 750 m high). A pit crater, about 200 m in diameter and 100 m deep occurs at the top of the cone. This edifice appears to have been built from crystal-rich, viscous flows in a manner similar to subaerial shield volcanoes. The lavas were mainly trachyandesite, with locally abundant plagioclase, consistent with a higher degree of fractionation than in the pyroxene-phyric, mafic lavas at Conical and TUBAF Seamounts. Flow breccias dredged from the top of the volcano were encrusted by Mn-oxides, probably precipitated from warm fluids emanating from the volcanic edifice.

Observations in 1994 suggested that the submarine volcanoes south of Lihir are examples of the earliest stages of island-building in the region. The volcanic rocks are dominantly alkali-olivine basalt and ankaramitic lavas with abundant clinopyroxene and trachybasalt with abundant phlogopite phenocrysts. Although the lavas are quite primitive, they also appear to have been very volatile rich. Several of the volcanic cones have distinctive pit craters and appear to have formed by explosive eruptions.

In addition to detailed bathymetric mapping, and tectonic and petrologic investigations, an important result of SO-94 was the successful application to the marine environment of genetic models which have been developed for epithermal deposits on land.

The initial work on samples from Conical Seamount led to a number of important criteria for the recognition of submarine analogs of epithermal gold deposits elsewhere on the seafloor. The discovery of hydrothermal activity on young volcanic cones near Lihir is the first documented evidence of seafloor venting associated with alkaline volcanism in a Tertiary forearc terrane, and the occurrence of high gold contents in the sulfides may have important implications for understanding the origins of large, Lihir-type gold deposits.

1.2 Cruise Objectives

BY PETER HERZIG AND MARK HANNINGTON

The objectives of SO-133 were to conduct detailed mapping and sampling of the young volcanic cones discovered in 1994. In comparison to Lihir, the Tabar, Tanga, and Feni island groups are relatively aseismic, and detailed mapping of these areas did not reveal any additional submarine activity. These areas were not examined further during SO-133.

Specific objectives of the cruise included:

(1) to establish the extent of recent volcanism and extension south of Lihir. In 1994, mapping and bottom photography focussed on just 3 volcanic cones. A number of additional bathymetric anomalies, including major boundary faults and possible volcanic cones, have not been examined. This area was remapped using differential GPS in order to document known structural features in greater detail (e.g., horst and graben structures south of Edison and Conical Seamounts).

(2) to investigate the possibility of new eruptions. The area mapped in 1994 has experienced continuing seismic activity and, judging from the youthful morphology of the recent volcanic cones may have been subject to renewed volcanism within the last 4 years. The large eruptions at Rabaul in September 1994 and the continuing volcanic and hydrothermal activity in the Manus back-arc confirm that extension beneath New Ireland is also ongoing. The emphasis during SO-133 was on Edison and TUBAF Seamounts, which were the youngest volcanic cones in 1994.

(3) to establish the present status and extent of hydrothermal venting at Edison Seamount. Indications in 1994 were that diffuse venting at the summit of Edison Seamount was mainly low-temperature. At the time it was unclear whether this system was decaying as a result of cooling of recent pyroclastic deposits or if sealing of the underlying pyroclastic cone might lead to a more robust system. Additional surveys of Edison Seamount were intended to document possible changes in the intensity of hydrothermal upflow around the cone and to document the nature of the substrate beneath the exposed clam beds and hydrothermally altered crusts.

(4) to document the status of vent communities at Edison Seamount. Since Edison Seamount is thought to have been a recent volcanic feature, the colonization of the diffuse vents may have been very rapid. The large clam beds in 1994 showed remarkable dispersal over large areas of diffuse venting, with local areas of very high densities. However, large portions of the two main clam beds were also littered with dead clams, indicating a collapse of the hydrothermal upflow. Subtle changes in the nature of the hydrothermal system in the intervening 4 year period are likely to be recorded by the migration, growth and distribution of vent fauna.

(5) to collect more representative suites of vent specific fauna, including smaller and rarer species and meiobenthos. A diverse collection of animals recovered in 1994 revealed the presence of several new species that required additional sampling and description for proper classification and

for comparison with vent fauna in nearby back-arc settings. A study of vent-related microbiology will also be carried out for the first time in a volcanic environment of this type.

(6) to determine the extent and character of alteration and gold mineralization at Conical Seamount. Only one sample was recovered from Conical Seamount in 1994, and only one camera-tow across the summit was possible. In order to determine the extent of mineralization, detailed mapping and sampling was carried out over a much larger area of the volcanic cone. Mineralogical and chemical studies of the alteration and gold mineralization were carried out to fully document the character of the deposit and to compare with nearby land-based deposits at Lihir.

(7) to determine the origin of near-bottom CH_4 anomalies south of Lihir. Strong near-bottom CH_4 anomalies were found in 1994 in association with hydrothermal activity at Edison Seamount. Preliminary data also indicated elevated concentrations of CH_4 in the water column between 1500 and 1600 m water depth at several other stations, however, a discrete source below 1500 m could not be located. Seismic profiles revealed possible gas hydrate layers and anticlinal structures which may be suitable traps for natural gas and a possible source for near-bottom methane anomalies. The large bounding faults defining the inter-island troughs within the New Ireland Basin may also be important channelways for gases. The possible sources of the methane (e.g., direct magmatic versus hydrocarbon sources) were tested during SO-133 by sampling for isotopic studies of dissolved gases.

(8) to sample volcanic rocks on individual volcanoes. Sampling of volcanic rocks in 1994 revealed compositions similar to those of mafic volcanic suites from the nearby islands. The youthful nature of the volcanoes suggests that this suite may be representative of the earliest stages of volcanism associated with local extension. However, a comprehensive suite of analyses from each volcanic cone, necessary to characterize the history of eruptions, was not obtained. Sampling for detailed geochemical studies was conducted to help characterize the origins of the various magmas. Sampling at TUBAF Seamount was also carried out in order to further evaluate the diversity of xenoliths in the lavas and to examine the melt characteristics (melt inclusions, mantle vein material).

(9) to sample the recent record of subaerial volcanic activity in deep sediments along the northwest part of the New Ireland Basin. Thin tuff beds recovered in 1994 are thought to represent the fall-out from the latest eruptions on Feni and Lihir (ca. 2300 yr.). Additional sampling and profiling (including Parasound) away from the Tabar-Feni chain was undertaken to improve stratigraphic correlation in the region.

1.3 Participating Institutions / Cruise Participants

TUBAF Technische Universität Bergakademie Freiberg
Institut für Mineralogie, Lehrstuhl für Lagerstättenlehre
Brennhausgasse 14; D-09596 Freiberg; Germany
Phone: +49-(3731)-39-2626 / 2662; Fax: +49-(3731)-39-2610
email: herzig@mineral.tu-freiberg.de (Prof. Dr. P. Herzig)

CODES Centre for Ore Deposit Research, University of Tasmania
GPO Box 252-79 Hobart; Tasmania, Australia
Phone: +61-(3)-6226-2893; Fax: +61-(3)-6226-7662
email: Bruce.Gemmell@utas.edu.au (Dr. J. B. Gemmell)

FSF Forschungsinstitut und Naturkundemuseum Senckenberg
Abteilung Zoologie II
Senckenberganlage 25; D-60325 Frankfurt am Main; Germany
Phone: +49-(69)-7542-240; Fax: +49-(69)-746238
email: mtuerkay@sng.uni-frankfurt.de (Dr. M. Türkay)

GPI Institut für Geowissenschaften der Christian-Albrechts Universität Kiel
Olshausenstrasse 40-60; D-24118 Kiel; Germany
Phone: +49 (431) 880-2850 / 2852; Fax: +49 (431) 880-4376;
email: pst@gpi.uni-kiel.de (Prof. Dr. P. Stoffers)

GSC Geological Survey of Canada
601 Booth Street; Ottawa, ON K1A 0E8; Canada
Phone: +1-(613)-996-4865; Fax: +1-(613)-996-9820;
email: mhanning@gsc.NRCan.ca (Dr. M.D. Hannington)

UF Department of Geology, University of Florida
1112 Turlington Hall; Gainesville, FL 32611; U.S.A.
Phone: +1-(352)-392-2128; Fax: +1-(352)-392-9294
email: perfit@geology.ufl.edu (Prof. Dr. M. Perfit)

UR Universität Regensburg; Institut für Biologie
Lehrstuhl für Mikrobiologie und Archeenzentrum
Universitätsstr. 31; D-93053 Regensburg; Germany
Phone: +49 (941) 943-3185; Fax: +49 (941) 943-2403
email: harald.huber@biologie.uni-regensburg.de (Dr. H. Huber)

UV Department of Biology, University of Victoria
P.O. Box 3020; Victoria, BC V8W 3N5; Canada
Phone: +1-(250)-721-7135; Fax: +1-(250)-721-7120
email: tunnshaw@uvvm.uvic.ca (Prof. Dr. V. Tunnicliffe)

GPNG Geological Survey of Papua New Guinea, Department of Mineral Resources
Private Mail Bag, Port Moresby, N.C.D.; Papua New Guinea
Phone: +675-322-4259; Fax: +675-321-1360
email: geoserv@online.net.png (Paul Kia)

Shipboard Scientific Party

Herzig, Peter (Chief Scientist)	TUBAF	economic geology
Hannington, Mark. (Co-Chief Scientist)	GSC	economic geology
Stoffers, Peter (Co-Chief Scientist)	GPI	sedimentology
Becker, Klaus-Peter	TUBAF	geochemistry, XRF
Drischel, Mario	TUBAF	documentation, XRF
Franz, Leander	TUBAF	petrology
Gemmell, Bruce	CODES	economic geology
Höppner, Bernd	TUBAF	voltammetry
Horz, Kersten	GPI	sedimentology
Horn, Christian	UR	microbiology
Franklin, James	GSC	economic geology
Jellineck, Thomas	FSF	macro/mega fauna
Jonasson, Ian	GSC	economic geology
Kia, Paul	GPNG	scientific observer
Mühlhan, Norbert	GPI	technician
Nickelsen, Sönke	TUBAF	documentation
Percival, Jeanne	GSC	alteration, XRD
Perfit, Mike	UF	petrology
Petersen, Sven	TUBAF	economic geology
Schmidt, Mark	GPI	gas chemistry
Seifert, Thomas	TUBAF	petrology
Thiessen, Olaf	GPI	gas chemistry
Türkay, Michael	FSF	macro/mega fauna
Tunnicliffe, Verena	UV	macro/mega fauna
Winn, Kyaw	GPI	sedimentology

Ship's Crew

Andresen, Hartmut	Master
Priebe, Roland	First Mate
Mallon, Lutz	First Mate
Sturm, Wolfgang	Radio Operator
Martin, Andreas	Chief Engineer
Schlosser, Thomas	Second Engineer
Guzman, Werner	Second Engineer
Freitag, Rudolph	Electrical Engineer
Duthel, Rainer	Electronics Engineer
Vöhrs, Helmut	Electronics Engineer
Grigel, Jens	System Operator
Klein, Andreas	System Operator
Schymatzek, Peter	Fitter
Nagelberg, Uwe	Motor Man
Paul, Gerhard	Motor Man
Rademacher, Hermann	Motor Man
Sosnowski, Werner	Motor Man
Erbelding, Klaus-Peter	Physician
Hermann, Klaus-Otto	Chief Cook
Falk, Volkhard	Second Cook
Bronn, Johann	Chief Steward
Grübe, Gerlinde	Stewardess
Wege, Andreas	Steward
Miscker, Joachim	Bosun
Basner, Alwin	Able Seaman
Becker, Siegfried	Able Seaman
Bosselmann, Karsten	Able Seaman
Dracopoulos, Eugenius	Able Seaman
Hödl, Werner	Able Seaman
vom Berg, Götz	Able Seaman

2 Summary of Results

BY PETER HERZIG AND MARK HANNINGTON

2.1 Seafloor Topography and Structure

Detailed mapping of the seafloor topography south of Lihir has revealed a number of important structural elements of the active tectonic zone which account for the location of recent submarine volcanic and hydrothermal activity.

The island group is situated on a large uplifted block, raised by regional southward compression along the Manus-Kilinailau trench (Fig. 2.1). During the late Miocene, nearly 7 km of sediment accumulated in the basin on top of Eocene to early Miocene volcanic basement. Volcanic activity on the islands, which began about 3.5 Ma ago, appears to have been related to extension along northeast-trending structures that cut across the New Ireland Basin. Since Pliocene-Pleistoncene time, partial melts associated with extension in the thickened crust of the New Ireland Basin have risen through the old forearc crust along reactivatd transfer faults to form the volcanic islands of the Tabar-Feni chain. These structures are thought to be related to regional plate rotation and extension of the old forearc crust of the New Ireland Basin (Exon et al., 1986; Stewart and Sandy, 1988; McInnes, 1992). Although plate rotation has isolated the Tabar-Feni chain from the presently active arc of New Britain, the present volcanism on the islands is most likely related in some way to subduction from the south along the New Britain-Solomon trench. Observations during SO-133 confirm that active extension is occurring between New Ireland and Lihir and that major strike-slip faulting associated with the plate rotation has localized recent eruptions along the pedestal of Lihir. A conjugate set of NE-NW striking faults that control the volcanism on the islands has been documented in Landsat and airborne magnetics surveys, and similar structures have been identified in the offshore areas (Gulf Research and Development, 1973; Exon et al., 1986).

Records of seismic activity between the Lihir group and New Ireland show that shallow earthquake epicenters are confined to a distinctive NE-SW corridor along the axis of the Lihir group. The earthquakes define a narrow seismic zone, and the recent tectonic activity along this corridor may be an indication of the beginning of the break up of New Ireland in response to the present subduction of the Solomon Plate and back-arc spreading in the Manus Basin. New Ireland is already noticeably thinned along the portion of the island immediately opposite Lihir (see Fig. 2.1).

During SO-94, several large NE-trending sedimented fault blocks were observed along the margins of the island pedestal, and these may also be related to the regional extension. Additional mapping during SO-133 confirmed that several major normal faults on New Ireland (the Ramat and Matakan fault zones) can be traced offshore and are likely responsible for extension within the active seismic zone (Fig. 2.2).

The most prominent structural elements in the area immediately south of Lihir have a NW orientation - at right angles to the implied regional extension - and are likely part of the Tabar Fault system (Fig. 2.3). The close association of these faults with the recent submarine volcanism suggests that they are deeply penetrating structures that may have tapped melts at considerable depth in the crust. A number of cross-cutting structures are also implied by the NE-trending alignment of several of the volcanic cones. However, obvious NE-trending pull-apart structures associated with extension in the Lihir block were not observed and my be concealed by recent sedimentation. It is unclear whether the offshore extensions of the Ramat and Matakan fault zones

on New Ireland cross the Tabar Fault. However, large fault blocks with NE orientation appear to dissect the main Tabar Fault in the area mapped.

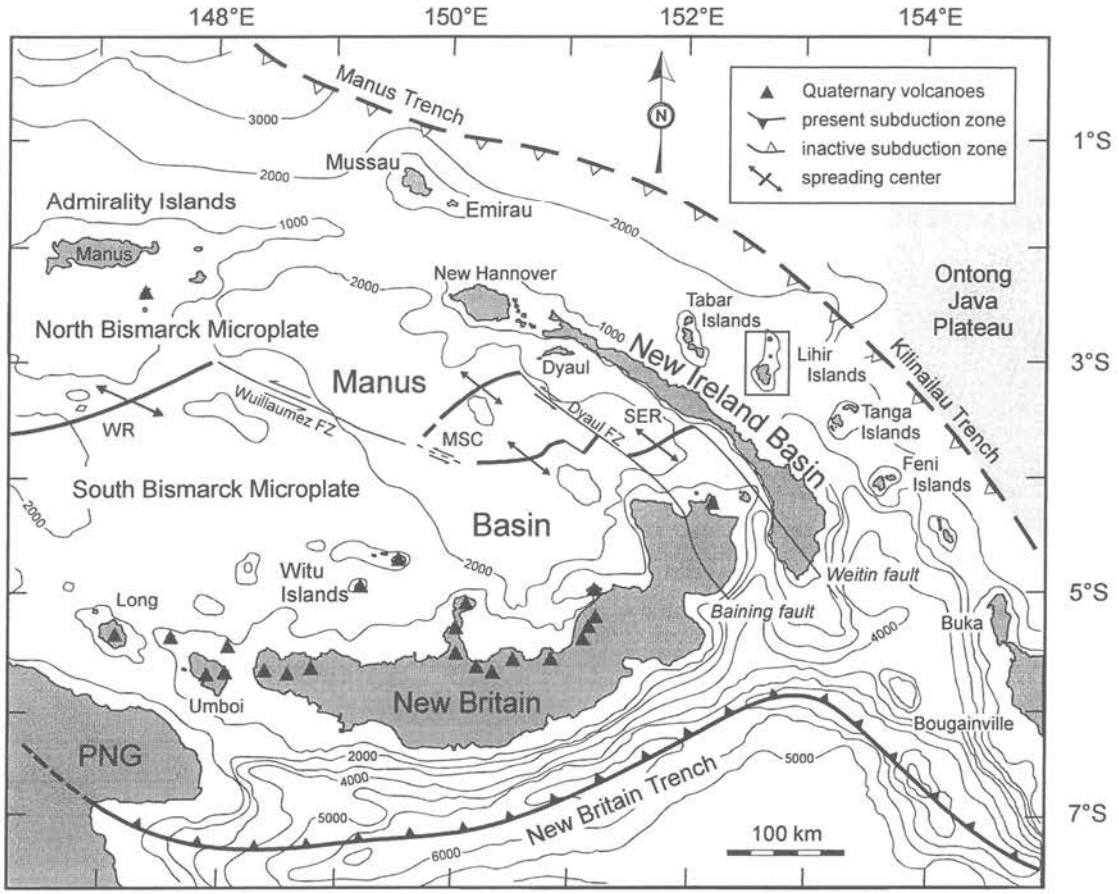

Figure 2.1: Regional map showing the location of the Tabar to Feni island chain and the principal structural elements of the New Ireland Basin and the Manus Basin. The box indicates the study area enlarged in Fig. 2.2.

A raised block of sediment southeast of Edison Seamount is bounded by one of the largest faults and is presently leaking methane along part of its exposed strike length. This fault is on line with the Edison and TUBAF volcanoes and may be the controlling structure for recent volcanic eruptions at these sites. At its eastern extremity, near TUBAF volcano, the trace of the fault appears to have been buried by recent debris flows from Lihir. TUBAF has erupted onto the debris apron and much of the pyroclastic material from the volcano sits on older sediments eroded from the flanks of the island. Nunmerous older volcanic cones also occur along the fault (e.g., small cones immediately north of Edison Seamount) and suggest that this structure may have been active for some time. Volcanic rocks outcropping on the sides of these cones appear to have been exposed by tectonic activity along the fault.

Major debris flows, associated with collapse features on the island of Lihir, dominate the seafloor topography east and west of the island. One debris flow, east of the Luise caldera (Fig. 2.4) is thought to be the outflow from a major sector collapse between 350,000 and 100,000 years ago. This collapse was coincident with the onset of late-stage epithermal gold mineralization in the caldera, tentatively dated at 100,000 to 150,000 years (K-Ar on K-Feldspar and alunite).

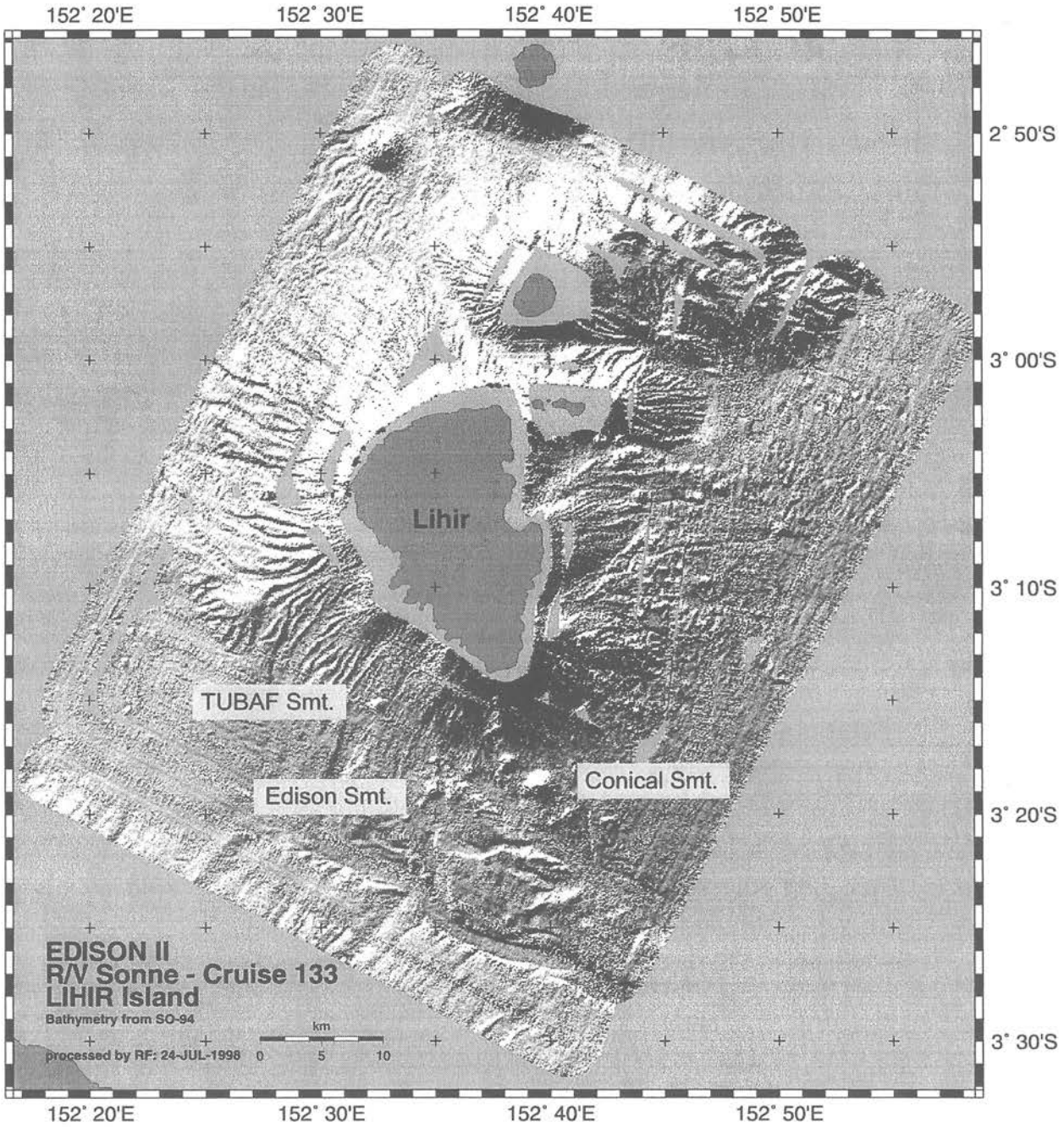

Figure 2.2: Bathymetric map of the New Ireland Basin, showing the location of twelve volcanic cones south of Lihir.

2.2 Submarine Volcanism

The few radiometric dates available indicate that the most recent volcanic eruptions on Lihir occurred at about 1.1 Ma (Johnson et al., 1976). The most recent dated eruption in the island chain occurred about 2,300 years ago at Feni to the extreme southeast (Licence et al., 1987). These eruptions covered wide areas with, ranging from 5 to 30 cm in thickness, some of which was recovered in sediment stations during SO-133. The discovery of even younger volcanic cones in the area south of Lihir implies that volcanism in the New Ireland Basin is now focussed in the active tectonic zone of the Lihir group.

Twelve (12) separate volcanic cones have now been mapped and sampled in the area (see Fig. 2.3), and a preliminary assessment of their age progression implies at least several episodes of volcanism. Five (5) of the cones have well-defined summit craters, up to several hundred meters in diameter and up to 50 m deep. Volcanic rocks are exposed at the summit of four of the cones, but the remaining volcanoes are heavily sedimented (up to 5-10 m thickness of sediment in the summit craters). The variable sediment thickness implies that volcanic activity in the area has likely been episodic for at least the past 10^5 years. A major swarm of volcanic eruptions during this time would coincide with the age of recent intrusive activity and associated geothermal systems on Lihir. Large blocks of carbonate-cemented foraminiferal ooze recovered from the summit of New World Seamount, northwest of Lihir, suggest that this volcano is older.

Edison, Conical and TUBAF seamounts appear to be the youngest volcanoes in the area. TUBAF volcano, which has erupted through the debris apron on the flank of Lihir, may have been active within the time frame of the available seismic records for the area (between 1900 and 1992). A broad heat flow anomaly associated with this area (up to 100 mW/m^2 at the base of the largest volcanic cone) is consistent with a young age for the volcanism.

The volcanics rocks recovered from Edison, Conical, and TUBAF seamounts consist of pyroxene-phyric alkali-olivine basalt and trachybasalt, with locally abundant phenocrysts of pyroxene, magnetite, and phlogopite. The highly alkaline, SiO_2-undersaturated character of the volcanics is consistent with a tectonic model which involves local extension and rifting of the old forearc crust of the New Ireland Basin. One model suggests that the alkaline melts may have been generated by partial melting of mantle material which has been subjected to metasomatism by H_2O, CO_2, and alkali-rich components derived from seawater-altered basalts (McInnes and Cameron, 1994).

Most of the smaller volcanoes with well-defined summit craters appear to be pyroclastic cones, composed of volcanic ejecta blown from the small pit craters. Much of the pyroclastic material comprises volatile-rich, phlogopite-bearing basalt, especially at TUBAF and Edison seamounts. New samples recovered from Edison Seamount also revealed distinctive pepperitic textures, indicating local extrusion of basalt into wet pelagic sediments. Some samples contained metasedimentary rocks, which appear to have been baked in contact with the basalt.

The ejecta blanket at TUBAF Seamount comprises mainly fresh, sand-sized ash, lapilli, and small rounded bombs (up to 10 cm). The absence of any pelagic sediment covering the pyroclastic deposits suggests that the last eruption of this cone was very recent. By comparison, the sediment within the crater at Edison is at least several meters deep, suggesting that the volcano has been dormant for thousands of years (sedimentation rates are approximately 5 cm/1000 yr). Nevertheless, Edison shows a similar eruptive style to TUBAF, which is much younger.

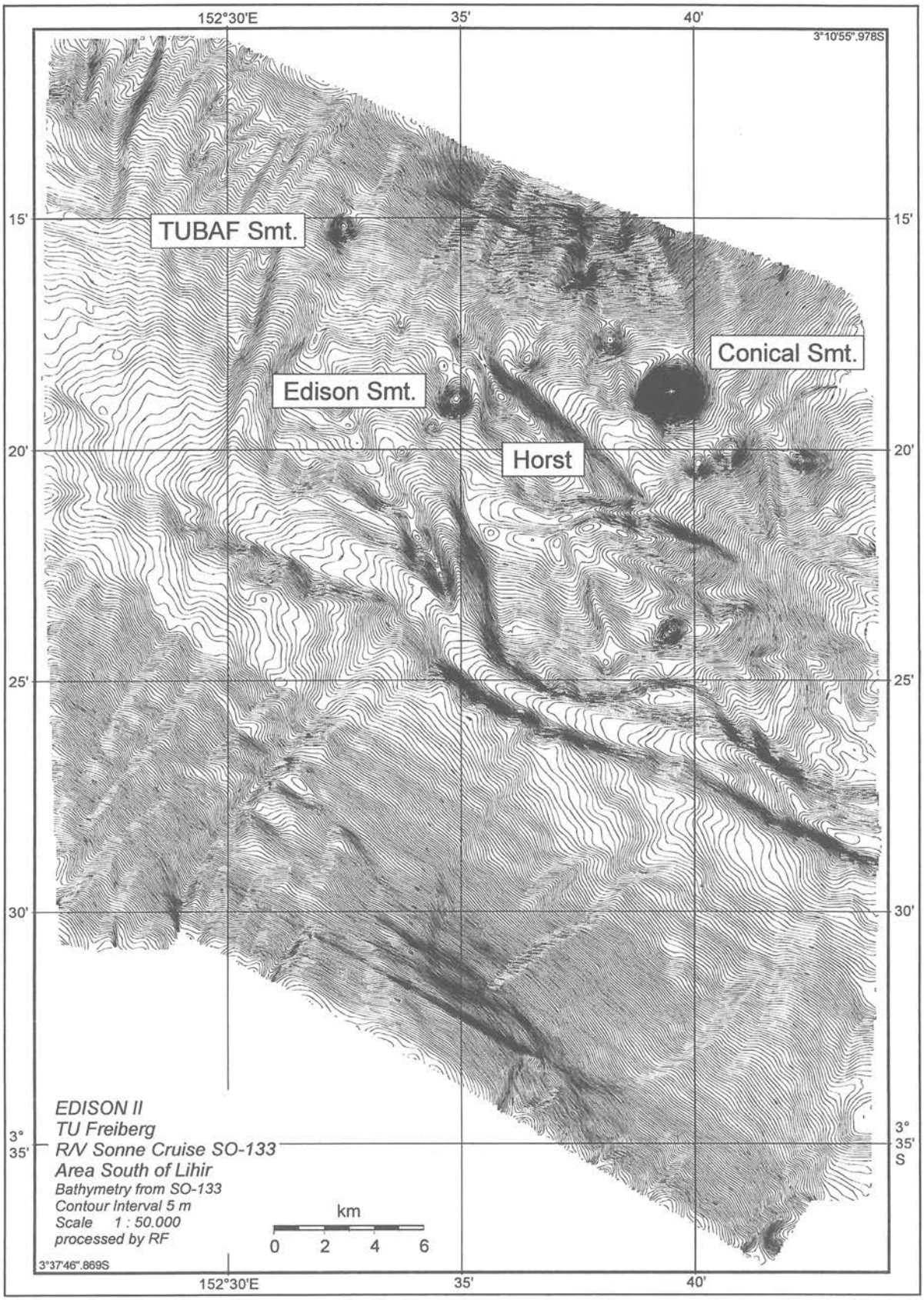

Figure 2.3: Hydrosweep bathymetric map (1:50.000) of volcanic and structural features in the area south of Lihir. TUBAF, Edison, and Conical Seamounts are shown. A major horst structure, southeast of Edison Seamount, is the location of extensive methane degassing. The large NW-SE trending fault structure which crosses the lower part of the map is the Tabar Fault.

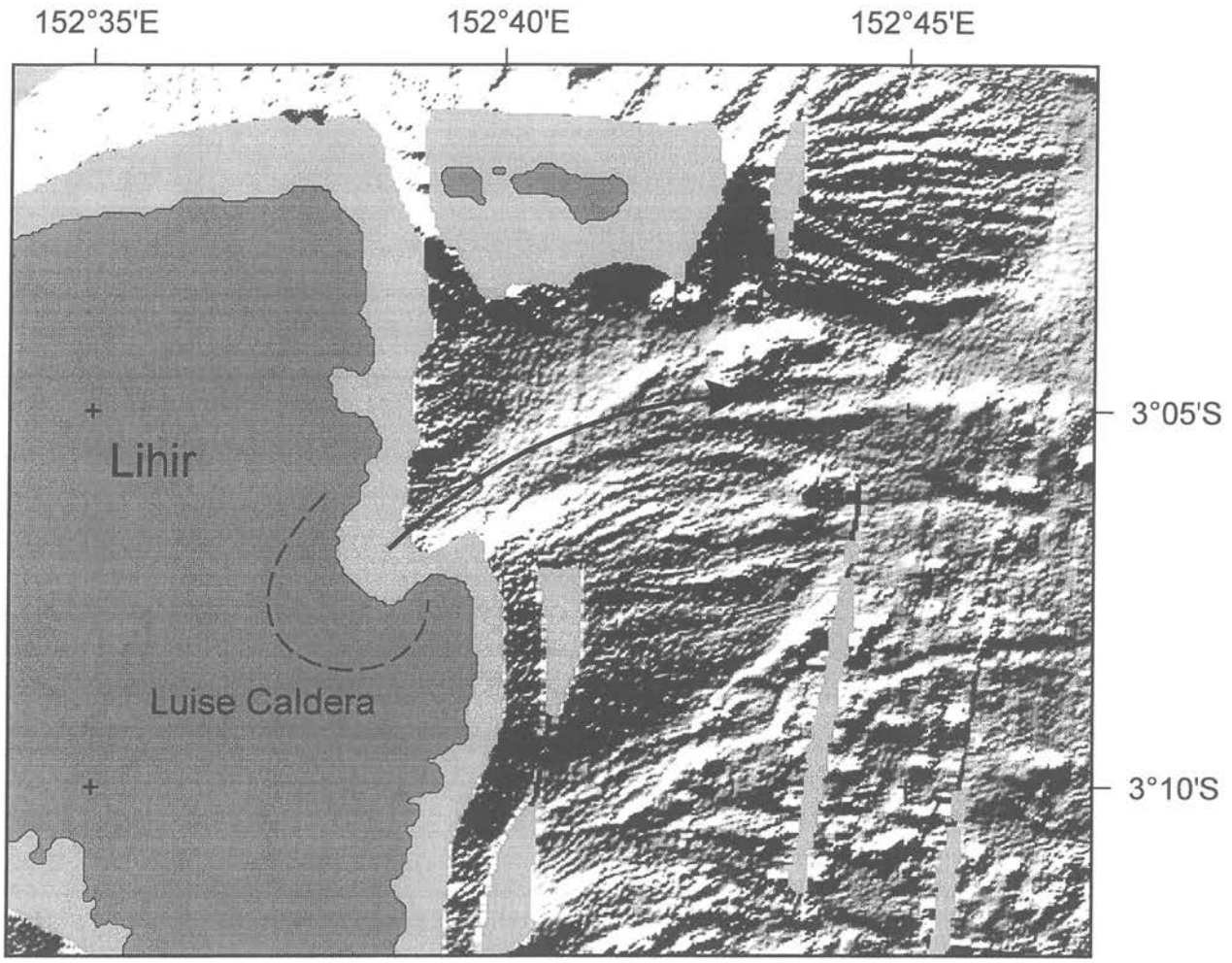

Figure 2.4: Portion of the processed Hydrosweep data showing the location of a major debris flow east of Luise Caldera. This feature is thought to be the outflow from a major sector collapse of the Luise volcano that occurred between 350,000 and 100,000 years ago.

The volcanic bombs at TUBAF consist of highly vesicular, phlogopite-bearing trachybasalt containing a wide range of nodules (up to 10 cm) of ultramafic, mafic, and sedimentary material. Almost every bomb or fragment large enough to cut contained a xenolithic core. The nodules first collected in 1994 included spinel lherzolite, dunite, harzburgite, wehrlite, gabbro, anorthosite, diabase, basalt, serpentitite, amphibolite, as well as carbonated mudstones and siltstones. As similar suite was collected during SO-133, with a larger proportion of gabbros, dunites, and pyroxenites, and similar samples were also collected for the first time from Edison Seamount. The xenoliths represent a cross-section of the oceanic lithosphere and forearc crust sampled by the basalt during its ascent through deeply penetrating fractures.

The larger volcanoes are dominanted by massive vesicular flows of mainly pyroxene-rich ankaramite. Several of the older cones, such as New World Seamount and at least one cone near Edison Seamount, have somewhat more evolved volcanic rocks (plagioclase-phyric trachyandesites) which may indicate a slightly different eruptive history for their magma.

Conical Seamount, which is the largest cone in the area, was built from a long-lived submarine fissure eruption. An elongate bathymetric feature at the summit of the volcano is interpreted to be the eruptive fissure. This was confrimed by mapping with the TV-grab, which revealed lobate flows

cascading down the sides of the summit plateau and locally draining back into an elongate summit depression (Fig. 2.5). The sediment on many of the flow surfaces is not more than a few centimeters thick, suggesting that volcanic eruptions at Conical Seamount have occurred within the last few thousand years. Single-channel seismic profiles from 1994 revealed structures in the sediment covering the flanks of the volcano which may be due to faulting. However, a systematic relationship to shallow faults was not observed, suggesting that the volcanism may be localized by deeper structures which are now buried beneath the debris flows from Lihir.

2.3 Seafloor Hydrothermal Activity and Cold Seeps

In 1994, evidence for active hydrothermal venting was found at Edison Seamount, where extensive clam beds associated with diffuse fluid flow were discovered near the crest of the pyroclastic cone (Fig. 2.6). Two distinct fields covering areas of approximately 100-200 m in diameter were mapped along the crater rim and on the outer flanks of the cone. Camera surveys during SO-133 suggest that these fields may have expanded onto the eastern rim of the crater. Clear, shimmering water was observed in at least two towed camera surveys during SO-94, and diffuse venting was mapped over an area of several 10s of meters at the center of each clam bed. In 1994, the field on the northern rim of the crater was littered with blackened, dead clam shells and was thought to be extinct. However camera tows during SO-133 showed a new clam bed at the northeast corner of the crater which was not observed in 1994. An OFOS survey appears to show a much larger area of live clams at the northern field than previously thought and an apparent increase in the population density of the southern field. Apart from the clam beds, no visual evidence for active fluid venting was found.

The clam beds occur on heavily sedimented surfaces at the crater rim and are surrounded by darkened muds that are stained by sulfide. Samples of the sediment collected in the TV-grab consist of pale green, foraminiferal carbonate ooze with minor smectite, amorphous Fe-sulfides and trace pyrite. The black, amorphous Fe-monosulfides occur in distinct, vermiform channelways through the sediment, similar to that observed in muds from the cold seeps. Large slabs of indurated sediments and semi-lithified, volcaniclastic breccias in a matrix of foramniferal ooze were also recovered from the clam fields. The altered muds and cemented breccias form a hardened layer up to10 centimeters thick, immediately surrounding the vent fields. 4.5 kHz bottom-profiling suggests that layers of indurated sediments may form an extensive carapace over the top of the cone and this may be important for concentrating fluid flow at the crater rim. The cement consists dominantly of calcite, which may be derived from the recrystallization of foraminiferal ooze or the partial dissolution of clam shells, which are also abundant in the sediment. However, detailed isotopic and mineralogical studies are required to determine whether this induration is due to hydrothermal alteration or cementation by methanogenic carbonate (i.e., methane oxidation).

The presence of a mussel type, known elsewhere to have methanotrophic symbionts normally associated with cold seeps, and the abundance of carbonate-cemented crusts at Edison Seamount suggests that some of the present diffuse venting may be of "cold seep" origin rather than hydrothermal. The age of the cone and its location at the intersection of several major fault structures that are leaking CH_4 support this idea. However, the high density and enormous biomass of the clam fields far exceeds that found at cold seeps, and more closely resembles that of H_2S-rich vents associated with higher-temperature hydrothermal activity.

During investigations of a large, near-bottom methane anomaly discovered in 1994, a major source of methane was located along the raised block (horst structure) southeast of Edison Seamount (Fig. 2.7). 4.5 kHz sub-bottom profiling indicates that the structure is an uplifted block of sediment.

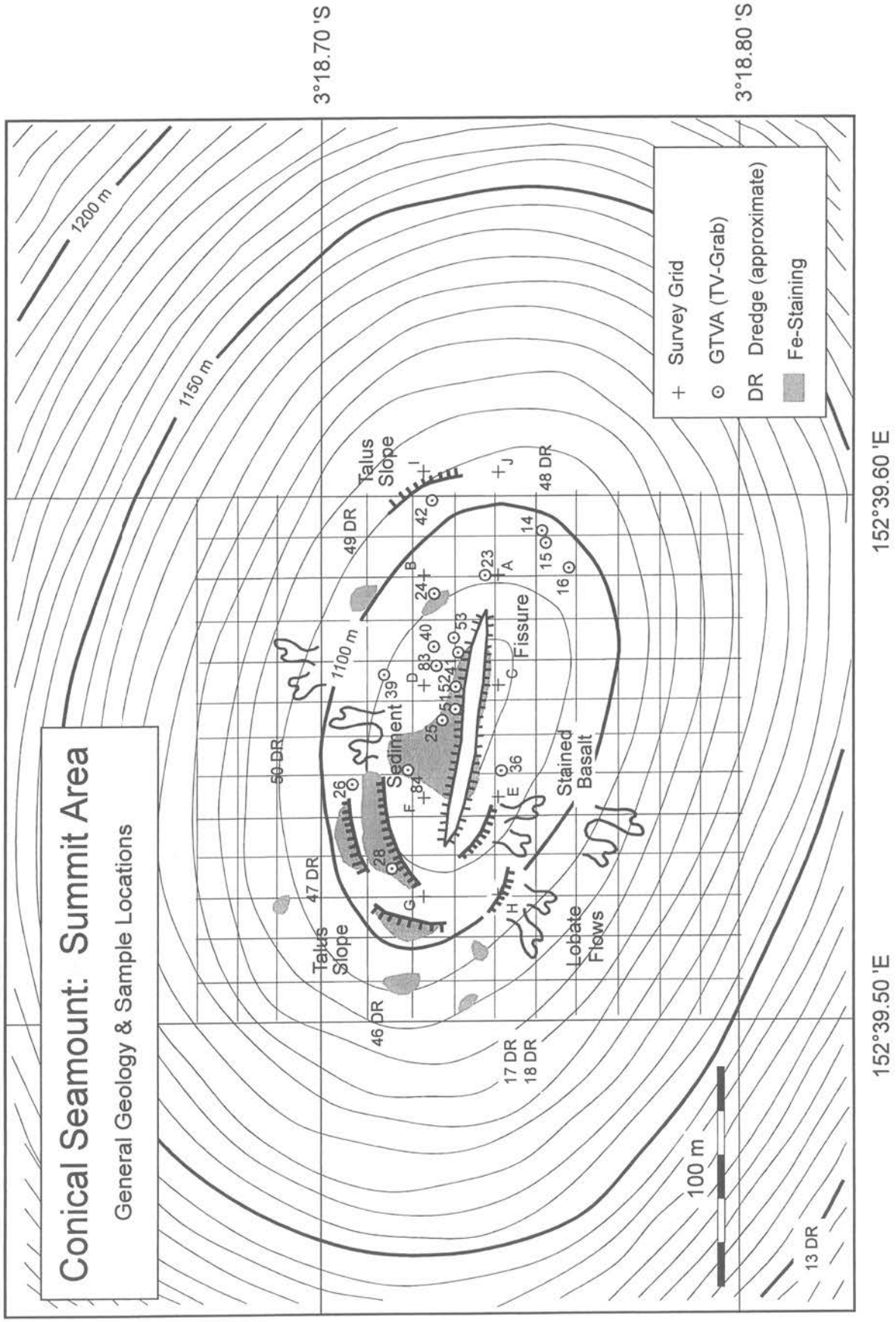

Figure 2.5: Detailed bathymetry and interpreted geology of the summit area of Conical Seamount.

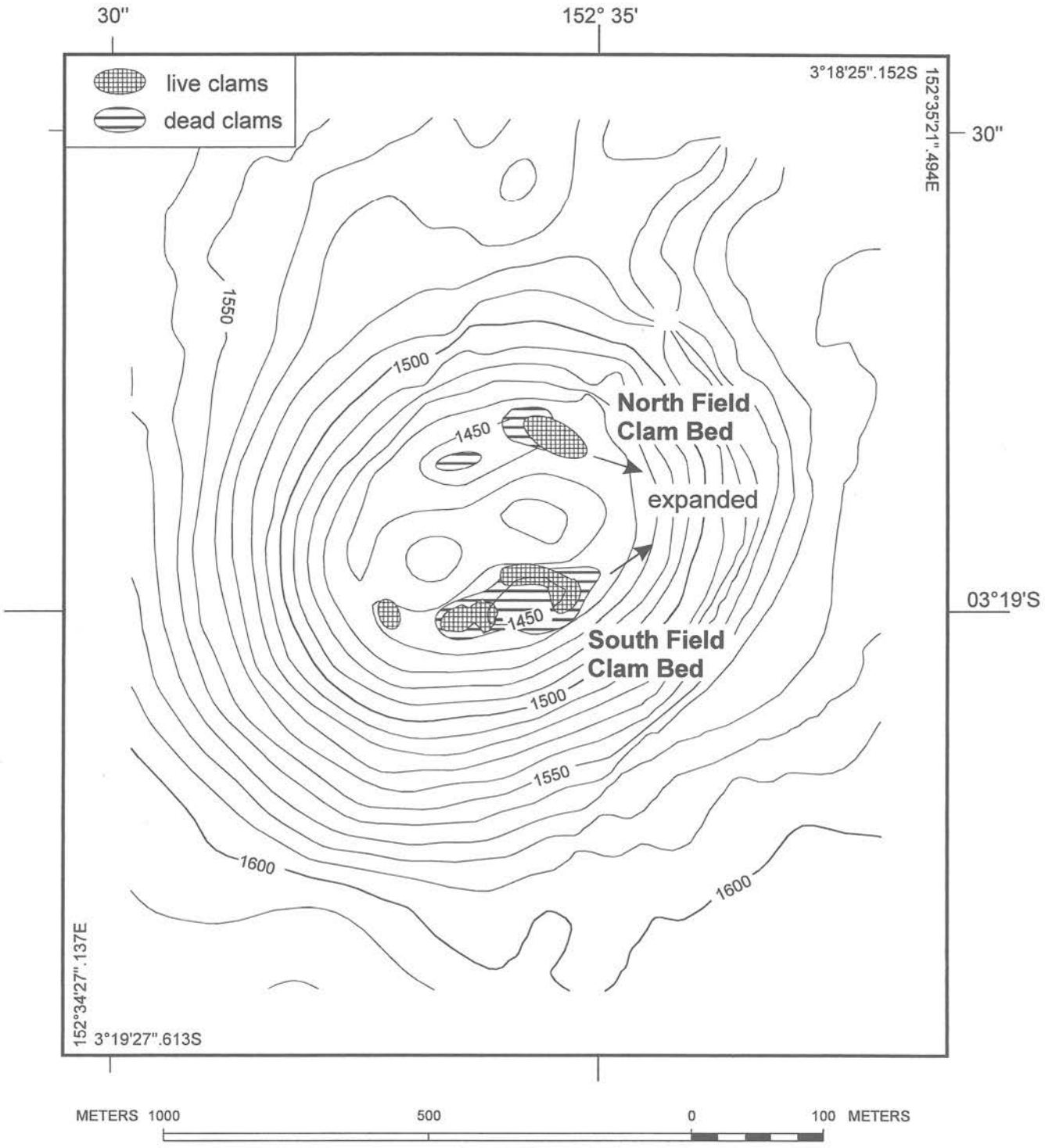

Figure 2.6: Detailed bathymetric map showing the distribution of large clam beds surrounding the summit area of Edison Seamount.

A maximum concentration of 9,000 nl/l CH_4 was measured along the east-facing slope of the horst, opposite Edison Seamount, and this source likely accounts for a widespread mid-depth anomaly in the area. No temperature anomaly was observed. The first dredge of the horst block recovered several large clam shells, indicating the presence of a chemosynthetic biological community. The association with high CH_4 suggests that the clam beds occupy cold seeps, and the presence of high ethane in the cold seep gases may suggest a petroliferous origin.

Several camera tows and TV-grabs in the area revealed discontinuous cold seep biota over a strike length of at least 2 km, centered on the highest methane anomaly. The cold seep area is characterized by sparsely populated but widespread patches of white clams, polycheate worms, vesitmentiferan tubes, and extensive beds of black mussels on stained patches of sediment and discontinuous outcrops of carbonate crust. The carbonate crusts are exposed on the steep slope of the raised block, and grey-black streaks of sulfide-stained sediment have been eroded from the slope face. Large blocks and slabs of carbonate-cemented muds recovered from the slopes contain abundant flow channels stained by sulfide.

Similar cold seeps were also observed on the southeast flank of a small volcanic cone north of Edison Seamount. This cone may be partly dissected by the fault which is presently leaking methane further to the south.

The discovery of methane degassing along major structural elements in an active tectonic zone of the New Ireland Basin and widespread animal communities along the faults may be an indication of the presence of cold seeps similar to those found at accretionary margins (e.g., Cascadia Margin). The seeps occur in an area of hummocky seismic refelctors and arched upward sedimentary sequences (Fig. 2.8), and flat subbottom reflectors observed in single-channel sesimic profiles in 1994 were interpreted to be possible gas hydrate layers. Similar features were also reported near this location by Exon and Marlow (1988) and Marlow et al. (1991).

The extensive carbonate cementation is thought to be related to the oxidation of methane within the upper part of the sediment profile. Gas charged (H_2S- and CH_4-rich) sediments were recovered in a core from this area, and obvious gas cavities were found in the sediment cores. White patches were also observed at the locations of the seeps, and these may be an indication of bacterial mats or solid gas hydrates. However, no samples of this material could be recovered. The liberation of methane from gas hydrates in the sediments may be related to the high heat flow in the area or local uplift associated with the rising basement high of the Lihir island group.

2.4 Chemosynthetic Biological Communities

The clam beds on Edison Seamount are mature chemosynthetic communities. Clams on both the north and south sides of the summit reach large sizes, and abundant dead shells point to long-term fluid flow at this site. The largest clams are 18-22 cm in length, with most of the population in the range of 13 to 20 cm. The large size of the individuals suggests that the venting has been ongoing for at least a decade. Parts of the southern field are colonized by smaller clams amid large empty shells, suggesting that fluid flow may have been recently rejuvenated at this site. The abrupt boundaries of the clam fields likely reflect the limits of fluid upflow around the summit of the cone. Preliminary observations and comparison with 1994 results suggest that the northern clam bed may be increasing in size and density.

Sulfide-specific fauna are absent at the edge of the clam beds, but a mussel type normally associated with cold seeps was observed (this type of mussel can have either sulfide- or methane-oxidizing

symbionts, and further work on the samples is required to identify the bacteria present). Evidence for both H_2S and CH_4 in the fluids would support the idea that a portion of the nutrient flux at Edison may be related to nearby leaky fault structures that are degassing CH_4. Indeed, some of the vent animals may have been recruited from the cold seeps nearby. However, the biomass associated with Edison Seamount is much greater than that observed at the cold seeps, suggesting that a thermal flux associated with the volcano may be enhancing the availability of reduced gases.

On the nearby fault structure, southeast of Edison Seamount, another assemblage of animals was recovered with quite a different character. Mussels and polycheates at this site have colonized areas of carbonate concretions, and both vesitmentiferans and polycheates were collected from the sediments. However, the biomass encountered was considerably lower than in the clam beds at Edison. Examination of Hydrosweep data south of Lihir suggests that several major structures could be focussing enriched fluid flow in this area. High concentrations of methane in the escaping fluids likely contribute the largest part of the nutrient base for the observed biological community. The sampled animals are similar to that of other cold seep environments and are characterized by a variety of CH_4- and H_2S-specific fauna.

The presence of diverse biological communities in the vicinity of Edison Seamount suggests two different but closely juxtaposed styles of venting (warm springs and cold seeps). The warm fluids are likely influenced by volcanic processes causing enrichment in reduced sulfur, whereas cold fluids channeled through tectonic features may be remobilizing buried carbon and emerging as fluids enriched in both methane and sulfur. The observation of both warm springs and cold seeps near Edison Seamount may be a unique juxtaposition of these different processes. Clams, mussels, and vestimentiferans are known at both warm vents and cold seeps, but many of the animals found at Edison (crabs, shrimps, barnacles, limpets) have their closest relatives at mid-ocean ridges and back-arc hydrothermal sites. Many of the animals at Edison and at the nearby cold seeps are likely to be new species and thus represent a fauna specific to this region. The animals are different from the vent fauna in the nearby Manus Basin and may indicate the presence of a large endemic population elsewhere in the New Ireland Basin.

2.5 Seafloor Mineralization

A compresehnsive sampling program at the summit of Conical Seamount recovered more than 1,200 kg of mineralized material at 26 separate stations (18 TV-grabs, 8 dredges) along a 150 m strike length of the eruptive fissure. Camera surveys across several hundred meters of the top of the cone revealed widespread but discontinuous patches of yellow, brown, and grey stained sediment. The abundant discoloration of the sediments suggest that low-temperature, diffuse hydrothermal vents were formerly active near the summit of the volcano. A gossan-like Fe-oxide crust was sampled at the perimeter of the mineralized zones, and appears to be the weathered product of altered (pyrite-bearing) basalt. The Fe-oxide staining is exposed over a strike length of at least 250 m, and dredging of the flanks of the volcano (from 1250 m water depth to 1100 m) also recovered intensely altered lavas with weak mineralization and thick Fe-oxide crusts. The abundance of Fe-oxide gossan implies that the hydrothermal system is now extinct and that the mineraliztion is old. Thick Fe-oxide crusts on some of the basalts are most likely a product of seafloor weathering, enhanced by the presence of abundant disseminated pyrite in the rocks. Some Fe-oxide crusts showed excellent preservation of the original mineralized crackle-breccia.

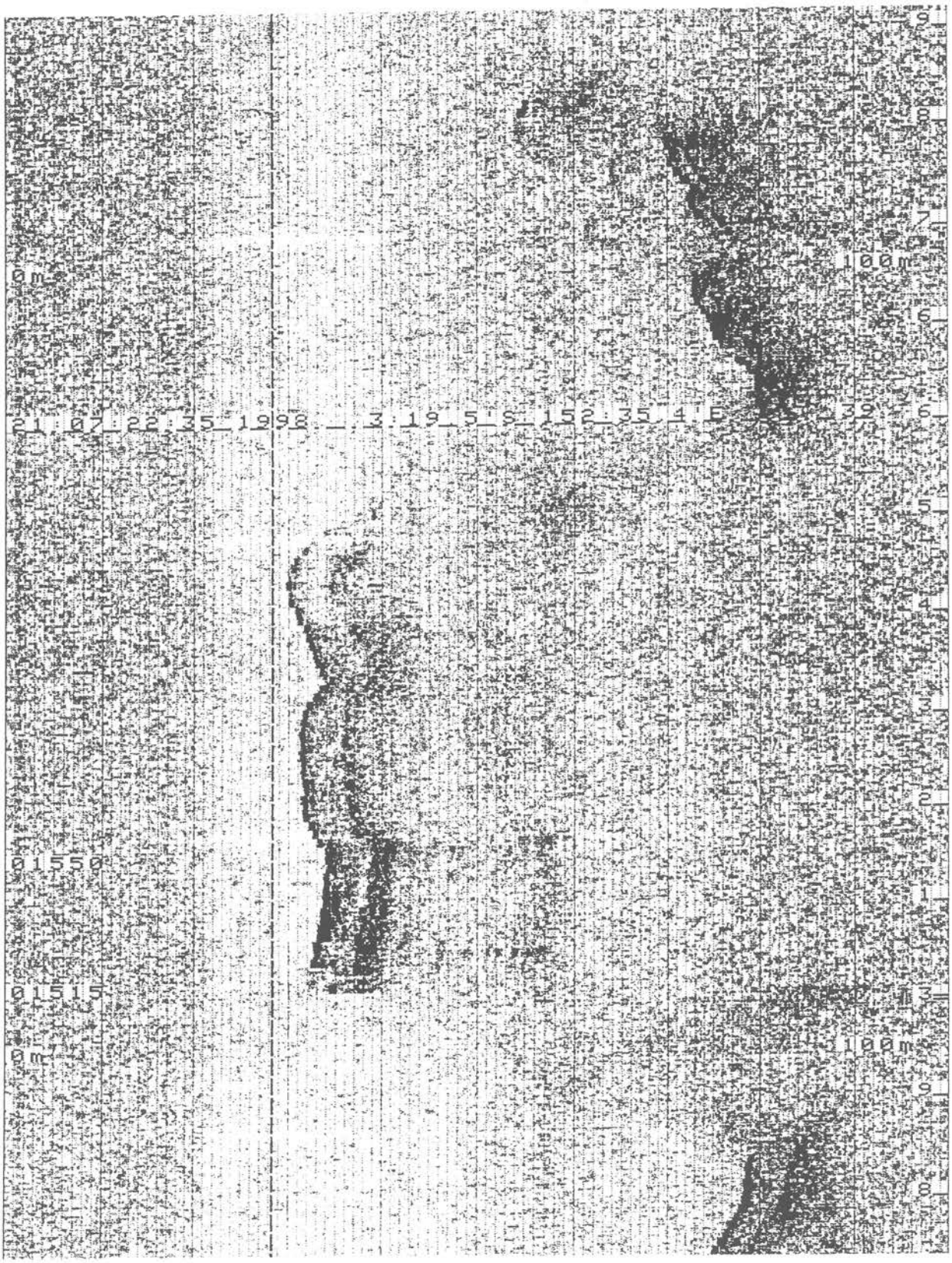

Figure 2.7: 4.5 kHz sediment profile of a large horst structure located southeast of Edison Seamount. This structure was identified as the likely source of a major near-bottom methane anomaly, most likely related to cold seeps.

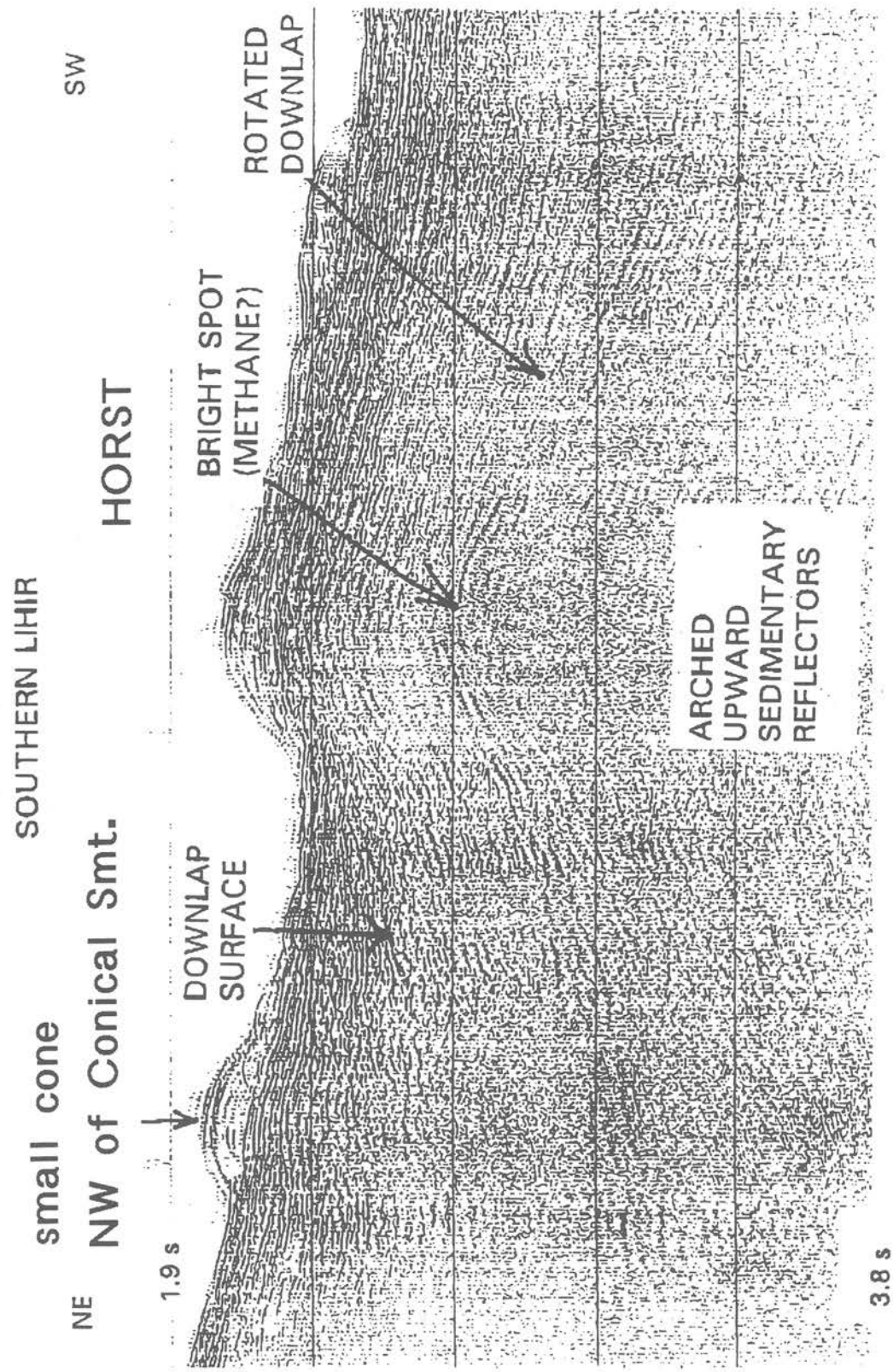

Figure 2.8: Single-channel seismic profile across large horst structure southeast of Edison Seamount (from SO-94). The profile shows several subbottom reflectors which may be gas hydrate layers.

The exposed mineralization is confined to the top of the seamount along the main eruptive fissure. Talus slopes leading away from the fissure and debris in the summit depression are heavily stained by Fe-oxides, and portions of the thicker lava flows adjacent to the fissure are intensely mineralized on exposed surfaces where large slabs of lava have spalled off. The most intense staining is often observed between large blocks of broken flows and where talus has accumulated at the top of the flow. Sediment which has ponded in the summit depression and is notably stained or mottled in appearance. Grabs of this material recovered large mineralized blocks and pyritic, clay-rich muds immediately beneath the sediment cover. Much of this material may be the erosional remnants of older mineralized lavas. All of the sampled lavas were originally pyroxene-rich ankaramite.

Samples collected from the summit area include distinctive polymetallic, epithermal-style vein mineralization and pyritic stockwork material with locally intense clay-silica alteration. A zonal distribution of the different styles of mineralization is evident, from a central clay-silica-pyrite stockwork to polymetallic vein mineralization at the margin (Figure 2.9). Two main types of mineralized breccias were recovered: (i) large blocks of fractured basalt with pyrite lining the fractures, and (ii) clay-altered breccias with abundant matrix silica and sulfides, with fine-grained disseminated pyrite within the breccia fragments.

The central clay-silica zone contains semi-massive and stockwork-like pyrite, with sulfide contents locally reaching more than 20 wt.%. The outer zone of less altered breccias contains abundant disseminated pyrite, pyrite-lined fractures, pyrite veining. The matrix of the breccias consists of clay minerals, pyrite, and polymetallic sulfides including pale yellow sphalerite, disseminated galena, minor chalcopyrite, sulfosalts, and As-sulfide. Realgar, together with abundant amorphous silica, are present in a large number of the samples collected at the outer margin of the mineralized zone, occuring as fine fracture-fillings in the silicified breccias and lining vesicles in the basalt. Many of the mineralized blocks are coated with a green stain, thought to be iron or copper arsenates (e.g., scorodite).

The top of the deposit, in the clay-silica zone, is deeply altered. The most intensely altered breccias are broken down into a grey, sulfide-rich mud consisting largely of smectite (+chlorite) and containing up to 10 wt.% fine-grained pyrite. Loose breccia fragments occur as rounded cobbles in the clay-rich matrix and exhibit a distinctive blue-grey alteration colour. The basalt in the clay-silica zone is completely replaced by illite+smectite+chlorite, kaolinite, K-feldspar and silica. The original pyroxene phenocrysts in these rocks are pseudomorphed by white clay minerals, and most of the primary magnetite has been destroyed. The intensity of alteration is clearly indicated by the state of preservation of pyroxene phenocrysts and disseminated magnetite. Alunite was found in the only sample recovered in 1994, but was not identified in any of the new samples. Anglesite ($PbSO_4$) and cerussite ($PbCO_3$), found in the 1994, are likely supergene.

The intense clay-silica alteration grades outward into weakly altered basalt breccias that are veined by pyrite. Many of the basalt fragments exhibit zoned alteration adjacent to the pyrite veins and pyrite-line fractures. The weaker alteration is closely associated with fine-grained disseminated pyrite (on microfractures and lining vesicles).

The most striking feature of the mineralization is the high concentrations of Pb, Zn, As, Sb, and Ag, which resemble typical polymetallic vein mineralization in subaerial low-sulfidation epithermal systems. Shipboard analyses of the sulfide-rich material contained an average of 0.8 wt.% Zn, 0.3 wt.% Pb, 0.04 wt.% Cu, 3400 ppm As, 160 ppm Sb, 36 ppm Ag, and 9.3 wt.% S based on 25 samples and 10 gram assays (see chapter 7.3.1). The most intensely mineralized material contains

up to 5.5 wt.% Zn, 2.9 wt.% Pb, 1.8 wt.% Cu, 2.6 wt.% As, 1950 ppm Sb, 1020 ppm Ag, and 39.0 wt.% S.

The gold contents of a sulfide vein sampled in 1994 ranged from 1 to 43 ppm Au. Trace amounts of native gold were found in the sample, but its distribution was highly variable. Shipboard analyses during SO-133, indicate high concentrations of gold in four of the mineralized samples. Three separate samples from 41-GTVA, 15-GTVA, and 23-GTVA contained 0.5, 1.0, and 3.0 ppm Au respectively, and two analyses of a fourth sample (25-GTVA-6A) indicated gold contents of 11 and 44 ppm Au. The gold-rich sulfides from 25-GTVA-6 also contained between 420 and 1020 ppm Ag. The remaining samples contained <0.5 ppm Au and <50 ppm Ag. First shore based analyses have indicated up to 45 ppm Au with an average of 16 ppm for 26 mineralized samples.

During the cruise, a suite of 11 bulk samples of altered and mineralized basalt (0.5-1 kg each) was sent to the nearby Lihir gold mine for fire assay. These samples included both vein material and the surrounding wallrock and returned an average grade of 0.3 ppm Au, together with 0.16 wt.% Zn, 0.11 wt.% Pb, and 0.05 wt.% Cu based on 50 grams (Table 2.1). The lower grades than in the sulfide veins reflect the incorporation of the surrounding wallrock in the samples analysed.

The present mapping and sampling suggests that the entire upper part of the volcano may be mineralized at depth, however, the difficulty of sampling the broken flows prevents a proper assessment of the 3rd dimension. Drilling of the summit area is required to determine the extent and character of mineralization at depth. None of the other seamounts appear to be mineralized. Sediments recovered from Edison contain only minor amorphous Fe-sulfides, pyrite, and marcasite, and sediment from a cone NE of Conical contained nontronitic, Fe-bearing clays in veins which may have been related to low-temperature hydrothermal activity.

Table 2.1: Geochemical results for bulk samples (0.5–1 kg each) performed on Lihir Island using the fire assay facilities of Lihir Gold Limited (values in ppm).

sample	Au	Cu	Pb	Zn
14-GTVA	0.01	140	33	85
15-GTVA-2F	0.01	150	85	75
23-GTVA-2	0.53	135	4760	6450
23-GTVA-3	0.35	150	2710	4850
39-GTVA (<0.5mm)	0.52	240	420	460
39-GTVA (0.5-1mm)	0.34	165	380	460
40-GTVA (<0.5mm)	0.62	1240	920	1080
40-GTVA (1-5mm)	0.26	740	680	1320
41-GTVA (<0.5mm)	0.28	1120	700	1380
41-GTVA (1-5mm)	0.24	880	700	1380
53-GTVA (avg. bag1)	0.15	180	600	180

2.6 Conclusions

The polymetallic (Zn-Pb-As+Ag) vein mineralization and associated pyritic stockwork on Conical Seamount is among the first documented examples of submarine epithermal-style mineralization on the modern seafloor. The base metal-rich sulfide assemblage and the presence of both clay-silica and K-feldspar alteration most closely resembles that of low-sulfidation epithermal vein systems on land. The intense acid alteration and pyritic breccias are similar to the material currently being

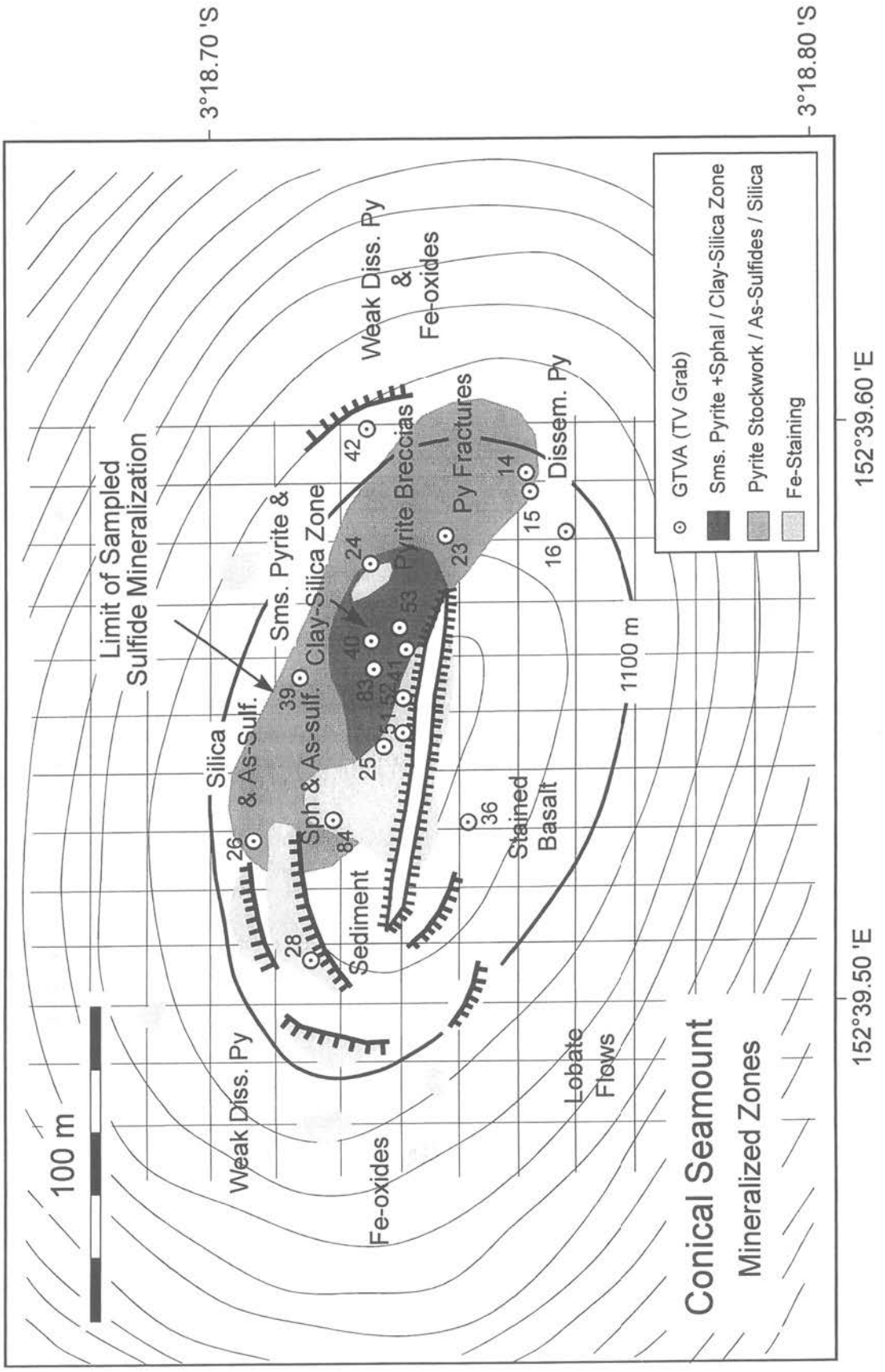

Figure 2.9: Simplified map of the summit of Conical Seamount showing sample locations and the distribution of mineralized zones.

mined at the nearby Ladolam gold deposit on Lihir, although the influence of seawater may account for the more abundant smectite (+chlorite) alteration. The distinctive polymetallic nature of the mineralization may also reflect enhanced base metal leaching more typical of submarine hot springs. However, massive sulfides were not observed, suggesting that relatively little of the hot spring fluid vented onto the seafloor. The absence of obvious seafloor mineralization may reflect boiling of the hydrothermal fluids and precipitation of metals at depth or mixing of the fluids with seawater and cooling prior to reaching the seafloor. The proximity of the Conical deposit to the presently active hot spring environment of the Luise Caldera suggests that both submarine and subaerial epithermal mineralization may be linked to the same district-scale magmatic events.

Detailed mapping of the active seismic zone south of Lihir has revealed a long history of submarine volcanism and a strong structural control on the location of the volcanoes. A post-subduction phase of extension in the old New Ireland forearc appears to be responsible for partial melting that has given rise to the highly alkaline lavas. These melts have risen along a conjugate set of major fault structures that penetrate through the entire forearc crust.

A combination of reactivated transform faults between the Manus-Kilinailau trench and New Ireland and extension within the thickened forearc crust provides an explanation for the recent volcanism and may account for the anomalous metallogenic history of the region. Further studies (e.g., sidescan sonar surveys) are required to fully document the interplay between extensional faults and the Tabar Fracture Zone. The major faults which have localized recent volcanic eruptions and hydrothermal activity may be reactivated transforms. These faults are still active and are presently leaking large amounts of methane. The combination of hydrothermal as well as cold seep gases venting along the faults has given rise to a diverse chemosynthetic biological community in the area.

Acknowledgements

Principal funding for the SO-133 cruise EDISON II was provided by the German Ministry for Research and Technology (BMBF FK 03G0133A) to Freiberg University of Mining and Technology. We thank Master Andresen and the officers and crew of the R/V SONNE for their expert assistence and cooperation during research activies around Lihir Island.

References

Exon, N.F., and Marlow, M.S., 1988. Geology and offshore resource potential of the New Ireland - Manus region - A synthesis. In: Marlow, M.S., Dadisman, S.V., and Exon, N.F. (eds) Geology and offshore resources of Pacific island arcs - New Ireland and Manus region, Papua New Guinea. Circum-Pacific Council for Energy and Mineral Resources Earth Science Series, Vol. 9, Houston, Texas, p.241-262.

Exon, N.F., Stewart, W.D., Sandy, M.J., and Tiffin, D.L. 1986. Geology and offshore petroleum prospects of the eastern New Ireland Basin, northeastern Papua New Giunea. BMR Journal of Australian Geol. Geophys. 10: p. 39-51.

Gulf Research and Development 1973. Regional marine geophysical reconnaissance of Papua New Guinea. Gulf Research and Development Company and Australian Gulf Oil Company, Sydney.

Hedenquist, J.W., and Lowenstern, J.B. 1994. The role of magmas in the formation of hydrothermal ore deposits. Nature, 370: p. 519-527.

Herzig, P.M. and Hannington, M.D. 1995. Hydrothermal activity, vent fauna, and submarine gold mineralization at alkaline fore-arc seamounts near Lihir Island, Papua New Guinea. Proceedings Pacific Rim Congress 1995, Australasian Institute of Mining and Metallurgy: p. 279-284.

Herzig, P.M., Hannington, M.D., McInnes, B., Stoffers, P., Villinger, H., Seifert, R., Binns, R., Liebe, T., and Scientific Party RV Sonne Cruise SO-94 1994. Submarine volcanism and hydrothermal venting studied in Papua New Guinea. EOS, Transactions American Geophysical Union, 75: p. 513-516.

Herzig, P.M., and Becker, K.-P. (eds) 1996. Tectonics, Petrology and Hydrothermal Processes in Areas of Alkaline Island-Arc Volcanoes in the Southwest Pacific: The Tabar-Lihir-Tanga-Feni Island Chain, Papua New Guinea. Final Report SO-94. 289 pp.

Johnson, R.W., Wallace, D.A., and Ellis, D.J. 1976. Feldspathoid-bearing potassic rocks and associated types from volcanic islands off the coast of New Ireland, Papua New Guinea: a preliminary account of geology and petrology. In Johnson, R.W. (ed) Volcanism in Australasia, Elsevier, Amsterdam: p. 297-316.

Licence, P.S., Terril, J.E., and Fergusson, L.J., 1987, Epithermal gold mineralization, Ambittle Island, Papua New Guinea: In, Proceedings Pacific Rim Conference '87: Australian Institute of Mining and Metallurgy, Melbourne: p.273-278.

Marlow, M.S., Exon, N., and Dadisman, S.V. 1991. Hydrocarbon potential and gold mineralization in the New Ireland Basin, Papua New Guinea. In: Watkins, J.S., Zhiqiang, F., and McMillen, K.J. (eds) Geology and Geophysics of Continental Margins. American Association of Petroleum Geologists Memoir No. 53, p.119-137.

McInnes, B.I.A. 1992. A glimpse of ephemeral subduction zone processes from Simberi Island, Papua New Guinea. Ph.D. thesis, University of Ottawa, Canada: 235 p.

McInnes, B.I.A., and Cameron, E.M., 1994. Carbonated, alkaline metasomatic melts from a sub-arc environment: Mantle wedge samples from the Tabar-Lihir-Tanga-Feni arc, Papua New Guinea, Earth Planet Sci. Letts., v.122, p.125-141.

Moyle, A.J., Doyle, B.J., Hoogvliet, H., and Ware, A.R. 1990. Ladolam gold deposit, Lihir Island. In Hughes, F.E. (ed) Geology of the Mineral Deposits of Australia and Papua New Guinea, Vol. 2: p. 1793-1805.

Port Moresby Geophysical Observatory, 1994. Earthquake map of the PNG region 1964-1994.

Stewart, W.D., and Sandy, M.J. 1988. Geology of New Ireland and Djaul Islands, Northeastern Papua New Guinea. In Marlow, M.S., Dadisman, S.V., and Exon, N.F. (eds) Geology and Off-shore Resources of Pacific Island Arcs - New Ireland and Manus region, Papua New Guinea. Circum-Pacific Council for Energy and Mineral Resources, Earth Science Series 9: p.13-30.

3 Bathymetry

BY SVEN PETERSEN

During Leg 133-2 the area south of Lihir Island has been intensly mapped using the HYDROSWEEP system (HYDROSWEEP DS, Krupp Atlas Electronic GmbH) installed on RV SONNE. The system uses 59 acoustic beams at a frequency of 15.5 kHz and an angle of 90 degrees, allowing a swath width that is twice the water depth.

A total of 18 HYDROSWEEP profiles with altogether 35.5 hours of ship time were performed in order to remap the area south of Lihir using differential GPS. Only small dislocations have been observed when the SO-133 HYDROSWEEP data was compared to the SO-94 dataset. Bathymetric maps on different scales have been produced on board using the Hydro Map System 300 (HMS 300). The main working area of cruise SO-133 south of Lihir island is shown on a bathymetric map (scale: 1:50,000) showing the major volcanic and structural features south of Lihir (Fig. 3.1). The datset has been further processed to produce a shaded relief map of this region (Fig. 3.2). The four main working areas (Conical Seamount, TUBAF Seamount, Edison Seamount , and Mussels Cliff) are shown on this map. Regional maps will be published by the Geological Survey of Canada as an Open File Report similar to the maps produced from SONNE cruise SO-94.

Two other maps show the area around Conical Seamount (Fig. 3.3) and Conical Seamount itself (Fig. 3.4). Ship tracks and the location of the stations are given in Figure 3.5, however, most stations are concentrated near the very top of the seamount (indicated by the white box). The location of TV-grab stations can be found in Figures 2.5 and 2.9 of Chapter 2. A detailed bathymetric map (contour interval 1 m) of the summit area of Conical Seamount is presented in Figure 3.6.

The ship tracks and the location of stations on TUBAF and Edison seamount are given in Figure 3.7.

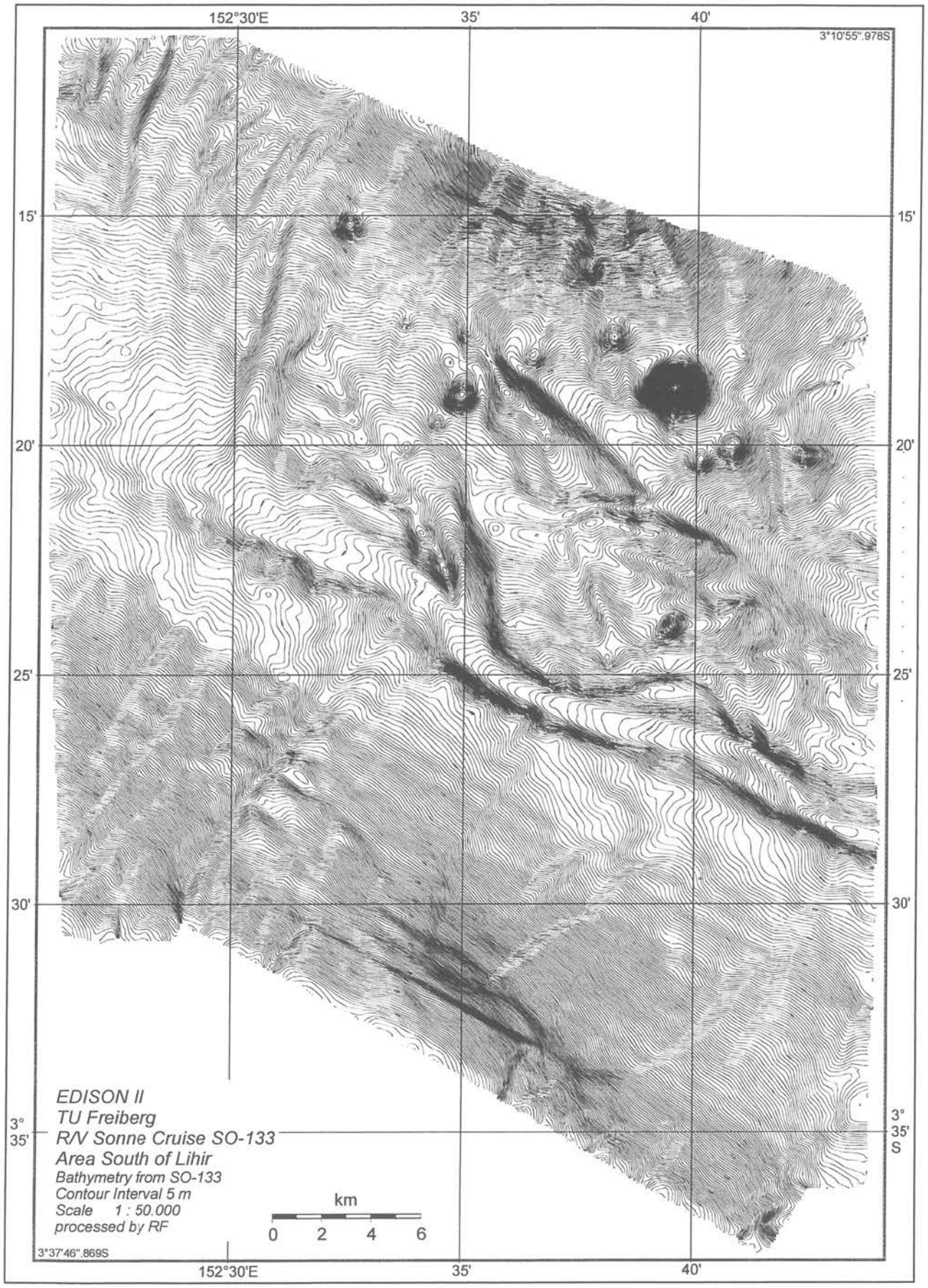

Figure 3.1: Bathymetric map of the area south of Lihir based on data of RV SONNE cruise SO-133.

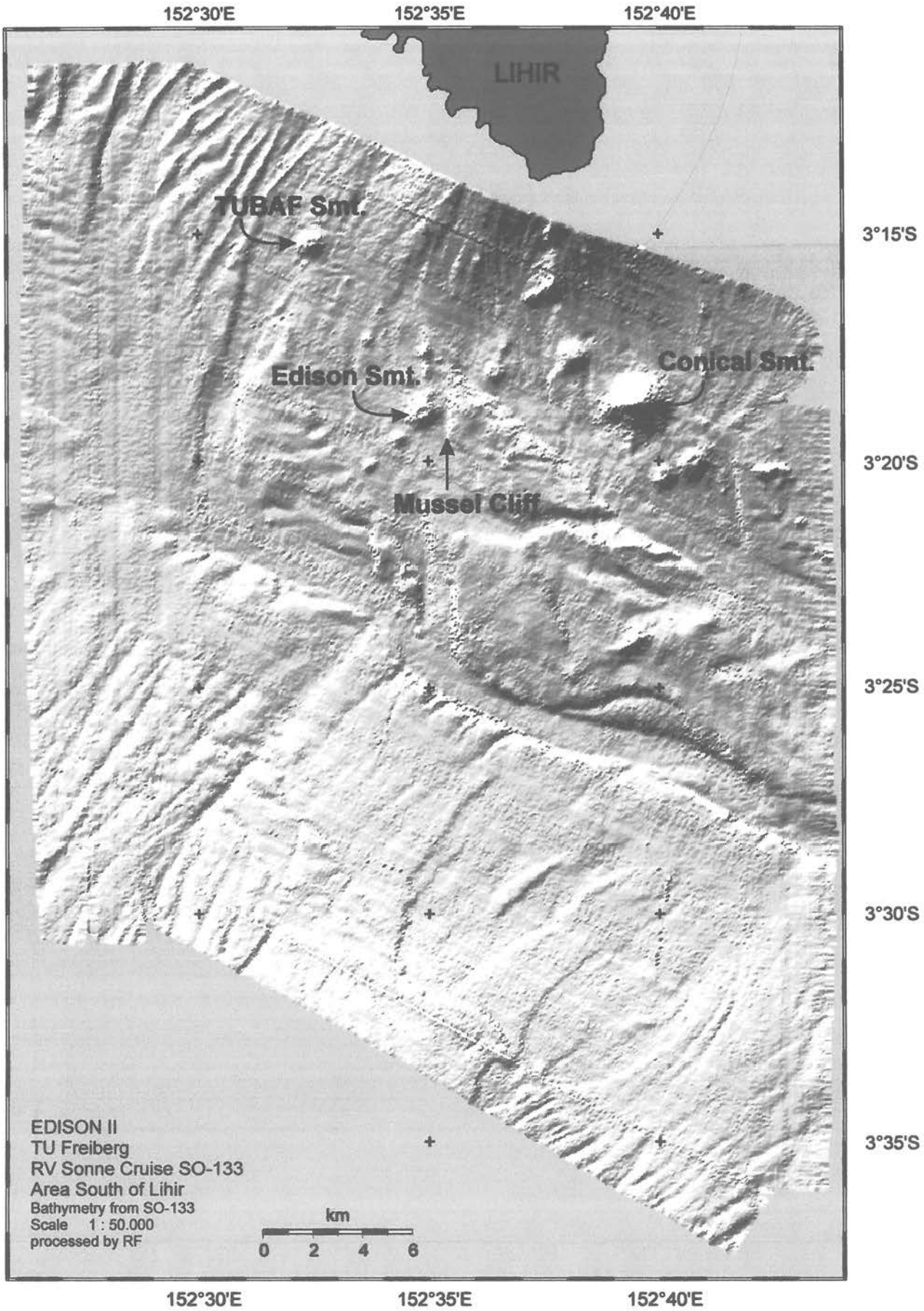

Figure 3.2: Shaded relief map of the area south of Lihir showing the location of major volcanic cones and the Mussels Cliff site.

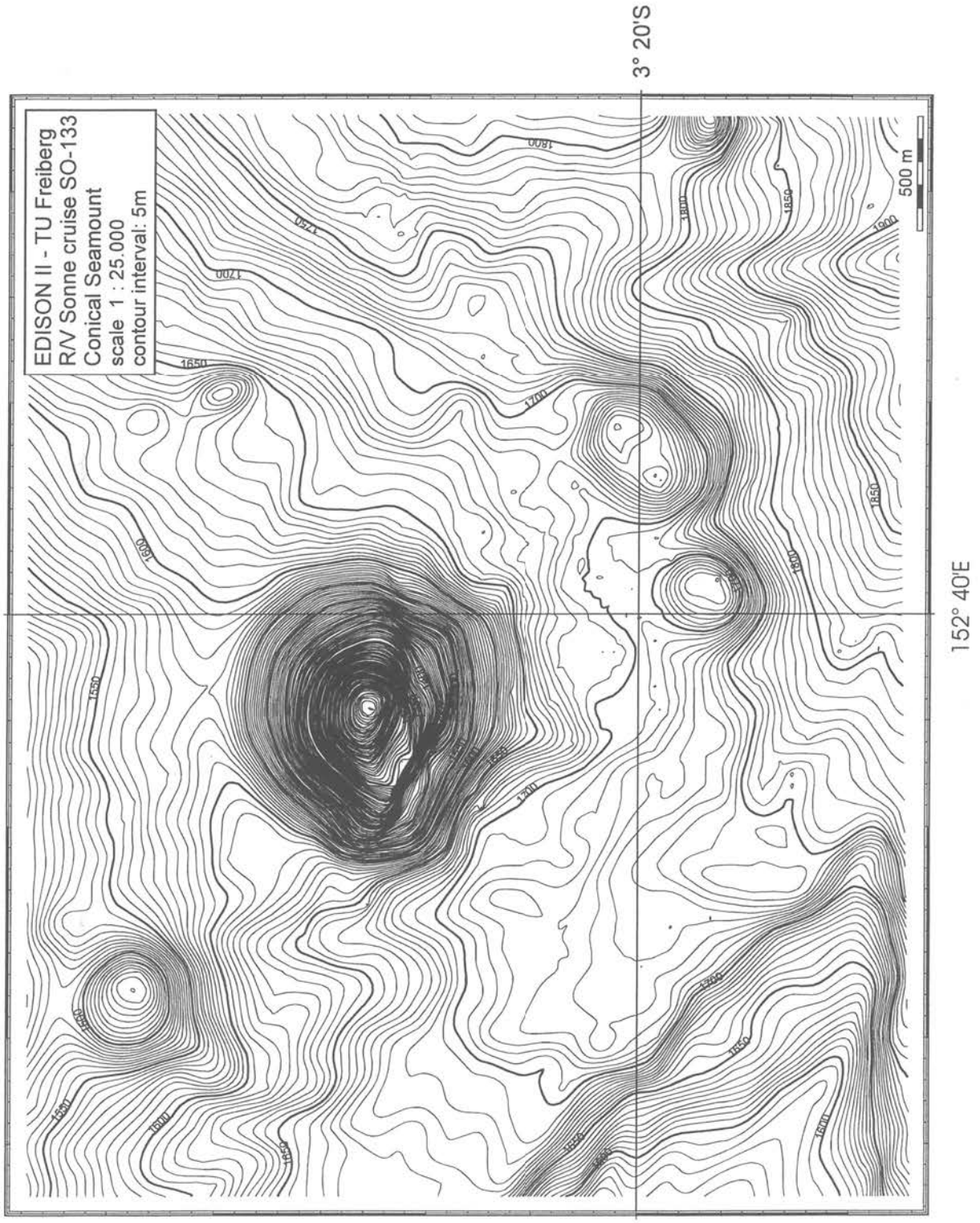

Figure 3.3: Detailed bathymetry of the area around Conical Seamount.

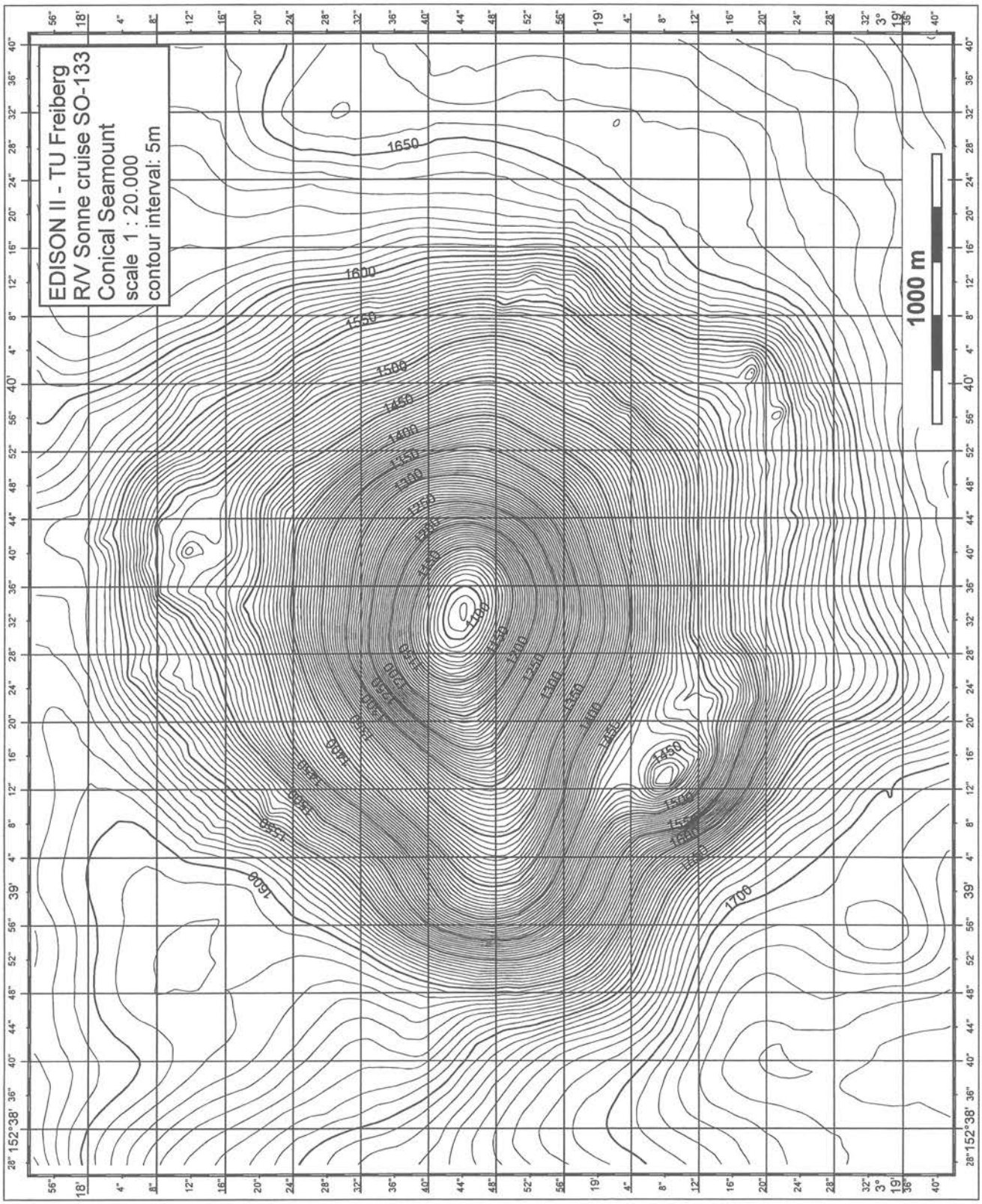

Figure 3.4: Detailed bathymetry of Conical Seamount.

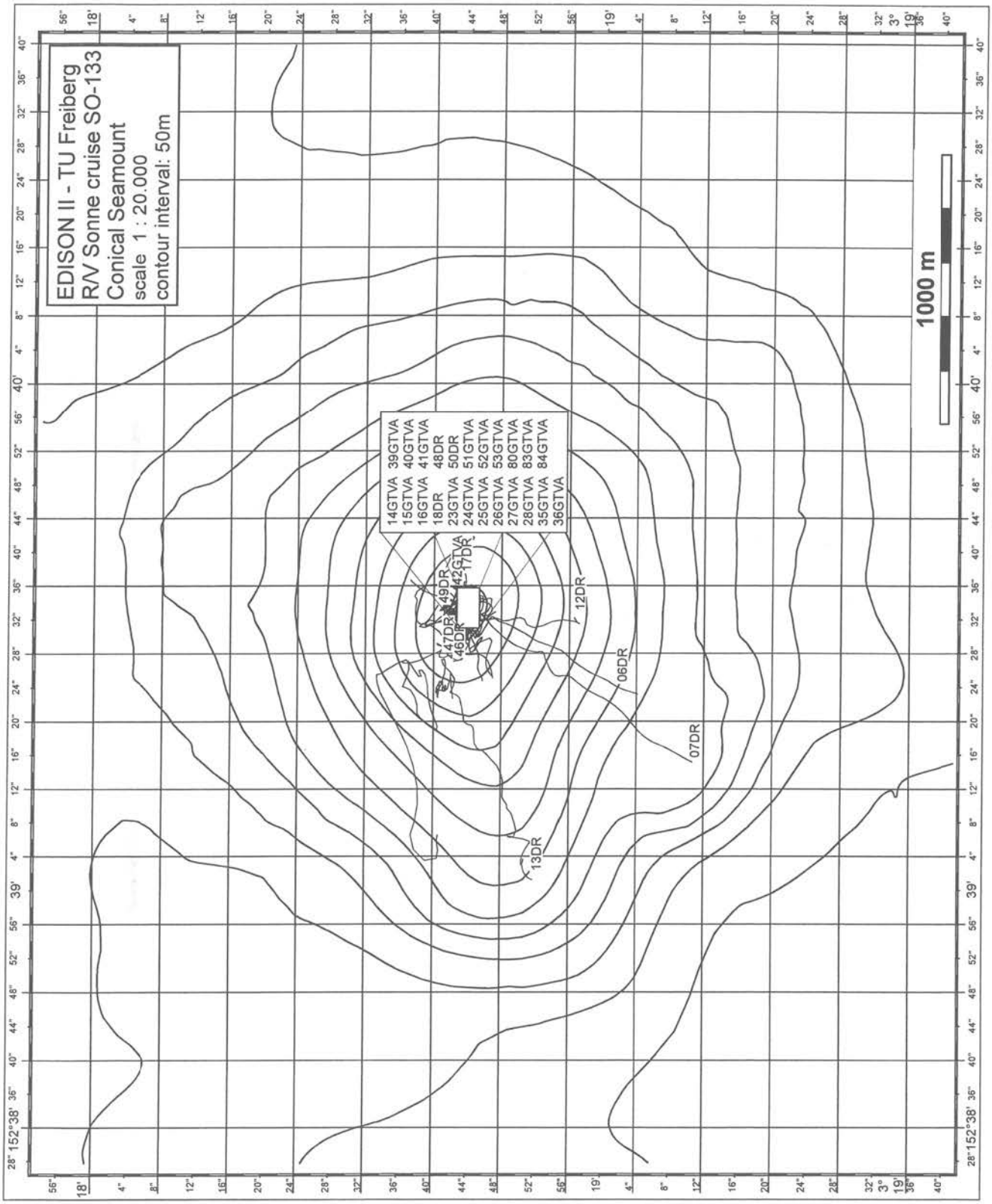

Figure 3.5: Detailed bathymetry of Conical Seamount showing the ship tracks and station locations.

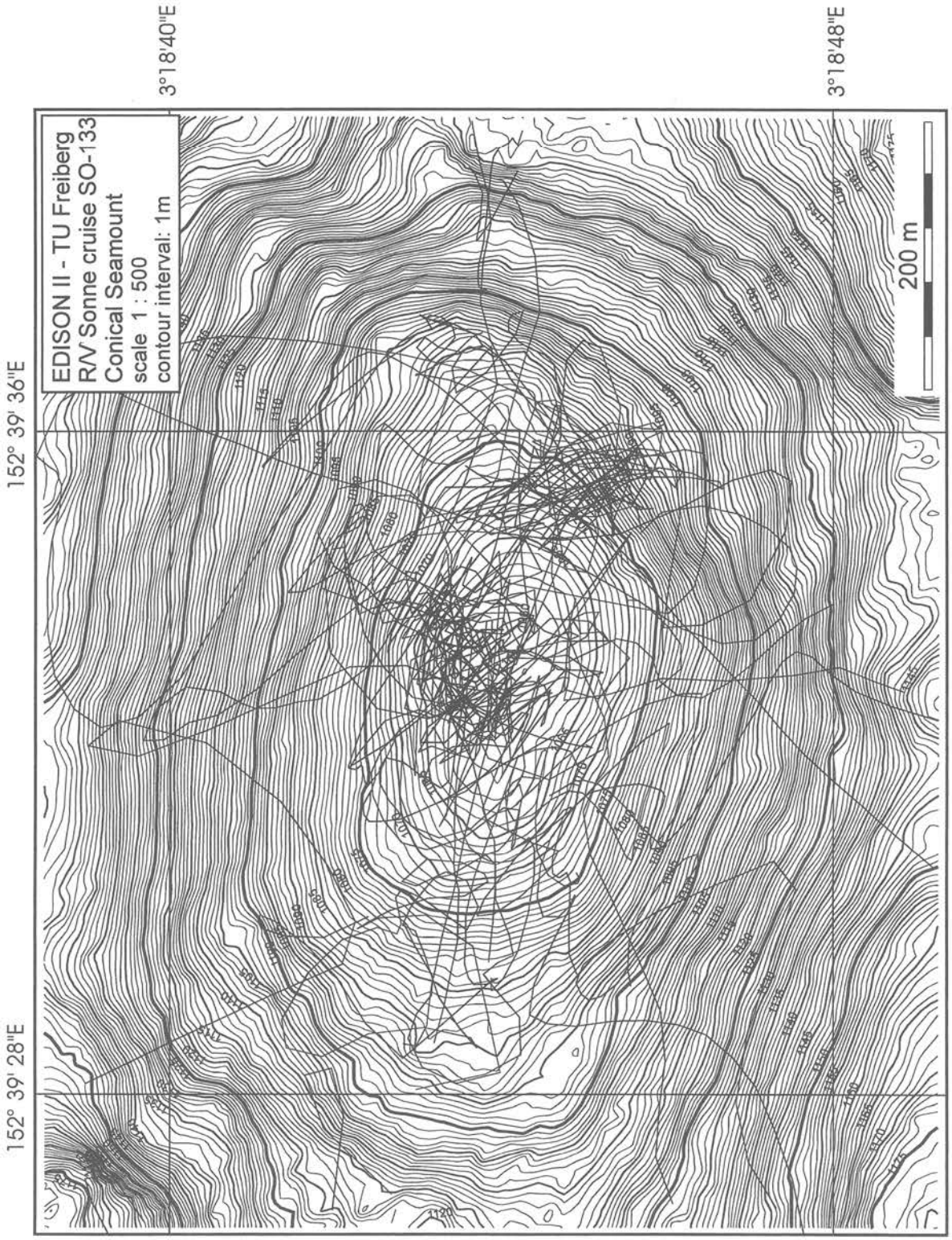

Figure 3.6: Detailed bathymetry of the summit plateau of Conical Seamount showing ship tracks. Sampling positions are given in Figures 2.5 and 2.9 of Chapter 2.

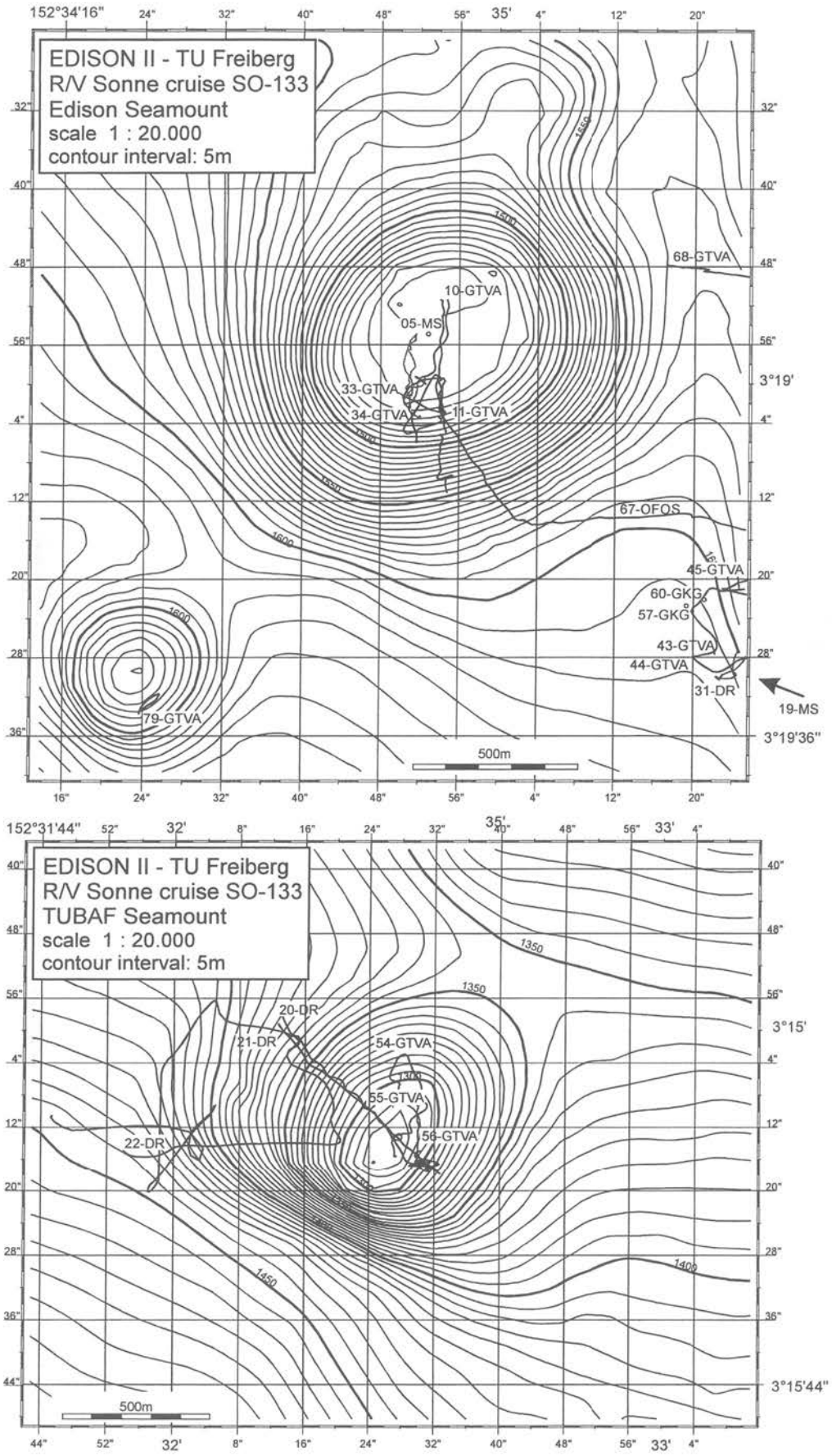

Figure 3.7: Detailed bathymetry of TUBAF Seamount and Edison Seamount showing ship tracks and sample locations.

4 Sample Descriptions of Dredge and TV-Grab Sampling Stations

BY JIM FRANKLIN, BRUCE GEMMELL, IAN JONASSON, MIKE PERFIT, LEANDER FRANZ, AND THOMAS SEIFERT

4.1 Introduction

During cruise SO-133, rock and sediment specimens that were recovered using the rock dredge (DR) or sampled with the TV-grab (GTVA) were categorized, described and distributed to interested parties (see below). The reports were done soon after the station was completed and were facilitated by cutting most of the samples into smaller slabs with a rock saw. Groups (1, 2, 3 etc.) were determined based on gross macroscopic features of all of the recovered samples and representative samples from each group (e.g. 1A, 1B) were described in greater detail. Individual descriptions were based on macroscopic features as well as those observed using a hand-lens. Mineral assemblages of individual samples are based solely on visual estimates and all sizes and percentages are approximate. Some samples (mostly of surface crusts or altered portions of rocks) were analyzed by X-ray diffraction techniques.

An attempt was made to distribute a portion of each sample to each interested scientific group [Freiberg (TUBAF), University of Florida (UF), University of Tasmania (CODES) and the University of Papua New Guinea (UPNG)]. In many instances, the largest sample or excess sample(s) was given to TUBAF. Some mineralized samples were also given to the Geological Survey of Canada (GSC).

4.2 Sample Descriptions

06-DR

21 July, 1998	SW flank of Conical Seamount; S of Lihir Island			
On bottom:	06:52	3°19.040' S	152°39.410' E	Depth: 1416m
Off bottom:	08:00	3°18.790' S	152°39.550' E	Depth: 1125m

Aim: Sample southeastern flank of Conical Seamount.

Operation: No bites during the first half of dredge but there were numerous small bites as the dredge was pulled up the steep SW flank of the seamount. The dredge was ended before the ship reached the top of the cone because it was felt that samples had been recovered from the flanks.

Recovery: No sample recovery

07-DR

21 July, 1998	SW flank of Conical Seamount			
On bottom:	09:37	3°19.170' S	152°39.280' E	Depth: 1591m
Off bottom:	12:35	3°18.700' S	152°39.610' E	Depth: 1107m

Aim: Sample southeastern flank of Conical Seamount. Repeat 06-DR.

Operation: Retry of sampling the SW flank, following the same track as 06-DR. Very few bites up-slope but larger ones recorded as the ship began to move north over the top of the edifice. Samples probably came from the upper flanks of S-SW portions of the seamount.

Recovery: ~ 200 kg of massive, vesicular, pyroxene-rich basalt (ankaramite). Surface textures are very irregular, with knobby or "globular" features that appear to be primary flow textures related to the extrusive process. Minor Mn-Fe coatings. Some sediment in surface depressions and vesicles. Only minor amounts of biologic material recovered.

Results: Porphyritic, vesicular basalt is the major lithology recovered at this dredge site. Vesicles (~10%) are small, rounded to elongate, irregular pipe vesicles (up to 2 cm diameter) that show some flattening parallel to flow direction (or from compaction?). Circumferential cooling fractures are common and many have rims that are glassy with abundant clinopyroxene crystals. Rocks contain clinopyroxene phenocrysts up to 1 cm long; many are euhedral and show compositional zoning. Some have open cavities that may have been inclusions. A second generation of clinopyroxene exists in the groundmass. Total clinopyroxene may exceed 30% by volume. Olivine is a rare (<1%) but common phase and exists as 0.25-0.5 cm phenocrysts. The matrix is fine-grained, dark and pyroxene-rich. Some irregularly shaped areas appear to have been replaced with secondary minerals.

Samples:

Group 1: Sediment on outside surface of basalt

Group 2: Pyroxene-phyric and ankaramitic basalt
- A. Small round lava
- B. Irregular shaped with more vesicles
- C. Small oblong lava with fewer vesicles
- D. Large lava (pieces cut) with some large vesicles
- E. Irregular, 3 kg lava, moderately vesicular
- F. Fine-grained, small lava fragment
- G. Lava with heterogeneous texture and prominent clinopyroxene euhedra
- H. Small crystalline piece
- J. Large vesicular lava with radial cracks, olivine xenocryst. (extra piece given to gas geochemists)

10-GTVA

22 July, 1998 Top of Edison Seamount in northern field of clam beds.

Sample Site: 12:04 3°18.855' S 152°34.913' E Depth: 1429-1479m (1440m)

Aim: Sample hydrothermal fauna in large clam field of Edison Seamount.

Operation: Rapidly found the northern-most clam beds that were documented in 1994. Grab was successful.

Recovery: 10 – 15 kg of basaltic pepperite with numerous small xenoliths; clam shells & barnacles

Results: Large amount of biological material including broken and whole clams (two varieties), shrimp, barnacles and limpets in a muddy matrix with numerous cobble to pebble sized rock fragments. Largest samples are 2-3 kg. Most are rounded to oblong with thick mud coatings on them. Larger samples have knobby or "globular" features similar to those in 07-DR. Some exhibit folded/contorted internal textures. Two samples have large sedimentary xenoliths that have prominent reaction rims.

Samples: Samples are basaltic pepperite with abundant sedimentary and volcanic xenoliths and rare small ultramafic xenoliths. Pyroxene and plagioclase phyric with rare biotite or olivine (+spinel) indicate that the predominant basalt type is trachybasalt (shoshonite). Most samples have abundant small vesicles throughout. Rocks are unusually magnetic and some have visible magnetite grains (some euhedral).

The samples are divided into eight groups:

Sample 1: 1 and 1A light colored mud

Sample 2: Dark colored mud

Sample 3: Mud

Sample 4: Basaltic lava with sedimentary xenoliths; subtypes include:
A. Complex sedimentary xenolith with prominent banding and layering. Angular fragment enclosed in lava.
B. Oblong, greenish-white, cross-bedded sedimentary xenoliths with thin 1-2 cm lava crusts.

Sample 5: Pepperite/vesicular basalt with dispersed small xenoliths.
A. Big piece
B. Medium size piece
C. Small cm-size piece.

Sample 6: Pepperite with moderate sized (<1 cm) xenoliths. Tend to be oblong with vesicles that are flattened and lineated.
A. Largest
B. Smaller

Sample 7: More rounded somewhat brecciated lava/pepperite with fewer xenoliths
A. Large
B. Smaller

Sample 8: Black ashy sediment washed out of grab. (for X - ray and to UF only)

11-GTVA

22 July, 1998 Edison Seamount, southern clam field, edge of crater wall on floor.
Sample Site: 14:42 3°19.049' S 152°34.887' E Depth: 1428-1522m (1445m)

Aim: To recover biota

Operation: Grab was successful in large clam field on the south side of the crater

Recovery: 900 kg of H_2S-rich mud and living as well as dead mussels, barnacles, and worms

Results: Basalt (probably shoshonitic) is the primary lithology recovered in this site. It is vesicular; with small xenoliths of various rock types - similar to 10-GTVA. Lava samples have a gnarly or knobby texture, look like they may have erupted into sediment in some cases.

Samples:
Sample 1: Sediment samples for XRD.

4 vials of ferrous sulfide(?) Impregnated sediment, 1/2 cm channelways abundant
A. Foraminiferal ooze, cut in three pieces: fragments of shale, shell, magnetite, and olivine?

Sample 2: Basalt
A. Basalt, contains abundant small xenoliths
B. Basalt with small phenocrysts of plagioclase and clinopyroxene; Knobby or gnarly surface textures; contains xenoliths of pyroxenite, olivine, and gabbro, Cr-diopside (?)
C. Basalt with plagioclase, plagioclase and olivine clots sedimentary xenoliths.
D. Basalt with pyroxene + magnetite xenolith (cumulate?).

12-DR

23 July, 1998	Conical Seamount, south slope			
On bottom:	18:01	3°18.955'S	152°39.552'E	Depth: 1391m
Off bottom:	19:33	3°18.691' S	152°39.129' E	Depth: 1308m

Aim: sample mineralized rocks close to the top of Conical Seamount.

Operation: Dredged up steep south side, probably deeper than 1300m on the south side.

Recovery: 60 kg of moderately Fe-oxide coated, vesicular, pyroxene-rich basalt.

Results: The basalt appears similar to the ankaramite recovered previously in 07-DR but have smaller and less abundant clinopyroxene and vesicles. Possible sub-trachytic texture is present. Surfaces are commonly irregular to gnarly or globular with cm sized voids and pipe vesicles. Microphenocrysts of clinopyroxene are prominent with minor plagioclase and rare olivine. Some textural alignment is obvious - flattening of vesicles towards the tops of samples. One basalt sample has vesicles coated with light grey amorphous silica (?). Some other ankaramitic basalt samples with large clinopyroxene phenocrysts and ovoid vesicles look very similar to those from previous dredge on Conical Seamount.

Samples: Samples were placed into three groups:
Sample 1: Fe-oxide crusts and coatings from lava surfaces
A. Black coating
B. Red-rusty coating

Sample 2: Ankaramitic Basalt
A. Lobate basalt with glassy rind (~2 cm), flattened vesicles. Contains 30-40% clinopyroxene phenocrysts in a dark, fine-grained matrix. Glassy rind has up to 60% phenocrysts of clinopyroxene.
B. As above, smaller piece

Sample 3: Basalt-Ankaramite
A-D. Different samples with variable amounts of glassy, clinopyroxene-rich rinds.

Highly vesicular (~10%), range in size from microscopic to 1 cm; small vesicles are rounded and larger are commonly elongate and flattened; matrices are brownish-green.

13-DR

23 July, 1998	SW side of Conical Seamount, probably 1200-1300m small bench over steep cliff.			
On bottom:	21:05	3°18.874'S	152°39.038'E	Depth: 1402m
Off bottom:	22:54	3°8.730'S	152°39.347'E	Depth: 1175 m

Aim: To sample for alteration, mineralization at the summit of Conical Seamount

Operation: Many bites, large sample obtained.

Results: The previous TV-grab showed the seamount to be fairly sediment-free, with lumpy lobate lava, and a few massive flows. About 300 kg of moderately altered and iron oxide and sulfide coated pyroxene-rich basalt. Pyroxene is unaltered in a greenish-grey matrix. Interiors of large samples are fairly fresh, very vesicular.

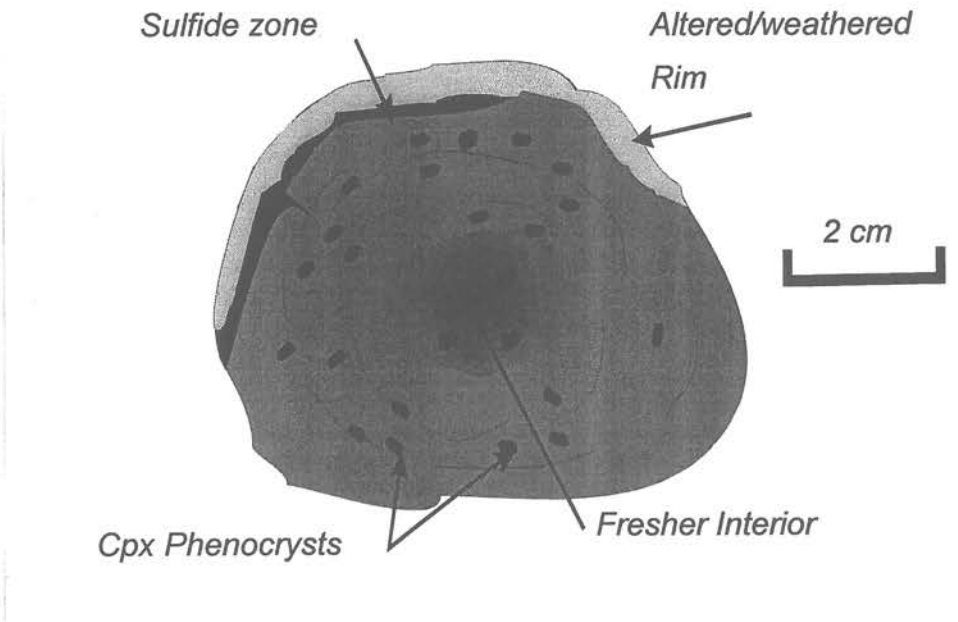

Figure 4.1: Cross section of zonally-altered ankaramite. Station 13-DR.

Plagioclase microphenocrysts are more common. Some samples have a 1-3 mm rind of black amorphous sulfide (H_2S released with 10%HCl). The rind sits on brownish-altered basalt. The rind is a 2-5 mm thick zone of brown oxide alteration on a tan-altered mesostasis. The tan zone is underlain by a grey-altered band, ~ 15-20 mm wide. Samples are cored by relatively unaltered dark grey basalt. Pyroxene phenocrysts appear unaltered, comprise ~50% of sample. The basalt contains some decorated vesicles with pyrite and fine pyrite in the altered matrix. These rocks are not magnetic.

Sample 2 has very well defined iron oxide crust.

Significance: The rounded lobate shape of the lava samples may be a primary eruptive feature, i.e. some form of submarine ejecta. The concentric cracks suggest that they had a lobate, tubular form. There is crude zoning from core to rim of vesicles, crystals, and alteration. The lack of sediment cover indicates that Conical Seamount has been volcanically active in the past few thousand years.

Samples:

Sample 1: Clays from rock surface for XRD

Sample 2: Fe-oxide crusts; variably dull brownish-red to glassy, thin black layers (lepidocrocite or limonite?).

Sample 3: Sample illustrates well zoned alteration with an outer rind (2-3 mm) of sulfide, underlain by an oxide layer (2-3 mm) then light-grey altered zone (2 cm wide), and dark-grey less altered core.
3A: To lab for Au analysis
3B: vial for XRF
3C: Sub-sample for alteration XRD
3D: Bulk sample

Sample 4: Relatively "fresh" pyroxene-porphyritic basalt; vesicular, some plagioclase microphenocrysts.
A: Sample to all institutions
B: Samples to UF and TUBAF
C: Very large sample with an oxide outer crust; distributed to all, plus big piece to TUBAF

Sample 5: Altered, sulfide-rich rind and bands, highly vesicular sample. Typically, parts of this sample have an outer bleached zone of clay-rich altered basalt. Phenocrysts are not visible in this zone. Below this, the next zone is a sulfide band in some samples mantled by an oxide zone. The sulfide band is semi-continuous around each piece locally becoming semi-massive over a width of 1-3 mm. The sulfide zone is underlain by a light-grey altered zone, which in turn surrounds a core of less altered dark grey basalt.
5A: sulfide on the outer surface; well – zoned alteration
5B: Less altered, no distinct sulfide zone
5C: Locally-thick sulfide accumulation on the outer edge; remainder of sample is highly oxidized
5D: Diffuse sulfide band below thin outer zone of white, clay-rich altered basalt
5E: Distinct outer zone of white-altered (clay) material, with 1-2 mm sulfide band in the sample.
5F: Locally distinctly banded sulfide zone; well-developed outer white alteration zone

Sample 6: Well-zoned pyroxene basalt with a prominent zone of sulfide alteration about 1-2 cm towards the centre; five zones of alteration. Very weathered exterior. The sample zonation is:
Outer Thin outer oxide zone -- Dark lava -- Thin dark sulfide-rich zone;
Centre Grey interior lava

Sample 7: Thick oxide zone (3 cm), distinctly banded with probable remnant sulfide. Four black oxide bands in oxide zone, each 1 to 2 mm thick. Oxide sits on highly altered phenocryst-rich basalt.

Sample 8: All samples have a distinct white-altered outer layer, 1-4 mm thick. The white layer is locally rust-stained, and in some samples is underlain by distinctive sulfide zone, then altered basalt (light grey).

A: no sulfide zone, distinct white zone
B: Thick white zone on one surface (2-5 mm), underlain by distinct sulfide band (1-3 mm), and then by poorly zoned altered basalt.
C: This white altered outer zone, no sulfide layer
D: similar to 8C: very vesicular, no sulfide zone.
Bag of extra sulfide material sent to GSC
Bag of extra oxide sent to GSC.

Sample 9: Banded oxide sample. Massive to banded Fe-oxide with multiple bands of amorphous iron oxide or lepidocrocite form crude layers, resembling iron formation.
subsample to lab for Au analysis

14-GTVA

23 July, 1998 Conical Seamount:
Sample Site: 02:54 3°18.752'S 152°39.591'E Depth: 1107 m

Aim: To sample hydrothermal, sulfide enriched zone

Operation: Grabbed from small area on the top of the seamount. Area was sampled because of prominent white staining seen in video. Excellent recovery of 300 kg sample

Results: Highly altered and mineralized lava mixed with viscous grey, green and brown mud was recovered. The lava samples have variable amounts of veining with amorphous silica and sulfides in the veins. Many of the mineralized rocks are light grey-blue and quite soft, with only a few preserved clinopyroxene phenocrysts. Some samples are stained to red, orange and green, and coated with iron oxides. Sizes of samples vary from 20 kg boulders to the more common irregular, oblong to round cobbles. Shapes and forms are similar to those observed in fresh lava, and many individual samples are probably individual spatter bombs. Vesicles are filled with crystalline silica. There is a variety of basaltic breccia, cemented by silica and rock fragments. Breccia zones mantle some larger pieces of basalt. Some of the samples are brecciated, with matrix formed of basalt pieces, pulverized rock and hydrothermal precipitate. Some may also be autobreccia, although this requires further petrographic examination.

The mud is grey-black, sulfide-rich, and greenish-grey to tan, nanofossil-bearing ooze.

Significance: Possibly at the margin of an extensively mineralized system

Samples: Seven sample groups were established:
Sample 1: Clay samples for XRD; dark grey and green clay taken for XRD.

Sample 2: Highly altered and mineralized pyroxene basalt; mineralization and alteration are quite variable in extent, with some containing remnant or little altered clinopyroxene, others with highly replaced clinopyroxene Silica seems to be the principal replacement phase. Pyrite lines vesicles and forms veins.
A: Crowded porphyritic basalt, groundmass altered to hard, dark brown, siliceous (?) mesostasis. Minor sulfide, rim of sample slightly bleached. This is a "least altered" sample.
B: Similar to 2A, but with 1-2% pyrite in vesicles and as coatings of small, euhedral

grains on vesicles and fracture surfaces.
C: More altered, with a calcified coral attached; about 1% pyrite throughout the matrix of the basalt, as well as in veins and vesicles; groundmass is buff to tan, hard and silicified.
D: Very black, highly altered porphyritic basalt; only minor pyrite visible in the vesicles, none in the groundmass.
E: Grey, less-altered basalt; strongly magnetic, no pyrite
F: Probably the most pyritic sample; about 5% pyrite, coarsely crystalline pyrite grains in both the matrix and vesicles. Some possible bornite (peacock stain) in composite sulfide grains.
G: Very abundant pyrite - bearing altered basalt; pyrite is in fractures and disseminated throughout, and also is in vesicles. The groundmass is altered (silicified) and even-textured. The crowded porphyry texture is well preserved (clinopyroxene crystals).
H: Moderately pyritic, highly altered basalt. This is a very hard sample, and is probably silicified. It contains locally very large (1-2 mm) fine-grained pyrite blebs and pyrite fills vesicles.
I: Massive pyrite rind on basaltic "bomb". The rind coats the outer surface on about 1/3 of the sample. Pyrite also forms about 1% of the groundmass of the rock as disseminations and vesicle fillings. Alteration is complete and homogeneous, with pyroxene replacement, silicification (?) and possible smectite. The sample is moderately magnetic.
J: (2 pieces only): Very pyritic (~5%), highly altered sample. Some phenocrysts are altered as well as the groundmass. Some coating of fine-grained to amorphous black mud (possible fine-grained pyrite) with local oxide development.

Sample 3: Zonally altered samples; includes a large sample taken by TUBAF for display purposes. Each sample has a partially preserved rim of oxidized altered basalt, about 1-3 mm thick. Each is concentrically altered, with the most intense alteration (light-colored) on the outside rim. The samples are progressively less altered inwards in a series of semi-discrete rings or zones. Disseminated and vein pyrite occurs throughout, plus vesicle-filling pyrite. This sample contains up to 10% pyrite, and is probably the most pyrite rich of this station.

Sample 4: Breccia Samples. Highly brecciated samples; fragments consist of subangular to sub-rounded basalt fragments, each zonally altered and pyritic. Fragments are 1-5 cm in diameter. The matrix is fine to medium-grained basaltic detritus, with some (minor) nanofossil ooze incorporated (?) into the breccia. Silica (amorphous) comprises about 10% of the matrix. Only breccia samples contain abundant silica.
A: Fragment – dominated breccia; 1% pyrite.
B: Large fragments, small amount of matrix.
C: Matrix-rich breccia, considerable pyrite in the matrix.
D: Very large fragments, about 20% matrix as well defined channels. These are larger samples, and illustrate the nature of the breccia. Silica and nanofossil ooze partially fill the matrix voids, which also contains about 1% pyrite. The fragments have pyrite in the vesicles and matrix fractures. The basalt is highly altered; each fragment displays the zonal alteration described above, with a lighter rim and pyrite zones.
E: Two samples of breccia: large fragments; small amount of matrix surrounding fragments. Up to 10% pyrite in fractures, 1% overall.
F: Large fragments, only minor amount of breccia.

Sample 5: Nodular basalt. One nodule is intensely altered basalt, with up to 5% pyrite. Surrounding matrix may be finely comminuted breccia material, containing several percent silica, possible broken foraminifers.

Sample 6: Altered phenocryst basalt. Replaced pyroxene phenocrysts, groundmass is hard, dark grey to black. Pyrite occurs in veins, vesicles and along some of the altered phenocrysts. One surface is iron oxide stained.

Sample 7: Taken for whole-rock analysis (shipboard). Consists of a large breccia fragment with about 10% matrix. This sample is very pyritic, including a pyrite rim on one surface. Matrix is very silica – rich.

15-GTVA

23 July, 1998 Conical Seamount
Sample Site: 06:26 3°18.750'S 152°39.568'E Depth: 1064m

Aim: To sample hydrothermal material.

Operation: Almost two hours were spent mapping the bottom and attempting to sample. After several attempts, about 10 kg were recovered.

Results: Two generalized sample types were recovered from this site. Most consist of breccia, similar to those collected in 14GTVA. A few samples are massive, altered lava.

Significance: May define the southern margin of the mineralized zone.

Samples:

Sample 1: Highly vesicular basalt with elongate pipe vesicles. Some vesicles are filled with green, smectite-like mineral(s). There is minor pyrite in the vesicles; some are filled with silica. Samples are distinctly zoned, with a light (bleached) pyrite-altered rim and darker, less altered interiors. Each fragment appears to be a primary volcanic bomb.
A: Well-zoned large bomb or spatter fragment; 4 pieces
B: Minor breccia on the surface: 2 pieces
C: Minor breccia on outer surfaces: 2 pieces
D: Elongate, bomb-shaped, flat vesicles, with minor pyrite; 3 pieces

Sample 2: Breccia
A: The brecciated portion of this sample comprises 50%. The matrix contains a trace of pyrite, and about 5% amorphous silica infill. The matrix is moderately comminuted; fragments are 1-2 cm, angular to subrounded. Most fragments are coated by silica, some with a thin veneer of pyrite.
B: Variably sized fragments make up 60-80% of the sample; trace sulfide, 1% silica in the matrix. Breccia fragments display zoned alteration.
C: Breccia with very well zoned fragments; these are highly vesicular, with vesicle filling of cryptocrystalline quartz and smectite. The matrix is highly comminuted rock fragments with silica coating on the larger fragments. Silica also coats a few pyrite grains, indicating late silica deposition.

D: Very similar to sample C, but with larger fragments, more silica in the matrix. Vesicle sizes are similar to samples A and B. The matrix contains about 1% pyrite.

16-GTVA

23 July, 1998	Top of Conical Seamount			
Sample Site:	10:09	3°18.785'S	152°39.549'E	Depth: 1118m

Aim: To sample hydrothermal material.

Operation: Grab tipped over and caught the cable.

Results: Two small rock chips recovered.

Significance: Still in mineralized zone.

Samples: These were so small as to not warrant general distribution.
Sample 1: Rusty coating on vesicular lava; sample 3x3x1 cm, not cut (in TUBAF collection).
Sample 2: Larger piece (5x4x4 cm) of same material, also in TUBAF collection

17-DR

23/24 July, 1998	Top of Conical Seamount			
On bottom:	12:36	3°18.730'S	152°39.629'E	Depth: 1128m
Off bottom:	13:01	3°18.746'S	152°39.707'E	Depth: 1216m

Aim: To sample hydrothermal material at the top of Conical Seamount, for definition of size of gold –bearing occurrence.

Operation: Dredge traversed the eastern margin of the mineralized zone. It contained representatives of both mineralized and unmineralized basalt.

Results: 15-20 kg of altered and mineralized basalt was recovered. A few large samples of basalt have oxidized and weathered outer surfaces, but are not intensely altered in their central portions. The remainder of the dredged samples consists of strongly altered, heavily veined and mineralized basalt. Some portions of these samples are clay-rich. Only on sawing the samples was the extent of the alteration and mineralization evident.

Significance: This dredge station defined the eastern margin of the mineralized zone.

Samples: The samples are divided into four groups:
Group 1: Relatively "fresh" basalt; 40% pyroxene phenocrysts in a light grey, highly altered groundmass. These samples have evenly distributed vesicularity. Fracture surfaces are coated or veined by alteration, consisting of silica and grey clay (kaolin?). The outer surfaces are rubbly-textured flow tops, coated by about 1 cm of oxide. The largest samples have pipe vesicles. There is minor sulfide in the vesicles and in fractures.

Group 2: Two large and 5 smaller samples of moderately to strongly altered basalt. Vesicles are still evident in these samples, but both the phenocrysts and groundmass are strongly altered to grey-black, clay and sulfide-rich material. Some native sulfur coats fractures. The outer surfaces of these

samples have a thick oxide coating. These inner portions of these samples are banded, formed of alternating layers of clay-rich and sulfide-rich alteration. H_2S was released on application of 10% HCl, indicating the presence of abundant sulfide, including some sphalerite.

Group 3: This group consists of 9 small and 2 larger (10x8x8 cm) samples of heavily silica-veined (amorphous) clay-altered basalt. Most samples have about 1 cm of oxide coating. Cut surfaces indicate well-developed brecciation, with phenocrysts and groundmass completely altered. Disseminated pyrite rims vesicles and coats some samples. Pyrite is also disseminated in the matrix and in veins.

Group 4: Clay-rich altered basalt samples. These consist of five small samples (1 kg each) of tan to grey, massive clay with some oxide coatings. A small selvedge of basalt is preserved in one sample; otherwise the samples are completely altered to clay, with some sulfide.

Sample 1: representing Group 1, above
A: Highly vesicular, slightly altered basalt.
B: Altered vesicular basalt.
C: Large sample with quartz-filled vesicles.

Sample 2: representing Group 2, above
A: Fractured highly altered basalt; alteration and veining very evident.
B: Vesicular altered basalt.

Sample 3: representing Group 3, above
A: Intensely altered, locally brecciated, quartz-rich altered basalt. Some native sulfur on fracture surfaces.
B: Highly brecciated, altered silica-veined, sulfide-rich basalt. Sample consists of many small pieces, some very fine-grained grey mineral (sphalerite, sulfosalt?), together with disseminated pyrite, and intense silica veining.

Sample 4: clay samples
A: For whole rock and gold analysis (ASV).
B: For clay mineral analysis.

18-DR

24 July, 1998	Top of Conical Seamount			
On bottom:	14:06	3°18.774'S	152°39.432'E	Depth: 1161m
Off bottom:	14:45	3°18.695'S	152°39.641'E	Depth: 1153m

Aim: To dredge the top of Conical Seamount, and sample hydrothermal material

Operation: Poor recovery.

Results: Obtained only 2 kg of plates and crusts of Fe-oxide-rich material, consisting of 8-10 pieces, each 4x10x10 cm. Also obtained one Fe-oxide-rich crust on sediment, and one sample of pyroxene-basalt

Significance: Possible alteration peripheral to mineralized zone

Samples: Two types of samples were recovered:
Group 1: Fe-oxide crusts; some have formed over a sediment substrate, others over volcanic rock. These are very similar texturally to those observed at TAG, and to the Cyprus ochres.

Group 2: Basalt; moderately fresh, vesicular pyroxene basalt. Phenocrysts are most abundant in the outer rimes of spatter bombs. Large vesicles are flattened, small are round.

Sample 1: A: Distinctly banded iron oxide sediment or crust, 3 to 6 cm thick, alternating tan, red and black layers of oxide. The black bands are 1 mm thick, red are 2-3 cm thick and tan are 2-5 cm thick. The darkest layers are slightly more crystalline.
B: Distinctly banded iron oxides with thick tan beds. The bands contain some quartz, pyroxene and minor magnetite on a substrate of hydrothermal weathered basalt. The basalt is completely altered. Banding is convolute, and appears to be diagenetic or low-temperature hydrothermal in origin.

20-DR

24 July, 1998	TUBAF Seamount			
On bottom:	18:49	3°14.971' S	152°32.221' E	Depth: 1403m
Off bottom:	19:43	3°15.303' S	152°32.543' E	Depth: 1307m

Aim: Sample xenoliths from the side of TUBAF Seamount

Operation: Dredged along a line from NW to SE, samples from near top to seamount.

Results: Two small pieces of very dark colored, fine-grained lava had with only a thin coating of sediment in places. The lava is fine-grained, pyroxene trachybasalt with abundant xenoliths (~10%) of sizes that range from microscopic to ~ 1 cm diameter. Lava appears very fresh with no obvious alteration. Surface textures are ropy to irregular-gnarly.

Samples:
Sample 1: Trachybasalt
A. This is a small oblong piece with a few % phenocrysts of clinopyroxene (< 0.2 cm) and elongate phlogopite. Vesicular with flattening in horizontal direction, greatly variable sizes. Contains xenoliths of dunite (olivine>opx>spinel), microgabbro (similar to 21DR), sedimentary rocks, other fine-grained basalt, and olivine xenocrysts. [2 pieces to TUBAF, 1 to UF]
B. Similar to A, but smaller piece (~100 g), contains xenoliths plus plagioclase clot, dunite that varies in degree of alteration [3 pieces to UF, 1 to TUBAF].

21-DR

24 July, 1998	TUBAF Seamount.			
On bottom:	21:12	3°14.988' S	152°32.214' E	Depth: 1404m
Off bottom:	22:46	3°15.298' S	152°32.546' E	Depth: 1306m

Aim: Sample xenoliths from the side of TUBAF Seamount

Operation: Dredge was taken from NW to SE

Recovery: 2 small pieces of xenolith-bearing basalt. Each sample 50-100 g.

Results: Vesicular trachybasalt, fine-grained, relatively fresh with more Fe-Mn coating than 20-DR but less sediment. Samples contain one large xenolith in each.

Samples:

Sample 1: Trachybasalt

A. Fine-grained, vesicular trachybasalt, vesicular with clinopyroxene (<5%) and phlogopite (<2%) phenocrysts. Similar to 20-DR but less vesicular. Contains large ~5 cm dunite xenolith that has minor amounts of pyroxene and spinel. Has a very granular texture, somewhat friable. Also contains some smaller microgabbro xenoliths. Sharp contacts with xenoliths, no reaction rims seen. (only to TUBAF and UF).

B. Same as A, but with large microgabbro xenolith (~4 x 7 cm). Gabbro is medium-grained, holocrystalline with subhedral plagioclase and pyroxene and minor opaque minerals (magnetite?). Lesser red-brown mineral that could be altered olivine or oxide. (only to TUBAF and UF)

23-GTVA

24 July, 1998: Top of Conical Seamount

Sample Site 05:03 3 18.739'S 152 39.581'E Depth: 1049m

Aim: To sample hydrothermal material, top of Conical Seamount

Operation: Successful grab of about 30 kg of altered basalt, consisting of six large pieces (2-5 kg each) and 20 smaller pieces. Some well-lithified pieces of grey mud, containing pyrite, were recovered. Non-lithified grey mud was also recovered.

Results: All samples are composed of highly altered clasts in a finer, more highly comminuted dark grey to black matrix. The breccia samples are variably altered. Some are entirely or zonally silicified (possible K-feldspar?), with an outer light colored rim of pyritized, silicified basalt, where pyroxene phenocrysts are entirely destroyed/replaced by smectite (?). Other samples are less altered, with only partially replaced or altered phenocrysts

Significance: This grab is from the centre of the mineralized zone, and displays strong alteration and pyritization.

Samples:

Sample 1: Grey mud, containing disseminated pyrite, silica subrounded white to grey nodules or granules, each about 0.5 mm in diameter.

This sample was sub-sampled for ASV, XRD and XRF analyses.

Sample 2: Large (8-10 kg) sample, plus many small samples of black, semi-lithified, highly altered basalt, with an outer strongly oxidized coating.

A: Large sample contains pink vein, 1 cm wide at one end. This vein may contain K-feldspar. The remainder of the sample is an intensely silicified breccia with finely disseminated pyrite throughout. Phenocrysts are totally replaced by silica and/or smectite (white to grey aphanitic grains). The matrix contains 10% pyrite is a dark grey, silicified matrix. Some fragments are surrounded by pink to tan veinlets, also possibly

K-feldspar (or quartz). One sample sent for XRD and ASV.
B: More massive basalt fragment, cut by hydrofracture vein. The phenocrysts are white, completely altered from pyroxene. The groundmass contains 5-10% pyrite in a black, very fine-grained matrix.
C: Zonally altered samples, consisting of a core of less altered basalt, which retains vesicularity, and contains "unaltered" (chloritized?) phenocrysts. The outside edge of these samples are intensely altered, silicified with white-altered pyroxene phenocrysts, some hydrofracturing, reticulate veining in the groundmass, and considerable (~10%) disseminated pyrite. The outer surface is composed of up to 2 cm of oxidized, weathered material.

Sample 3: Excellent development of breccia.
This sample consists of fragments up to 4 cm in diameter that are zonally altered, with white, highly silicified rims (smectite/clay?) and black, pyritized cores. These samples contain some pink to tan areas that may contain K-feldspar.

Sample 4: Very coarse breccia.
Fragments are totally altered, 5 cm in diameter, and subrounded, with phenocrysts completely dissolved, leaving skeletal outlines of pyroxene. The fragments contain about 10% pyrite. The matrix occupies only about 10% of the sample, and is black, very fine grained, highly comminuted basalt with disseminated sulfide.

Sample 5: An exceptional sample of zonally altered breccia. The fragments are defined by a white silicified margin, with their centres composed of dark grey to black pyritized basalt. All phenocrysts are replaced (silicified?). Sampled for XRF and ASV.

Sample 6: Altered basalt.
This sample has a green outer surface and black interior, with white, complexly replaced phenocrysts. Anastomosing veins of amorphous silica (or possibly K-feldspar) cut this small sample. Subsampled for XRF.

Sample 7: Very large sample, with breccia at one end, massive basalt at the other. The brecciated portion has angular to subrounded fragments, defined by silica coatings. The fragments are less altered than in previous samples, with the largest retaining "unaltered" (chloritized) phenocrysts. There is some pyrite throughout the fragments, and lining some vesicles. Most of the pyrite is disseminated. One or two grains of possible bornite, chalcopyrite or sphalerite (peacock tarnish). The matrix is silicified, pyritic and highly comminuted basalt. The end of this sample that is massive basalt is zonally altered, retains its vesicles, and has a white outer rim with disseminated pyrite, which decreases in amount inwards.

The remaining samples from this site are placed in bags and bubble-wrapped for further work.

24-GTVA

24 July, 1998 Top of Conical Seamount
Sample Site: 06:08 3°18.725'S 152°39.576'E Depth: 1099m

Aim: To sample hydrothermal material.

Operation: Successful TV-grab, with 8 large sample and numerous small pieces recovered.

Results: Each of the eight large pieces weighed 3 to 6 kg. All have highly oxidized rusty surfaces. These samples are more massive, and apparently less altered than samples from 23-GTVA. The samples contain minor fine-grained disseminated pyrite. These samples are zonally altered, with pyroxene phenocrysts silicified (or clay-replaced) at the margins, preserved (chloritized) in the cores. The smaller samples were bagged as a single set of samples.

Significance: Weakly sulfidic and altered zone, at the periphery of the epithermal system.

Samples:

Sample 1: Highly vesicular (10%) basalt; phenocrysts are chloritized to fresh, with only local silicification/replacement. The matrix is dark tan to dark grey, about 10% pyrite, silicified and much less altered than previous samples (e.g. 23-GTVA). The samples contain a few veins of amorphous silica, and pyrite occurs as vesicle linings, as well as disseminated grains in trace amounts in the matrix.
A: Weakly developed zonal alteration, white to tan at the outer edge, darker in the centre.
B: " Glassy" top which contains crowded (>60%) phenocrysts. Vesicles contain disseminated pyrite in the grey part of the sample.
C: Moderately fresh basalt, with fresh pyroxene phenocrysts. The outer surface is altered, and is mantled by comminuted, partially degraded basalt, with variably oxidized pyrite.
D: Thick coating of oxidized, silicified vein infill material, composed of silica granules in an oxide-rich (hematite) matrix. The basalt substrate is zonally altered, but the alteration is incipient, with only partial degradation of pyroxene and partial silicification. The oxide coating is in sharp contact with the basalt.

25-GTVA

24 July, 1998 Top of Conical Seamount
Sample Site: 07:57 3°18.728'S 152°39.543'E Depth: 1093m

Aim: To sample hydrothermal material

Operation: Successful grab of about 75 kg of basalt.

Results: Two basic types of samples were recovered. Group 1: Basalt samples with little evidence of strong alteration/mineralization. Pyroxenes are altered (partially) to chlorite. The surfaces of the samples are more altered than the centres, indicating that fragmentation is primary (basalt spatter). Group 2: Breccia samples: This group contains a variety of intensely altered, pyritic breccia composed of 80% fragments, 20% matrix. The breccia fragments are zonally altered, with silicified (clay–altered?) rims, infilled (silica) vesicles, altered pyroxenes, and disseminated pyrite. Some samples have orange and yellow minerals infilling fractures, probably realgar and orpiment. Sulfides include some chalcopyrite, fine-grained sphalerite, and possible arsenopyrite. Brown veins of very fine-grained material emit H_2S with application of 10% HCl, and appear to be composed of sphalerite.

Significance: These samples define a new assemblage in this area. They contain significant quantities of zinc, some lead and copper, and late arsenic and possibly other related elements (Sb, Hg). They are paragenetically complex, and represent a probably intense phase of mineralization. The presence of base metals and abundant arsenic suggest that this may be a lower temperature, and perhaps spatially peripheral phase of mineralization system. The chloritic alteration of otherwise unaltered samples may represent the peripheral part of the system, affected primarily by heated seawater.

Samples: These are representative of both "least altered" (2,3) and more altered to intensely altered portions of the grab.

Sample 1: Clay: for XRD.
A: Various size fractions sieved from the mud sample.

Sample 2: Slightly altered pyroxene-rich basalt. The vesicles are not filled. Phenocrysts are mildly altered and the sample is still magnetite–rich.

Sample 3: Altered basalt
A: More extensively altered basalt, with strongly developed, somewhat weathered alteration rind. This sample contains minor pyrite.
B: Similar to A.

Sample 4: Green-altered breccia
The outside 1 cm rind is green-stained brecciated basalt (possibly Cu or Fe Arsenate stain?). This sample is very sulfide-rich (10% pyrite), and contains minor but distinctive orange orpiment and red realgar (possible cinnabar? Not confirmed by x-ray). Some sphalerite, galena and chalcopyrite occur in veins and as disseminations throughout the altered volcanic rock samples. We also identified (tentatively) tennantite. The crust on this sample contains bands of chalcedony.

Sample 5: Mineralized breccia
A: Coarse breccia, with highly altered clasts and matrix. Pyrite is disseminated throughout both. The matrix is finely comminuted basalt, and may be an "in situ" breccia. It contains fine-grained pyrite, sphalerite and a trace of chalcopyrite. Some of the matrix appears to retain vesicles as well as the fragments. The vesicles contain coarser grained (0.05 mm) euhedral pyrite grains.
B: Similar to A, with a strongly silicified matrix and smaller breccia clasts. This sample is very pyritic (~10%). Pyrite occurs as discrete polycrystalline blebs, 1-3 mm in diameter, and in vein fillings. Copper stains are prominent, and the sample contains abundant realgar and orpiment. C: Coarse breccia, with 2-5% realgar and orpiment. The green stain may indicate copper (either chalcopyrite or tennantite/tetrahedrite). This is the most arsenic-rich sample observed thus far.
The sample has only a little matrix, which is highly silicified.
Most of the altered parts of this sample are not magnetic, but the least altered fragments have retained some magnetite, and are quite vesicular. Some vesicles are infilled with chalcedony.

Sample 6: This large (30-kg) sample was broken into numerous sub-samples; all are similar. It is comprised of coarse breccia with distinctive grey to white silicified fragments and less silicified cores. Both the fragments and the matrix contain vesicles, indicating that the

brecciation occurred as an in situ hydrothermal fracturing (hydrothermal auto-brecciation), not involving any transport.
The sample contains some very distinct black veins, 2-3 mm wide that cut through several of the sample fragments. If treated with 10% HCl, these veins turn brown and emit H_2S, and are probably sphalerite.
A: Sphalerite-veined sample.
B: Breccia with vesicular matrix and very altered clasts.
C: Massive basalt portion of this sample.

Sample 7: Realgar/orpiment sample. Sample contains about 8-10% realgar (9%) and orpiment (1%) and has some green staining (scorodite?), probably indicating chalcopyrite or tetrahedrite/tennantite. The entire sample is intensely altered, silicified basalt. The phenocrysts are all replaced by silica/clay, and the matrix is altered to a fine-grained black anastomosing network of pyrite veinlets cutting a granular cherty groundmass. Realgar occurs as linings in veins, which infill the most silicified parts of the fragments and groundmass.

Sample 8: A. This is a very large (25 kg) sample of ropy lava, with a base of altered, veined and brecciated lava. The basalt portion is about 7 cm thick, underlain by a one cm boundary zone of incipient brecciation and alteration, underlain in turn by 3 cm of brecciated mineralized basalt (see Figure 2, below).
B. Large sample of the same flow and breccia units as shown in Figure 1. Vesicles contain native sulfur crystals.
C. Similar to A and B. Large sample showing flow and underlying breccia, with semi-massive sulfide. Sample contains 20% pyrite, 20% sphalerite, orpiment, realgar, some copper mineral.

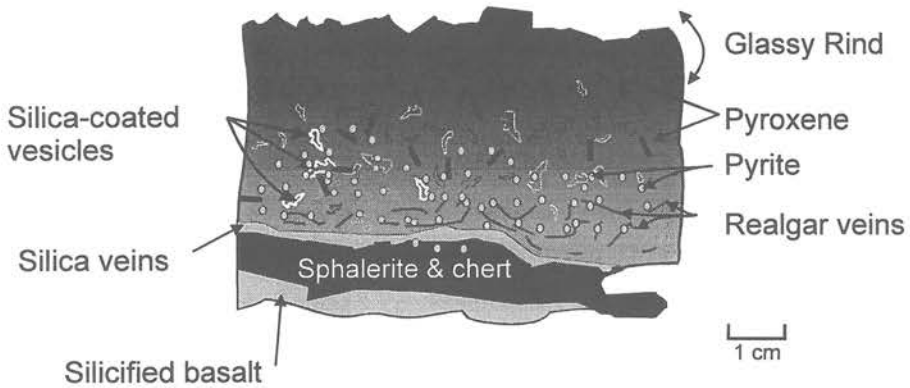

Figure 4.2: Cross section of sample 25-GTVA-8A, illustrating the distribution of alteration and sulfide/arsenic minerals.

26-GTVA

24 July, 1998 Top of Conical Seamount
Sample Site: 10:35 3°18.707'S 153°39.528'E Depth: 1103m

Aim: To sample hydrothermal material

Operation: A successful grab of 2 large (25 and 15 kg) and about 12 smaller (1-2 kg) samples.

Results: Most of the samples have rusty coatings, and are heavily (1 cm or more) oxidized. The large samples are moderately altered with large patches of realgar, orpiment, and silica on fracture surfaces (x-ray work will confirm identifications). Large vugs (possibly dissolution cavities) and vesicles are coated with iron oxides, silica and sulfur. The basalt is moderately altered (pyroxenes are chloritized, groundmass is locally silicified), and contains about 5% disseminated pyrite in the largest sample. Only partial pyroxene replacement by silica or clay minerals is evident.

Significance: This suite of samples may define an outer edge of the hydrothermal system, where As (and Hg?) were deposited.

Samples:

Sample 1: Fairly fresh basalt. Highly vesicular basalt contains about 35% pyroxene. Fracture surfaces are coated in realgar +/- orpiment, minor pyrite and silica. Most of the basalt is not strongly altered. Pyroxene phenocrysts are slightly retrograded to chlorite.
A: Samples with realgar and orpiment on fracture surfaces
B: No coating on this sample; otherwise it is moderately fresh basalt.

Sample 2: Weathered, silicified basalt. This sample is strongly weathered. Both groundmass and pyroxene phenocrysts are silicified. Some pyroxene crystals show partial replacement. The groundmass is altered from its original grey green to yellow, and cut by both vein and massive silicification. Realgar is abundant on fracture surfaces.

Sample 3: Small sample of highly altered basalt has a sucrose texture with preserved euhedral pyroxene grains. It appears to be strongly altered (or weathered), and silicified. (2 pieces only).

Sample 4: Very weathered but only slightly altered basalt. The vesicles are slightly iron-oxide coated. The surface is black, weathered; one surface is composed of a 3 cm-thick layer of oxide and sandy material (degraded or weathered basalt).

28-GTVA

24 July, 1998 Top of Conical Seamount
Sample Site: 14:54 3°18.715'S 152°39.507'E Depth: 1102m

Aim: To sample hydrothermal material

Operation: Obtained 100 kg of 2 to 5 kg boulders

Results: Four types of samples were recovered. Group 1: The most abundant sample type is composed of boulders of relatively unaltered pyroxene-phyric basalt. Each boulder is rimmed by an Fe-oxide coating typically about 2 mm wide (except on sample 4, which has a five to ten mm oxide layer and contains a trace of pyrite). Generally the basalt is moderately vesicular (10%, vesicles 1-3 mm), pyroxene-phyric (40% phenocrysts) in a dark-grey matrix. A few olivine grains are observed. Most pyroxene grains are variably chloritized with some grains containing fresh cores and altered rims or patches.

Group 2: One sample of siliceous breccia. This sample is a weathered breccia containing 50-60% clasts of variably altered porphyritic basalt. Clasts are 3-6 mm, subangular, and matrix supported. They do not contain open vesicles. The matrix is brown to pale green granular silica. Granules are 0.5 to 1.0 mm, and well packed.

Group 3: Banded Fe-oxide crusts. Crusts are 8-10 cm thick, composed of nodular and banded Fe-oxide layers. Most of the layers and nodules consist of bright to deep orange, well-indurated hematite/goethite. Banding is defined by thin (~2 mm) bands of dark brown to black siliceous? or better crystallized/indurated Fe-oxide.

Group 4: One large sample of basalt consists of a thick coating of black, fine-grained reduced mud. The sample is composed of basalt, similar to the samples of Group 1, but with a trace of pyrite. The black mud resembles reduced organic ooze. The basalt samples have 3-5 mm oxide rinds, and may be a bit more mineralized than those of Group 1.

Significance: This area seems less well mineralized than some others, and may be peripheral to the central epithermal system. Nevertheless the pyroxene grains are altered to chlorite, and some pyrite is present.

Samples:

Sample 1: Group 4, black mud sub-sample for clay mineral determination (XRD). The sample has a small amount of black mud attached to Fe-oxide coated basalt. It contains traces of sulfide.

Sample 2: "Fresh" basalt of Group 1, with 1-2 mm oxide rinds, no sulfide, vesicular.

Sample 3: Fe-oxide coating (Group 4).

Sample 4: Siliceous breccia sample (Group 2).

31-DR

24 July, 1998 Southwest facing slope of horst that is SW of Edison Seamount, in region of methane anomaly.

On bottom:	21:08	3°19.492' S	152°35.372' E	Depth: 1630m
Sample Site:	22:20	3°19.072' S	152°35.756' E	Depth: 1506m

Aim: Characterize nature of horst structure.

Operation: Dredge of SW slope of steep side.

Recovery: ~ 1 kg of large, broken clam shells

Results: Clam shells have thin coatings of Fe-sulfide on external portions of the shells. Shells show very little dissolution suggesting they are relatively youthful.

Samples:

All to biologists.

33-GTVA

25 July, 1998 Edison Seamount, southern clam field, edge of crater wall on floor.
Sample Site: 02:19 3°19.041' S 152°34.854' E Depth: 1342-1456m (1446m)

Aim: To obtain biological samples and possible rocks from top of the cone.

Recovery: ~200 kg, mostly of biologic samples enclosed in muddy, sulfurous sediment. Also recovered within the sediment were, ~50 cobble to pebble sized knobby, xenolith-bearing basalt samples.

Results: Fine-grained, vesicular, pyroxene and phlogopite bearing trachybasalt was recovered. Phenocryst content is generally below a few percent with clinopyroxene > phlogopite. All trachybasalt includes xenoliths that have a wide range of compositions and sizes (microscopic to cobble sized). A number of the basalt samples have unusual oblong, ropy (turdiform) surface textures that may be a kind of submarine "spatter". One sample (#1) appears to have spheroidal exfoliation. Many of the samples were cut to look for xenoliths.

Samples: Samples were placed in two groups, metasedimentary rocks and basalt.

Sample 1: 0.5 kg of metasediment. Carbonate-bearing wacke with circumferential banding/layering that appears to be related to contact metamorphism by lava that may have erupted into it or enclosed it at one time. No lava exists on it now.

Sample 2: Trachybasalt, xenolith-bearing with minor clinopyroxene and phlogopite phenocrysts set in a dark, fine-grained matrix. The groundmass is very fine-grained, and vesicular. Vesicles are unevenly distributed, and commonly concentrated in the cores of rounded lava fragments. They get smaller and less abundant towards the rims (suggesting the rounded pieces are individual lava bombs or "spatter").

A. Basalt with 8 x 4 cm ultramafic xenolith which appears to be a wehrlite or clinopyroxene-websterite with modal layering and/or secondary veining by pyroxene (orthopyroxene and rare phlogopite) that exhibit very little reaction with the lava. (2 samples to TUBAF, 1 to UF, small to CODES)

B. Basalt (1 kg) with large pipe vesicles in core. Abundant microxenoliths that range from sediments to altered gabbro to dunite (larger gabbroic xenolith to UF).

C. Basalt with cm-sized metasediment or metavolcanic rocks (only to TUBAF and UF)

D. Basalt with vesicular core (0.5 kg) containing small xenoliths but not as many as other samples.

E. Small round pebble with fresh? gabbro xenolith. Gabbro contains plagioclase, clinopyroxene, olivine, and possibly amphibole, magnetite and sulfide. (TUBAF and UF only)

F. Basalt with small xenoliths (2 kg one of larger pieces).

G. Small basalt with vesicular, olivine-basalt xenolith. Two different samples distributed

H. Microgabbro xenolith (TUBAF and UF only).

I. General sedimentary xenolith-bearing lava.

J. Irregularly shaped vesicular basalt with a variety of small xenoliths. (TUBAF and UF only)

K. Elongate (turdiform) lava with small ultramafic xenoliths. (TUBAF and UF only)

L. Similar to K with clinopyroxene xenocryst.

M. Phlogopite-bearing trachybasalt. (UF only)

34-GTVA

25 July, 1998 Edison Seamount; clam field
Sample Site: 05:45 3°19.051' S 152°34.864' E Depth: 1448-1484m (1448m)

Aim: To obtain biological samples and possible rocks from top of the cone.

Recovery: Mostly biologic samples in a pebbly/sandy mud. Only a few rock samples - 2 kg sized basalt samples. The remaining samples are mostly smaller than 7 cm in diameter. Inspection of the mud showed the pebbles are rock fragments on glass. No evidence of hyaloclastite.

Results: Basalt is slightly pyroxene- and phlogopite - phyric, but phenocrysts are small and sparse (< few %). All samples contain abundant small xenoliths of compositions that range from ultramafic to gabbroic, to sedimentary (very much like samples from TUBAF Seamount.). Large samples have a knobby/gnarly surface texture (similar to TUBAF basalt).

Samples: All samples are basically the same, but two distinct larger samples are numbered separately.

Sample 1: One of the largest basalt samples which contains a 6x5x4 cm pyroxenite xenolith with abundant magnetite (possibly spinel) and sulfides (chalcopyrite and pyrrhotite and pyrite). Basalt host is vesicular and has phenocrysts of clinopyroxene, phlogopite and olivine (? could be xenocrystic). [2 slices to TUBAF, 2 to UF, 1 to GSC].

Sample 2: Complex xenolith-bearing bomb enclosed in another lava. Inner "bomb" contains a large 7x5x5 cm angular clast of limestone that includes microfossils and is partially metamorphosed. Inner lava is more vesicular than outer enclosing lava. [Large piece to GSC, see Fig. 4.3].

Sample 3: Other large sample, that could be the other half of sample #. 1Vesicular basalt is clinopyroxene, phlogopite and olivine phyric (olivine looks xenocrystic).

Sample 4: Smaller basalt samples. Appear to be the same as #1 and 3. Small pieces distributed to all groups.

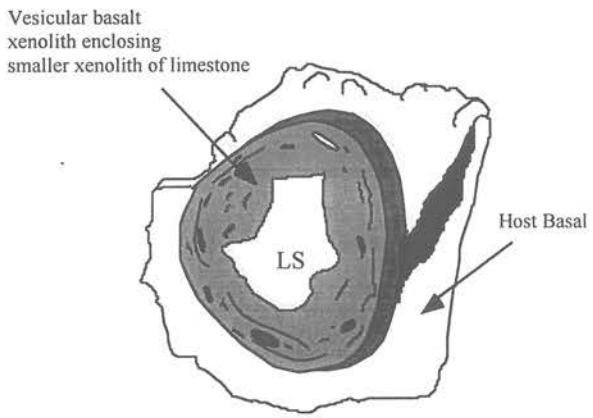

Figure 4.3: Sample 34-GTVA-2 illustrating mantled xenolith.

36-GTVA

25 July, 1998 Conical Seamount.
Sample Site: 12:00 3°18.741' S 152°39.531' E Depth: 1081-1154m (1088m)

Aim: To sample hydrothermal material from the top of the deposit.

Operation: Grid sampling to determine extent of mineralization

Recovery: One 3 kg basalt

Results: Moderately fresh basalt was recovered, with little evidence of hydrothermal alteration.

Significance: The lack of alteration and pyrite in this sample indicates that this site may be outside the mineralized zone. However, the sample is very small, and given the variability of larger grabs, the site should not be considered as conclusively defining the zone of hydrothermal deposition.

Samples:
Sample 1: Pyroxene-phyric basalt, with ~1% vesicles as small elongate pipes (0.5 - 1.5 mm), ~ 60% pyroxene phenocrysts, fresh to slightly chloritized, minor magnetite. Surface is ropy with thin (1 mm) Fe-oxide coating.

39-GTVA

26 July, 1998 Top of Conical Seamount
Sample Site: 00:22 3°18.714'S 152°39.557'E Depth: 1059m

Aim: To sample hydrothermal material.

Operation: Recovered 75 kg of rocks and mud.

Results: Many of the samples have pyrite coatings on fracture surfaces and vesicles. The mud is black and sulfide-rich. Most of the samples are cobble to boulder-sized pieces of ankaramitic basalt with a range of alteration and mineralization. The least-altered basalt samples have fresh-looking pyroxene euhedra set in a grey, vesicular altered groundmass. The least altered basalt sample has the least pyrite; the latter is most abundant in vesicles, veins and finely disseminated in the groundmass. The samples include lightly altered and sulfide bearing to those that are completely altered (chloritized pyroxene) with veins and more massive infilling of vesicles and fractures. Colloform textures predominate in the larger veins and vesicles. A few samples are semi-massive to massive sulfide.

Significance: This is the most intensely mineralized portion found thus far, and represents the core of the mineralization zone.

Samples: The samples are divided into 5 groups:
Group 1: Massive sulfide samples, containing > 75% sulfide (pyrite +/- marcasite).
Group 2: Veined and sulfide coated basalt.
Group 3: Altered basalt with disseminated pyrite.
Group 4: Completely altered pyritized grey mud.
Group 5: Oxide crusts.

Sample 1: Semi-massive pyrite.
Several samples, each 0.3 to 1 kg, of massive to semi-massive pyrite - marcasite were recovered. Pyrite occurs as distinct, intricate colloform bands and framboids. Layering occurs at the microscopic to sub-mesoscopic scale, and is defined by alternating growth zones of bright (marcasite?) pyrite and dusty brown pyrite. Some samples contain aggregated ooids of pyrite, which define excellent framboid texture.
The largest sample is composed of a botryoidal to framboidal and colloform pyrite matrix surrounding apparently "fresh" pyroxenes. The matrix of the basalt has been almost completely replaced. Some samples have white amorphous silica in open spaces, surrounding or overgrowing pyrite bands.
A: Massive, colloform sulfide
B: Massive colloform sulfide with a dark sulfide zone (possible sphalerite?).
C: Very fine-grained sulfide portion of the sample group, showing some excellent colloform banding.
D: Medium-grained colloform banding.
E: Pyroxene crystals in massive to colloform sulfide.

Sample 2: Basalt with veins of massive pyrite/marcasite.
Basalt is highly vesicular (15-29%), with curved pipe vesicles, 1 mm to 8 mm long. Vesicles are usually coated by pyrite. The matrix is composed of fine-grained, medium brown mesostasis, with about 1%-disseminated pyrite. Phenocrysts comprise about 30%, and are chloritized pyroxene. A few olivine grains (rounded, possibly xenocrysts) are dispersed through all samples. Veins are typically 1 cm thick, complexly colloform banded, with a coarser grained band on their margins, intimate colloform bands in the interior and about 20-30% open space (locally occupied by amorphous silica). A thin (0.5 mm) pyrite band mantles several samples. Although most of the veins are on the margins of the samples, one has a vein in the centre, illustrating the variable nature of the vein thickness.
A: Thin layer of pyrite coating the outer surface plus vesicles. One narrow zone of sulfide "breccia" or colloform band.
B: Pyrite coating vesicles only.
C: Thick pyrite vein on one surface, about 1 cm thick.
D: Pyrite band, 3 mm thick, coating one surface.
E: Thin pyrite band on the surface of the sample, disseminated pyrite in the matrix.
F: Pyrite-coated veins and vesicles, plus some silica infill of vesicles.
G: Pyrite coating the surface of the sample and also coating large vesicles.
H: Excellent colloform banding within bands of pyrite, and on much of the outer surface of the sample. Sample includes several small samples with pyrite on the outer surface.

Sample 3: Altered basalt. Moderately vesicular (5-20%) pyroxene-phyric basalt. Almost all samples are non-magnetic. Pyroxene phenocrysts vary from black (unaltered) to green (chloritized), and comprise 30-40% of the sample. Some feldspar microlites are evident, in a few samples, and all have rare olivine xenocrysts. Samples contain about 0.5% disseminated pyrite, mainly in vesicles.
A: Moderately altered pyroxenes
B: Very pyrite–rich sample, containing disseminated pyrite, with pyrite replacing pyroxene grains. Pyroxene is chloritized.
C: Remaining "fresh" basalt samples, all with altered pyroxene.

Sample 4: Completely altered basalt
This sample is composed of light grey, kaolinized and pyritized basalt. Pyroxene phenocrysts are totally replaced by clay and pyrite. The groundmass is intensely silicified, and may contain some K-feldspar. The sample contains about 10% pyrite. The sample is highly friable, and thus few large pieces are available. The small pieces and matrix material were saved in a bucket. This sample is quite similar to that in 40-GTVA.
A: Hard samples.
B: Mud.

Sample 5: Oxide crusts. This sample is composed of oxide crusts up to 3 cm thick, formed on moderately to weakly altered basalt. There is a trace of pyrite in the matrix of the pyroxene-phyric basalt. The crusts are not well banded, and appear to replace weathered basalt.
A: Most oxide-rich samples.
B: Less oxide rich samples.

40-GTVA

26 July, 1998 Top of Conical Seamount
Sample Site: 02:19 3°18.714'S 152°39.556'E Depth: 1096m

Aim: To sample hydrothermal material.

Operation: After 4 unsuccessful attempts, a rusty area was sampled. 150 kg of cobbles to small boulders, Fe-oxide crust and basalt, and one very large boulder (about 150 kg) were recovered.

Results: Most of the samples are moderately altered pyroxene-rich basalt with variable amounts of disseminated pyrite content. Smaller samples are more altered basalt that contain 5-10% pyrite, kaolin (?), possible K-feldspar, and appear to be silicified. In the most altered samples, the pyroxenes are replaced by clay minerals. Bulk fine grained material was sieved and sulfide concentrate given to XRF and ASV.

Two groups of samples were defined: Group 1. Moderately altered and vesicular ankaramitic basalt. Clinopyroxene is partially altered to chlorite. The matrix varies form dull brown to greenish-grey. Iron oxide coatings (<0.5 cm thick) are layered, with alternating thin black and thicker red-orange (limonite) layers. The ankaramite has disseminated pyrite in the vesicles and groundmass. Amounts are highly variable, but generally less than 0.5 %. Many of the samples have circumferential cooling fractures.

Group 2: These samples are totally altered light-grey sulfidic ankaramite. The samples vary from dark grey pieces that contain remnant pyroxene grains in a totally altered matrix to light grey samples that contain no primary pyroxene, but excellent pseudomorphs after pyroxene. The samples with remnant dark pyroxene are moderately veined by silica, with about 2% pyrite in the matrix and partially replacing pyroxene. Pink and tan aphanitic vein filling and patches may be K-feldspar. Silica fills remnant vesicles. Pyroxene grains are partially replaced by smectite (?). The samples with no remnant pyroxene. Its texture is retained, but all crystals are totally replaced by a white to green-white mineral (smectite?) and mantled by silica. The groundmass is an intensely reticulate set of dark grey veinlets, each 0.05-mm wide, which enclose white, pink and tan matrix granules of

replaced matrix. The matrix contains 1-5% pyrite. Some pyroxene grains are completely dissolved but not replaced, leaving skeletal pits in the samples. Native sulfur occurs on one fracture surface.

Significance: Sample is from the highly mineralized core of the system.

Samples:

Sample 1: Less altered basalt, group 1.
A: Ankaramite with partially chloritized clinopyroxene, trace of pyrite. Fe-Oxide crust contains fragments of basalt.
B: Small fragment similar to 1A, but weathered more strongly, with a distinct rind on one surface. Vesicles contain a trace of pyrite.
C: Partially altered ankaramite from very large (150 kg) sample. This sample is a ropy lava flow, and it is vesicular, with chloritized pyroxene.

Sample 2: Altered, sulfide-bearing samples, group 2.
A: Remnant pyroxene in highly altered basalt.
B: Selection of highly altered basalt fragments. Pyroxene in some parts of these samples is pyritized, with silica rims.

41-GTVA

26 July, 1998 Top of Conical Seamount; definition of mineralized zone.
Sample Site: 04:55 3°18.731'S 152°39.562'E Depth: 1097m

Aim: To sample hydrothermal material.

Operation: About 150 kg of boulder and mud were recovered.

Results: The majority of the boulders are light to medium grey, highly altered, sulfide bearing basalt. Few pieces (about 10% of the total sample) is less altered basalt and oxide crust.

Significance: Sample site is in the strongly mineralized part of Conical Seamount.

Samples: Samples were divided into three groups:
Group 1: Light grey, intensely altered samples with pyroxene totally or partially replaced. On cut surfaces, most samples display distinct zoning of alteration. The outer rim (2-3 cm) is bleached, sulfide rich (5%), and pyroxene-replaced. The core is darker, with more chloritized pyroxene, and is less pyritic (1-2%). Several samples have large holes, which may be dissolution cavities or augmented vesicles. These are filled with amorphous silica and marcasite crystals. The holes are 1-1.5 cm wide, 2 cm deep and may have formed by corrosion. The groundmass is a reticulate mass of smectite (?) veinlets and granular silica, paragonite (XRD determination) and possible K-feldspar.

Group 2: Dark grey, more pyroxene–rich samples. The matrix tends to have coarser-grained pyrite, and vesicles filled with marcasite. The alteration is less distinctly zoned, and resembles the core alteration of type 1. The bleached rims may have been milled off during sampling.

Group 3: Least altered basalt. This group comprises a couple of samples of dark green, partially altered ankaramite. These contain finely disseminated pyrite in the groundmass, and partially chloritized pyroxene crystals.

Sample 1: Highly altered basalt
A: This sample is concentrically zoned, highly altered, clay-rich,and moderately vesicular basalt. The outer rim is bleached, and contains 1-5% pyrite. The core contains about 1% coarse grained (1 mm) pyrite. Pyroxene is partially replaced, altered to clay, but with at least 50% chlorite remaining.
B: Well-zoned sample with a light (bleached) band at the top and bottom. Each band is about 1 cm thick. These light bands have most of the sulfide in them. Pyroxene is intact in the dark central portions of the samples.
C: Darker grey, less altered pyroxene-phyric rock, containing 1-2% pyrite as disseminations and veins. This sample is less sulfide-rich than A or B.
D: Highly altered, non-zoned sulfide-bearing samples. These were randomly selected to represent typical altered rock from this grab.

Sample 2: Basalt with oxide rinds.
These samples have 1 cm-thick oxide rinds on moderately altered, chloritic basalt.

Sample 3: Oxide crusts.
These are typical of the oxide crust group (4).

A pyrite and magnetite concentrate was made from this sample by sieving the mud and fine fragments and given to XRF and ASV.

42-GTVA

26 July, 1998 Top of Conical Seamount
Sample Site: 06:48 3°18.724'S 152°39.599'E Depth: 1051m

Aim: To sample hydrothermal material, and to define limits of mineralized zone

Operation: After 4 unsuccessful attempts, a small set of samples was obtained. About 12 small pieces and 2 larger pieces were recovered.

Results: Samples include small highly weathered/oxidized pieces and two larger pieces of basalt. Oxide coatings are about 3 cm thick, and mantle slightly altered, dark green to dark grey basalt. Pyroxene phenocrysts are chloritized, and comprise 40% of the samples. The groundmass is aphanitic and dark grey. Disseminated pyrite occurs as a trace throughout. Some portions of the larger samples are brecciated, with iron oxides filling fractures that displace less altered, but somewhat oxidized basalt.

Significance: Probably defines the outer edge of the mineralized area.

Samples:
Sample 1: Basalt, minimal crust, and minimal alteration.
Sample 2: Iron oxidized crust (no sample for UF).
Sample 3: Basaltic breccia
Sample 4: Small sample of freshest basalt contains trace of disseminated pyrite.

43-GTVA

26 July, 1998 South side of horst, SE of Edison Seamount.
Sample Site: 08:37 3°19.461' S 152°35.370' E Depth: 1599-1624m (1624m)

Aim: To look for and sample possible "cold seep" fauna.

Operation: Grab was attempted in the area of methane anomaly and observed biologic activity. Grab was taken on white-coating and black dendritic stains. Worms and clams in area.

Recovery: 300(?) kg of mud and biota.

Results: Hemi-pelagic mud with localized dark staining no lithified material. Mud contains some, dark granular material, possibly sulfides. Some biota.

Samples:
Sample 1: Hemipelagic mud sample (to UF).

44-GTVA

26 July, 1998 South side of horst, SE of Edison Seamount.
Sample Site: 12:26 3°19.352' S 152°35.462' E Depth: 1451-1610m (1598m)

Aim: Sample fauna and crusts observed earlier.

Operation: Grab taken in area of methane anomaly and observed biologic activity. Grab fell on side, only partial recovery.

Recovery: 50 kg of mud and biota

Results: Several 1 kg samples of indurated mud. Samples consist of foraminiferal ooze penetrated by gas discharge holes (5 mm in diameter.). Samples contain fine-grained to cryptocrystalline black material (probably Fe-sulfide) and some surfaces are lightly oxide coated. The cementing material is not obvious but some silica coated or partially filled discharge holes are present. In addition, needles of silica are associated with small clams.

Samples:
Sample 1: Indurated mud

46-DR

27 July, 1998 Conical Seamount
On bottom: 18:43 3°18.716' S 152°39.468' E Depth: 1120m
Off bottom: 19:11 3°18.748' S 152°39.538' E Depth: 1097m

Aim: To sample hydrothermal material and define limits of the hydrothermal system

Recovery: 5 cobble-sized rock fragments, 15 kg of basalt with Fe-oxide stains.

Results: Ankaramite, partially altered, slightly to moderately vesicular.

Samples:

Sample 1: Ankaramite

A. Pyroxene-rich basalt (ankaramite), slightly altered with pyroxenes partially chloritized, rare olivine. Vesicular (typically 2-3 mm) some flattened pipe vesicles. Some finely disseminated pyrite (trace). Thin Fe-oxide coating (1-2 mm) on surface of flow. Large sample.

B. Smaller sample; as above

47-DR

27 July, 1998	Top of Conical Seamount			
On bottom	20:07	3°18.715'S	152°39.477'E	Depth: 1118m
Sample Site	20:21	3°18.749'S	152°39.582'E	Depth: 1114m

Aim: To sample hydrothermal material and define limits of the hydrothermal system.

Operation: Bites at 20:15:22, 20:17:37, 20:20:07; successful dredge, about 12 kg of sample material

Results: Three small, hand-sized samples of Fe-coated basalt and Fe-oxide crusts each about 4 kg, were recovered. The basalt is vesicular (1 cm vesicles), and contains no sulfide. Pyroxene partially altered to chlorite

Significance: Out of primary mineralized zone. May be in peripheral alteration system.

Samples:

Sample 1: Typical ankaramite; fresher than previous dredge hauls and TV-grabs. Sample contains 40% pyroxene phenocrysts in a dark grey matrix. The pyroxene is slightly altered to chlorite. The sample contains a trace of olivine. It has minimal oxide coating, large pipe vesicles, and no sulfide. It has minimal oxide coating.

Sample 2: Fe-oxide coated, pyroxene-phyric, sparsely altered basalt. The matrix is brown-green. The sample is vesicular, and no sulfides observed.

Sample 3: Fe-oxide crusts. These are brecciated, granular black, brown and tan crusts. A few remnant pyroxene grains are evident in the oxide, indicating that it has replaced the weathered portion of the basalt. Banding is irregular.

50-DR

27 July, 1998	Conical Seamount, east side of cone.			
On bottom:	23:40	3°18.739' S	152°39.541' E	Depth: 1150m
Off bottom:	24:00	3°18.717' S	152°39.656' E	Depth: 1097m

Aim: To define limits of the hydrothermal system.

Operation: Dredge up east side of cone.

Recovery: 60 kg of mostly cobble-sized ankaramite, Fe-oxide cemented basaltic breccia, Fe-oxide crust. One relatively large (~15 kg, 30 cm thick) basalt.

Results: Ankaramite with abundant clinopyroxene (~40%), rare olivine microphenocrysts. Very vesicular. Alteration is variable but mostly slight, with clinopyroxene altered to chlorite, matrix is light grey.

Samples:

Sample 1: Basalt.
A: Ankaramite, vesicular, small cobble with ~40% clinopyroxene phenocrysts (< 0.5 cm), minor olivine microphenocrysts. Abundant round micro-vesicles and lesser flattened pipe vesicles (no sample to CODES)
B. More typical ankaramitic basalt. Vesicular. Clinopyroxene is chloritized, rare
C. Ankaramite, larger slabby piece. Abundant clinopyroxene, rare olivine. Rounded xenolith of clinopyroxene -rich, vesicular xenolith.
[Extra bag of Group 1 to TUBAF]

Sample 2: Weathered Ankaramite.
A. More altered/weathered variety of ankaramite described above.

Sample 3: Fe-oxide cemented basaltic breccia.
A. Breccia composed of angular fragments of ankaramite (exhibiting different extents of alteration). Breccia also includes pockets of sediment.

51-GTVA

27 July, 1998 Top of Conical Seamount
Sample Site: 01:38 3°18.730'S 152°39.553'E Depth: 1096m

Aim: To sample hydrothermal material and to define limits of the hydrothermal system.

Operation: About 10 kg of mud and indurated mud, containing small rock samples was recovered.

Results: Gritty mud containing a few shell fragments and about 20 2x2 cm rock fragments was recovered. Two 5x5 cm samples of altered basalt were included in the grab recovery.

Significance: Significant alteration and sulfide indicate that this site is within the alteration/hydrothermal zone, and is distinctly mineralized. Sphalerite and galena indicate very strong mineralization.

Samples:

Sample 1: Completely altered pyritic basalt, with pyroxene phenocrysts; 80% replaced by silica/clay. Pyrite (2-3%) is disseminated through the groundmass and in vesicles. The outer surface is rusty. Traces of sphalerite and galena were observed in one sample (identification was confirmed with microscopic examination).

Sample 2: Slightly less altered basalt, otherwise similar to sample 1.

Sample 3: Rusty indurated oxide crust on highly silicified and altered sulfide-bearing samples. Sphalerite and galena occur in the largest piece; other samples are silicified and sulfidic.

Sample 4: Mud (TUBAF only)

52-GTVA

27 July, 1998 Top of Conical Seamount
Sample Site: 02:44 3°18.730'S 153°39.546'E Depth:1096m

Aim: To sample hydrothermal material and to define limits of the hydrothermal system.

Operation: Recovered several large (10 kg) pieces of heavily oxide-coated basalt. Sample weighed about 30 kg.

Results: All samples are of pyroxene–phyric basalt. Oxidized surfaces on some samples range up to 8 mm in thickness, and are typically 2 mm thick. Below the oxidized zone is a 5 cm-wide bleached zone, with minor disseminated pyrite.

Significance: At the edge of the mineralized system.

Samples:
Sample 1: Samples all contain about 40% pyroxene phenocrysts in a dark grey-brown matrix. One sample has pyrite coating vesicles, and contains trace of disseminated pyrite.
A: Trace of sulfides in slightly altered basalt. Sample has incipient silicification.
B: Least altered basalt. The matrix is grey-green, and only slightly altered. Pyroxene grains are all chloritized.
C: Most oxidized sample, with a thick coating (1 cm) of bleached yellow-orange outer surface.

53-GTVA

27 July, 1998 Top of Conical Seamount, to define limits of hydrothermal system
Sample Site: 03:52 3°18.730'S 153°39.565'E Depth: 1057m

Aim: To sample hydrothermal material.

Operation: Recovered about 100 kg of basalt blocks, weathered basalt, altered, sulfide-rich material, and silicified breccia samples.

Results: This grab recovered some excellent examples of the various phases of mineralization in the Conical Seamount area. All "facies" of mineralization were found, including sulfide-rich breccia, sulfide-metasomatized basalt, vein sphalerite, minor galena, possible sulfosalts, iron oxide crusts and some less altered ankaramite.

Significance: This is possibly the best example of epithermal (Lihir) style mineralization recovered on Conical Seamount.

Samples: Five types of samples were identified:
Group 1: Grey, brecciated sulfide-silica (pyrite breccia).
Group 2: Bombs of basalt mantled by black-grey breccia.
Group 3: Green-stained sulfide-rich samples (include some galena-sphalerite).
Group 4: Less-altered basalt.
Group 5: Fe-oxide crusts.

Group 1: Sulfide-silicate breccia.
These are composed of intensely brecciated, totally altered basalt. Fragments appear shattered, angular to subrounded, typically 5 mm in width (2-15 mm range) and formed primarily as an "in situ" breccia. The matrix is a granular silicified replacement of ankaramite and ankaramitic detritus. The fragments are mantled by silica, and contain skeletal and totally replaced pyroxene grains. The mesostasis of the fragments is medium grey and strongly silicified. The groundmass (matrix) to the fragments is dark grey to black, and is composed of 80 to 100% fine-grained to cryptocrystalline reticulate pyrite, and pyrite fracture fillings. Some vugs and solution cavities are filled with amorphous silica. Thick oxide coatings mantle a few samples. In some samples, silica veining is well developed, in others, silica forms the cement to the fragments. These samples are totally demagnetized.

Group 2: Large ankaramitic bombs mantled by breccia.
These bombs or pieces of spatter breccia are typically 10 cm in diameter, well rounded and vesicular, and are mantled by finer angular to finely comminuted ankaramitic breccia (1 cm fragments typically). The bombs are commonly mantled by silica, and retain some magnetic signature. Their pyroxene phenocrysts are chloritized. The matrix is not magnetic, is silica-cemented, and the pyroxene phenocrysts are variably, but usually intensively altered. The fragments in the breccia are not vesicular, in contrast to the bombs that they are mantling.

Group 3: Green-stained breccia samples.
These are breccia samples that have an outer "weathered" coating that is stained bright green, similar to that found in association with copper (chryscolla), scorodite ($Fe_2[AsO_4]_3$) or annabergite. The breccia samples contain anastomosing networks and veins of disseminated and reticulate pyrite, with sphalerite, galena, chalcopyrite, Cu-sulfosalts (tennantite?), possible arsenopyrite, all in a siliceous matrix. These samples have 10% sulfide disseminated throughout the matrix. They are not as altered as the breccia samples.

Group 4: Basalt
These are samples of vesicular basalt with ovoid vesicles, typically 2 mm in width. Some are pipe-like. Pyroxene phenocrysts are chloritized but otherwise not affected. All samples are magnetic. A few have traces of pyrite. Some have concentric or sector fractures along which zoned incipient alteration is present. The alteration style seems to be silicification, with a trace of sulfide diffusing outwards from the fractures.

Group 5: Iron-oxide crusts
These crusts are 2-4 cm thick, and are composed of banded red-yellow-black oxide minerals as weakly banded outer surfaces to the altered, sulfide-rich basalt.

Sample 1: Group 1 samples of sulfide-silicate breccia

A: Excellent example of finely comminuted matrix, silica vein, semi-massive sulfide in the matrix. Fragments are totally altered, and these samples have a well-developed oxide rim.

B: Zonally altered fragments with distinct silica rims. The fragments are densely packed (form 80% of sample). Very sulfide rich as the matrix is black, and composed of 80% reticulate pyrite.

C: 90% fragments cemented by silica. Exceptionally black matrix, but sulfide abundance appears to be lower (less visible discreet sulfide grains than in the above samples). This sample may be transitional to Group 2.

D: Breccia: Highly silicified matrix, that is moderate to coarse grained. This sample may be a bit less altered and sulfide-rich, with pyroxene grains more evident.
E: Excellent example of breccia, with angular to subrounded fragments in a finely comminuted, poorly consolidated matrix. This sample has a well-developed oxide coating.
F: Excellent example of sulfidic breccia.

Sample 2: Bombs
A: Mainly a bomb, with little matrix (10%) attached
B: Distinctive bombs, 30% matrix attached, with considerable silica infill in the matrix. The bombs have relatively coarse disseminated pyrite, whereas the matrix has 5-8% reticulate pyrite veinlets throughout.
C: Small bombs cemented by 30% matrix. Sulfide content is minor, at about 1-25 in the matrix, similar (but coarser grained) in the bomb.
D: Bombs with large vesicles very little matrix
E: Possibly the best example of bombs cemented in breccia with silica and sulfides in the matrix. Bombs are 7-8 cm in diameter
F: Large bomb mantled by breccia.

Sample 3: Green-stained breccia
A: Galena-sphalerite-pyrite-sulfosalt (?) chalcopyrite sample, with massive sulfide veins.
B: Disseminated pyrite in massive basalt, with a well-developed green alteration zone on the rim of the sample.
C: Minor sulfide in a large "bomb", more sulfides in the silica-rich breccia zone.
D: Very sulfide-rich basalt
E: Not assigned
F: Low sulfide massive basalt with no matrix
G: Mixture of sulfide-rich and sulfide-poor smaller samples, all with green margins.

Sample 4: Least altered basalt
A: Incipient alteration along fractures in otherwise "fresh" basalt
B: Unaltered basalt, with chloritized pyroxene phenocrysts.
C: Slightly more weathered, but otherwise unaltered basalt

Sample 5: Fe-oxide crusts
A: Various crust samples

54-GTVA

27 July, 1998 TUBAF Seamount, NE side of crater rim
Sample Site: 06:10 3°15.135' S 152°32.499' E Depth: 1243-1274m (1263m)

Aim: To sample basalts and xenoliths.

Operation: Grab was run from SW to NE across the central, sediment-filled crater. Rim of crater has the coarsest material. Much of the area on the crater rim is densely covered with sand/pebble/cobble basaltic tephra. Pelagic sediment is light or concentrated in shallow depressions. Grab was taken where larger basalt fragments were present.

Recovery: 250 kg of mostly cobble and pebble sized trachybasalt that commonly contain xenoliths. These samples are in a sandy to pebbly mud mixed with minor pelagic ooze. The mud is viscous with rock fragments embedded within it.

Results: Basalt fragments range from large cobbles to small pebbles. Nearly all contain xenoliths (peridotite, gabbro, basalt, sedimentary rock) with sizes ranging from a few mm (maybe smaller) to ~10 cm. Some rock fragments (mostly metasedimentary rocks, peridotite) are the same composition as the xenoliths and probably represent detached xenoliths broken out of the basalt. Rare pumice fragments. Basalt samples are relatively fresh with only thin Fe-oxide coatings on some surfaces.

Basalt is believed to be trachybasalt (or shoshonitic basalt) based on analysis of similar material from 1994 cruise. Samples are highly vesicular, but vesicles are mostly small, rarely more than 0.5 cm in longest direction. Phenocrysts of phlogopite are common (~5%), some euhedral crystals up to 1 cm long. May be as much as 10% phlogopite microphenocrysts in the fine-grained, cryptocrystalline groundmass. Clinopyroxene phenocrysts are rare but microphenocrysts are more common in groundmass. Nearly all of the basalt contains a xenolith or a variety of xenoliths, which can include: ultramafic rocks, gabbro, basalt, and/or metasediment. Xenocrysts of clinopyroxene and olivine are also present. There is very little reaction of lava with enclosing xenoliths in most cases. Only some sedimentary xenoliths appear to be altered around their rims.

Outer surfaces of samples are knobby to gnarly, only minor, thin sediment on some, with thin coatings of Fe-oxides common. Small samples are generally round or oblong and nearly always contain a xenolith in their core. Texture of larger samples are similar to "cow pies" associated with spatter cones.

Most samples were cut in half, so sample distribution was first to TUBAF and UF. Over 150 samples were cut to give a representative sampling of the types of xenoliths in the basalt. Groups were divided based on major types of xenoliths: ultramafic rocks, gabbro (including pyroxene-rich dolerite and basalt), sediments (including metasediment), and basalt with a mixed variety of different xenoliths (generally small, dispersed). Xenoliths no longer enclosed in lava are noted as "detached" in descriptions below. In this grab the estimated distribution of xenoliths is >1/3 peridotite, 1/3 gabbro, and <1/3 sedimentary and mixed.

Samples:

Group 1: Sediment

A. 0.5 kg random sample of sandy-gravely sediment comprised of basaltic clasts. To examine for volcanogenic features.

Group 2: Trachybasalt with peridotite xenoliths

A. Spinel dunite; largest xenolith (0.5 kg), granular texture, broke away from enclosing basalt.
B. Spinel dunite (250g)
C. Lherzolite (250g)
D. Spinel lherzolite (veined)
E. Fresh spinel lherzolite; "detached"
F. Spinel harzburgite, granular texture; 4x5 cm
G. Spinel dunite, with rare orthopyroxene, some size grading, 5x4 cm; detached
H. Spinel harzburgite with clinopyroxene
I. Light colored spinel harzburgite 3x3 cm

J. Spinel lherzolite with small amount of Cr-diopside; spinel rich layer
K. Spinel lherzolite, detached 5x5 cm
L. Spinel lherzolite (2 different pieces in basalt L1 and L2) 2x3 cm
M. Spinel lherzolite, fine grained

Note: All the above samples were distributed between TUBAF and UF only

N. Trachybasalt with small dunite, basalt and sedimentary xenoliths (to UPNG and GSC)
O. Dunite 2x3 cm
P. Pyroxenite with long (2 cm), black clinopyroxene, and interstitial chalcopyrite and malachite; appears to be slightly vesicular. (TUBAF and GSC only)
Q. Typical trachybasalt with small peridotite xenoliths. (Various representative pieces distributed to UPNG, CODES, and GSC)
R. Large trachybasalt with large dunite and various small xenoliths exhibits typical knobby surface texture.
S. Spinel lherzolite, extremely fine grained, 7x4 cm
T. Small Spinel lherzolite dunite, detached
U. Spinel lherzolite fragment

Group 3: Gabbroic xenoliths

A. Gabbro or dolerite, subophitic texture, veined, medium-grained, slightly altered; 6x5 cm
B. Gabbro, detached, medium-grained, plagioclase and clinopyroxene crystals, slightly altered. 6x7 cm
C. Gabbro, enclosing a clinopyroxene-rich microgabbro xenolith. 6x8 cm
D. Gabbro, mottled appearance, partially altered, clinopyroxene altered to amphibole?
E. Clinopyroxene-rich gabbro, partially altered. 7x4 cm

Note: All the above samples were distributed between TUBAF and UF only

F. Gabbro, medium-grained, altered (Kiel and GSC)
G. Gabbro, clinopyroxene-rich, partially altered, magnetic. Large 1/2 kg piece.
H. Gabbro (10 cm diameter). (UF and TUBAF)
I. Gabbro, broken up by lava and partially digested. (GSC and CODES)
J. Microgabbro, small round piece (UPNG, GSC)
K. Gabbro, coarse, altered with biology on it (TUBAF and biologists)
L. Gabbro with elongate clinopyroxene or amphibole crystals. (TUBAF and UF)
M. Gabbro, small (TUBAF and UF)
N. Microgabbro, detached, fairly fresh (TUBAF and UF)
O. Magnetite-rich gabbro (GSC and UF)
P. Olivine gabbro (GSC and UF)
R. Basalt xenolith (UF)

Group 4: Trachybasalt with mixed xenolith population; xenoliths are generally smaller and lava that contains it tends to be bigger.
Samples not distinguished, all labeled "4"

Group 5: Epidote-rich, altered gabbro ? that looks cataclastic and has an unusual veined texture. 10x10 cm

Group 6: Sedimentary xenoliths: some are carbonate-rich that show thin <1/2 cm reaction (metamorphosed?) rims.
A. Sandstone, grey-green, bedded. 0.5 kg.
B. Limestone? Calcilutite.
C. Carbonaceous mudstone, zoned 3x5 cm.
D. Mudstone, small with convoluted bedding, parts are calcareous.
E. Fine calcareous sandstone, similar to 6B.
F. Interbedded mudstone and carbonate siltstone (UF).
G. Sandstone, small rectangular fragment (UF).

55-GTVA

27 July, 1998 TUBAF Seamount; SW slope
Sample Site: 07:36 3°15.149' S 152°32.447' E Depth: 1220-1255m (1220m)

Aim: To sample basalts and xenoliths.

Operation: Sample taken quickly along a part of the slope that was densely covered with rock fragments (tephra) and very little pelagic sediment. Looked like a hard "pavement" of pebbles and cobbles.

Recovery: 75 kg of mostly pebble and cobble sized basalt clasts (tephra), only minor amounts of pelagic sediment. Half-dozen larger samples, most others were golfball to baseball sized.

Note: 2 bags (2 kg ea.) of smaller nodular basalt were distributed to the GSC and one 5 kg bag to UF.

General description: Grab was very similar to 54-GTVA. The counted distribution of xenolith sample types was: 19 ultramafic, 13 gabbro, 32 basalt samples with mixed xenolith populations, but commonly more sedimentary types.

Samples:

Group 1: Sediment
2 kg sample of sandy-gravely sediment comprised of basaltic clasts or cinder mixed with a small amount of pelagic ooze. (To UF to examine for volcanogenic features).

Group 2: Trachybasalt with peridotite xenoliths. Basalt has a highly vesicular (almost pumiceous) groundmass that contains flattened, irregular shaped vesicles (some pipe vesicles up to 0.5 cm long). Phenocrysts and microphenocrysts of phlogopite and clinopyroxene (phlogopite>>clinopyroxene). Estimate. 5 % phlogopite euhedral phenocrysts. Very little reaction of lava with enclosing xenoliths.
A. Spinel harzburgite with thin layer of Cr-diopside, granular. 7x3 cm
B. Dunite; spinel rich. 3x1 cm
C. Spinel lherzolite, fine-grained, inhomogeneous, light colored metasomatized zones and darker layers. 4x2 cm
D. Spinel harzburgite, fine-grained. 3x4x4 cm
E. Spinel harzburgite fine-grained, inhomogeneous. 3x4 cm
F. Harzburgite, fine-grained, inhomogeneous
G. Spinel harzburgite, coarse grained. 6x2.5 cm

F. Two samples of spinel harzburgite (spinel lherzolite with inhomogeneous distribution of minerals)
G. Spinel harzburgite, secondary fracture in the alteration
H. Harzburgite with spinel, granular. 4x2.5 cm
I. Spinel Lherzolite. 2x3 cm
J. Spinel Harzburgite, 4x2 cm

Note: All samples above were distributed to TUBAF and UF only because of their small and unique nature.

K. Peridotite (UPNG, CODES)
L. Dunite (UF only)

Group 3: Gabbroic xenoliths
A. Gabbro, partially assimilated or infiltrated with vesicular melt that is interstitial to crystals, weathered. 8x5 cm
B. Microgabbro, homogeneous with plagioclase, clinopyroxene, and magnetite; slightly altered with epidote common; magnetite rich zones; detached (6 cm diameter)
C. Microgabbro, clinopyroxene, plagioclase, magnetite; elongate plagioclase crystals. 2x3 cm
D. Microgabbro, intruded by host lava.
E. Gabbro, pyroxene-rich with magnetite and lesser plagioclase. 4x2 cm
F. Melanocratic gabbro, cut by veins of lava. 5x4 cm
G. Gabbro, medium-grained, olivine-bearing; granular (possibly cataclastic), partially altered

Note: All the above samples were distributed between TUBAF and UF only

Group 4: Basalt xenoliths
A. Basalt, fine grained, altered with olivine (?) phenocrysts (UF only)
B. Basalt, vesicular, clinopyroxene, olivine and plagioclase crystals; detached 3 cm diameter (UF only)
C. Epidotized lava (similar to 54-GTVA-5)

Group 5: Trachybasalt with mixed xenolith population; xenoliths are generally small and well dispersed throughout the sample.
A. Contains various small xenoliths and a layer of sediment
B. Larger sample with small dunite, sedimentary rock and gabbro
C. Small round basalt with sedimentary. and wehrlite xenolith
D. Contains sedimentary, gabbro and dunite xenoliths (TUBAF, UPNG)
E. Large basalt with few xenoliths (UF and UPNG).
F. Contains dunite, gabbro and small sedimentary xenoliths (CODES, UF).

Group 6: Sedimentary xenoliths: some are carbonate-rich that show thin <1/2 cm reaction (metamorphosed?) rims.
A. Lithic wacke with large component of basalt clasts (UF and UPNG)

56-GTVA

27 July, 1998 TUBAF Seamount, N side of crater on top of cone
Sample Site: 10:07 3°15.140' S 152°32.487' E Depth: 1243-1297m (1258m)

Aim: To sample basalts and xenoliths.

Operation: Grab traversed from SW to NE side of cone across the crater. Much of the crater was filled with pelagic sediment with ripple marks. Basaltic tephra was prominent on the rims of the crater and down the walls of the cone. In many places the tephra was so dense that it formed a hard pavement on the seafloor with only small, thin pockets of pelagic sediment. The traverse to the north side of the cone showed that basaltic clasts/tephra extends quite far down the flanks of the seamount but seem to get finer, further from the top. The sample was taken from the northern rim of the crater where the clasts started to become larger.

Recovery: 100 kg of pebble to cobble sized xenolith-bearing trachybasalt in a finer cinder-like sediment with minor pelagic sediments. Samples recovered were very similar to those in 54- and 55-GTVA (see above). Distribution of xenolith types is: 37 (large) + 28 (small) ultramafic, 31 gabbro, 13 sedimentary rocks, and 40 lava samples with mixed xenoliths.

Samples:

Group 1: Sediment; sand and pebble sized, rounded clasts/ejecta with minor amounts of pelagic ooze.

Group 2: Peridotite xenoliths in trachybasalt

A. Metasomatized, granular spinel lherzolite. Spinel in layers. 7 cm diameter
B. Peridotite; inhomogeneous with one portion dunite with veins and the other is lherzolite. 3x2.5 cm
C. Harzburgite, metasomatized
D. Spinel dunite, strongly veined. 4x2 cm
E. Spinel harzburgite, fine grained, light colored.
F. Spinel harzburgite, fine grained, granular, light colored. 4 cm diameter
G. Dunite, inhomogeneous, coarse grained, part may be wehrlite. 5x7 diameter
H. Spinel lherzolite with clinopyroxene veins; detached 8 cm diameter
I. Spinel websterite; detached
J. Spinel websterite, metasomatic veins; detached 4x4 cm
K. Spinel websterite, medium grained with veins and small fragment of spinel dunite in same trachybasalt. 4x3 cm
L. Spinel websterite, 4x2 cm
M. Dunite/websterite, heterogeneous larger sample; lower zone has odd texture where melt/lava has infiltrated the intergranular spaces and reacted with the mineral grains forming a white reaction zone around the black, vesicular lava.
N. Websterite or dunite, small layered sample
O. Spinel lherzolite (2 pieces), 4x3 cm
P. Spinel hartzburgite. 7x4x4 cm
Q. Spinel harzburgite. 1x2 cm
R. Spinel harzburgite 5x2.5 cm
S. Spinel harzburgite, coarse grained. 5x6 cm
T. Dunite, layered with concentrations of spinel and ortho/clinopyroxene, coarse grained. This is a very large sample, ~ 3 kg, originally 15x12x10 cm

U. Harzburgite, 2 separate samples, small round in basalt 5x4 and 4x3 cm
X. Small lherzolite with metasomatic vein.

Note: Smaller peridotite samples distributed to all groups in 2 separate bags. Largest piece of 2T to TUBAF.

Group 3: Gabbro, including pyroxene-rich types.
A. Melanocratic gabbro, rich in magnetite 2.5x3 cm.
B. Melanocratic gabbro, 4x3 cm.
C. Gabbro, medium grained, altered, detached small piece.
D. Melanocratic gabbro. 3x3 cm.
E. Gabbro, medium grained with magnetite rich zone. 4x3 cm.
F. Epidotized Gabbro, epidote appears layered and granular surrounded by different amounts of very dark, non-crystalline or cryptocrystalline material (replaced clinopyroxene?).(GSC, CODES, TUBAF, UF)
G. Olivine gabbro, medium grained with intercumulus plagioclase, possibly cumulate clinopyroxene, fairly fresh rock. detached (8x5x3).
H. Clinopyroxene-rich gabbro, layered with some secondary veining, intercumulus plagioclase.
I. Melanocratic gabbro with schlieren. 7x7 cm.
J. Melanocratic gabbro.
K. Pyroxene phyric basalt, chloritized?, 2.5x3 cm.
L. Gabbro with unusual, layered and epidotized texture, plagioclase xenocrysts (?).
M. Gabbro, magnetite-rich, medium grained. 3x2.
N. Melanocratic dunite and dunite.
O. Subophitic altered basalt.
P. Augen-shaped basalt xenolith.

Note: Bulk gabbroic samples (~10) distributed to UPNG, GSC and CODES.

Group 4: Sedimentary xenoliths
A. Bedded wacke, feldspar and clinopyroxene-rich interbedded with a small piece of fine mudstone.
B. Layered mudstone.
C. Sandstone/wacke.
D. Calcareous mudstone, detached.
E. Interbedded dark and fine mud and lighter calcareous siltstone: detached.
F. Fossiliferous limestone.

Note: Various others to CODES and UPNG.

Group 5: Trachybasalt with mixed assemblage of xenoliths, generally small.
A. Plagioclase granite (?), small felsic fragment.
B. Gabbro and peridotite.
C. Dunite and basalt.
D. Various basalt samples with xenoliths.

Note: Large unaltered basalt sample (3 kg) to UF (for possible dating).

61-GTVA

28 July, 1998 New World Seamount
Sample Site: 01:24 2°50.719' S 152°32.705' E Depth: 1127-1134m (1134m)

Aim: To sample igneous rocks for petrogenetic comparison with other islands and seamounts.

Operation: TV-grab sample.

Recovery: 90 kg of mud and crusty indurated sediment.

Results: Nanofossil ooze, no igneous rocks.

Samples:
Sample 1: Sediment for X-ray
Other samples to biologists and sedimentologists

62-GTVA

28 July, 1998 New World Seamount
Sample Site: 03:01 2°50.731' S 152°32.691' E Depth: 1126-1137m (1134m)

Aim: Map top of New World Seamount.

Operation: One hour spent mapping, grab taken of suspected igneous rocks or sedimentary crusts.

Recovery: Carbonate concretions and sediment.

Samples:
Sample 1: Sediment for X-ray

68-GTVA

29 July, 1998 Horst structure south of Edison SMT
Sample Site: 09:30 3°18.742'S 152°35.731'E Depth: 1485 m

Operation: Extensive survey of the base of the cliff, possibly sample gas hydrates

Aim: To look for gas hydrates or hydrothermal activity.

Recovery: Carbonate concretions and sediment.

Results: A large sample of pelagic sediment with some crusts.

Samples:
Sample 1: Sediment for X-ray

72-GTVA

29 July, 1998 Small seamount SSE of Conical Seamount
Sample Site: 23:39 3°20.413'S 152°40.110'E Depth: 1688

Aim: Looking for igneous rocks.

Operation: Surveyed on bottom for 38 minutes, large sample taken.

Recovery: 400 kg of tan-brown hemipelagic mud and foram. ooze. Some darker layers and filled bore holes are apparent. No coarse material was obtained. Some carbonate concretions, sediment thickness minimum of 50 cm.

Samples:
Sample 1: Sediment for X-ray (250 g to UF).

73-GTVA

30 July, 1998. Slightly larger seamount to ESE of Conical Seamount.
Sample Site: 01:30 3°20.051'S 152°40.713'E Depth: 1668

Aim: Looking for igneous rocks.

Operation: Heavy sediment cover (like 72-GTVA) made it impossible to grab any rocks. Reflection profile suggests more than 5 m of sediment cover top of seamount (at 5+ cm/ka sedimentation rate the age would be over 100,000 years).

Recovery: No samples.

74-GTVA

30 July, 1998 Small seamount NW of Conical Seamount
Sample Site: 05:20 3°17.775'S 152°38.208'E Depth: 1489m

Aim: Looking for igneous rocks.

Operation: Towed grab around the edge of the cone and down the flanks. Mostly covered with pelagic sediment but has a significantly greater amount of coarser material that is mostly pebble sized or smaller. Upper flanks of cone have rarer, slabby outcrops that were difficult to find. One outcrop on south side and another found on NW side (which was sampled).

Recovery: 200 kg of mostly indurated and veined, carbonate sands.

Results. Vari-colored and extensively veined, indurated sediments. Most are soft enough to break by hand. Anastomosing veins of red, green and black material are common.

Samples:
Group 1: Sediments for X-ray
A. Buff colored sediment
B. Pale green colored unconsolidated clay
C. Brown crusty rubble

D. Deep green sediment from veined area
E. Black/dark green sediment from vein

Group 2: Indurated sediment
A. Variegated with veins and lenses of material in Group 1. Veins are parallel to bedding, but some are crosscutting, anastomizing. Give a "braided" pattern to cut surfaces of sediment. Green veins are thought to be nontronite which grades upward into red-brown oxidized zones.
Also contains worm burrows and highly permeable zones filled with darker green sediment/clays. Pteropod shell zones are common. Rare small clam shell also found in sediment.

75-GTVA

30 July, 1998 Small seamount (Edi's Daughter), NW of Edison Seamount, in line with TUBAF Seamount.
Sample Site: 07:22 3°17.643'S 152°34.895'E Depth: 1470m

Aim: Looking for igneous rocks.

Operation: Grab samples up SW wall of cone where much slabby and nodular appearing basalt was observed covered with thin sediment. Clam/mussel shells were also observed along the flanks of the seamount. Grab was taken near large lava blocks and cobbles near the top of the cone.

Recovery: 70 kg of angular to rounded boulders (a few up to 10 kg and 30 cm wide) and cobbles. Pelagic sediment mixed with basaltic sand.

Results: Lava samples include ankaramite and more evolved clinopyroxene and plagioclase phyric basalt showing various amounts of weathering and low-temperature alteration (zeolite). Samples were divided into 3 groups based on mineralogy and vesicularity, but they are probably gradational in nature. Samples are partially coated with thin (mm) Fe-Mn oxide layer.

Samples:
Sample 1: Clinopyroxene and plagioclase-phryic basalt (trachybasalt?) with minor vesicularity. Most show some degree of alteration or weathering that is commonly concentrated on the outer rinds or along fractures.
A. Basalt, partially weathered with small clinopyroxene and plagioclase phenocrysts; plagioclase abundant in groundmass; non-vesicular, weathering concentrated in outer rind and along fractures, core is fresh. (UF, TUBAF, UPNG)
B. Angular, slightly vesicular clinopyroxene and plagioclase-phyric basalt
C. Slightly weathered slabby basalt similar to above with distinct weathered rind. Possible rare olivine.
D. Basalt, round, vesicular with pilotaxitic texture; plagioclase and clinopyroxene in equal amounts, rare olivine.

Note: all above to TUBAF and UF only except were noted.
E. Various different types of basalt, mostly more weathered, some quite oxidized

Sample 2: Ankaramite, clinopyroxene-rich, clinopyroxene generally large euhedra and microcrystalline part of groundmass, rare olivine.
A. Ankaramite; relatively low vesicularity, fine-grained groundmass, slightly altered; trace chalcopyrite and possible native copper; 1 kg.
B. Pyroxene-rich basalt fairly fresh but clinopyroxene partially altered to chlorite, small amount of plagioclase in groundmass, 500 g. (UF, TUBAF).
C. Ankaramite; slightly vesicular with rare olivine, fairly fresh, 300 g.
D. Similar to sample B. 500 g (UF, TUBAF)
E. Two small, somewhat weathered basalt (TUBAF and UPNG).

Sample 3: Vesicular ankaramite
A. Ankaramite; euhedral clinopyroxene partially altered to chlorite, trace of olivine; round to flattened ovoid vesicles up to 2 cm long; zeolite in some vesicles and fractures. 500 g (UF, TUBAF, UPNG)
B. Ankaramite, vesicular, partially altered with zeolite minerals (stilbite, chabazite) in vesicles.

80-GTVA

31 July, 1998 Conical Seamount
Sample Site: 09:24 3°18.725'S 152°39.569'E Depth: 1092m

Aim: To sample hydrothermal material and to define limits of the hydrothermal system.

Operation: Surveyed for mineralized samples; grab did not close properly (batteries low).

Recovery: Mud.

Results: Pelagic ooze and some crust material

Samples: Sample 1: Sediment for X-ray

83-GTVA

31 July, 1998 Top of Conical Seamount
Sample Site: 01:51 3°18.725'S 152°39.558'E Depth: 1091m

Aim: To sample hydrothermal material and to define limits of the hydrothermal system.

Operation: Surveyed for almost 3 hours to locate a suitable sample; grab successful.

Recovery: 75 kg of boulder and cobble-sized highly altered samples recovered.

Results: Sample contained homogenous grey, zonally altered ankaramite, some with thick oxide crusts. All contained disseminated pyrite. The larger samples demonstrate that the zonal alteration proceeded along propagating fractures, and that fluids diffused outwards to develop distinct zones of clay-rich, silica rich and sulfidized ankaramite. The rock disintegrated into cobbles on sampling, breaking along intensely altered fractures. Bulk sample has been sieved to sample sulfides enriched in the fine fraction.

Samples: Three groups of samples are defined:
Group 1: Sandy grey mud
Group 2: Zonally altered ankaramite.
Group 3: Oxide crusts.

Group 1: Clay-rich grey ooze
A: Fine-grained, clay-rich mud.
B: Coarser and highly altered mud; probably represents most altered fraction of ankaramite.

Group 2: Altered basalt. Very consistent, homogeneous sample of altered ankaramite. All samples have about the same content of pyroxene (usually altered) and of vesicles (locally filled). Two sizes of samples were collected. Most are cobble-sized (6x6x10 cm), and several are larger (20x20x20 cm). All samples are completely non-magnetic (demagnetized due to alteration). Most contain about 1%-disseminated pyrite, plus pyrite coated vesicles. A few samples have distinct discontinuous pyrite veinlets, up to 2 mm in width. Where pyrite replaced pyroxene phenocrysts, it is coarser grained (~1 mm cubes). All pyroxene is altered to white clay/silica, with ghost remnant pyroxene (probably chlorite) in a the less altered cores of the zonally altered samples. Regular zonal alteration occurs around the subgroup of ovoid, cobble - sized samples. Alteration consists of a dark grey, locally oxidized rim zone, typically 0.5 cm wide, followed inwards by a white, silica-rich zone, 1-2 cm thick that contains 1-2% pyrite, all cored by a zone of darker grey, less altered ankaramite that contains about 1% pyrite.

The subgroup of larger samples, cu on the large saw, illustrate the zoning relationship very well. The alteration zones are concentric about propagating fractures in the more massive or lobate forms. The fracture patterns are orthogonal, resulting in a regular jointing and disintegration of the larger samples into sub-equally sized cobbles. The larger samples provide an indication of the overall process that led to the disintegration of the altered ankaramite.

Sample 1: Grey mud, taken for XRD.

Sample 2: Zonally-altered ankaramite
A: Small (4x5x5)sample of zonally altered absalt with disseminated pyrite (0.5%) throughout. Distinct silica zone, about 8 mm inside the surface, and 4 mm wide. The core of this sample is darker grey, and may be more sulfide-rich.
B: Similar to A, but with a darker core, and less silica. It seems more sulfide-rich (1%).
C: Large sample of fractured basalt, illustrating the fracture relationship of the zonal alteration.
D: Large sample of lobate flow, also illustrating alteration and fracture relationships.

Sample 3: Several small pieces of oxidized crust material. All given to XRD specialist (J. Percival)

84-GTVA

01 Aug., 1998 Top of Conical Seamount
Sample Site: 03:29 3°18.717'S 152°39. 539'E Depth: 1092m

Aim: To sample hydrothermal material and to define limits of the hydrothermal system.

Operation: After about one hour of surveying, did not get a good bite.

Recovery: About 10 kg of mud containing a few small fragments of rock.

Results: Recovered a small amount of pyritic weathered basalt and oxide crusts.

Samples:

Sample 1: Hemipelagic mud (to XRD only).

Sample 2: Pyritic (~1%) weathered basalt; pyroxenes are chloritized, highly vesicular, with most of the pyrite in the vesicles. There is a trace of disseminated pyrite in the matrix.

Sample 3: Oxide crusts: These are yellow to red, locally highly brecciated and silicified (silica granules). Some pieces of crust have remnant basalt textures, which are very weathered and oxidized.

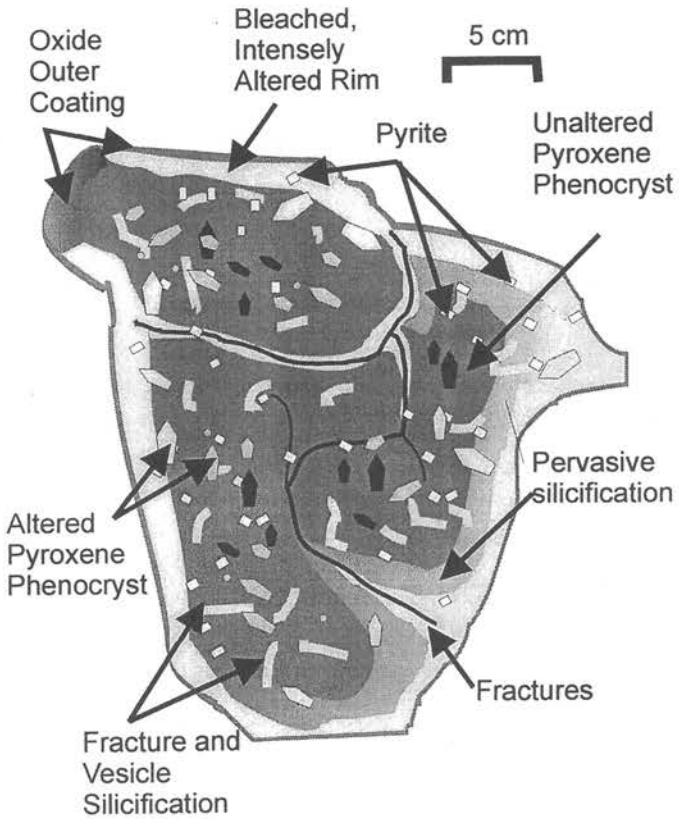

Figure 4.4: Sample 83GTVA-2c, illustrating zoned alteration.

7-DR

12-DR

13-DR

13-DR

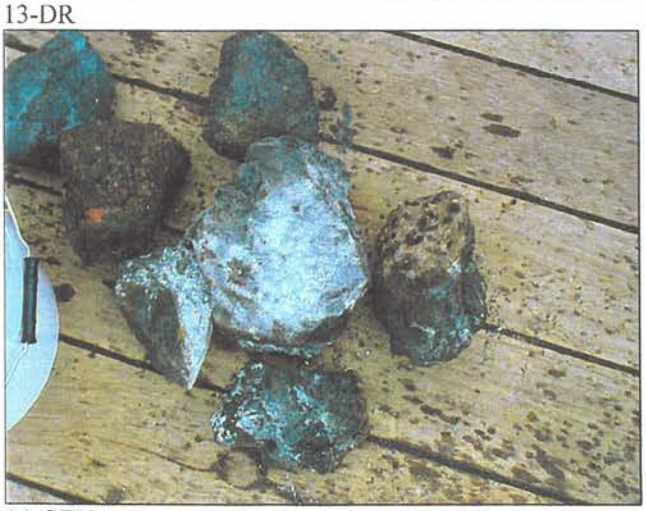

14-GTVA

15-GTVA

Figure 4.5: Sample photographs representing material recovered from Conical Seamount.

a	b
c	d
e	f

a) Vesicular pyroxene-phyric and ancaramitic basalt (sample 07-DR)
b) Ancaramitic basalt showing Fe-Mn-oxyhydroxide staining (sample 12-DR)
c) Highly vesicular ancaramitic basalt with Fe-oxide rim (sample 13-DR)
d) Porous Fe-oxide crust (sample 13-DR-2)
e) Various pieces of highly altered and mineralized pyroxene-bearing basalt with silica lining fractures and vesicles (sample 14-GTVA)
f) Various pieces of mineralized basalt similar to material recovered at station 14-GTVA (sample 15-GTVA).

15-GTVA

15-GTVA

20-DR

21-DR

26-GTVA

26-GTVA

Figure 4.6: Sample photographs representing material recovered during RV SONNE cruise SO-133.

a	b
c	d
e	f

a) Large subsample of altered basalt showing intense silicification (sample 15-GTVA, Conical Seamount)
b) Close-up of amorphous silica lining vesicles and fractures (sample 15-GTVA)
c) Dark-pyroxene-rich lava from TUBAF Seamount (sample 20-DR)
d) Xenolith-bearing basalt from TUBAF Seamount (sample 13-DR-2)
e) Large pieces of intensly mineralized gold-rich basalt (sample 26-GTVA)
f) Close-up of intensly mineralized basalt showing amorphous silica, realgar and auripigment lining fractures and vesicles (sample 26-GTVA).

Figure 4.7: (opposite page)
Sample photographs representing material recovered during RV SONNE cruise SO-133.

a	c
b	d
e	f

a) Intensly altered and mineralized basalt (sample 39-GTVA, Conical Seamount)
b) Close-up of slabs showing pyrite/marcasite veins cutting vesicular basalt (sample 39-GTVA)
c) Vesicular basalt rimmed by intensly mineralized breccias (see arrows; sample 53-GTVA)
d) Selection of peridotitic xenoliths in basalt from TUBAF Seamount (sample 56-GTVA)
e) Peridotite and meta-sediment inclusions in basalt (sample 54-GTVA, TUBAF Seamount)
f) Selection of various xenoliths including microgabbros (front right, sample 54-GTVA).

39-GTVA

53-GTVA

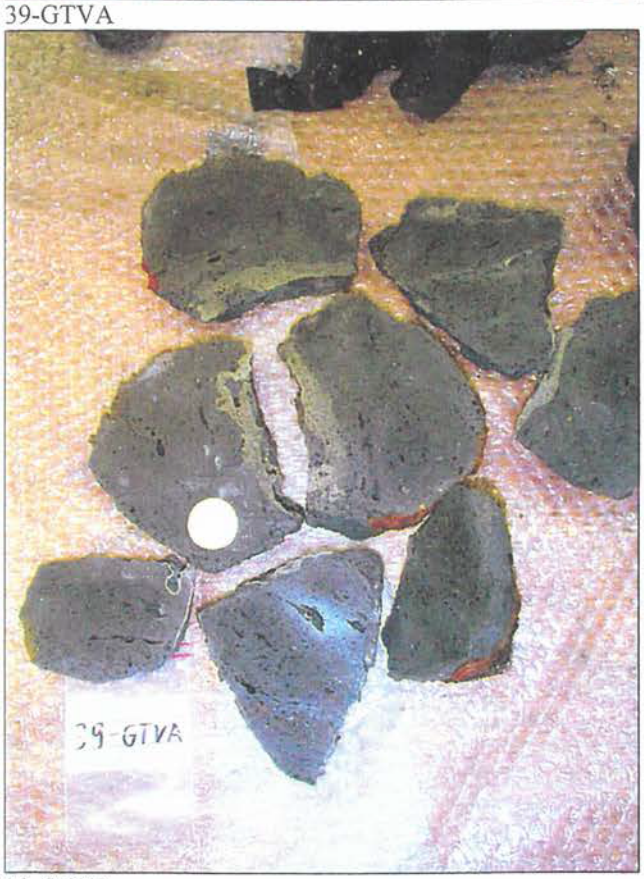

39-GTVA

56-GTVA

54-GTVA

54-GTVA

74-GTVA

74-GTVA

75-GTVA

75-GTVA

83-GTVA

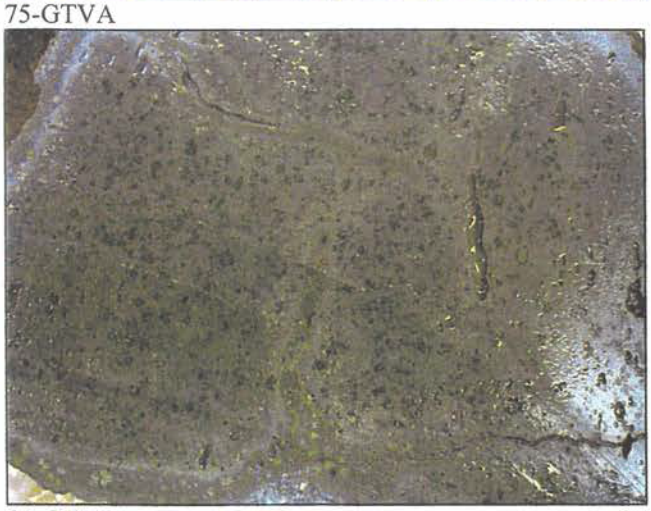

83-GTVA

Figure 4.8: Sample photographs representing material recovered during RV SONNE cruise SO-133.

a	b
c	d
e	f

a) Indurated sediment with green surface coatings suggesting the presence of nontronite (sample 74-GTVA, from small seamount NW of Conical Seamount)
b) Close-up of indurated Fe-oxyhydroxides (sample 74-GTVA)
c) Vesicular pyroxene-rich and plagioclas-phyric lava (sample 75-GTVA, Edi's Daughter)
d) Close-up of cut surface showing intense weathering (sample 75-GTVA, Edi's Daughter)
e) Slightly altered and mineralized basalt (sample 83-GTVA, Conical Seamount)
f) Close-up of cut slab showing small pyrite veinlets in vesicular basalt (sample 83-GTVA)

5 Sedimentology

BY KYAW WINN, KERSTEN HORZ & PETER STOFFERS

5.1 Objectives

The aim of the sediment studies is the reconstruction of the volcanic history of the New Ireland Fore Arc based on discrete ash layers within the sediment cores. The detailed petrography and geochemical study of these ash layers together with the acoustic data from the parasound should allow the estimation of the amount of ash input as well as the identification of their origin and provenance.

5.2 Sediment Stations

5.2.1 Geological Considerations

The coring stations were sited in a geographical grid required to define and delineate the possible transport means and directions of the volcaniclastics. During the EDISON II cruise, we could close the profiles around the Tabar-Simberi Group and the Lihir Island. Two stations (GIK-17674, GIK-17675, see Fig. 1, Tab. 5.1) were located west and northwest of Simberi Island complementary to core GIK-16992 of the EDISON I cruise. GIK-17676 sited south of the Lihir-Tabar Islands should give information on the depositional history and on the volcanic activity. A core profile with 3 main stations (GIK-17681, GIK-17682 and GIK-17683/84) north of the Lihir and Tanga were intended to supplement our knowledge not only on the eruptive history of the nearby volcanoes but also to clarify if more distant sources (e.g. Feni, Rabaul) should also be taken into consideration.

Supplementary to the sediment program on the EDISON I cruise, the present sediment cores were taken further away from the islands or in areas between the islands not covered by the earlier survey. A list of the coring stations is given in Table 5.1, and a description of the cores which have been worked on so far is listed in the appendices.

5.3 Coring Operations

Raising cores with recovery of reasonable length sufficient for sedimentological-geochemical investigations has always been a problem in volcanic areas because of lava flows and volcanic ejectamenta, especially thick ash, pumice, and turbidites. The first cores with recoveries over a meter (max. 7 m) from this area were raised during the EDISON I expedition. In problematic areas of the last cruise as, for example, the sector west and northwest of Simberi Island, where coarser sediments combined with hard volcanic ash dominate, core penetration and recovery also remained minimal (< 2m) during this cruise,. It also resulted in damaged core barrels during the first three sediment stations. In the biologically active methane area discovered during this cruise, a core over 3 m length could be recovered with 3 thick concretionary crusts "hardground" which, however, also caused a bent corer. Better core recovery, as expected, was attained in the area north of Lihir-Tanga. A record length for the area of 8.32 m was raised with a gravity corer released through a trigger weight (Table 5.1).

5.4 Parasound Profiles

Parasound profiles onway to the core stations provide a first insight into the expected sediment sequence (seismic-stratigraphy). In areas with variable but normal deep sea sediments, acoustic reflectors were very irregular and dominantly parallel to each other. In our area, strong parallel

reflectors could also be caused by tephra layers, and dependent upon their lithological characteristics, grain size and degree of compaction, limit the length of recovery (e.g. GIK-17674, Fig. 2a; GIK-17675, Fig. 3a; GIK-17684, Fig. 11a).

Table 5.1: Location of cores, New Ireland Basin, Papua New Guinea

Date (UTC)	Shipboard No. SO133/2	Archive No. GIK	Latitude (°S)	Longitude (°E)	water depth (m)	core length (m)	remarks
20.07.98	01-GKG	17674-1	2°07.17	151°33.98	1716	0.45	NE Simberi Is.
	02-SL	17674-2	2°07.15	151°34.01	1716	1.20	NE Simberi Is.
20.07.98	03-GKG	17675-1	2°29.95	151°33.28	1898	0.43	W Simberi Is.
	04-SL	17675-2	2°29.97	151°33.25	1897	2.05	W Simberi Is.
22.07.98	08-GKG	17676-1	3°02.00	152°21.02	1860	0.46	SE Tabar Is.
	09-SLS	17676-2	3°02.00	152°21.01	1861	2.94	SE Tabar Is.
25.07.98	37-GKG	17677-1	3°37.24	152°57.29	2516	0.40	SW Tanga Is.
	38-SLS	17677-2	3°37.28	152°57.18	2516	3.60	SW Tanga Is.
27.07.98	57-GKG	17678-1	3°19.37	152°35.31	1610	0.43	SSW Lihir Is.
	58-SLS	17678-2	3°19.36	152°35.45	1574	3.21	SSW Lihir Is.
27.07.98	59-GKG	17679-1	3°19.34	152°35.46	1573	0	SSW Lihir Is.
27.07.98	60-GKG	17680-1	3°19.36	152°35.35	1625	0.46	SSW Lihir Is.
28.07.98	63-GKG	17681-1	2°23.99	152°50.83	1831	0.40	NNE Lihir Is.
	64-SLS	17681-2	2°23.95	152°50.85	1830	7.41	NNE Lihir Is.
28.07.98	65-GKG	17682-1	2°38.96	153°01.93	2040	0.45	NE Lihir Is.
	66-SLS	17682-2	2°38.98	153°01.90	2045	8.32	NE Lihir Is.
29.07.98	69-GKG	17683-1	3°04.60	153°04.05	2408	0	E Lihir Is.
29.07.98	70-SLS	17684-1	3°06.40	152°59.86	2387	3.18	E Lihir Is.

Abbreviations: GKG = big box core, SL = gravity core, SLS = gravity core with triggerweight.

Irregular reflectors, whose thicknesses lay below the resolution of the parasound (e.g. black ash layers in GIK-17677, Fig. 5a) do not themselves prevent penetration, but the total sedimentary sequence is very hard and compact. Volcanic debris (e.g. pumice) has variable spatial distribution and was observed as discontinuous reflectors on the sea floor. Because of their lightness, the pumice could be transported over large distances, and deposited far from their source (GIK-17683, Fig. 10a).

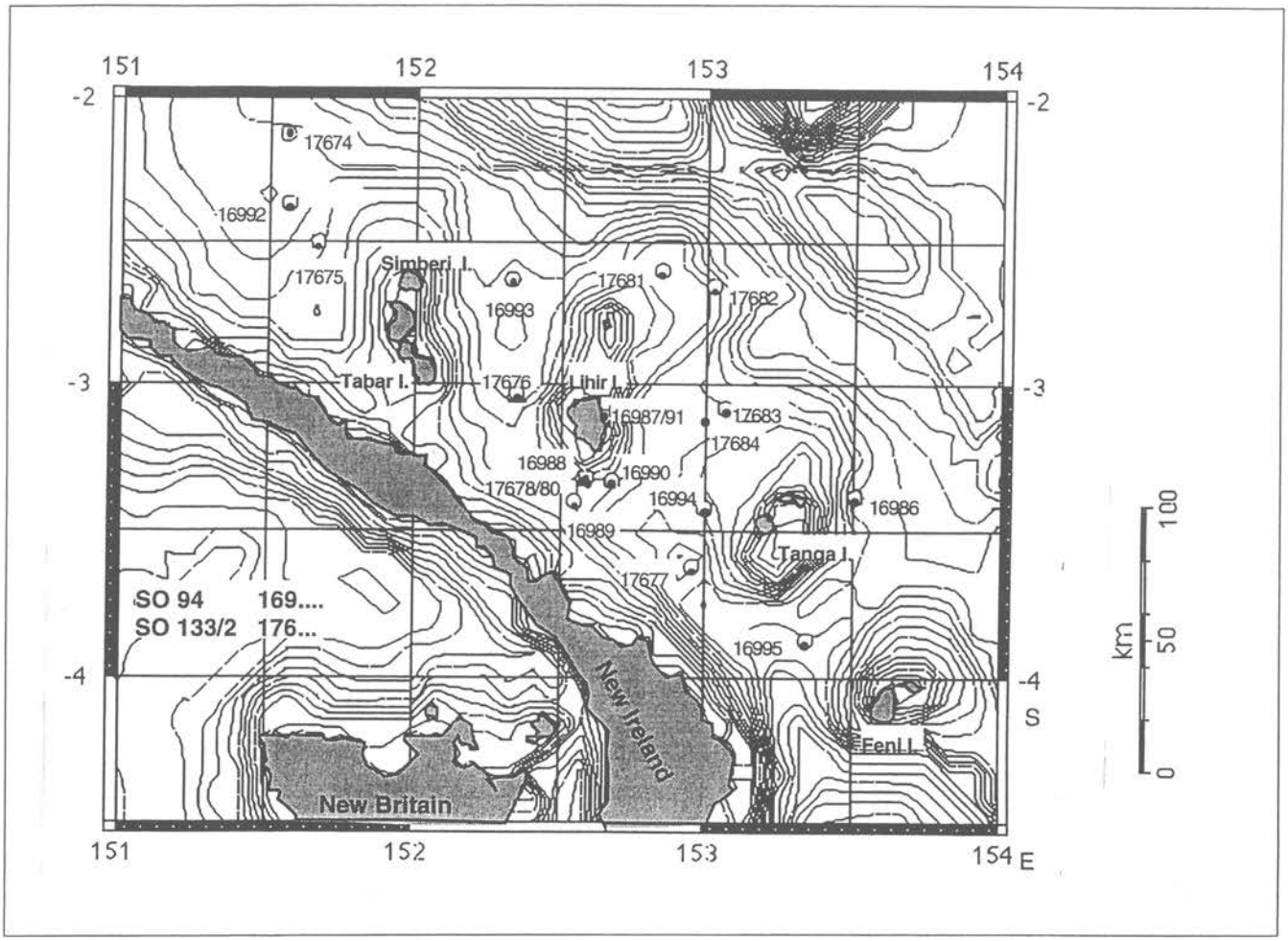

Figure 5.1: Locations of sediment core stations: EDISON I (SO-94, GIK-169.. series) and EDISON II (SO-133/2, GIK-176.. series). Prefix GIK-= Geological Institute Kiel

During the EDISON II cruise, extremely gas rich sediments populated with clams were discovered at a horst and graben structure south of Lihir Island. Here, the variable reflectors turned out to be concretionary crusts that were lithified through calcareous cement forming "hardgrounds". The core recovery was moderate (GIK-17678, Fig. 6a, 6c). A box core (GIK-17680) had a sinuous opening representing the path of gas escape to the sediment surface measuring 2.5 cm in diameter. Numerous other holes are all less than 1 cm in diameter. Parasound recordings were also made parallel to the hydrosweep mapping of the Lihir area. However, the quality of the records were generally poor due to the highly variable sea-bottom morphology which required frequent manual setting on the bottom echo, and the relatively high speed (8 Knots) with which the surveys were conducted.

5.5 Magnetic Susceptibility

Magnetic susceptibility is a useful tool for the identification of volcanic ash layers and in core to core correlation. It has no dimensions and reflects the amount of magnetic minerals in the sediment. For uniformity, we measure at 1 cm intervals and report in cgs units, with the zero value equal to the measurement in air. As with the EDISON I cruise, magnetic susceptibility was measured on the whole core on all the gravity cores we raised. In the case of the big box cores, the measurements were made on the 12 cm core liners pushed through the sediment layers (Fig. 2b to 11b). Correlation with the gravity core from the same station then showed the amount of surface sediment missing in the gravity core.

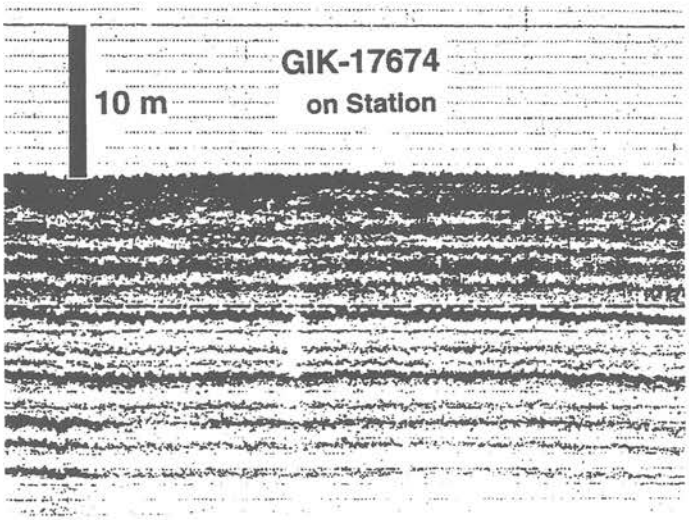

Fig. 2a: Parasound record of SO 133/2-1 GKG, -2 SL (GIK-17674). Note very strong near surface reflectors.

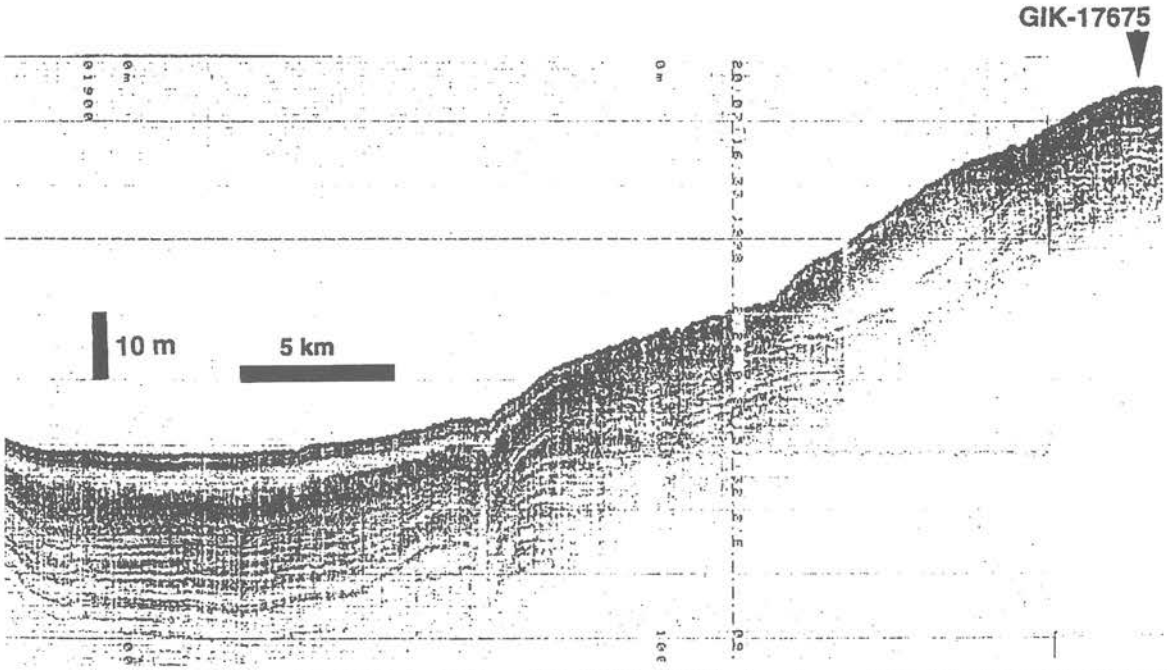

Fig. 3a: Parasound profile to SO 133/2-3 GKG, -4 SL (GIK-17675), showing sediment wedges and erosional boundaries.

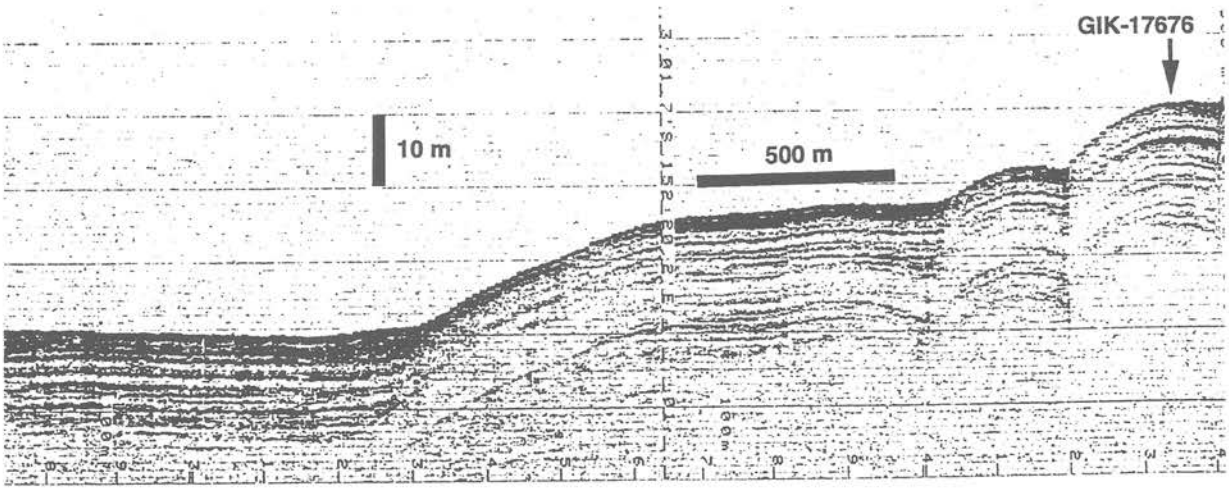

Fig. 4a: Parasound profile to core station SO 133/2-8 GKG, -9 SLS (GIK-17676).

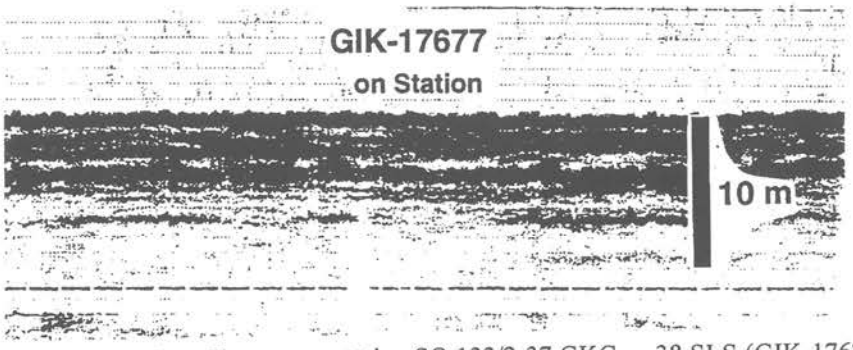

Fig. 5a: Parasound profile on core station SO 133/2-37 GKG, -38 SLS (GIK-17677).

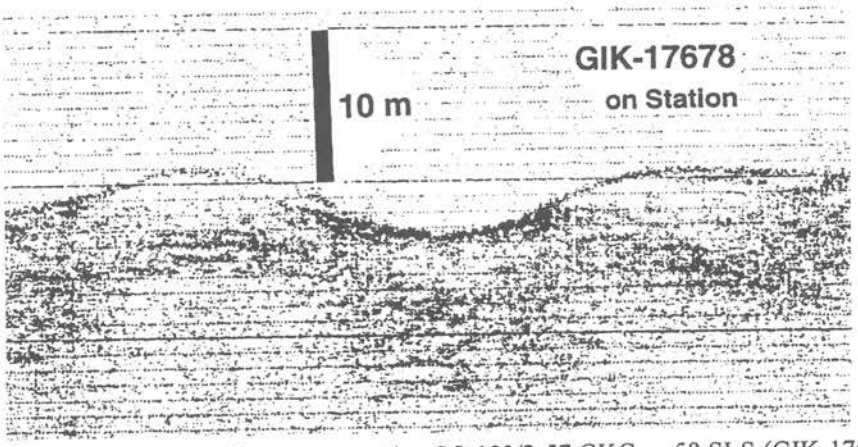

Fig. 6a: Parasound profile on core station SO 133/2-57 GKG, -58 SLS (GIK-17678). Note interference through side reflectors.

Fig. 7a: Parasound profile on core station SO 133/2-60 GKG (GIK-17680).

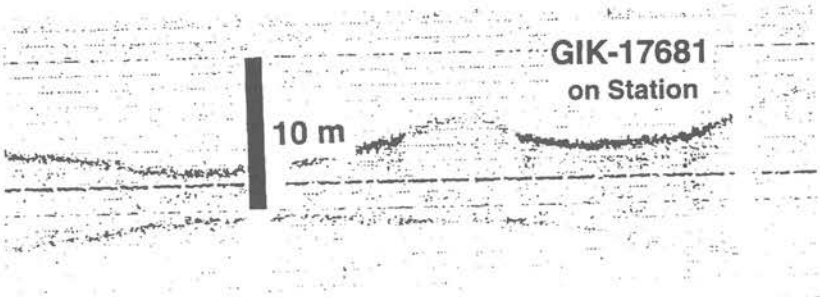

Fig. 8a: Parasound profile on core station SO 133/2-63 GKG, -64 SLS (GIK-17681).

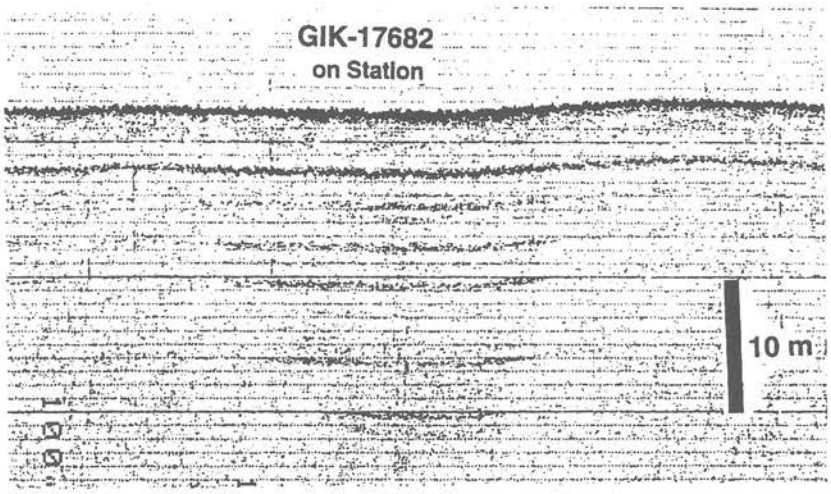

Fig. 9a: Parasound profile on core station SO 133/2-65 GKG, -66 SLS (GIK-17682).

Fig. 10a: Parasound profile on core station SO 133/2-69 GKG (GIK-17683).

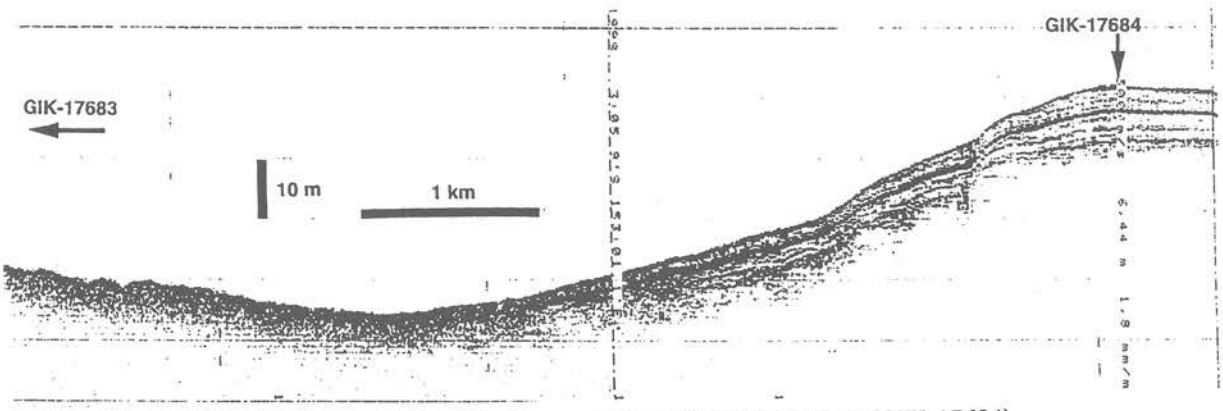

Fig. 11a: Parasound profile to core station SO 133/2-70 SLS (GIK-17684).

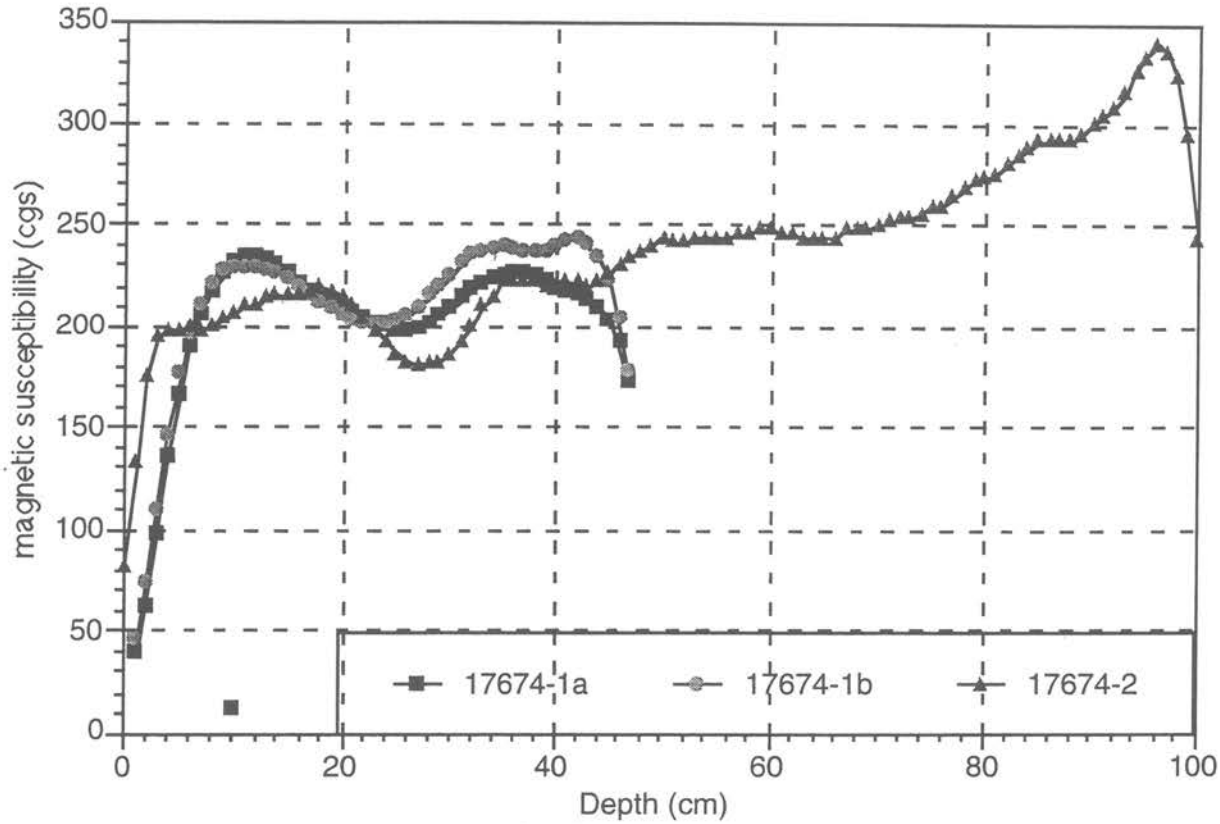

Fig. 2b: Magnetic susceptibility measurements in GIK-17674-1 GKG and -2 SL.

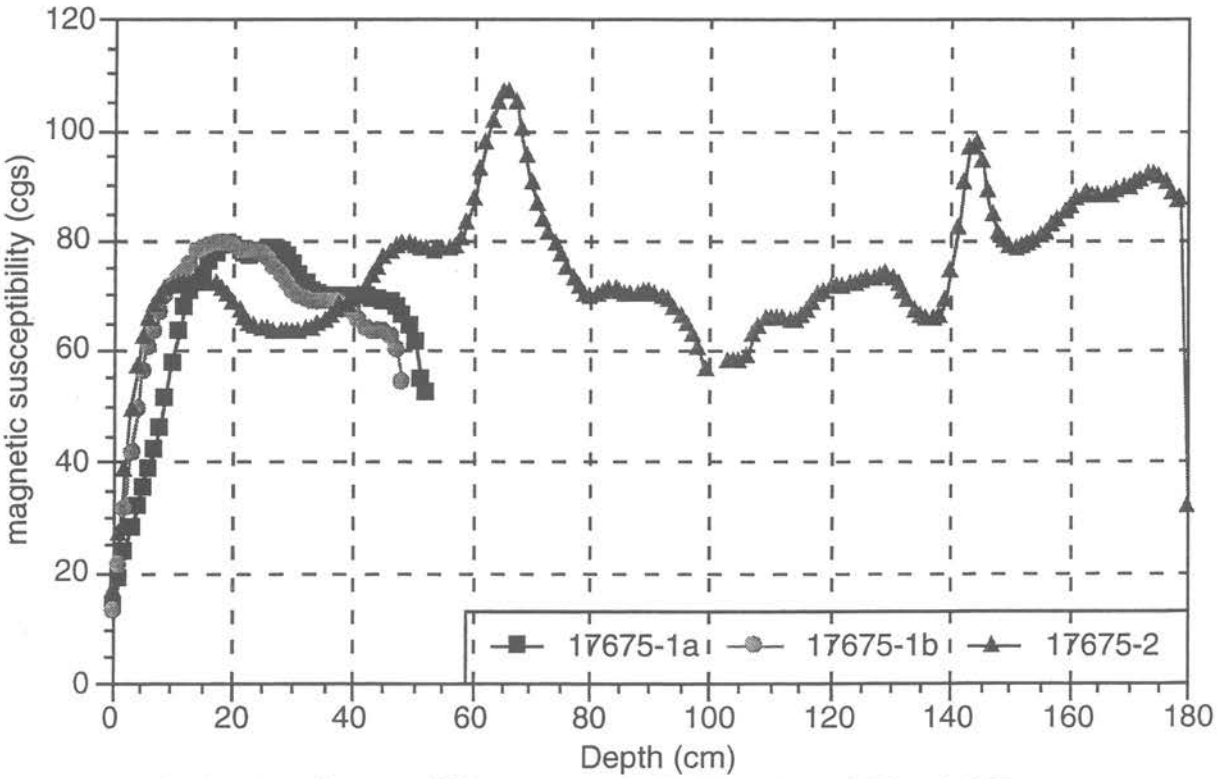

Fig. 3b: Magnetic susceptibility measurements in GIK-17675-1 GKG and -2 SL.

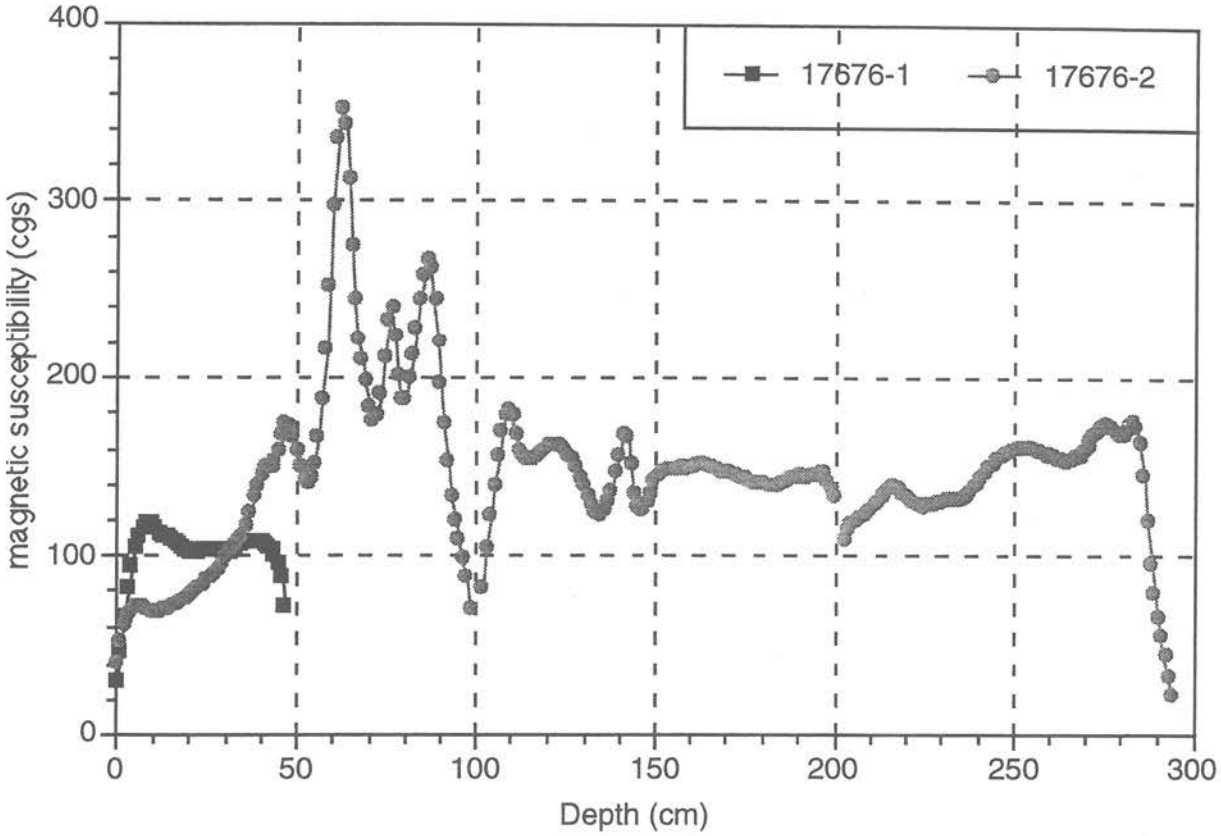

Fig. 4b: Magnetic susceptibility measurements in GIK-17676-1 GKG and -2 SLS.

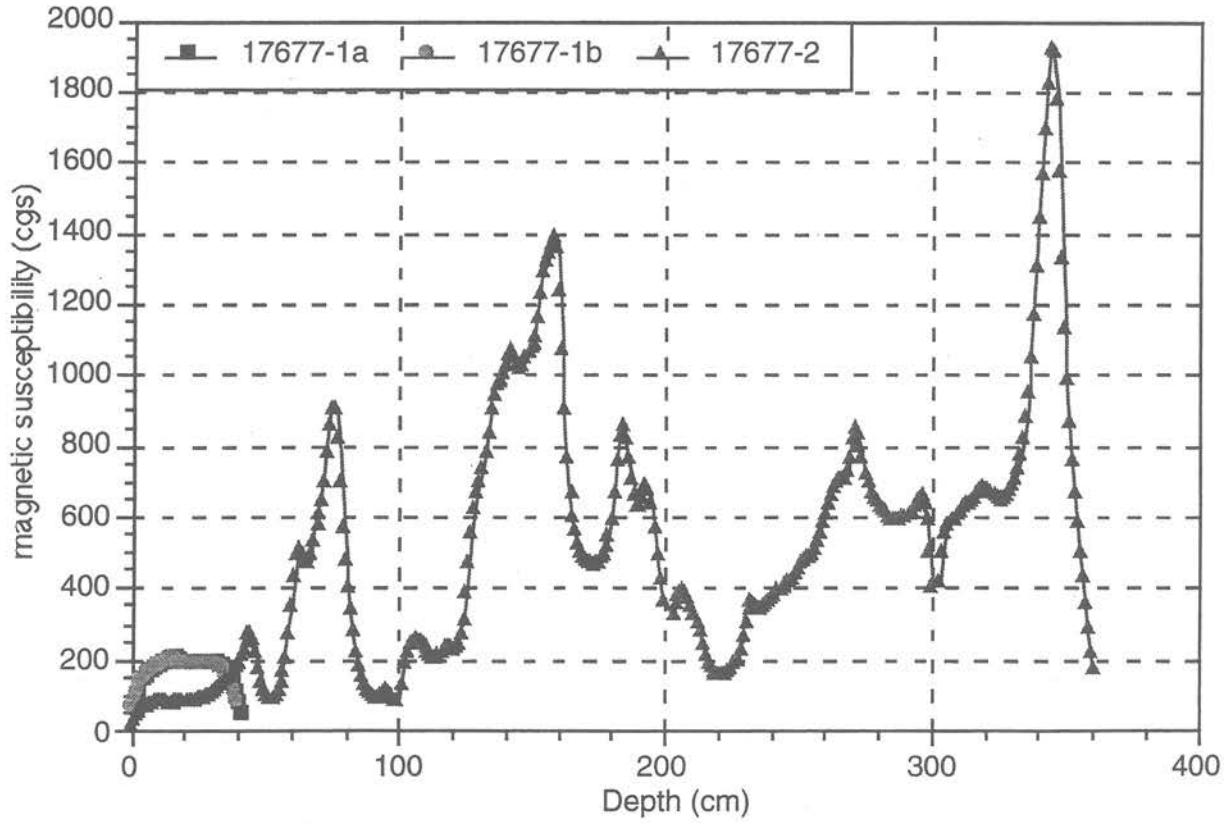

Fig. 5b: Magnetic susceptibility measurements in GIK-17677-1 GKG and -2 SLS.

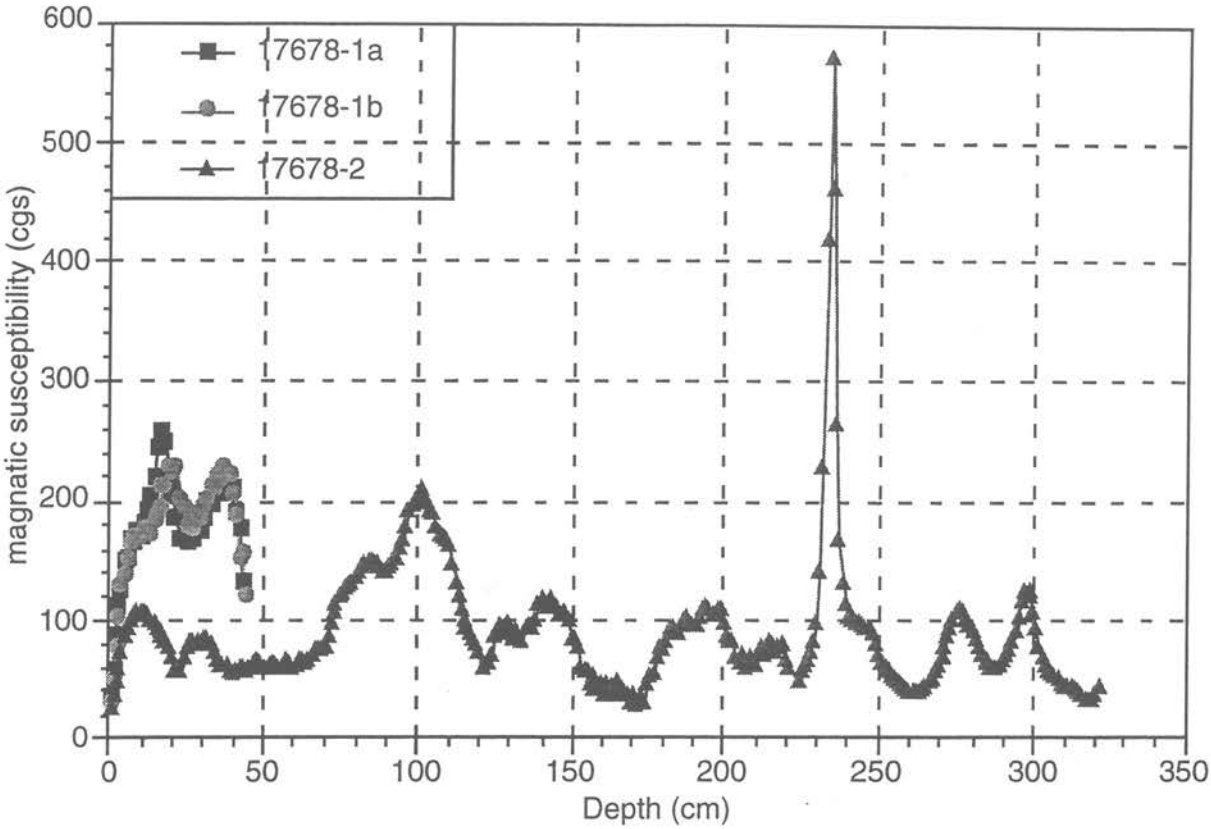

Fig. 6b: Magnetic susceptibility measurements in GIK-17678-1 GKG and -2 SLS.

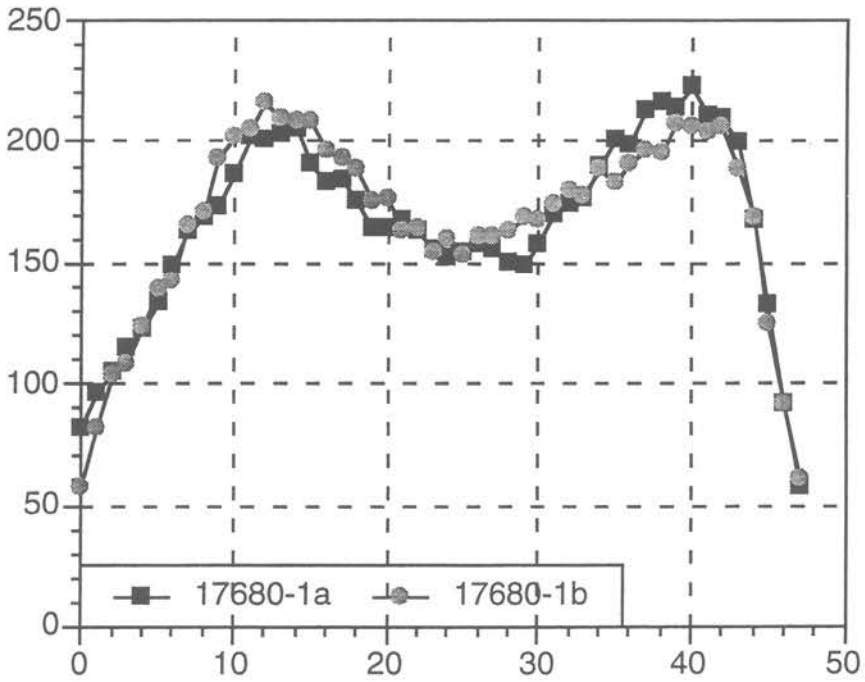

Fig. 7b: Magnetic susceptibility measurements in GIK-17680-1 GKG.

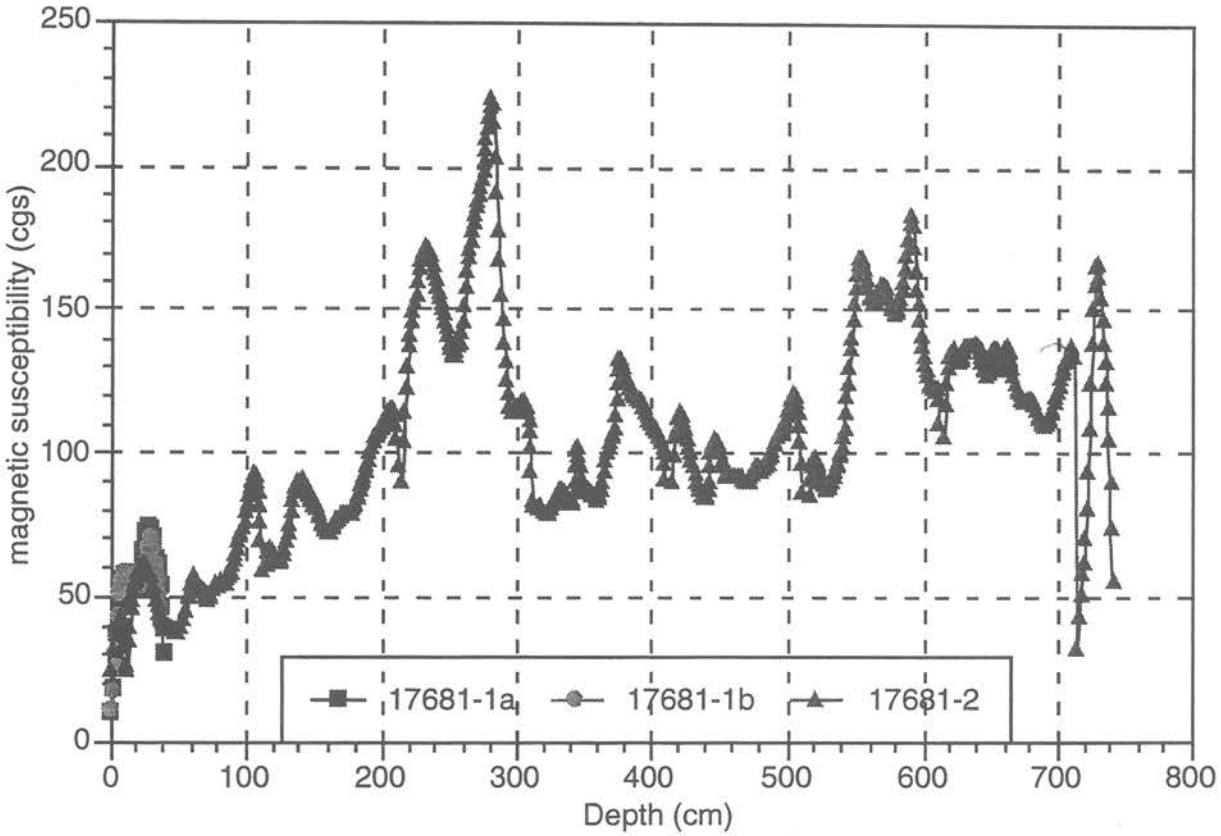

Fig. 8b: Magnetic susceptibility measurements in GIK-17681-1 GKG and -2 SLS.

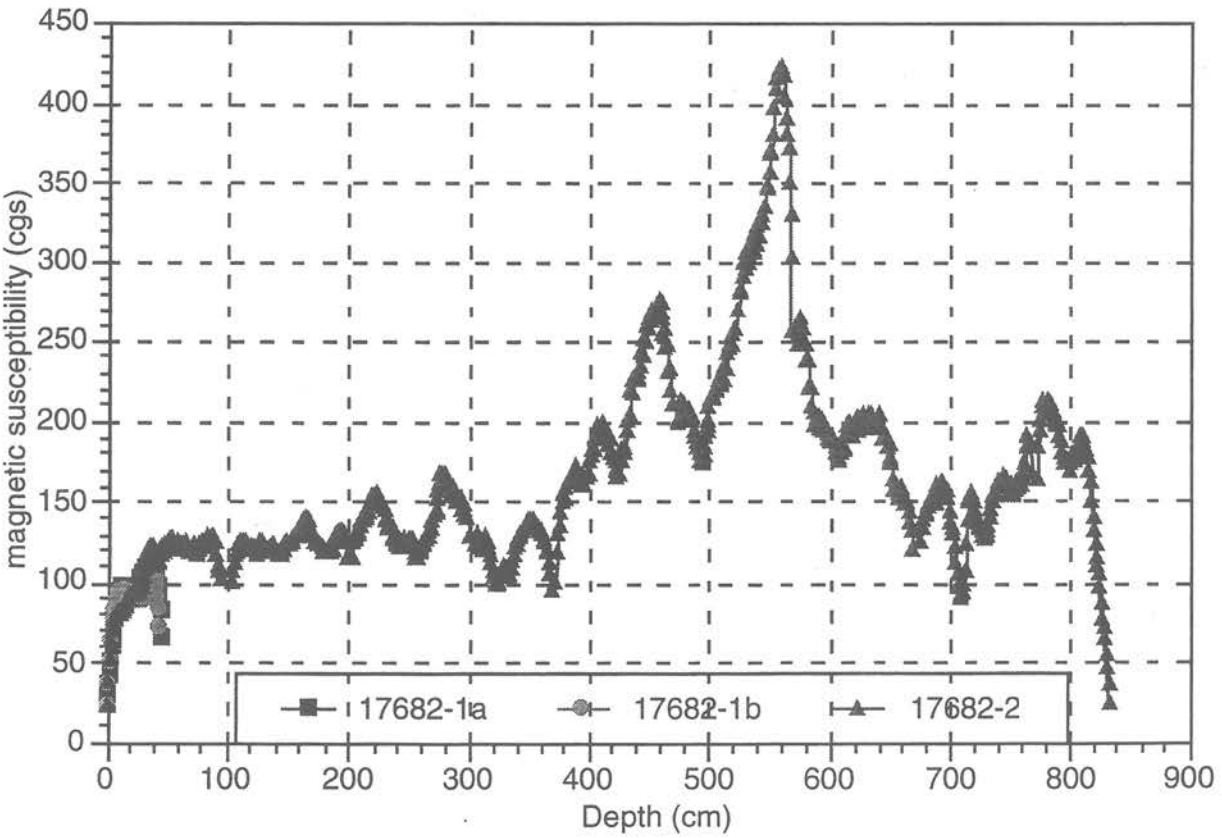

Fig. 9b: Magnetic susceptibility measurements in GIK-17682-1 GKG and -2 SLS.

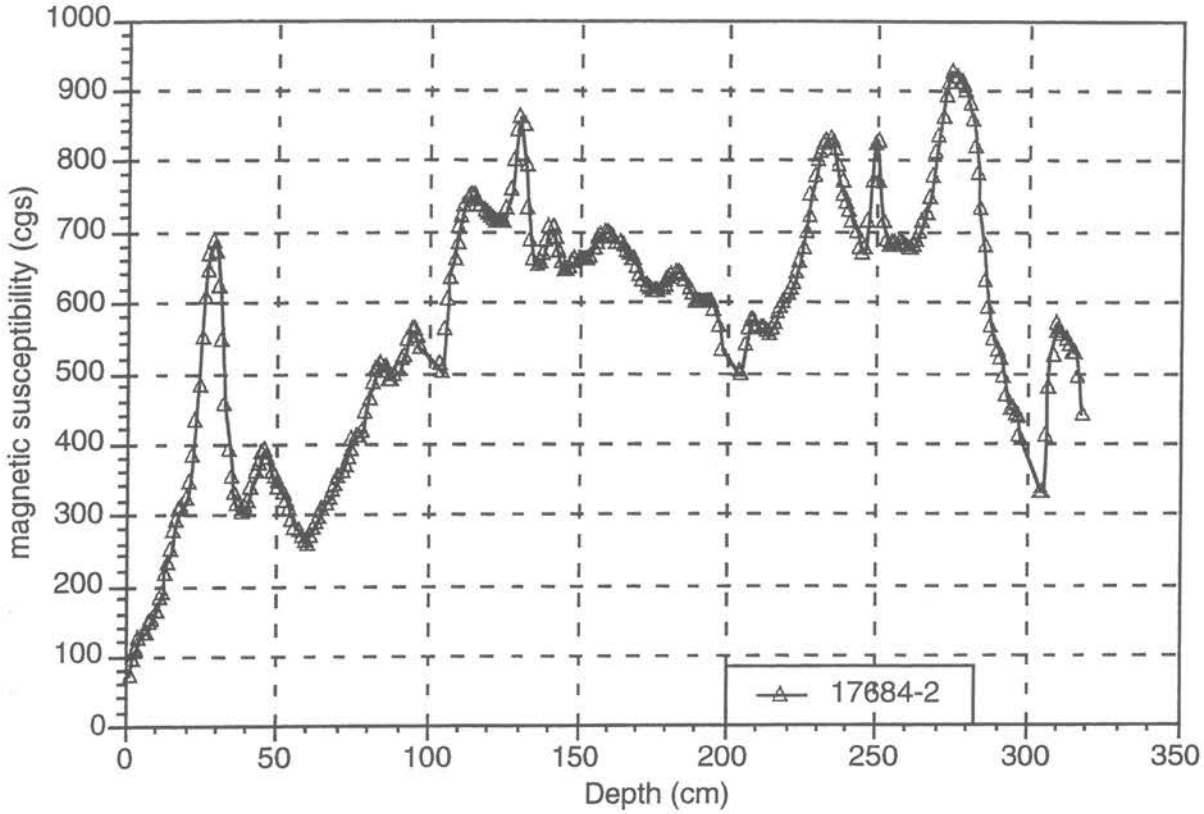

Fig. 11b: Magnetic susceptibility measurements in GIK-17684-1 SLS.

5.6 Sediment Handling

Photographic documentation and lithological descriptions of cores GIK-17674 to 17678 were made after they were cut in halves. Because of time and manpower limitations, cores GIK-17681, GIK-17682 and GIK-17684 were not opened. Sampling for measurement of the physical properties of the sediment and oxygen/carbon isotopes was made at close intervals of 3 to 5 cm in the upper segment and between 7 cm and 10 cm in the lower part of the cores. Volcanic ash layers were specially sampled for geochemical analyses. In every box core, bulk sampling of the ash layers was also carried out. In addition, subsamples of prominent ash layers in the gravity cores was also made. All samples were subsequently treated with dilute HCl. A few layers were selected for XRD analyses (see chapter 8). Smear slides were made wherever necessary for component identification.

5.7 Previous Results

Seven cores which were taken during the EDISON I cruise were studied in detail. Based on $\delta^{18}O$ and $\delta^{13}C$ measurements on 674 samples, a time-stratigraphic correlation of the 26 individual ash layers detected in the cores was possible. As indicated by the parasound data, many of the more pronounced ash layers represent major eruptive episodes having regional significance, and could be mapped over large areas. The isotope data clearly showed that some of the cores reached beyond the $\delta^{18}O$- Isotope Stage 4 (ca. 65,000 a BP). The sediment succession from the small crater in the vicinity of the Conical Seamount evidenced that it was dormant for at least the last 70,000 years. The pronounced volcanic activity in the New Ireland area could have substantially contributed to the global cooling indicated during this stage, an aspect that will be further pursued with the EDISON II cores. Fallout layers, graded turbidites, sediment slumps, gravity flows, and finely dispersed ash could be distinguished in the tephra layers which varied in thickness from a few mm

to several dcm. The fraction 63 µm to 500 µm of the ash layers consisted to more than 80% of volcaniclastic glass, mineral crystals and biogenic components, mainly foraminifera.

Highly vesicular rhyolitic glass and pumice are most abundant. The high grade of fractionation suggests formation from explosive eruptions. Less common are blocky brown glasses of basaltic-andesitic composition and latites. Crystals can reach more than 60% of the volcaniclastics and consists of plagioclase, biotite, pyroxenes, and less common hauyn. The presence of hauyn is of special interest as the mineral would need at least 5-7% SO_2 in the magma.

Detailed geochemical studies including trace and rare earth elements gave patterns which can be correlated with the data obtained from the islands thus pointing to a possible source area of the individual ash layers.

5.8 Sediment Cores SO-133

A total of 11 core stations (see Tab. 5.1) mainly west of Tanga were conducted during this cruise. As stated above, core recovery was generally very limited, but similar to the recovery during the SO-94 cruise.

SO-133/2 - 01-GKG GIK-17674-1; - 02-SL GIK-17674-2
SO-133/2 - 03-GKG GIK-17675-1; - 04-SL GIK-17675-2

These core stations are located on slopes to the north and south of the broad flat basinal area of EDISON I station GIK-16992 (Fig. 1). Parasound and magnetic susceptibility profiles (Fig. 2a-b, 3a-b) showed that the base of the GIK-17674 and GIK-17675 reached down to around 25 ka and 30+ ka respectively. The sandy nature of the sediments (see core descriptions Fig. 2c, 3c) did not allow deeper penetration than in core GIK-16992 of the previous EDISON I cruise.

SO-133/2 - 08-GKG GIK-17676-1; - 09-SL GIK-17676-2

This core station is located between GIK-16989 and GIK-16993 of the former cruise (Fig. 1). Pelagic foraminiferal oozes and numerous ash layers typical for this area were also penetrated in this core (Fig 4c). Core recovery of under 3 m is much less than in the EDISON I cores. The magnetic susceptibility measurements (Fig. 4b), however, indicated that the age at the base of the present core is comparable to the neighbouring cores ($\delta^{18}O$ Stage 4, 65 ka). The thick ash layer at the base of GIK-16993 was not reached.

SO-133/2 - 37-GKG GIK-17677-1; -38-SL GIK-17677-2

This core is located to the SW of Tanga Island and penetrated five black ash layers.(Fig. 5c). Parasound records showed that the reflectors were lensing out towards the core station, with an accumulation of several reflectors in the upper meters of sediment.. The numerous ash layers in the upper meter of the core as indicated by the magnetic susceptibility measurements (Fig. 5b), and confirmed as ash layers (Fig. 5c) means that in spite of its short length, this core probably penetrated much older sediments than GIK-16994.

SO-133/2 - 57-GKG GIK-17678-1; -58-SL GIK-17678-2
SO-133/2 - 59-GKG GIK-17679-1
SO-133/2 - 60-GKG GIK-17680-1

This set of stations was located in the vicinity of the new clam beds from the newly discovered gas rich sediment area south of Lihir Island (see also CTD report, chapter 7.1). GIK-17678 was located directly at the sites of the clam beds on the slope. GIK-17680 came from the valley area close by. As GIK-17678 was raised up, a strong smell of rotten eggs (H_2S) was noted when the corer neared the sea surface, and upon opening the core onboard in the laboratory. On deck, a odourless gas escape was also observed. Four major concretionary "hardgrounds" each about 10 cm in thickness were encountered between 1 and 2 m depth in sediment. Calcareous concretions were also present in the sandy beds between the hard layers. Below 2 m (Fig. 2c), the sediment was clayey and concretions were not observed. The large grab became entangled in its own wire during station GIK-17679, fell on its side, and there was no sediment recovery.

In GIK-17680 (Fig. 8c), a large sinuous open hole 2.5 cm in diameter was observed almost reaching the surface. Smaller openings (< 0.8 mm) in a cluster were also observed. No correlation through magnetic susceptibility profiles (6b, 8b) with the neighbouring cores GIK-16989 and GIK-16990 was possible.

SO-133/2 - 63-GKG GIK-17681-1; - 64-SLS GIK-17681-2
SO-133/2 - 65-GKG GIK-17682-1; - 66-SLS GIK-17682-2
SO-133/2 - 69-GKG GIK-17683-1; - 70-SLS GIK-17684-1

These stations form part of a profile extending the coring northwards of the first expedition's GIK-16994 core. The ash layers are expected to be less dominant, in numbers as well as in thickness, accompanied by a corresponding increase of normal deep sea sediments.

Core recovery was very good at the first two locations. Most of the sediment, estimated to be about 5m, slipped out again from the last core barrel due to a damaged core catcher (GIK-17684). The last big box corer (GIK-17683) also had no penetration in sediment and brought back some pieces of brown and black coated pumice.

A tentative correlation between the above three cores with the previous (anchor) locations GIK-16993 and GIK-16994 showed that the outermost core GIK-17681 recovered the sediment sequence extending down beyond ($\delta^{18}O$- Stage 4).

5.9 Summary and Conclusions

During the SONNE Research Cruise 133/2, we were able to extend and complete the systematic core sampling around the Lihir and Tabar-Simberi Group of Islands. The core profile northwards of the Lihir and Tanga Islands should provide information on the provenance of the ash layers, particularly on the volcanoes further to the east and south. The magnetic susceptibility profiles of the sediment cores proved to be a useful tool for correlation, especially since the stratigraphy of the EDISON I cores was known.

The gas rich area south of Lihir needs further detailed investigations, both geochemically and sedimentologically. From the tectonically rooted escarpments seen on the acoustic records, more pathways for gas escape and deep sea biological communities are likely.

SO 133/2 - 01 GKG GIK 17674-1 NE Simberi Is.
2°07.17'S 152°33.98'E Water depth 1716 m

SO 133/2 - 02 SL GIK 17674-2
2°07.15'S 152°34.01'E Water depth 1716 m

Core fit :37 cm in -1 = 12 cm in -2 (from magnetic susceptibility profiles)

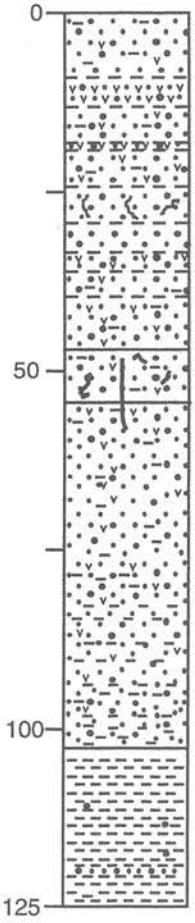

Colour	Depth	Lithological description
10YR 7/4	0- 9 cm	grayish orange, loosely consolidated, fine to medium grained foraminiferal sand speckled with larger forams, passing into
10YR 4/2	9- 13 cm	dark yellowish brown foram. sand as above, with darker hues from ash fallout.
10YR 7/4	13- 18 cm	grayish orange foram. sand as above, compacter.
10YR 4/2	18- 19 cm	dark yellowish brown foram. sand with irregular dark stains, as above.
10YR 7/4	19- 24 cm	grayish orange, compact, foram. sand, speckled with larger forams, as above.
10YR 7/2-4/2	24- 29 cm	foram. sand as above, mottled, with open worm burrows.
10YR 4/2	29- 33 cm	dark yellowish brown foraminiferal sand as above, coarser.
10YR 4/2	33- 35 cm	sand as above, with irregular darker flecks from ash.
10YR 7/4	35- 39 cm	grayish orange, compact, fine to medium grained foraminiferal sand, speckled.
10YR 4/2	39- 47 cm	dark yellowish brown foram sand as above, with darker streaks (ash fallout).
10YR 7/4-6/2	47- 54 cm	grayish orange to pale yellowish brown foraminiferal sand as above, coarser with open worm tubes. Vertical burrow 48-65 cm.
10Y 4/2	54-101 cm	lighter grayish olive, sandy foraminiferal ooze speckled with larger forams, brown mottled (bioturbation) 85-87 cm, from 87 cm to base more clayey layers.
10Y 4/2 to 5YR 4/1	101- 125 cm	grayish orange to brownish gray plastic clays, without larger forams, foram sand at 111.8-112.2 cm with larger forms.

Legend (for Fig. 2c-7c)

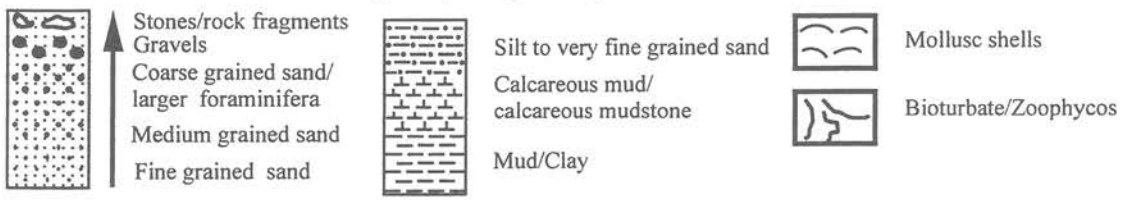

Fig. 2c: Composite lithological column and core description, GIK- 17674-1/2, New Ireland Basin.

SO 133/2 - 03 GKG GIK 17675-1 W. Simberi Is.
2°29.95'S 151°33.28'E Water depth 1898 m

SO 133/2 - 04 SL GIK 17675-2
2°29.97'S 151°33.25'E Water depth 1897 m

Core fit :21 cm in -1 = 11 cm in -2 (from magnetic susceptibility profiles)

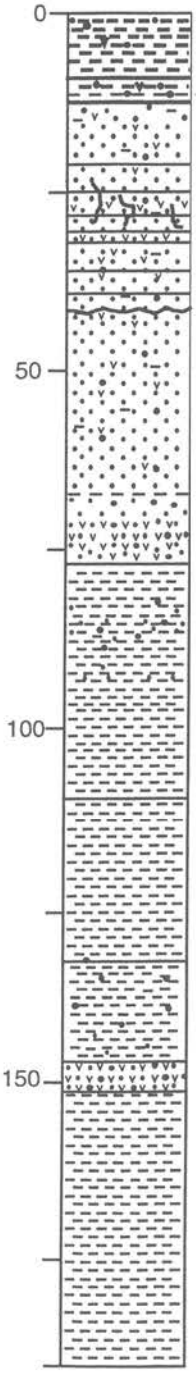

Colour	Depth	Lithological description
10YR 7/4	0- 9 cm	grayish orange, soft, poorly consolidated foraminiferal mud, passing into
10YR 7/4-6/2	9- 12 cm	grayish orange to pale yellowish brown compact clays with brown streaks and layers, floating larger foraminifera.
10YR 7/4	12- 18 cm	grayish orange foram. sand as above, compacter.
10YR 4/2	18- 21 cm	light brown sand, with black stains.
10YR 4/2	21- 25 cm	darker than above, occasional enrichment of foraminifera in nests.
10YR 7/4-4/2	25- 28 cm	browner hues than above, coarser with larger foraminifera, higher ash content.
10YR 4/2	28- 30.5 cm	dark grayish olive foram sand, with lighter streaks, bioturbated.
10YR 2/2	30.5- 32 cm	dusky yellowish brown foram and ash layer.
10YR 4/2	32- 36 cm	brown sand as above with black streaks and layers.
10YR 4/2	36- 39 cm	brown sand, mottled, with larger forams, as above.
10YR 5/4	39- 42 cm	darker brown foram sand, speckled with larger forams, irregular lower boundary.
5Y 3/2-5/6	42- 67 cm	olive gray to light olive brown sand, darker and compacter especially between 57-67 cm. Transitional boundary to
5Y 3/2	67- 77 cm	olive gray volcanic sand, darker below 75 cm. Sharp boundary to
5Y 3/2	77-110 cm	olive gray clays, coarser at 84-90 cm, greenish layer at 92.5-93 cm
5Y 3/2	110-133 cm	as above, lighter.
5Y 3/2	133-147 cm	light olive gray clays with a few floating larger forams. Bioturbated, mottling >1cm diameter to 140 cm. Bioturbation not observed below 140 cm.
5Y 3/2	147-151 cm	olive grey, fine to medium grained, volcanic sand.
5Y 3/2	151-190 cm	dark olive gray clays with coarse grains below 162 cm, mottling frequent to 180 cm, less coarse particles to base.

Fig. 3c: Composite lithological column and core description, GIK- 17675-1/2, New Ireland Basin.

SO 133/2 - 8 GKG GIK 17676-1 SE Tabar Is.
3°02.00'S 152°21.02'E Water depth 1860 m
SO 133/2 - 9 SL GIK 17676-2
3°02.00'S 152°21.01'E Water depth 1861 m
Core fit 9 cm in -1 = 6 cm in -2 (from magnetic susceptibility profiles)

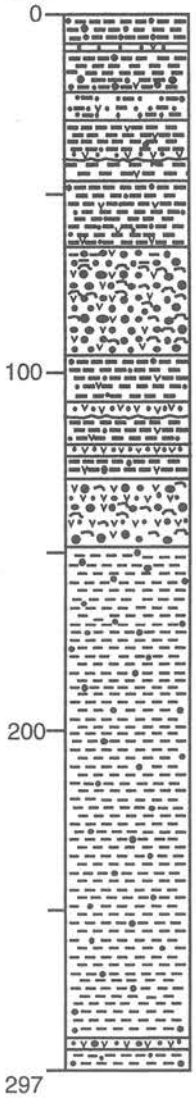

Colour	Depth	Lithological description
10YR 5/4	0- 8 cm	moderate yellowish brown, slightly sandy foraminiferal ooze.
10YR 4/2	8- 10 cm	dark yellowish brown, fine grained, foram sand with dark stains.
10YR 6/6-5/4	10- 18 cm	light yellowish brown to dark yellow clays with olive tint. .
10YR 4/2	18- 21 cm	clay as above, darker, speckled with larger forams.
10YR 6/6	21- 29 cm	dark yellowish orange, very fine grained, foram sand, with grayish olive green hue.
5Y 5/2	29- 40 cm	light olive gray, silty clays with small pelecypod, coarser at 35.5-36.5 cm with more ash, forming irregular layer.
5 Y 2/1-4/2	40- 46 cm	olive black to light olive gray, mottled clays.
5Y 3/2	46- 65 cm	olive gray, silty clays with ash pockets at 49.5-50 cm, 59-60 cm and 62.5-63.5 cm and irregular layers 4-5 mm in thickness.
5Y 7/2 to 10Y 8/2	65- 95 cm	whitish gray to yellowish gray, medium to coarse grained volcanic and shell debris with two 1-2 cm olive gray, silty layers as above, near the top.
5Y 4/4-5/2	95-108 cm	light olive gray to moderate olive brown clays with greenish streaks and occassional larger forams.
10YR 6/2	108-112 cm	dark yellowish brown, very fine grained ash, with irregular lower boundary.
5Y 3/2	112-120 cm	olive gray clays, slightly silty, large greenish streaks at 116.7-117.1 cm.
10YR 6/2	120-123 cm	dark yellowish brown, very fine grained ash, as above.
5Y 3/2	123-129 cm	clay as above, with larger foraminifera.
5Y 7/2 to 10Y 8/2	129-149 cm	medium to coarse grained debris with dark yellowish brown, fine grained ash, coarser grained at 131-133 cm, large black grains at 141-141.5 cm.
5Y 3/2	149-286 cm	olive gray clays, monotonous, hard and compact (plastic) with greenish streaks and thin dark brown layers, speckled. Dark brown streaks at 173-173.5 cm, 188.5-189 cm, 209,5 cm (1 mm), 229-231 cm, 252-253 cm. Two nests with material from 133-149 cm at 240.5 cm (6mmØ) and 266 cm (2 mm Ø)
10YR 2/2	286-289 cm	dusky yell. brown fine grained ash layer (core catcher).
5Y 3/2	289-297 cm	olive gray clays with larger forams.

Fig. 4c: Composite lithological column and core description, GIK-17676-1/2, New Ireland Basin.

SO 133/2 - 37 GKG GIK 17677-1 S Tanga Is.
3°37.24'S 152°57.29'E Water depth 2516 m
SO 133/2 - 38 SLS GIK 17677-2
3°37.28'S 152°57.18'E Water depth 2516 m
Core fit : 10 cm in -1 = 16 cm in -2 (from magnetic susceptibility profiles)

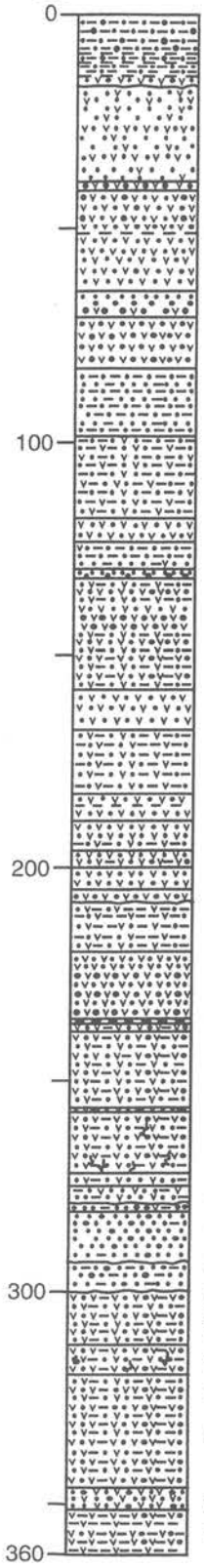

Colour	Depth	Lithological description
10YR 4/2-5/4	0- 9 cm	dark yell. brown, silty clay and very fine grained sand, speckled with forams.
+ 5YR 3/4	9- 11 cm	dark yellowish brown, fine sandy clay.
5Y 5/6	11- 14 cm	light olive brown silty clay, as above.
5Y 5/2	14- 16 cm	light olive gray, fine grained ash, speckled with larger forams. Irr. boundary to
10YR 5/4-4/2	16- 38 cm	dark yell. brown, fine grained, peppery sand. Ash layers at 32.1-32.3 cm and 36.0-36.9 cm and at the base, occasional brownish-black nests of ash.
10YR 4/2 to 5Y 3/2	38- 39 cm	dark yellowish brown to olive gray, peppery fine to medium grained volcanic ash.
10YR 5/4	39- 51 cm	dark yell. brown foram. sand as above, coarser.
10YR 5/4	51- 64 cm	moderate to dark yell. brown, very fine grained, silty ash with thin fine to medium grained layers.
5Y 6/1 - 5/6	64- 70 cm	light olive gray to light olive brown turbidite, very coarse grained at base to fine grained at top, core recovery about 40% 64-68 cm.
N1+10YR 5/2	70- 82 cm	black, medium grained, volcanic ash, with coarse grained parts, bedded with moderate yellowish brown layers 70-77 cm, occassional white specks (forams).
5Y 5/6	82- 98 cm	light olive brown, fine silt, and very fine grained, clayey sand, with greenish streaks and floating larger forams 200-500 µm.
5Y 3/2	98-117 cm	olive gray, fine grained clayey sand and ash, almost homogeneous without distinct layering, speckled with larger forams, especially near the base.
5Y 6/1-4/1	117-123 cm	olive gray, fine grained clayey sand and ash, almost homogeneous with no distinct layering, speckled with larger forams, especially near the base.
5Y 4/1	123-129 cm	olive gray, sandy clays, white speckled with forams, darker towards the base. Moderate dark gray (N5), fine grained, volcanic ash in pockets.
N5	129-131 cm	Dark gray, ash fallout, graded, medium grained at base to very fine grained at top.
N5	131-158 cm	medium gray, fine to medium grained ash with clayey component, speckled with forams. 5 mm thick alternations of fine & medium layers at 135-140 cm. Coarser at 140-143 cm, finer at 143-148 cm. Clay content higher at 148-158 cm
N1 to 5Y 2/1	158-167 cm	black to olive black, fine grained ash. Two thin "pearly" layers of individual larger pl. & ben. foraminifera separated by 2 mm black ash at 162.1 & 162.3 cm.
5Y 3/2	167-182 cm	olive gray, fine grained clayey sand and ash, almost homogenous, larger forams enriched in nests, and also floating in matrix, more clayey 176-179 cm.
N1	182-189 cm	black, very fine grained to silty ash, with clayey intercalation 183-186 cm.
5Y 2/1	189-196 cm	Olive black, very fine grained ash, very fine silty with clayey nests 192-196 cm.
N2	196-200 cm	grayish black ash, with fine to medium grained ash lenses, speckled with forams.
5Y 4/1	200-205 cm	Olive gray very fine grained ash, occassional large forams.
5GY 4/1	205-208 cm	dark greenish grey fine to medium grained ash, salz und pepper texture (forams).
N3	208-219 cm	Medium dark gray silty clay with ash streaks, some larger forams, and thin (1-2 mm) fine grained ash layers especially towards the base.
5YR 4/1 to 5Y 4/1	219-235 cm	Brownish to olive gray, medium grained to fine silty, graded ash. Upper 4 cm almost homogeneous, silty ash. 223-235 cm with at least 7 cycles, 1.5 cm thick.
N3	235-236 cm	Medium dark gray clay with ash streaks.
5Y 3/2	236-238 cm	Olive gray, medium to coarse grained ash, speckled with forams.
5GY 4/1	238-256 cm	Dark greenish gray, fine silty sand, speckled with forams, enriched in nests. Grayish bluish green (5BG 5/2) streaks and thin mm-thick layers.
5Y 2/1	256-257 cm	Olive black, very fine grained silty ash.
5GY 4/1	257-271 cm	Dark greenish gray, fine silty sand, speckled with forams, greenish streaks. More bioturbate in basal 2 cm with ash pockets
5Y 2/1	271-274 cm	Olive black, very fine grained silty ash, darker als above, fine grained ash pockets.
5Y 2/1 N1	274-278 cm	Olive black to black, very fine grained silty ash. Two graded layers each 2 cm thick. Darker at base.
5YR 2/1	278-280 cm	Brownish black, almost homogeneous, very fine silty ash.
5Y 4/1	280-293 cm	Olive gray, very fine grained sand with coarser parts and greenish streaks.
N3	293-300 cm	Dark gray clayey sand with coarser lenses > 1 cm, speckled with larger forams.
N3-N2	300-312 cm	Dark gray to grayish black, very fine silty ash with floating larger forams.
N4 5YR 5/1	312-319 cm	Moderate dark gray to brownish gray very fine silty ash with few floating larger forams, enrichment of foraminifera in nests.
5YR 4/1	319-346 cm	Brownish gray, fine silty ash rich clay. Speckled with larger forams, more frequent by 330-335 cm, frequent streaks and lenses below 335 cm.
N1	346-351 cm	Black, fine grained ash, with medium grained parts. Lighter layer in the middle.
5YR 4/1	351- 366 cm	Dark brownish gray, ash rich clay, speckled with forams.

Fig. 5c: Composite lithological column and core description, GIK- 17677-1/2, New Ireland Basin.

SO 133/2 - 57 GKG GIK 17678-1 SSW Lihir Is.
3°19.37'S 152°35.31'E Water depth 1610 m
SO 133/2 - 58 SLS GIK 17678-2
3°19.36'S 152°35.45'E Water depth 1574 m
Core fit : 10 cm in -2 = 18 cm in -1 (from magnetic susceptibility profiles)

Colour	Depth	Lithological description
10YR 5/4	0- 5 cm	dark yellowish brown, soft, fine silty mud.
5YR 3/2	5- 16 cm	olive gray, silty clay, occasional forams.
N4	16- 21 cm	dark gray, fine grained, volcanic ash mixed with forams, dark stains.
10YR 5/4	21- 29 cm	Moderate to dark yellowish brown, fine to medium grained sand. Black to grayish black stains 22-25 cm, enriched in larger forams at 25-26 cm.
5Y 3/2	29- 35 cm	olive gray, silty clay as above.
N5	35- 41 cm	gray, fine grained ash, clayey, with forams, dark stained.
5YR 3/2	41- 53/65 cm	Olive gray, soft, fine to medium grained sand with coarse parts, local foram enrichment, small *Bathymodiolus* at 43-45 m. Below 53 cm increasing presence of very hard sediment consolidated with calcareous cement.
5Y 6/1	53/65- 76/79 cm	light gray, clayey, medium grained sand, occasional "floating" larger forams.
5Y 4/1	76/79- 83 cm	olive gray, clayey, medium grained sand, with less larger forams.
5Y 4/2-2/1	83- 102 cm	olive gray to olive black, fine grained clayey sand, lighter below 91 cm, sporadic very hard calcareous concretions from 89 cm downwards.
5Y 2/1- 4/1	102-118 cm	olive black to gray, very fine grained silty sand, with lighter irregular bands at around 108 cm.
5Y 6/1 N4	118-162 cm	gray, hard, sandstone "hardground" with calcareous cement at 120-126 cm and 150-162 cm. Wavy and irregular lower boundaries. Rest of section with frequent concretions in dark grey, fine to medium grained, silty sand. Strong H_2S smell.
5GY 6/1-4/1	162-175 cm	greenish gray to dark greenish gray, sandy clay with sporadic larger foraminifera, frequent hard concretions with calcareous cement. Continuous structures from soft into hard consolidated sediment.
N4	175-185 cm	gray hardground as above, strong H_2S smell. Two preserved worm burrows with calcareous cement
N5 5GY 4/1	185-208 cm	dark to medium gray, fine grained sand, 6 mm greenish gray layer at 196 cm, with sporadic calcareous concretions.
N5	208-218 cm	gray hardground as above, strong H_2S smell.
N4	218-243 cm	gray, soft, clay with thin (mm) very fine grained ash between 223 cm and 228 cm. Calcareous concretions frequent below 229 cm.
5Y 6/1	243-249 cm	light olive gray, very hard muddy sandy hardground as above.
10GY 5/2	249-276 cm	greenish gray silty clay with brownish pockets.
10GY 5/2 5G 5/2-3/2	276-291 cm	greenish gray, very fine grained sand with grayish and dusky green pockets and streaks.
5GY 5/2	291-311 cm	grayish green, fine grained sand, occasional pockets.
5GY 6/1 5B 5/1	311-329 cm	Greenish gray to medium bluish gray clay with larger forams enriched in nests.

Fig. 6c: Composite lithological column and core description, GIK- 17678-1/2, New Ireland Basin.

SO 133/2 - 60 GKG GIK 17680-1 SSW Lihir Is.
3°19.36'S 152°35.35'E Water depth 1625 m

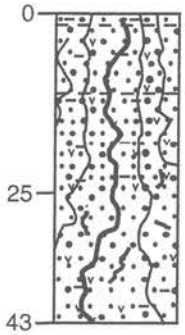

Colour	Depth	Lithological description
10YR 6/2	0- 1.5 cm	light yellowish brown, fine grained silty sand. passing into
10YR 5/4 5GY 4/1	1.5- 11 cm	moderate yellowish brown, fine grained sand, speckled white with foraminifera. Worm burrows and admixture of gray pockets 6.5-11 cm. Dark stains 1.5 to 8 cm.
5GY 4/1 5G 4/1	11- 43 cm	sand as above with enrichment of forams (whitish gray) in pockets between 15-cm, in nest 35-39 cm. Dark stains 15-24 cm, irregular to 30 cm. Dark greenish gray lense between 15-16 cm. A large sinuous opening about 2.5 cm in diameter is present almost to the surface. Smaller open holes having diameters ≈0.8 mm are numerous at the upper right sector of the box core.

Fig. 7c: Composite lithological column and core description, GIK- 17680-1, New Ireland Basin.

SO 133/2 - 60 GKG GIK 17681-1 NNE Lihir Is.
2°23.99'S 152°50.83'E Water depth 1831 m

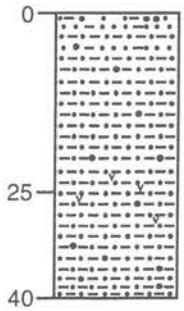

Colour	Depth	Lithological description
10YR 8/4 10YR 2/1	0- 40 cm	pale yellowish brown, very fine silty mud, almost homogeneous, lightly speckled with foraminifera. Sporadic darker stains 5-23 cm, more consistent from 23 cm to 30 cm.

Fig. 8c: Composite lithological column and core description, GIK- 17681-1, New Ireland Basin.

SO 133/2 - 65 GKG GIK 17682-1 NE Lihir Is.
2°38.96'S 153°01.93'E Water depth 2040 m

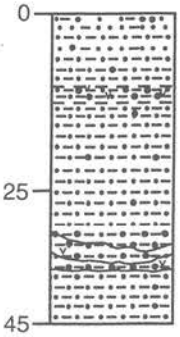

Colour	Depth	Lithological description
10YR 7/6 N 8	0- 10 cm	yellow, very silty mud, speckled white with abundant foraminifera 0-4 cm .
10YR 7/6	10- 12 cm	Dark brown stain on silty mud.
10YR 7/6 10YR 3/4 N 8	12- 45 cm	yellow, very fine silty mud, speckled white with foraminifera in enriched layers. Dark brown stain as irregular wavy band 32 to 37 cm with abundant foraminifera in lenses and pockets. 1 mm thick almost horizontal, lightly irregular foraminifera layer at 38 cm.

Fig. 9c: Composite lithological column and core description, GIK- 17682-1, New Ireland Basin.

6 Biology

6.1 Report on the Macrobiological Work

BY VERENA TUNNICLIFFE, MICHAEL TÜRKAY & THOMAS JELLINEK

6.1.1 Collections of Hydrothermal Seep Fauna from Edison Seamount

Four GTVA-grabs were executed on Edison Seamount in the North and South Clam Fields. Three of them returned a great number of live vesicomyid clams with a rich associated fauna. The first grab in the North Field had only dead shells. After the detection of high methane values in the water column above the horst-structure ESE of Edison Seamount two GTVA-samples were taken at the western escarpment. The area proved to have a rich fauna dominated by *Bathymodiolus*-like mussels and thus differing from that of Edison Seamount. This new site was called the „mussel cliff" with reference to the dominant faunal element.

Clams and mussels were collected, measured and a representative sample of each species was preserved. Most of the sediment from the grabs was sieved through 1 mm and 0.5 mm screens plus a subsample through a 0.25 mm mesh. Barnacles were examined on board (see below) and the remainder of the material was fixed for subsequent examination. Formalin fixation allows systematic and histological work, alcohol preserves for molecular work and glutaraldehyde for ultrastructural studies. The great majority of material will be sorted at the Senckenberg Museum. New species will be loaned to the appropriate systematists for description. While the dominant, larger species were collected in 1994, many novel forms were seen and much will emerge upon closer sorting.

Table 6.1 lists the collections taken on board.

6.1.2 Visual Observations

Observation of the sea floor was mainly carried out by the TV-grab (GTVA) before sampling. Only one track was performed by OFOS. While the video-grab has the advantage that its position more ore less matches that of the ship and samples can be taken upon sight of interesting objects, it is not suitable for mapping larger areas. After having sampled the „mussel cliff" site, the OFOS was used to examine the coverage and distribution of the biota along the escarpment.

During the surveys the locations of the two clam fields on Edison Seamount were confirmed, both by grab and OFOS. The northern field that looked smaller and more weakly developed during the surveys proved to be quite densely populated in its centre, but still narrower than the southern one. Shrimps were especially abundant in the southern field and the barnacles of the genus *Neolepas* seemed to increase in density towards the edges of the fields. They were also seen in large clusters outside the mussel population and were after the dead shell fragments the first sign of the seep community.

The OFOS tow at the „mussel cliff" site was not successful in detecting a larger seep community. Apart from isolated clusters and individuals of *Neolepas,* only normal deep sea fauna was observed. This shows that the seepage sites are very localised and do not occur along the whole escarpment.

Table 6.1: Biological samples from vent/seep sites around Edison Seamount

GTVA	Jar size	Preserve	Contents	Site	Comment
10	1	formalin	barnacles	Edison North	
10	1	formalin	0.5fraction	Edison North	
10	1	formalin	0.5fraction	Edison North	
10	sm.buck.	formalin	1 mm	Edison North	
10	0.5	formalin	*Phymorhynchus*	Edison North	Alcohol
10	0.5	formalin	shrimp	Edison North	
10	0.5	formalin	polychaetes	Edison North	
10	1	formalin	barnacles	Edison North	Verena
10	0.25	Trumps	barnacles	Edison North	O. Giere
11	1	formalin	barnacles	Edison South	
11	1	formalin	mixed: *Phymorhynchus*, polychaetes	Edison South	
11	1	formalin	1 mm fraction	Edison South	
11	bucket	formalin	clams	Edison South	
11	0.5	formalin	shrimp, galatheids	Edison South	
11	1	formalin	barnacles	Edison South	Verena
11	1	formalin	barnacles	Edison South	Verena
11	0.5	Trumps	*Phymorhynchus*	Edison South	O. Giere
11	0.25	Trumps	shrimp	Edison South	O. Giere
33	0.5	formalin	0.25 fraction	Edison South	
33	0.5	formalin	0.5 fraction	Edison South	
33	sm.buck.	formalin	1 mm fraction	Edison South	
33	bucket	formalin	clams	Edison South	
33	sm.buck.	formalin	barnacles	Edison South	
33	bucket	formalin	barnacles	Edison South	
33	0.5	formalin	shrimp	Edison South	
33	0.25	formalin	limpets	Edison South	
33	1	formalin	shrimp, galatheids	Edison South	
33	1	formalin	barnacles	Edison South	
33	1	formalin	assorted gastropods, polychaetes etc.	Edison South	
33	1	formalin	barnacles	Edison South	Verena
33	bucket	dried	clam shells	Edison South	Verena
33,34	sm.buck.	formalin	clams	Edison South	Verena
34	sm.buck.	formalin	clams	Edison South	
34	0.5	formalin	assorted polychaetes, limpets, shrimp	Edison South	
43	0.5	formalin	tubicolous polychaetes	Mussel Cliffs	
44	1	formalin	0.5fraction	Mussel Cliffs	
44	1	formalin	shucked mussels	Mussel Cliffs	
44	1	formalin	1 mm	Mussel Cliffs	
44	1	formalin	1 mm	Mussel Cliffs	
44	bucket	formalin	mussels	Mussel Cliffs	
44	0.5	formalin	polynoids	Mussel Cliffs	
44	0.5	formalin	1 *Solemya*	Mussel Cliffs	
44	0.5	formalin	galatheids, gastropods, polychaetes	Mussel Cliffs	
44	0.25	alchohol	polynoids, chitons	Mussel Cliffs	
44	1	alchohol	mussels	Mussel Cliffs	
44	sm.buck.	formalin	mussels	Mussel Cliffs	Verena
44	0.25	Trumps	mussels gill	Mussel Cliffs	O. Giere
44,45	bucket	formalin	vestimentifera	Mussel Cliffs	Verena
45	1	formalin	*Solemya*, polychaetes	Mussel Cliffs	
10,11,33	bags	dried	clam shells	Edison	

A small hydrothermally influenced area was discovered at the south-western slope of „Edi's Daughter Seamount". The two most abundant organisms were a vesicomyid clam and a vestimentiferan tube worm. The profile was too steep for sampling so we have only pictures that do not allow further identification. No further such assemblages were seen on either side of the seamount. Attempts to relocate the patch failed in spite of extensive cruising in the area near the first encounter. This means that the area is very localised and small.

Conical and TUBAF Seamounts were also extensively surveyed before grab sampling. Neither showed signs of hydrothermal fauna, nor did any of the other nearby seamounts that were surveyed less extensively. On Conical Seamount, there were abundant populations of gorgonarian horny corals and less common hexactinellid sponges. Both faunal elements, especially abundant at the slopes, show that there is a considerable flux of particulate matter around and/or down the slope, on which they feed.

6.1.3 Collections of Non-vent Fauna

On all GTVA and dredge stations the recovered macrofauna was collected. Because of the large mesh sizes of the dredges only very large animals were recovered, i. e. gorgonarians and crinoids. In one station, a homoloid crab was also collected. Most gorgonarians belonged to the family Isididae. Later analysis in the lab will give the full range of diversity. Presently, the deepwater horny coral fauna of the Bismarck Archipelago is only poorly known. A comparison to the much better known New Caledonian fauna will be effected and will give an idea on regional differences.

The sediments from all box cores were sampled after the sedimentological working group took what they needed. Sediments were taken to a depth of 20 cm and sieved through a minimum mesh-size of 0.5 mm; a subsample also sieved to 0.25 mm. The 1 mm, 0.5 mm, and 0.25 mm fractions were preserved separately in seawater-formalin (4% formaldehyde concentration). There was not much visible macrofauna and the 1 mm fraction was, as a rule, small (abt. 200ml maximum for the whole grab). After sorting in the laboratory, the samples will be analysed as baseline values in comparison to the respective fractions of the hydrothermal samples. This is of importance as in hydrothermal vent expeditions usually the adjacent deep sea fauna remains unsampled. This may bias results as it is not known which animals of the smaller size fractions are really unique in the hydrothermally influenced sediments. With the reference samples, we can obviate this problem for this area.

6.1.4 Small Fauna of Sediments

Nearly nothing is known about sediment fauna below the size class of macrobenthos. With the opportunity of recovering sediments from both hydrothermally influenced and non-influenced areas the meiofauna can be studied in detail. Unsieved sediment was preserved in seawater-formalin (4% formaldehyde) for meiofauna analysis from all grabs (GTVA and GKG). Furthermore, about 2 litres of sediment were taken for the study of microshells and especially ostracods. These sediment samples will be processed in the laboratory in Frankfurt by sieving and sorting the shells before identification.

We now have samples from comparable depths of sediment with and without hydrothermal influence so that any peculiarities in the fauna of hydrothermal sediments can be easily detected. This portion of the study will be done partly in Frankfurt (ostracods and small molluscs) and for the meiofauna by further collaborative partners.

6.1.5 Notes on the Clam Populations of Edison Seamount

During SO-133, four grabs were taken on Edison Seamount and all returned clam shells. These collections are most unusual because of the shear volume of animals returned. Usually, studies on hydrothermal vents are conducted by a submersible that is able to collect only a few large animals at a time. Using the guided TV-grab, a single population can be retrieved without any selective bias. With such a collection, we can get some idea of population characteristics.

Clam Biology

We know, from the 1994 collections, that this species has not been previously described. It belongs to the group called Vesicomyidae but systematics in this clam family is very difficult. This animal will likely belong to the genus *Calyptogena* or *Vesicomya*. At present, molecular studies on the vent and seep vesicomyids show a distinct separation of species in the two habitats. Vent vesicomyids of the western Pacific are currently known from the Okinawa Trough - they may be the closest relatives to these Edison specimens.

There is extensive information available on the biology and physiology of the clams of the East Pacific Rise (*Calyptogena magnifica*). There is no reason to believe that the Edison clam has a substantially different character. Examination of the body shows it has no gut and that there are symbiotic bacteria present in the gills (E. C. Southward, pers. comm.). Therefore, the animal relies on the chemosynthetic fixation of carbon by its microbial symbionts. For this autotrophic process, it requires a reliable flux of hydrogen sulphide, oxygen and carbon dioxide. The animal captures H_2S using the foot and O_2 using the gills; the blood transports the gasses to the symbionts that mediate the energy-generating oxidative reaction. These microbes fix carbon dioxide using the stored energy. Fixed carbon is transferred to the clam for growth.

We can't know how old the large individuals are. On the East Pacific Rise, 25 cm clams may be between 10 and 20 years. Embryos from gametes released into the water and larvae develop in the water column to recruit back to the vent sites. Clams are capable of movement using the active foot. They prefer a position vertical in the sediment with the foot down and the gills up. However, they do live on hard substrata if a sulphide source is available. Predators are poorly known - crabs and octopus probably eat the smaller individuals but there is likely little that can tackle a large clam successfully.

Abundance

Several images of the Edison clam beds show very high densities of clams restricted to two beds flanking the seamount summit. In places, clams are packed extremely tightly. The grab is not a quantitative tool, but it can give an estimate of density. The bite is a little less than 2 m^2. 11-GTVA returned 110 whole clams; about another 25 were smashed upon recovery. Thus density was about 70 clams/m^2. Numbers in 33-GTVA and 34-GTVA were 85 and 82 respectively.

It will be interesting to weigh the clams and calculate a biomass. Because of the large size and the high densities, the clam community of Edison (along with several other known seep sites around the world) may represent the highest biomass known on the seafloor. Based on measurements of the cross-sectional areas of the animals in 33-GTVA, clam body occupies at least 25% of the seafloor at this station.

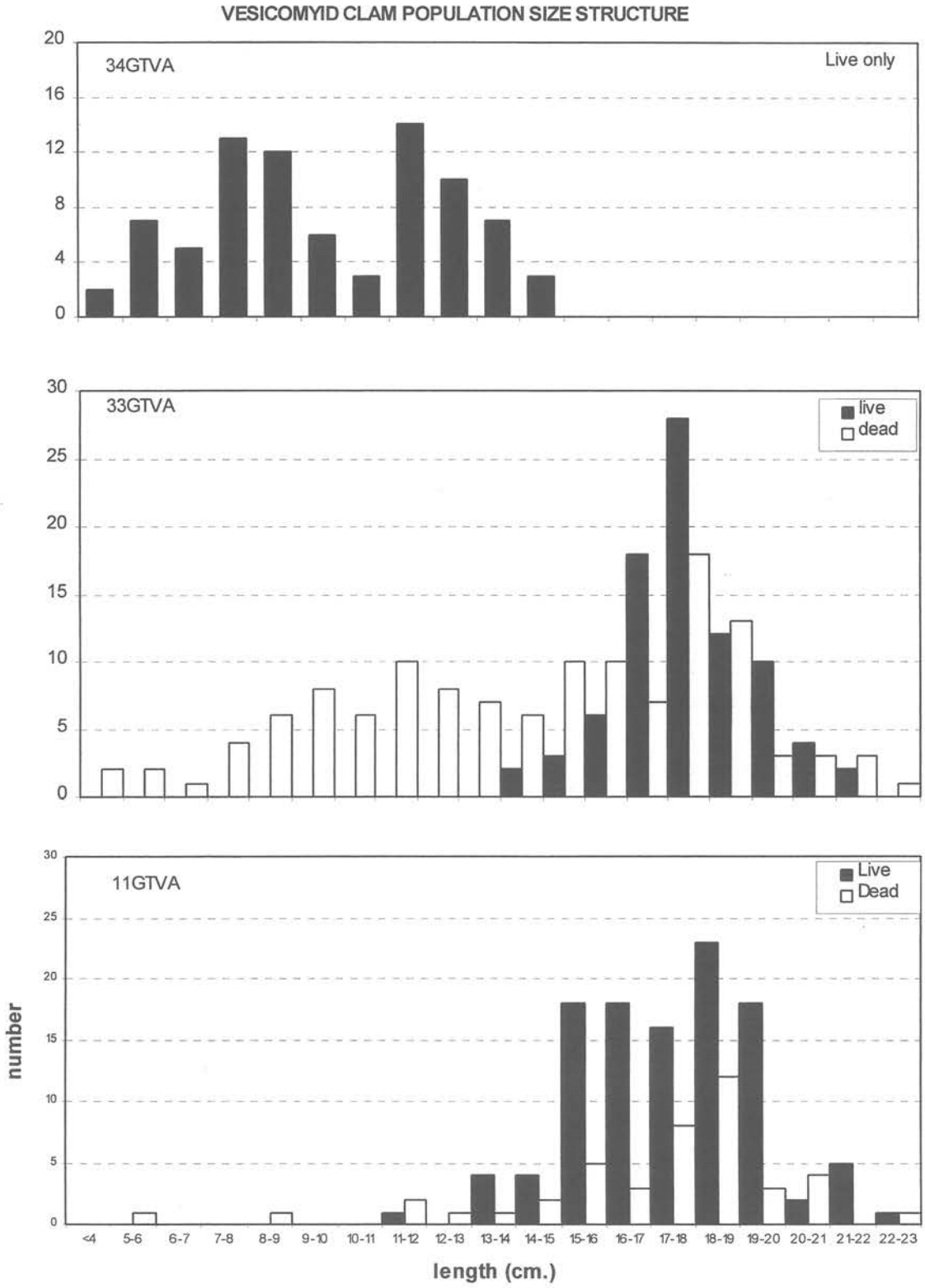

Figure 6.1: Distribution of size classes in three TV-grab collections on Edison Seamount. Dead clams from 34-GTVA were too broken to measure.

Shell debris was abundant in all grabs. 10-GTVA comprised entirely empty shells while 34-GTVA contained more shell debris than sediment. Debris appeared to be deeper in the sediment which is likely caused by living clams pushing weak or dead individuals down or to the side of the colony. Space in optimum fluid flows is likely a limiting commodity.

Population Structure

It is possible to make some interpretations of populations processes from the distribution of sizes in a community. Figure 6.1 presents the measurements from three grabs. Measured sizes ranged between 2.7 cm and 22 cm length. There was a marked difference in sizes and apparent ages between 34-GTVA and the other two grabs. It is possible that this population is a similar age but growth conditions are suboptimal, however, the abundance of gold periostracum on the outer shell layer supports a relatively young age. The extensive mass of dissolving, broken shells under the live clams suggests renewed sulphide flow and recolonization.

In contrast, only large clams inhabited 33-GTVA and 11-GTVA sediments. As these animals appeared to be healthy, it is difficult to believe they are not reproducing. Either larvae are not recruiting or juveniles do not survive. The size frequency of the dead shells suggests the latter circumstance in 33-GTVA. A large range of dead shells is present indicating ongoing mortality of smaller clams. Movement by the larger adults would be an effective competition mechanism excluding smaller animals. Relatively few small dead clams were retrieved from 11-GTVA.

Further work

Material will be offered for systematic, morphological and molecular study to determine the relationship of the Edison clam to other known vesicomyids. Gill tissue will be examined to determine the nature of the symbionts (O. Giere) and confirm their identity as sulfur-oxidizers.

6.1.6 Notes on the Vent Barnacle of Edison Seamount

One of the most abundant animals associated with the clam beds on Edison Seamount is the stalked (or 'gooseneck') barnacle. From specimens collected in 1994, we know this animal is a new species in the barnacle group Neolepadinae that is endemic to hydrothermal vents. The species, to be placed in the genus *Neolepas*, will be named in a publication by W. C. Newman and A. E. Southward.

The vent barnacles are of particular interest to biologists because they display characteristics of extinct groups in the evolutionary lineages of barnacles. The subfamily Neolepadinae represents one of these lineages and the western Pacific *Neolepas* is closely related to an Eocene fossil. There are three other *Neolepas* species known from Okinawa, Fiji, and Southeast Indian Ridges. A study of the relationships of these four species will contribute to interpretation of biogeographic and historical relations of these vent areas.

Distribution

The Edison *Neolepas* was encountered at all the bivalve beds sampled: north Edison, south Edison and Mussel Cliffs. The barnacle was not seen at other sampling sites. It appeared most abundant on South Edison where extensive bushes obscured the underlying clams in places. While it appears to do best where sulphide emissions are also supporting the clams, it appears in tows on dead shells on the periphery of the clam beds. It is a good indicator that there are live clams - and therefore sulphide - nearby.

The barnacle requires a hard substratum for settlement and thus may be limited in its distribution more by substratum availability than by food or sulphide. It attaches to rocks, clams, mussels and others of its own species. Thus, it can be found in clumps with a single 'stem' individual supporting up to 30 other individuals. Juveniles settle everywhere along the host barnacle – including on the plates of the capitulum.

Behaviour

Neolepas is a suspension feeder that uses its cirri (legs) to extract particles from the water. While another species in the genus from Fiji appears to 'farm' bacteria growing on the cirri, the Edison species has no such epibiosis. One can assume it is extracting organic debris, benthic plankton and bacteria associated with venting fluids. The cirri extend 2 to 3 cm and are held in a cupped-fan position. Specimens maintained in seawater on the ship rarely retracted the cirri but remained extended for minutes at a time. The animal is capable of moving the stalk although its base is fixed. It may move quite rapidly to reposition the capitulum (head) or escape provocation.

Size

Animal sizes ranged from 2 mm to 33 cm in length. Three populations were examined shipboard. The collection from Edison North had notably smaller individuals; this grab was associated with dead clams and may not represent an optimal growing condition. Mature individuals dominated the collections: 75% were over 1.2 mm capitulum length – apparently the minimum size for reproducing. Recently settled barnacles were rare – only 18 were less than 0.4 cm.

Reproduction

These collections are unique in the multitude of specimens returned. Information on reproductive biology of these unusual animals is completely lacking but the retrieved animals show all stages of development. The species is hermaphroditic (as are all barnacles) having both male and female capabilities. However, they do outcross and copulation takes place with adjacent individuals. Eggs develop in the ovary, which extends down the stalk. Fertilised eggs are brooded in two masses inside the mantle of the capitulum. One mid-sized individual contained 870 embryos. Differentiation of the larvae occurs in these masses but nauplii larvae capable of independent movement are found dispersed inside the mantle.

Specimens maintained overnight on the ship released nauplii into the buckets on July 23. These larvae are filled with fat vesicles and floated to the surface of the water. They floated ventrum-up and showed only weak movements of the swimming antennae initially. In another day, they were moving for long periods turning to swim dorsum-up. In two days, they had sustained swimming movements and swam to the bottom of the dish. By five days, moults appeared in the dish and elongation of the abdomen has occurred. At the end of the cruise a goood deal of the larvae were still living.

Further Work

Information on this species will be added after examination of towed photos, video, and preserved specimens. Images will give us an idea of preferred habitat and relation to the clams as well as orientation. We can determine if they can live at large distances from the clam beds. We (Tunnicliffe & Southward) will detail feeding structures including gut contents in preserved specimens. Information on reproductive stages will be extended with further work and we will examine gametogenesis (egg and sperm development). Developmental stages of the larvae will be photographed using scanning electron microscopy.

6.2 Microbiological Investigations

BY CHRISTIAN HORN

6.2.1 Water Sampling (CTD)

Methods

Water samples were obtained with a rosette water sampler, equipped with a Seabird CTD for temperature, oxygen and salinity measurements and 24 Niskin bottles (10 l volume). Samples were taken at different water depths. Filtration experiments were done with 4.5 l of the sampled water using 0.45 µm MicroClear (Roth, Germany) polycarbonate membranes. One part of the filter membrane was fixed with para-formaldehyde for phylogenetic staining experiments. The rest of the filter membrane was stored in vials filled with sterile seawater of the same depth (gasphase nitrogen) and sealed with rubber stoppers. Further investigations will be carried out in Regensburg, Germany.

Sampling sites

For details and sampling sites see Fig. 7.1.1 (Chapter 7.1, Gas Geochemistry).

Table 6.2: Samples and CTD data for water stations 05-MS, 19-MS, and 29-MS.

Station 05-MS	Position 3°18.906 S	152°34.878 E	top of Edison seamount		
depth (m)	Salinity (‰)	temperature (°C)	oxygen (mg/l)	sample (l)	pH
5	34.1569	29.04	4.56	4.5	7.0
50	34.3473	29.05	4.80	4.5	7.0
150	35.6579	20.64	3.07	4.5	7.0
400	34.7597	10.40	3.60	4.5	7.0
700	34.4789	5.65	4.41	4.5	7.0
100	34.5434	4.27	3.15	4.5	7.0
1200	34.5509	3.78	3.63	4.5	7.0
1400	34.5844	3.10	3.46	4.5	7.0
1420	34.5875	3.06	3.42	4.5	7.0
1450	34.5955	2.89	3.44	4.5	7.0

Station 19-MS	Position 3°19.505 S	152°35.442 E	S of Edison seamount		
depth (m)	Salinity (‰)	temperature (°C)	oxygen (mg/l)	sample (l)	pH
50	34.68	28.38	4.47	4.5	6.5
200	35.40	17.04	4.32	4.5	-
500	34.50	7.33	5.04	4.5	6.0
1000	34.54	4.29	3.37	4.5	-
1200	34.56	3.44	3.60	4.5	6.0
1400	34.59	2.96	3.49	4.5	-
1600	34.60	2.85	3.42	4.5	-
1610	34.60	2.67	3.43	9.0	6.0

Table 6.2 (continued): Samples and CTD data for water stations 05-MS, 19-MS, and 29-MS.

Station 29-MS	Position 3°19.326 S	152°37.225 E	SE of Edison seamount		
depth (m)	Salinity (‰)	temperature (°C)	oxygen (mg/l)	sample (l)	pH
1450	34.59	2.94	3.50	4.5	6.0
1500	34.5975	2.84	3.47	4.5	-
1550	35.610	2.64	3.48	4.5	-
1580	34.6123	2.60	3.47	4.5	6.0
1600	34.6137	2.57	3.47	4.5	-
1620	34.6157	2.60	3.42	4.5	-
1650	34.6163	2.57	3.50	4.5	-
1660	34.6172	2.52	3.456	4.5	6.0
1670	34.6181	2.51	3.46	4.5	-
1681	34.6182	2.51	3.45	4.5	6.0

6.2.2 Water and Sediment Samples

Methods

Additional anaerobic and aerobic samples of sediments and water were obtained from off-shore and on-shore locations. The material was filled into 100ml Schott bottles sealed with rubber stoppers. Anaerobic samples were reduced with 1.0ml of a natriumsulfide solution (2.5% w/v). Further investigations will be carried out in Regensburg, Germany.

Table 6.3: Water and sediment samples obtained off-shore and on-shore.

Sample	Location	Description	temperature	pH
Sediment sampling south of Lihir island				
10-GTVA (ED 1)	3°18.995' S 152°34.872' E	Grey sediment sample between mussles from Edison seamount	cold	9.0
14-GTVA (ED 2)	3°18.795' S 152°3.564' E	White surface layer on basaltic breccias from Conical seamount	cold	-
43-GTVA (ED 3)	3°19.457' S 152°35.370' E	greyish black sediment, samples rich in H_2S	cold	-
45-GTVA (ED 4)	3°19.458' S 152°35.409' E	greyish black sediment, samples rich in H_2S	cold	-
On-shore sampling at Lihir island				
ED 5	Capit area, field of acidic hot springs	grey, muddy, heavily degassing hot spring	96°C	2.0
ED 6	"	grey, heavily degassing hot spring	86°C	2.0
ED 7	"	greyish hot spring	73°C	2.0
ED 8	"	clear water, heavily degassing hot spring	95°C	2.0
ED 9	Capit beach, hot sandy beach	sediment sample, area with thermal activity, places with gas exhalations	70 to 85 °C	7.0
ED 10	"	sediment sample	97 °C	8.0
Off shore sampling at Lihir island				
ED 11	6m water depth	sediment sample from hot, heavily degassing hydrothermal vent	110 °C	

7 Shipboard analyses

7.1 Gas Geochemistry

BY MARK SCHMIDT & OLAF THIEßEN

7.1.1 Introduction

Determination of trace gases (e.g. CH_4, C_nH_n, CO_2 and He) in the water column and sediments of hydrothermal active areas can give information about the local vent situation and the origin of fluids. Abiogenic volcanic gases, gases from thermal processes in the sediment column and gases of biogenic origin (e.g. bacterial oxidation) can be described by their stable isotope signatures. Furthermore the stable isotope composition of gases in fluid inclusions provides information about the primary source conditions of magmatic fluids.

Recent hydrothermal activity in the Tabar-Lihir-Tanga-Feni Island chain was determined during RV Sonne cruise SO 94 in 1994. From these data a major hydrothermal plume source is supposed to exist in the seismicly active zone near Edison Seamount, south of Lihir Island. Localization of this vent and determination of gaseous compounds in the vent fluids should provide better information about the primary source of hydrothermal activity and possible secondary processes indicated by intensive biological activity (vent fauna) in the New Ireland Fore-Arc system.

7.1.2 Sampling Area

Water sample profiles were taken at four stations in the area south of Lihir island (05-MS, 19-MS, 29-MS, 71-MS) with a maximum water depth of 1717 m. Gas was sampled from gas vents at Lihir Harbor (LH 01, LH 02) and onshore Lihir Island (ED 07, see Fig. 7.1.1 for sampling locations and Table 7.1.1 for measured data).

7.1.3 Methods

Hydrographic data were taken by a multiprobe Seabird-CTD. Continuously logged data of dissolved oxygen, temperature and conductivity of vertical depth profiles are shown in the Appendix.

Water samples were taken with 24 × 10 l Niskin bottles attached to a CTD device. For the later measurements of dissolved He, water samples were stored in gas tight and air free copper tubes immediately after the sample device was on-board. Deep water samples for on-board degassing were filled in 1l air free glass bottles and stored in the cooling room until further preparation. Degassing of the water samples was done in 12 hours after sampling with the vacum ultrasonic method described by Schmitt et. al. (1991). In addition, water samples for CO_2 determination were treated with 2 ml conc. HCl each (sample pH=1,5) during vacum release.

Hydrocarbon gases from sediment samples were released by acid attack (H_3PO_4, conc.) in a vacuum line. Sediment samples were taken for total gas analyses, <63 µm fractions were used for adsorbed gas analyses. On-bord determination of extracted hydrocarbon trace gases was done with a DANI-Educational gaschromatograph. The light hydrocarbon gases were qualified with a Al_2O_3/KCl column, 30m, 0,32 mm diameter and were detected with a flame ionisation detector (FID). Carrier

gas was nitrogen. For shore-based stable isotopic analyses the gas samples were stored in evacuated, gas tight glass containers.

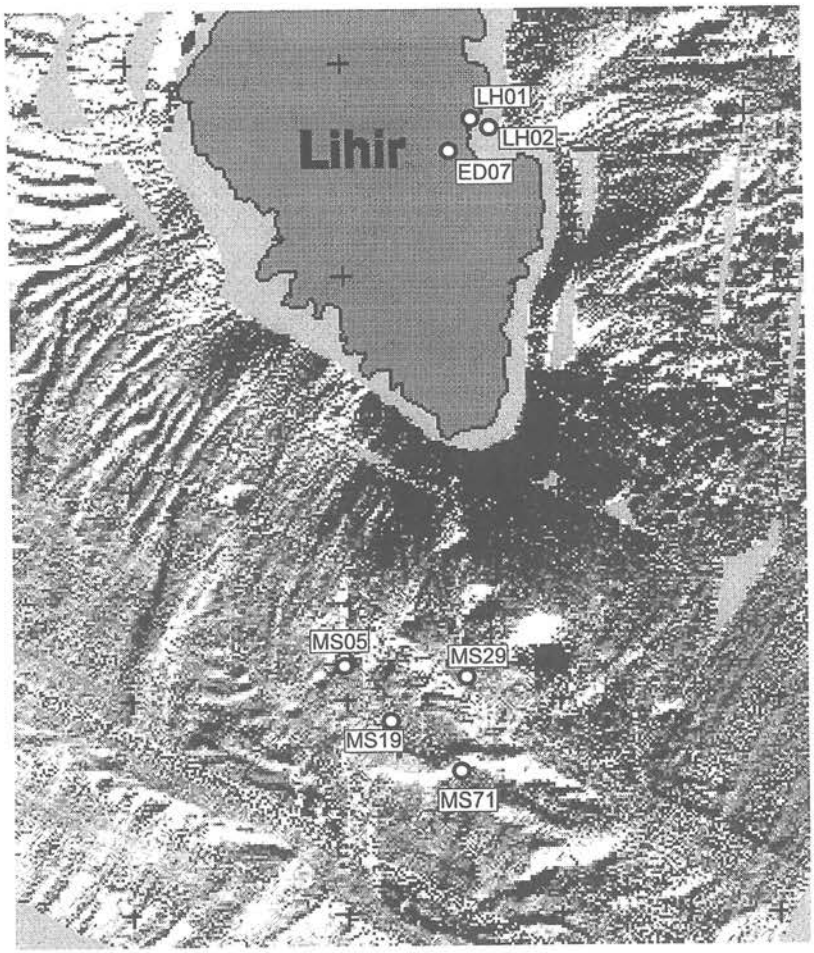

Figure 7.1.1: Sampling area

7.1.4 First Results

An active vent input was postulated by methane 3D-mapping based on SO-94 data. Highest concentrations were expected at 3°19.5S and 152°35.4E. This location matches also with a horst structure detected by Parasound and an observed biological activity (clam fields). Methane concentration data from the cruise report SO-94 and new data are plotted in Figure 7.1.2. Highest methane concentration of close to 10,000 nl/l were found in a water sample from station (19-MS) at 1610 m water depth. Sediment samples of this area show high contents of hydrocarbon gases (C1-C4) with max. concentration of 7,700 ppm CH_4 (see Tab. 7.1.3). Isotope measurements of released gases from water and sediment samples will be measured on shore after the cruise. Samples taken for He-isotope measurements (Tab. 7.1.2) will be investigated at the Institut für Umweltphysik (Heidelberg) by Quadrupol-IRMS.

Rock samples from Edison Seamount and TUBAF Seamount area (olivine and pyroxene containing basalts) were sampled for fluid inclusion measurements. Furthermore, large carbonate crusts were

sampled for further investigations from muddy sediments where high methane concentrations were found. Sediment and rock samples are listed in Table 7.1.3.

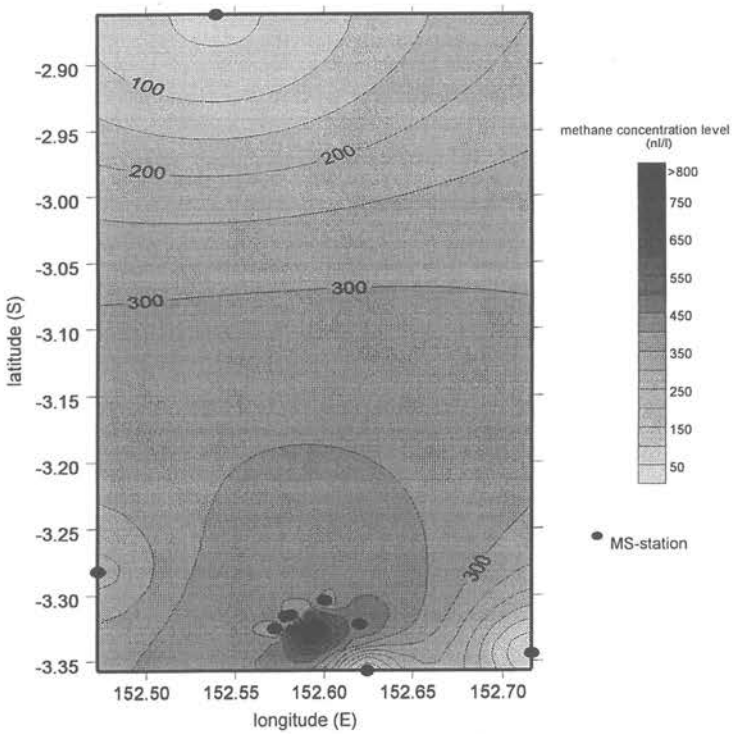

Figure 7.1.2: Methane concentration contour plot (1450-1680 m water depth; data from SO-94/133)

Table 7.1.1: Water and gas samples for hydrocarbons and CO_2 investigations

Station: 05-MS		Date: 21.7.98		Time:04:00 UTC	
WD: 1470m (HS)		Position:	03°18.906'S	152°34.878'E	
Depth [m]	Temperature [°C]	Oxygen [mg/l]	Salinity [‰]	CH_4 [nl/l]	vaccutainer No.
50	29.0582	147.9938	34.3473	46.8	05MS-23
1000	4.2806	97.5387	34.5434	10.0	05MS-22
1300	3.4876	108.9809	34.5635	12.7	05MS-18
1400	3.1051	105.8773	34.5844	20.2	05MS-15
1410	3.1013	105.6376	34.5846	25.0	05MS-06
1440	2.9368	105.0219	34.5944	58.4	05MS-12
1450	2.904	105.0105	34.5955	125.6	05MS-14

Station: 19-MS		Date: 23.7.98		Time:15:00 UTC	
WD: 1624m (HS)		Position:	03°19.505'S	152°35.442'E	
Depth [m]	Temperature [°C]	Oxygen [mg/l]	Salinity [‰]	CH_4 [nl/l]	vaccutainer No.
50	28.4143	149.3422	34.6298	66.2	19MS-05
200	17.1926	131.6632	35.4171	54.0	19MS-24
500	7.3256	153.9250	34.5493	55.6	19MS-23
800	5.3225	111.5678	34.5117	22.7	19MS-22
1000	4.2568	102.3422	34.5368	37.0	19MS-21
1300	3.1993	107.1483	34.5782	33.9	19MS-19
1500	2.9581	104.5673	34.5925	54.8	19MS-16
1570	2.9532	103.7260	34.5931	48.9	19MS-07
1590	2.8542	104.1818	34.5986	256.9	19MS-09
1610	2.6467	104.8345	34.6094	9874.6	19MS-11
1614	2.6467	104.8345	34.6094	6555.2	19MS-13

Table 7.1.1: (continued) Water and gas samples for hydrocarbons and CO_2 investigations

Station: 29-MS		Date: 24.7.98		Time:16:38 UTC	
WD: 1689m (HS)		Position:	03°19.326'S	152°37.225'E	
Depth [m]	Temperature [°C]	Oxygen [mg/l]	Salinity [‰]	CH_4 [nl/l]	vaccutainer No.
50	28.2193	149.4737	34.6296	47.4	29MS-01
500	7.2783	162.2548	34.5463	41.7	29MS-02
1000	4.3841	101.5978	34.5395	26.5	29MS-03
1500	2.8147	105.3397	34.6007	18.4	29MS-22
1550	2.6409	105.5637	34.6101	34.3	29MS-21
1580	2.5977	105.4195	34.6129	74.8	29MS-07
1600	2.5543	105.7169	34.6152	101.5	29MS-19
1620	2.5365	105.5592	34.6163	448.2	29MS-09
1650	2.5182	105.1987	34.6175	71.3	29MS-17
1660	2.5156	105.2333	34.6176	99.3	29MS-11
1670	2.5133	105.2537	34.6179	117.5	29MS-15
1681	2.5133	105.2537	34.6179	207.0	29MS-13

Station: 71-MS		Date: 29.7.98		Time:20:36 UTC	
WD: 1717m (HS)		Position:	03°21.456'S	152°37.272'E	
Depth [m]	Temperature [°C]	Oxygen [mg/l]	Salinity [‰]	CH_4 [nl/l]	vaccutainer No.
5	29.0051	142.807	34.3647	45.1	71MS-04
50	28.7223	141.3645	34.4508	59.0	71MS-24
500	7.8063	146.0104	34.5777	28.6	71MS-23
1000	4.2943	98.62491	34.5387	16.4	71MS-22
1300	3.147	106.7502	34.5817	30.4	71MS-21
1400	3.0357	104.9838	34.5877	23.9	71MS-20
1500	2.7655	104.7633	34.6027	19.6	71MS-19
1550	2.715	104.2096	34.6056	11.7	71MS-18
1600	2.6807	103.2495	34.6077	22.7	71MS-17
1630	2.6855	103.722	34.6074	17.1	71MS-05
1650	2.6887	103.7234	34.6074	36.0	71MS-15
1680	2.6733	102.6336	34.6082	14.9	71MS-13
1690	2.6348	102.9714	34.6106	26.1	71MS-07
1700	2.6348	102.9714	34.6106	14.2	71MS-11
1707	2.6348	102.9714	34.6106	65.8	71MS-09

Station: Lihir habor		Date: 28.7.98		Time:02:00 UTC	
WD: 6m (HS)		Position:	03°06.2'S	152°38.0'E	
Depth [m]	Temperature [°C]	pH	flow	note	vaccutainer No.
6m	110°C	~7	~400ml/s	H_2S	LH-1(12)
6m	110°C	~7	~400ml/s	H_2S	LH-1(56)
gas analyses	methane [ppm]	ethane [ppm]	propane [ppm]	butane [ppm]	
LH-1	1428.4	6.1	n.d.	n.d.	

Station: Lihir onshore		Date: 28.7.98		Time:02:00 UTC	
		Position:	03°06.8'S	152°37.5'E	
Depth [m]	Temperature [°C]	pH	Flow	note	vaccutainer No.
capit hot spring	98°C	~2	-	H_2S	ED-7(06)
capit hot spring	98°C	~2	-	H_2S	ED-7(94)
beach area	31°C	~7	-	H_2S	LH-2(89)

Table 7.1.2: Water samples for He-isotope measurements

Station: 05-MS	Date: 21.7.98		Time:04:00 UTC	
WD: 1470m (HS)	Position:	03°18.906'S	152°34.878'E	
Depth [m]	Temperature [°C]	Oxygen [mg/l]	Salinity [‰]	tube
50	29.0582	147.9938	34.3473	05MS-24
1000	4.2806	97.5387	34.5434	05MS-21
1430	3.0519	105.407	34.5875	05MS-14
1440	2.9368	105.0219	34.5944	05MS-12
1450	2.904	105.0105	34.5955	05MS-10

Station: 19-MS	Date: 23.7.98		Time:15:00 UTC	
WD: 1624m (HS)	Position:	03°19.505'S	152°35.442'E	
Depth [m]	Temperature [°C]	Oxygen [mg/l]	Salinity [‰]	tube
50	28.4143	149.3422	34.6298	19MS-05
200	17.1926	131.6632	35.4171	19MS-24
1550	2.9632	104.6891	34.5923	19MS-15
1610	2.6467	104.8345	34.6094	19MS-11
1614	2.6467	104.8345	34.6094	19MS-13

Station: 29-MS	Date: 24.7.98		Time:16:38 UTC	
WD: 1689m (HS)	Position:	03°19.326'S	152°37.225'E	
Depth [m]	Temperature [°C]	Oxygen [mg/l]	Salinity [‰]	tube
500	7.2783	162.2548	34.5463	29MS-02
1600	2.5543	105.7169	34.6152	29MS-19
1670	2.5133	105.2537	34.6179	29MS-15
1681	2.5133	105.2537	34.6179	29MS-13

Station: 71-MS	Date: 29.7.98		Time:20:36 UTC	
WD: 1717m (HS)	Position:	03°21.456'S	152°37.272'E	
Depth [m]	Temperature [°C]	Oxygen [mg/l]	Salinity [‰]	tube
1600	2.6807	103.2495	34.6077	71MS-17
1680	2.6733	102.6336	34.6082	71MS-13
1707	2.6348	102.9714	34.6106	71MS-09

Station: Lihir habor	Date: 28.7.98		Time:02:00 UTC	
WD: 6m (HS)	Position:	03°06.2'S	152°38.0'E	
Depth [m]	Temperature [°C]	pH	flow	tube
6m	110°C	~7	~400ml/s	LH-1(12)

Table 7.1.3: Sediment samples

Station: 43-GTVA	Date: 24.7.98				Time: 09:14 UTC	
WD: 1624m (HS)	Position:	03°19.471'S	152°35.374E			
sample no	gas analyses	weigth [g]	methane [ppm]	ethane [ppm]	propane [ppm]	butane [ppm]
43-GTVA-1	total	20.8	110.2	2.2	0.7	0.2
43-GTVA-2	adsorbed	19.5	173.2	22.3	6.7	2.0

Table 7.1.3: (continued) Sediment samples

Station: 45-GTVA		Date: 27.7.98			Time: 04:40 UTC	
WD: 1606m (HS)		Position:	03°19.340'S	152°35.464E		
sample no	gas analyses	weigth [g]	methane [ppm]	ethane [ppm]	propane [ppm]	butane [ppm]
45-GTVA-1	total	16.8	7705.1	663.3	2.6	0.7
45-GTVA-2	adsorbed	18.2	121.5	11.3	2.9	0.9

Station: 57-GKG		Date: 27.7.98			Time: 14:15 UTC	
WD: 1606m (HS)		Position:	03°19.340'S	152°35.464E		
sample no	gas analyses	weigth [g]	methane [ppm]	ethane [ppm]	propane [ppm]	butane [ppm]
57-GKG	total	17.9	107.3	16.4	5.1	1.8

Station: 58-SLS		Date: 27.7.98			Time: 14:15 UTC	
WD: 1614m (HS)		Position:	03°19.355'S	152°35.453'E		
sample no	gas analyses	weigth [g]	methane [ppm]	ethane [ppm]	propane [ppm]	butane [ppm]
58-SLS	total	20.5	299.7	26.4	8.1	2.1
sample from core catcher (5mbs)						

Tab. 7.1.4: Rock samples

Station: 07-DR	Date: 21.7.98	Time:04:00 UTC	
WD: 1591-1107m (HS)	Position:	03°19.170'S	152°39.280'E
	to	03°18.700'S	152°39.610'E
sample no: 2i vesicular pyroxene-rich basalt (ankaramite) with minor olivine phenocrysts			

Station: 44-GTVA	Date: 26.7.98	Time:10:06 UTC	
WD: 1630m (HS)	Position:	03°19.352'S	152°35.462'E
sample no: 44-GTVA Carbonate crust, increasing density of mussels and barnecles			

Station: 45-GTVA	Date: 26.7.98	Time:14:40 UTC	
WD: 1606m (HS)	Position:	03°19.340'S	152°35.464'E
sample no: 45-GTVA Carbonate crust, sediment with dark patches			

Station: 47-DR	Date: 26.7.98	Time:19:38 UTC	
WD: 1129m (HS)	Position:	03°18.683'S	152°39.481'E
	to	03°18.731'S	152°39.595'E
sample no: 47-DR vesicular pyroxene-rich basalt (ankaramite)			

Station: 54-GTVA	Date: 27.7.98	Time:06:09 UTC	
WD: 1269m (HS)	Position:	03°15.135'S	152°32.499'E
sample no: 54-GTVA Olivine xenolith from TUBAF seamount			

7.1.5 Appendix

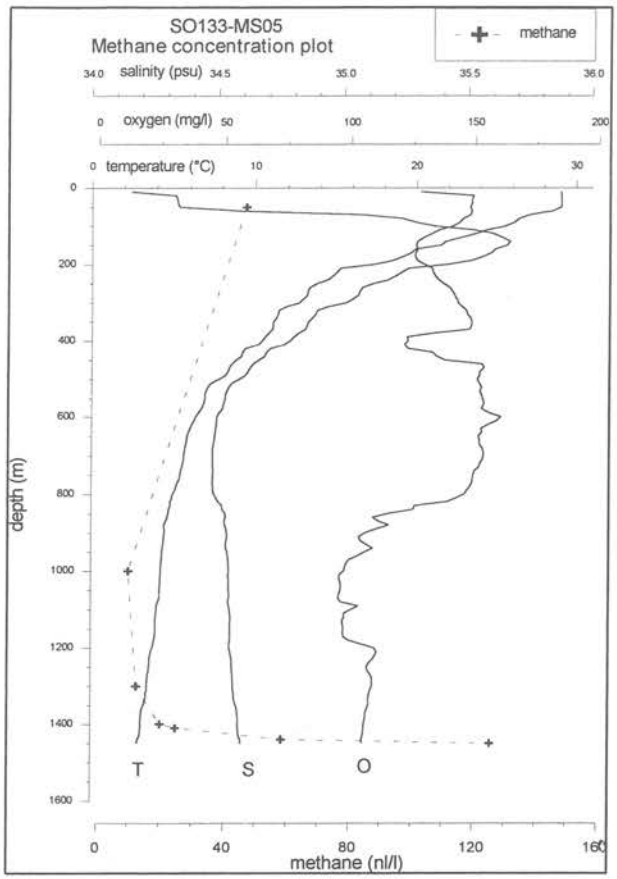

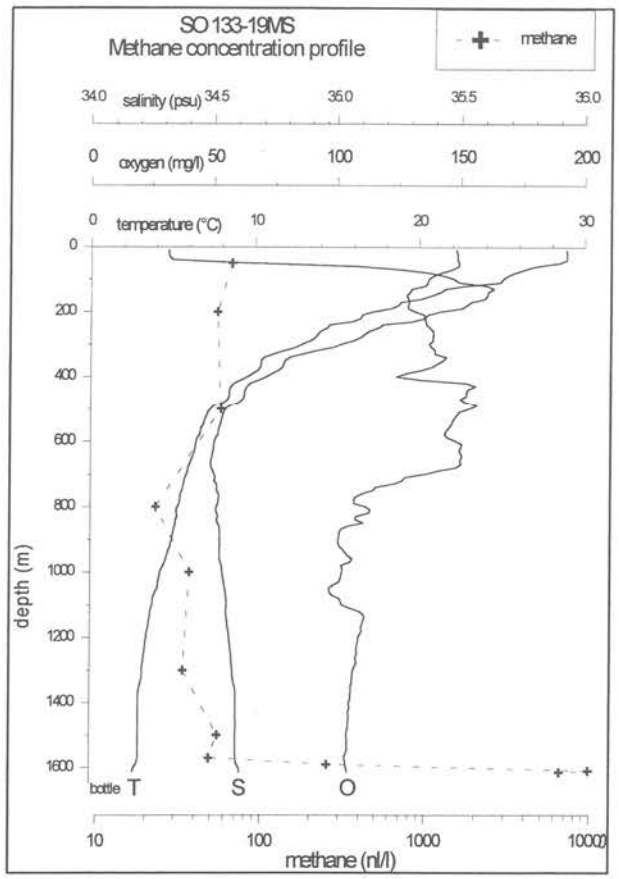

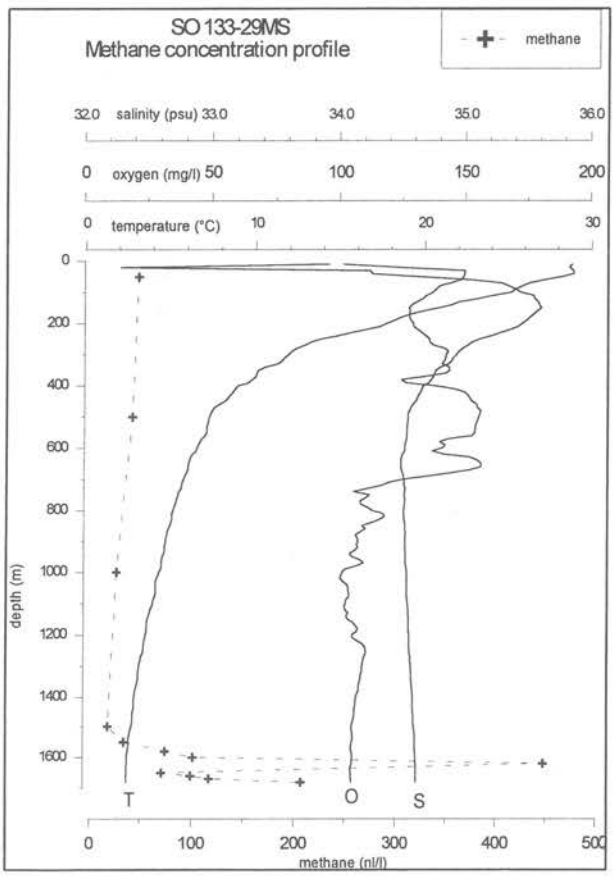

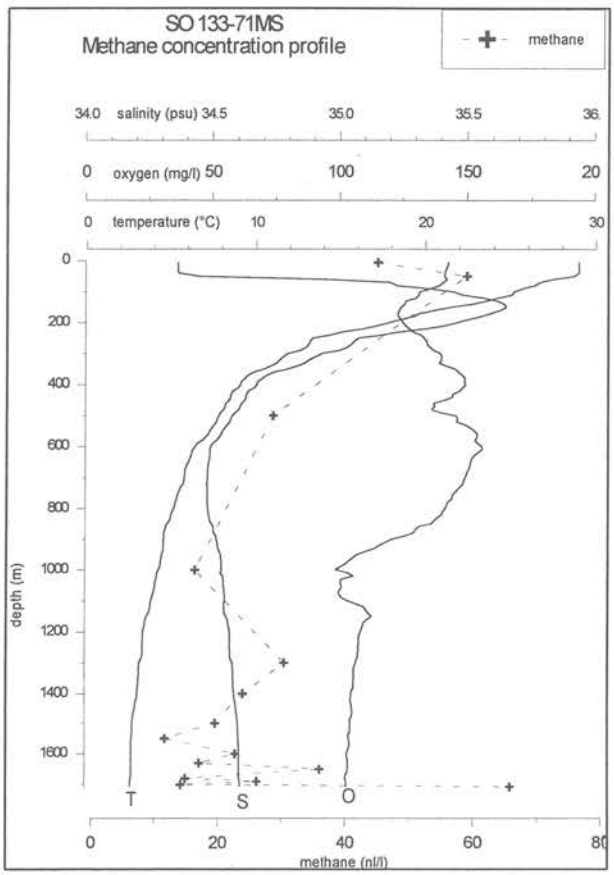

7.2 Mineralogical Analyses of Selected Samples Using X-Ray Powder Diffraction

BY JEANNE B. PERCIVAL

7.2.1 Introduction

A suite of samples were selected from TV-grabs, dredges, box cores and piston cores for qualitative mineralogical analysis using X-ray powder diffraction (XRD). This suite included basalts, breccias and unconsolidated and indurated sediments. Particular emphasis was placed on surface coatings and crusts, which may indicate hydrothermal alteration, and on sulphide-bearing samples. During the SO-133 cruise 78 sample analyses were completed.

7.2.2 Methods of Analyses

Most samples were lightly crushed in distilled water in an agate mortar. This procedure will not disaggregate all the minerals but is used to concentrate any clay minerals present. Oriented mounts were prepared by pipetting between 1 and 2mL of the suspension onto glass slides. The samples were air-dried overnight and X-rayed from 2 to 72° 2θ. Any samples with detectable amounts of clay minerals were then set in a desiccator containing ethylene glycol for 2 days and the X-rayed again from 2 to 35° 2θ. Eighteen samples were treated and reanalyzed to verify presence of smectite. For a few samples, the clay-size fraction was separated using the sedimentation technique (2 cm intervals) followed by centrifugation to spin down the sediment. Whole rock samples were also prepared using pressed powder mounts of finely ground material initially prepared for X-ray fluorescence analysis.

Samples were analyzed on the *RV Sonne* using a Philips PW1840 compact XRD set at 40kV and 50mA with Cu Kα radiation and Ni filter. The X-ray data was collected and processed using PC-APD (automated powder diffraction) software provided by Philips. Any samples containing abundant iron provided poor X-ray patterns due to excessive fluorescence using the Cu tube. Some samples were re-analyzed at the GSC as air-dried smear mounts. A Philips PW1830/PW1710 XRD equipped with a graphite monochromator, Co Kα radiation set at 40kV and 30mA was used. In addition, individual red and orange crystals from one sample (26-GTVA) were analyzed using routine X-ray powder diffraction by film methods (Debye-Sherrer camera). This same sample was then examined under an environmental scanning electron microscope, Hitachi S-3200N VP-SEM, in order to preserve the specimen for any additional analyses. Other samples (grain mounts) were examined under a Leica Cambridge Stereoscan S360 SEM equipped with an Oxford/Link eXL-II energy-dispersion X-ray analyzer, Oxford/Link Pentafet Be window/light element detector and an Oxford/Link Tetra backscattered electron detector at an accelerating voltage of 20kV. The grain mounts were prepared by pipetting a dilute suspension (in water) of fine material onto carbon double-sided tape, followed by coating with carbon.

7.2.3 Results

Results are summarized in Table 7.2.1 Minerals are listed in order of decreasing abundance. Abundance was estimated based on intensities of the each mineral's main X-ray peak.

Selected unconsolidated sediment samples were taken from box (GKG) and gravity (SL) cores. These buff-coloured, foraminiferal sands are interlayered with volcanic ash and consist of calcite with subordinate plagioclase, with or without quartz, aragonite and traces of chlorite and smectite. A typical example is shown in Figure 7.2.1 One sample of an ash layer (38-SL) was dominated by plagioclase and may contain traces of analcime and smectite. In order to verify the presence of other trace components, calcite should be removed.

Other samples of sediment and mud were taken from the dredges (DR) and TV-grabs (GTVA). These silty to sandy materials ranged in colour from buff to pale green, grey to black and brown to reddish brown, and in consistency from unconsolidated to highly indurated. The buff and brown muds were similar in composition to the foraminiferal sands. The pale green and grey to black muds contained variable proportions of pyrite and/or marcasite, magnetite, smectite and chlorite. Some are dominated by calcite and most usually contain minor to abundant amounts of plagioclase. Plagioclase composition is anorthite-rich. The reddish muds were very Fe-rich (probably goethite and ferrihydrite). However, when these samples were analyzed the pattern went off scale due to excessive fluorescence of the Fe.

One of the indurated muds, 74-GTVA, is layered and variegated in colour. Induration may have been caused by circulation of hydrothermal fluids, baking by extruding lavas, or by low temperature cementation by carbonates. In 74-GTVA, the dark green to black layer was dominated by smectite as well as minor amounts of marcasite. The smectite may be nontronitic (based on colour) but must be verified with further refined analyses and chemistry. If nontronite does occur, it would be further evidence for a hydrothermal origin. The presence of montmorillonite, on the other hand, is more typical of volcanic ash. Figure 7.2.2 is an SEM photomicrograph of the black material from this variegated mud. The smectite is completely coated by Mn oxide. Further analyses of the smectite will require removal of the oxide coating by means of a partial extraction method.

Another sample of interest was a pale-green indurated carbonate mud containing a myriad of gas holes (sample 44-GTVA). This mud, containing calcite, plagioclase, quartz and traces of kaolinite or chlorite, was intimately associated with a mussel field and may have been formed through methane expulsion.

A variety of crusts and coatings were visible on breccia and basalt sampled during dredging and TV-grab operations. Reddish crusts were very Fe-rich and could not be analyed using the Cu X-ray tube. The black crusts (e.g., 10-GTVA-2) generally contain plagioclase (anorthitic) with sulphides (pyrite and/or marcasite). The yellowish crusts (e.g., 17-DR-4BY) contained abundant sphalerite with pyrite.

Some basalt samples have a green altered surface. For example, sample 23-GTVA-6 contains abundant smectite in addition to minor amounts of plagioclase, kaolinite, marcasite and illite (Fig. 7.2.3). The green colour may indicate the presence of nontronite suggesting a hydrothermal origin for the alteration. Nontronite cannot be differentiated from other smectites without extensive pre-treatments.

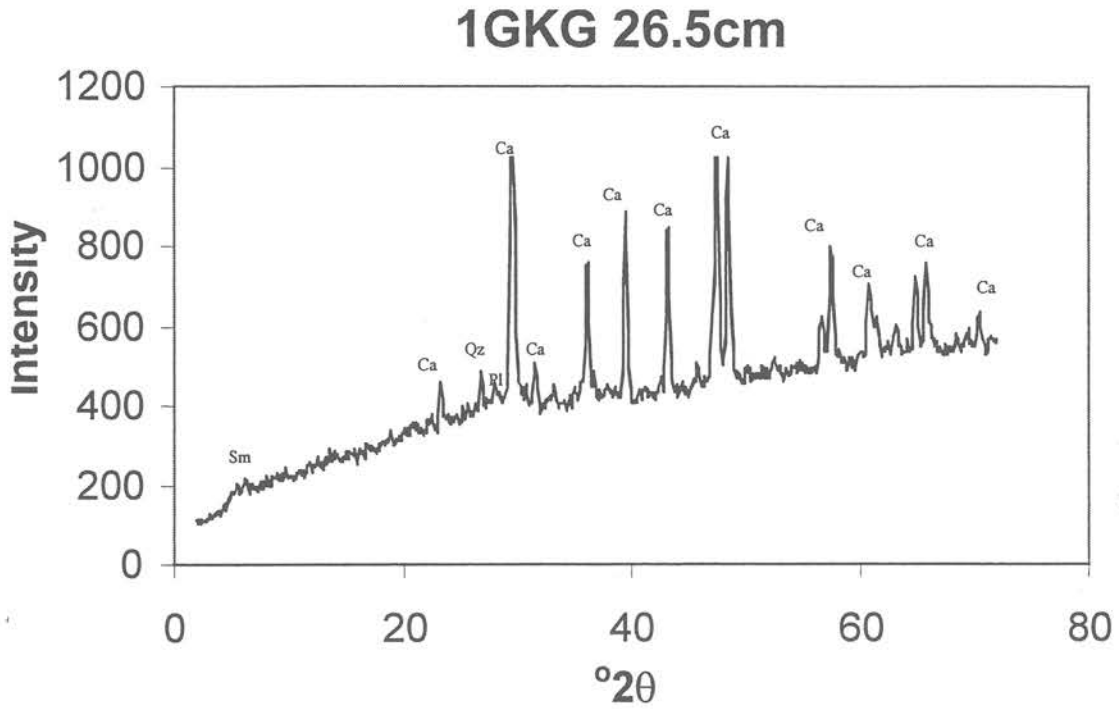

Figure. 7.2.1: XRD pattern of unconsolidated formaminiferal sand composed of calcite (Ca), minor to trace plagioclase (Pl) and quartz (Qz) and trace amount of smectite (Sm).

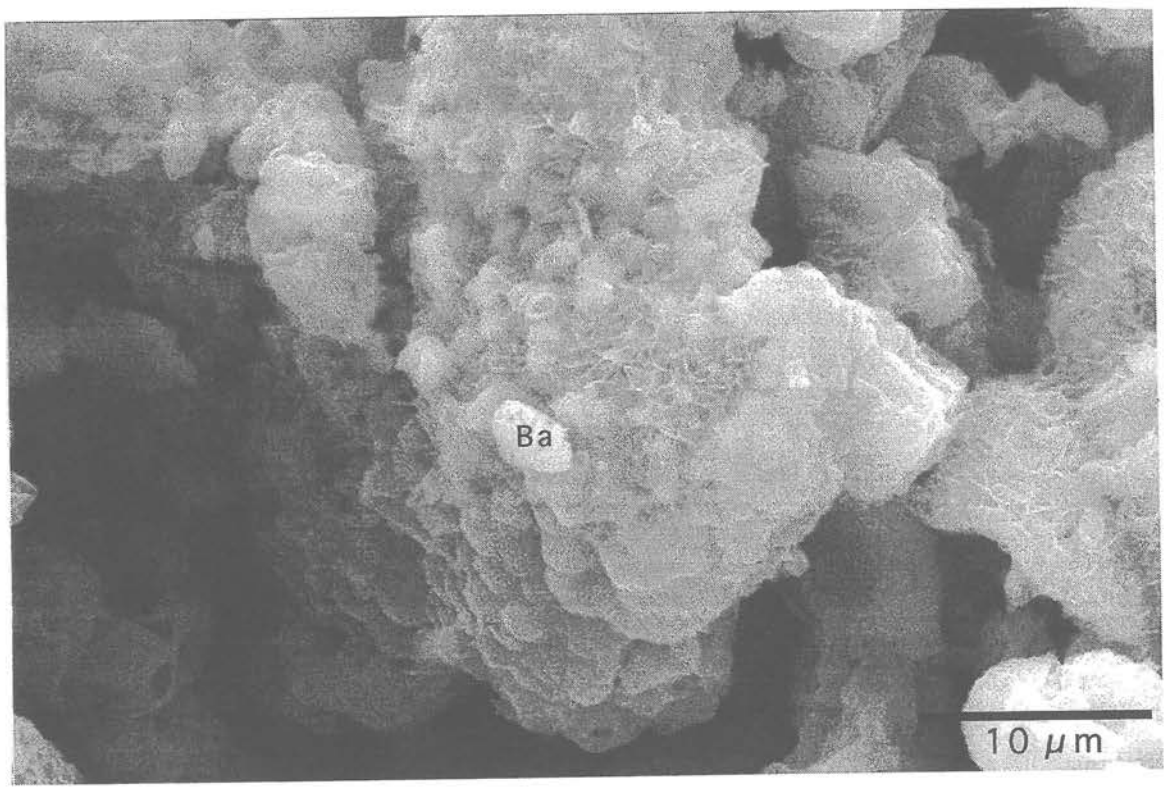

Figure 7.2.2: Secondary electron image of Mn-oxide coating on smectite (sample 74-GTVA, black layer). Small bright grain at centre is barite (Ba) (bar scale = 10 µm).

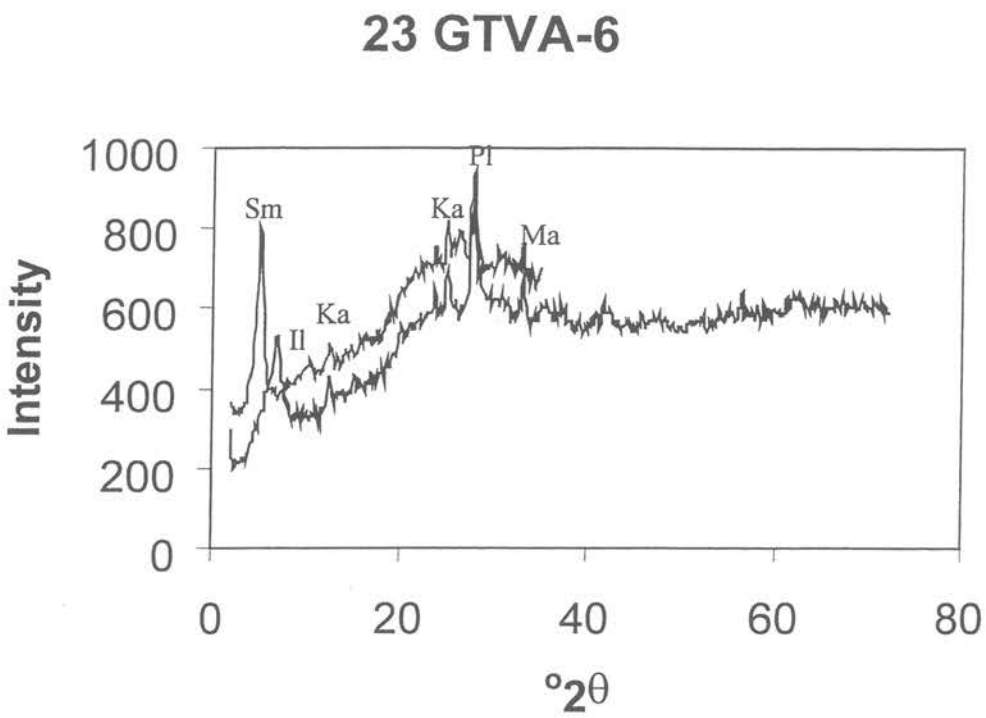

Figure 7.2.3: XRD pattern of green alteration material from basalt surface consisting of smectite (Sm), llite (Il), kaolinite (Ka), plagioclase (Pl) and marcasite (Ma). The lower pattern is air-dried, the upper is glycol-solvated. Note the shift towards the low angle verifying the presence of smectite.

During this cruise only a small number of rocks (basalts and breccias) were analyzed. Some samples were prepared for geochemistry (crushed) and will be analyzed after the cruise at the GSC. Many of the samples were highly altered to clay. For example, samples 40-GTVA-2 (altered basalt) and 39-GTVA-4A (ankaramitic basalt) contained abundant chlorite and pyrite with traces of plagioclase and possibly mixed-layer clay minerals. These results may not reflect the true mineral content as whole rock powders were not analyzed. For details see petrological sample description notes (chapter 4) in this volume.

Figure 7.2.4 shows an example of a highly altered basalt that is mineralized. Sample 17-DR-4B contains sphalerite, marcasite and pyrite in a matrix of plagioclase with traces of illite and smectite. Note that the main X-ray peaks for the sulphides overlap making it difficult to identify. In one highly mineralized sample, 25-GTVA-6, there were veins containing tiny, euhedral red crystals. These were identified as realgar (Fig. 7.2.5). The presence of realgar points to As-rich hydrothermal fluids at this locality. This mineral was not identified in the previous cruise (SO-94).

Detailed X-ray analyses at the GSC of the red and orange crystals from sample 26-GTVA revealed that realgar (red) was associated with alacranite, a rare polymorph of realgar (Fig. 7.2.6a). Both realgar and alacranite were embedded in a crust of white, amorphous silica (Fig. 7.2.6b).

Another unusual occurrence is the presence of paragonite in vesicles in basalt samples from station 41-GTVA (Fig. 7.2.8). The Na-rich mica probably precipitated following breakdown of Na-bearing feldspar or groundmass due to interaction with hydrothermal fluids.

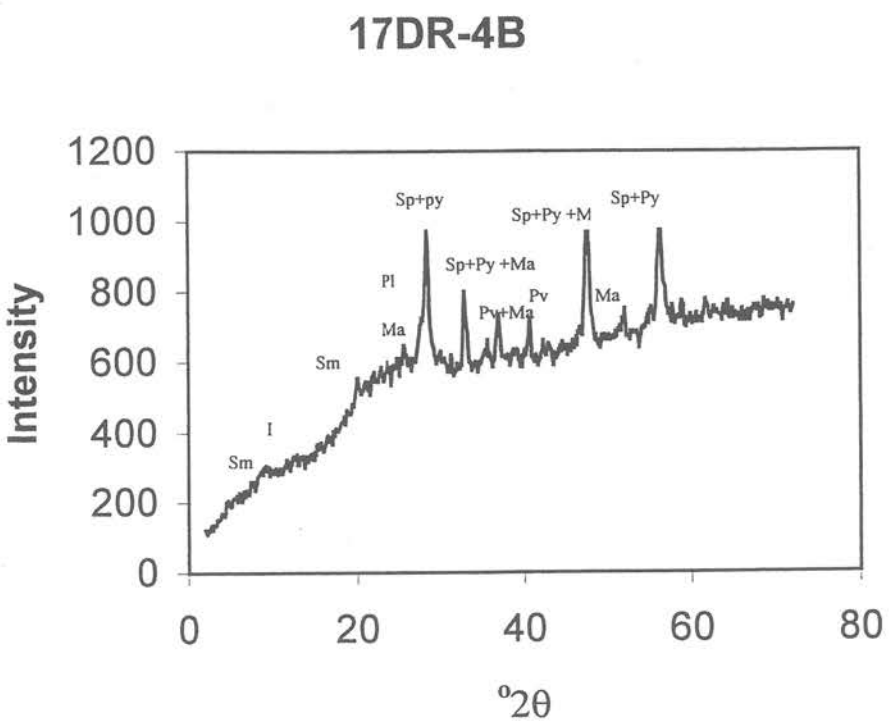

Figure 7.2.4: XRD pattern of altered basalt containing sphalerite (Sp), pyrite (Py), marcasite (Ma), minor plagioclase (Pl) and trace of illite (Il) and smectite (Sm).

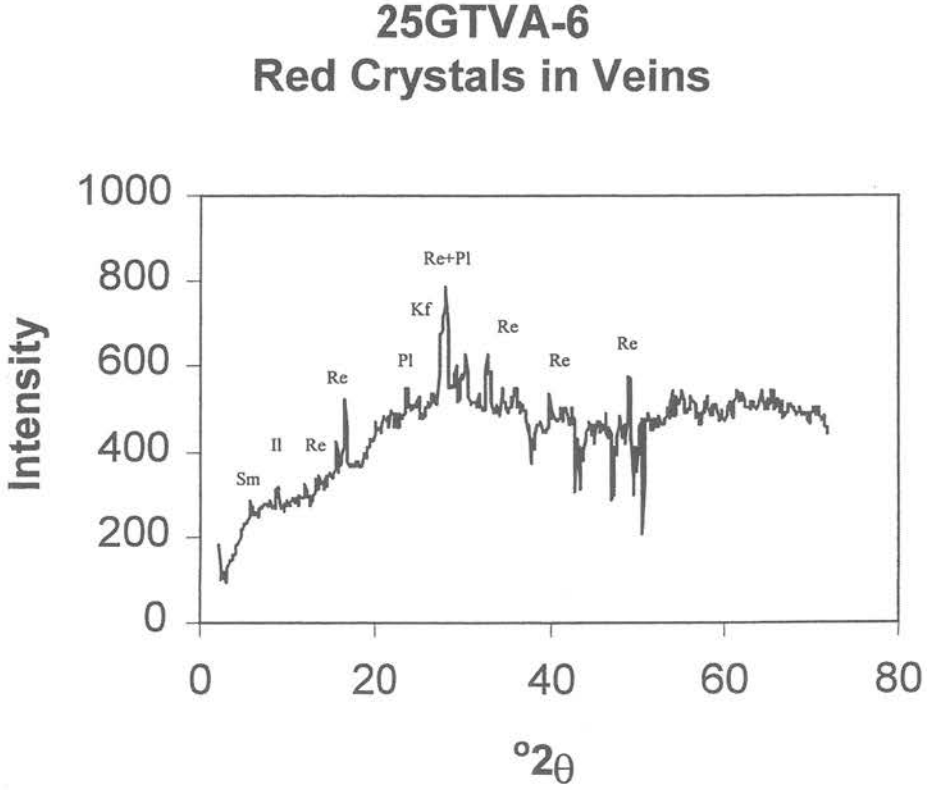

Figure 7.2.5: XRD pattern of realgar (Re) crystals from veins in mineralized basalt. Other minerals (Kf = K-feldspar, Pl = plagioclase, Il = illite, Sm = smectite) were scraped from the rock surface.

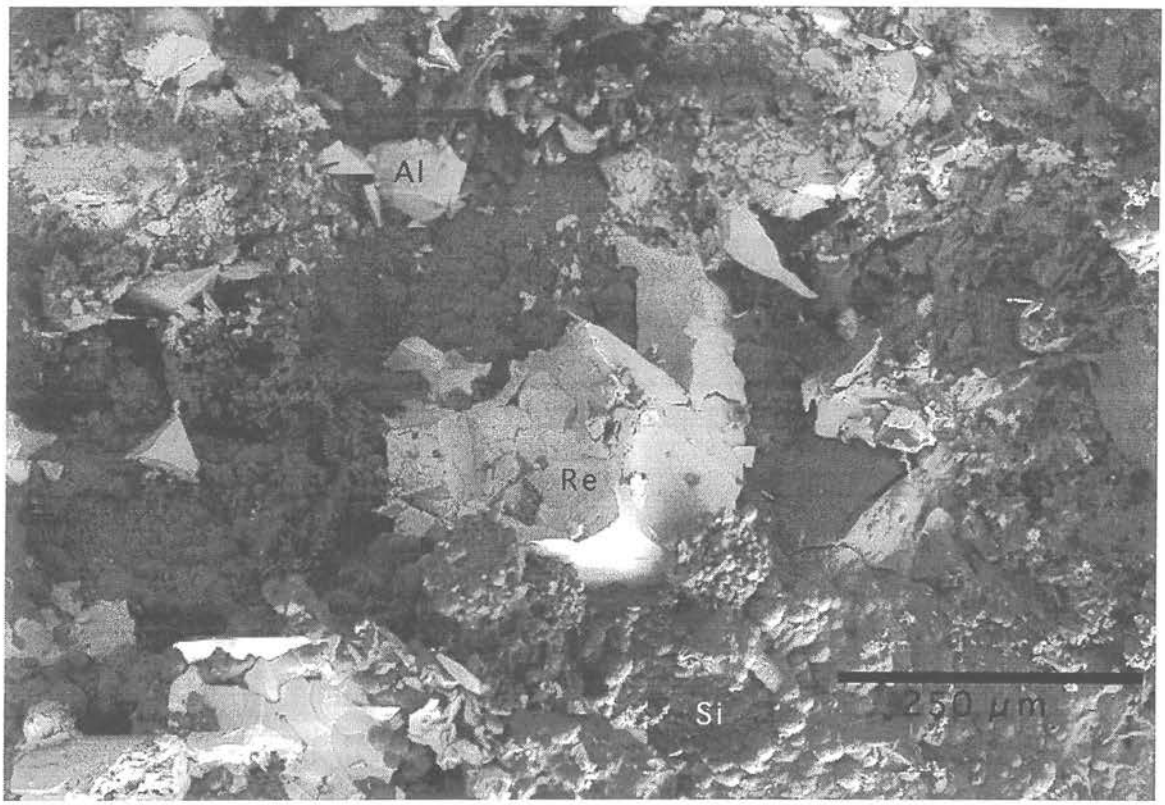

Figure 7.2.6a: Backscattered electron image of realgar (Re; whitish, central crystal) surrounded by alacranite (Al; other whitish crystals) in amorphous silica (Si; dark grey) (sample 26-GTVA).

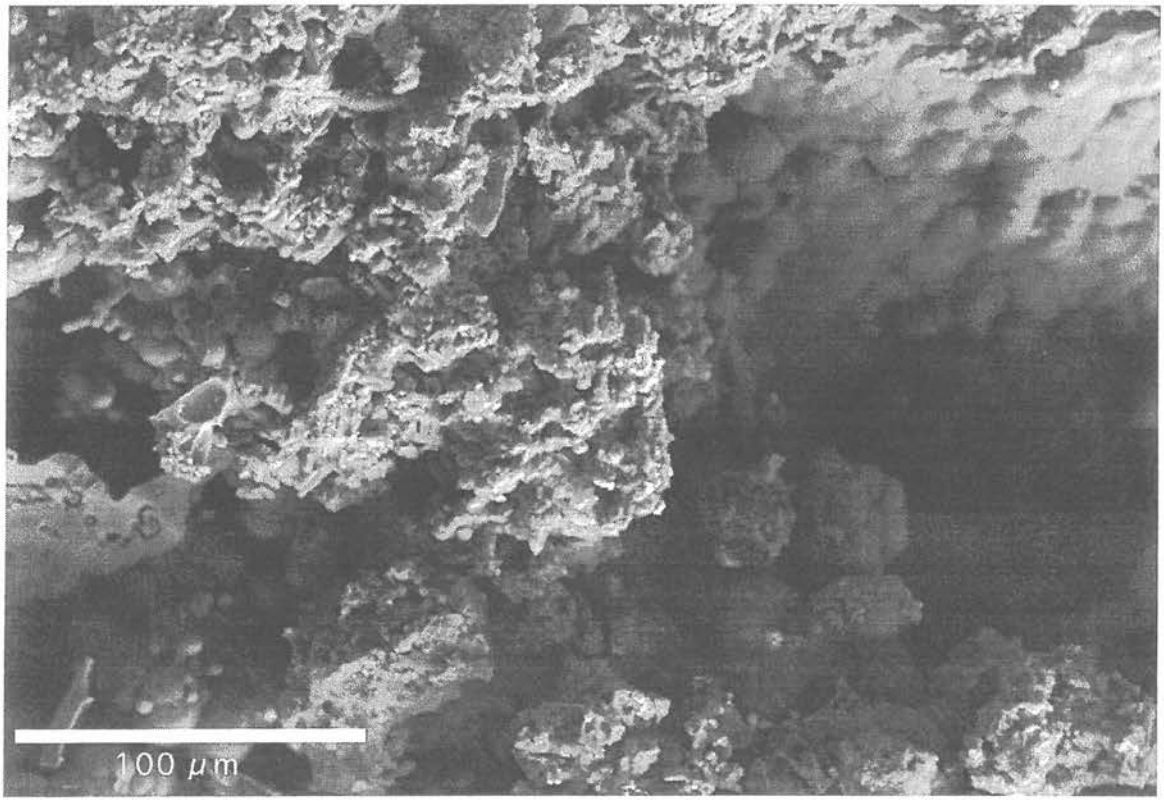

Figure 7.2.6b: Backscattered electron image of amorphous silica (Si) (sample 26-GTVA).

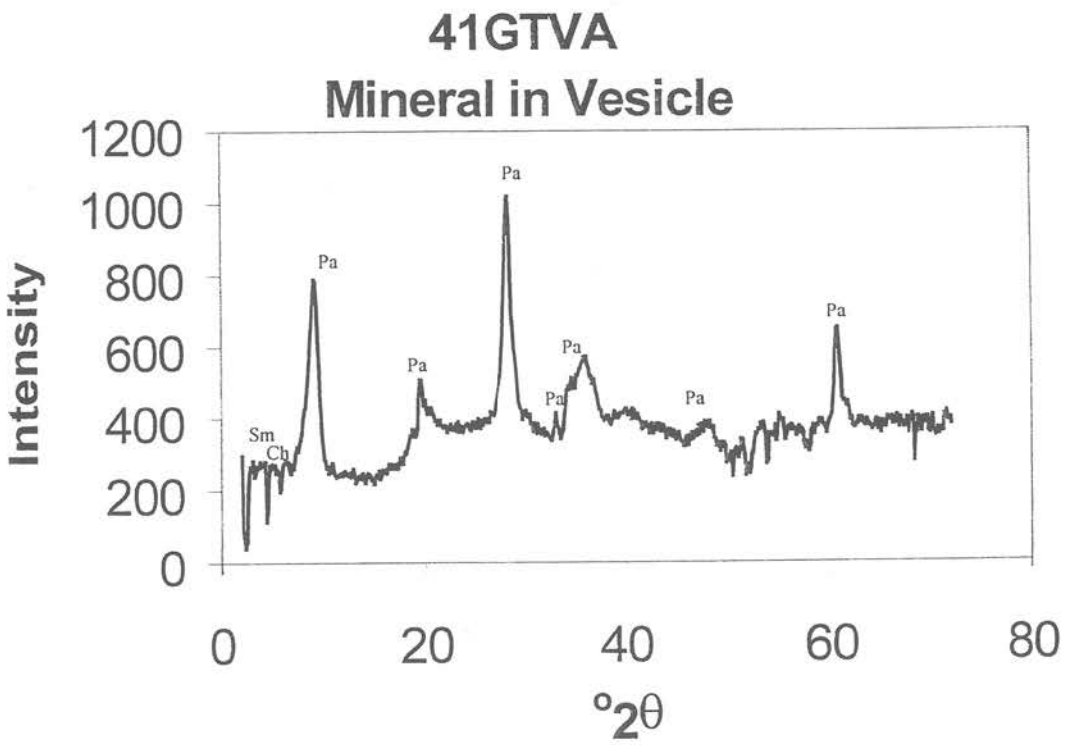

Figure 7.2.7: XRD pattern of paragonite (Pa) with traces of smectite (Sm) and chlorite (Ch) found in vesicles.

In the Lihir Au deposit, many of the mineralized samples contain alunite and kaolinite, minerals typical of a high sulphidation, epithermal environment. The altered samples analyzed from dredges and TV-grabs on this cruise do not appear to contain any alunite, but a few do contain kaolinite. Some of the X-ray peaks of the chief minerals (i.e., plagioclase) overlap with alunite and pyroxene. More refined analyses will be required as follow-up to look for these diagnostic minerals.

The author is grateful to J.M. Franklin for his patience and assistance in converting X-ray patterns to digital images; to A. C. Roberts (GSC) for Debye-Sherrer analyses; to R. Lastra (CANMET) and P. Hunt (GSC) for SEM analyses and photomicrographs; and to R. Lacroix (GSC) for computer graphics.

Table 7.2.1: Qualitative mineralogical (XRD) analysis of samples from the Lihir area, Papua New Guinea (A = abundant, m = minor, tr = trace).

Station/Area	Sample No.	Mineralogy	Comments
01-GKG NW of Simberi Island	01-GKG 3.5 cm	Calcite (A) Plagioclase, Quartz (m-tr) Chlorite	Brownish mud. Quartz was identified by only 1 peak. Will need to be confirmed with additional analysis.
	01-GKG 26.5cm	Calcite (A) Plagioclase, Quartz (m-tr) Smectite (tr)	
	01-GKG 42.5cm	Calcite (A) Plagioclase, Quartz, Aragonite (m-tr) Chorite? (tr)	

Station/Area	Sample No.	Mineralogy	Comments
02-SL NW of Simberi Island	02-SL 61 cm	Calcite (A) Plagioclase, Quartz (m-tr) Illite, K-Feldspar? (tr)	Greyish mud. See above concerning quartz.
	02-SL 87 cm	Calcite (A) Plagioclase, Quartz (m-tr) Chlorite, Illite?, K-Feldspar? (tr)	
03-GKG W of Simberi Island	03-GKG 29 cm	Calcite (A) Plagioclase, Quartz, Chlorite, Aragonite (m-tr) Illite/Smectite (tr)	Brown mud. XRD pattern poor. See above concerning quartz. Illite/ smectite = mixed layer clay mineral.
04-SL W of Simberi Island	04-SL 10.5 cm	Calcite (A) Plagioclase, Quartz (m-tr) Illite/Smectite, Chlorite, K-Feldspar? (tr)	Buff mud. See above concerning quartz. Poor XRD pattern, cannot readily distinguish clay mineral peaks from background. Second sample is grey.
	04-SL 150 cm	Calcite (A) Plagioclase, Quartz (m-tr) Chlorite, Smectite K-Feldspar? (tr)	
07-DR Conical SMT SE flank	07-DR-1A	Calcite, Halite (A) K-Feldspar, Plagioclase (m) Pyroxene (m-tr) Quartz? (tr) Amorphous component	Reddish mud. K-Feldspar may be orthoclase; very poor pattern. Halite formed from sea salt.
09-SL between Lihir and Tabar	09-SL 113.5 cm	Calcite (A) Plagioclase (m) Quartz, Smectite (m-tr) Chlorite, K-Feldspar? (tr)	Greyish mud. Peak intensities at low angle are very low.
	09-SL 158 cm	Calcite (A) Plagioclase, Smecite, Quartz (m-tr) K-Feldspar, Chlorite (tr)	
10-GTVA Edison SMT	10-GTVA-1	Calcite (A) Plagioclase, Quartz, Aragonite (m-tr) Illite, Chlorite? (tr)	Soft green mud.
	10-GTVA-1A	Calcite (A) Plagioclase, Quartz (m-tr)	Slightly more indurated green mud.
	10-GTVA-2	Plagioclase (A) Quartz, Smectite (m) Pyrite? (m-tr) Calcite, Chlorite? (tr)	Black crust.
	10-GTVA-3	Calcite (A) Plagioclase (m) Quartz (m-tr) Magnetite?, Pyrite?, Chlorite? (tr)	Yellowish crust
	10-GTVA-8	Calcite (A) Plagioclase, Quartz, K-Feldspar, Marcasite, Aragonite (m-tr)	Note that only two marcasite peaks were observed.
	10-GTVA-BG	Calcite (A) Aragonite, Marcasite?, Plagioclase, K-Feldspar (m-tr)	Bright green coating on shell; poor XRD pattern at high angle end.

Station/Area	Sample No.	Mineralogy	Comments
11-GTVA Edison SMT	11-GTVA-1A	Calcite (A) Plagioclase (m) Quartz, Pyrite (m-tr) Chlorite, Illite?, Aragonite?, Magnetite? (tr)	Greenish-black mud.
	11-GTVA-1B	Calcite (A) Plagioclase (m-tr) Quartz, Magnetite?, Marcasite? (tr)	Black mud.
	11-GTVA-1C	Calcite (A) Plagioclase, Quartz , Pyrite (m-tr) K-Feldspar, Magnetite? Marcasite?(tr)	Black fines (along fissures) taken from inside mass of mud.
	11-GTVA-1D	Calcite (A) Plagioclase, Quartz (m-tr) Magnetite, Pyrite, K-Feldspar?, Aragonite?, Chlorite? (tr)	Black mud.
12-DR Conical SMT	12-DR-1A	Calcite (A) Plagioclase (m) Quartz (m-tr) Smectite?, Magnetite, Pyrite (tr)	Black coating/mud. May contain a Mn-bearing calcite in addition to calcite. The 2.98Å of this Mn-calcite is also the main x-ray peak for alunite, however, there are no other alunite peaks present.
	12-DR-1B	Plagioclase (A) Quartz, Pyrite? (tr)	Rusty coating/mud. Poor XRD pattern due to high Fe content. Plagioclase is anorthitic.
13-DR Conical SMT	13-DR-1	Probably Fe-oxide	Not analyzed.
	13-DR-1A	Plagioclase (A) Illite (m) Pyrite or Marcasite (m-tr)	Plagioclase is anorthitic; illite is Fe-rich (biotitic or phlogopitic).
	13DR-2	Probably Fe-oxide.	Not analyzed.
14-GTVA Conical SMT	14-GTVA-GC	Plagioclase (A) Marcasite or Pyrite (m) Quartz? (m-tr) Illite, Smectite? (tr)	Greenish crust on, or alteration of basalt. Plagioclase is probably anorthitic.
	14-GTVA-7	Plagioclase (A) Marcasite or Pyrite (m) Quartz?, Illite, Kaolinite (tr)	Pressed powder mount (whole rock)
15-GTVA Conical SMT	15-GTVA	Halite (A) Marcasite? (m) Calcite (tr) Amorphous	White, soft coating found on most samples, probably amorphous silica.
17-DR Conical SMT	17-DR-4BY	Sphalerite, Pyrite (A) Marcasite? (m) Illite?, Smectite? (tr)	Yellowish coating on altered basalts.
	17-DR-4B	Sphalerite, Pyrite (A) Marcasite (m) Plagioclase (m-tr) Illite, Smectite (tr)	Altered basalt.

Station/Area	Sample No.	Mineralogy	Comments
23-GTVA Conical SMT	23-GTVA-1A	Pyrite (A) Smectite (A-m) Magnetite, Chlorite (m-tr) Illite/Smectite (tr)	Grey mud.
	23-GTVA-1B	Calcite (A) Plagioclase, Quartz? (m-tr) Chlorite?, Illite?, Smectite? (tr)	Brown mud.
	23-GTVA-2	Pyrite (A) Plagioclase (m) K-Feldspar (m-tr) Kaolinite or Chlorite, Illite? (tr)	Black soft material coating basalts (scrapings).
	23-GTVA-2 Whole Rock	Pyrite (A) Plagioclase (A-m) K-Feldspar, Marcasite (m) Magnetite?, Illite?, Smectite? (tr)	Altered basalt. Pressed powder.
	23-GTVA-3	Pyrite, Marcasite (A) Halite (m-tr) Quartz?, Illite?, Smectite?, Calcite (tr)	
	23-GTVA-6	Smectite (A) Plagioclase (A-m) Kaolinite, Marcasite (m)	Green alteration material scraped from surface.
	23-GTVA-8	Pyrite, Smectite (A) Chlorite (A-m) Halite (m-tr) Plagioclase (tr)	Basalt.
25-GTVA Conical SMT	25-GTVA-1A	Pyrite, Marcasite (A) Calcite (m) K-Feldspar (m-tr) Plagioclase, Illite, Smectite? (tr)	Grey mud. K-Feldspar is orthoclase.
	25-GTVA-1B	Calcite (A) K-Feldspar, Plagioclase (m-tr) Kaolinite or Chlorite (tr)	Brown mud.
	25-GTVA-4	Fe-rich	Green altered breccia, no results as too Fe-rich.
	25-GTVA-6	Realgar and Alacranite (A) Plagioclase, K-Feldspar, Illite Smectite (tr)	Red crystals-closest, but imperfect match, is realgar. Other minerals scraped from the rock surface.
28-GTVA Conical SMT	28-GTVA-1	Pyrite, Marcasite, Arsenopyrite (A) Plagioclase (m)	Dark grey mud.
33-GTVA Edison SMT	33-GTVA-1	Calcite (A) Plagioclase, Quartz? (m-tr) K-Feldspar, Smectite, Chlorite or Kaolinite (tr)	Mud.
	33-GTVA-1 < 2 m	Calcite (A) Smectite (m) Chlorite, Marcasite or Pyrite, Plagioclase, Aragonite? (m-tr)	Clay-Size separate.

Station/Area	Sample No.	Mineralogy	Comments
38-SLS between Tanga Island and New Ireland	38-SL 70 cm	Plagioclase (A) Smectite (m) Illite, Quartz?, K-Feldspar?, Analcime? (m-tr)	Dark grey ash. If K-Feldspar is present it is probably orthoclase.
39-GTVA Conical SMT	39-GTVA-M	Pyrite or Marcasite (A) K-Feldspar, Smectite? (m-tr)	Mud.
	39-GTVA-4A	Chlorite, Pyrite (A) Smectite (m-tr) Quartz (tr)	Altered basalt.
40-GTVA Conical SMT	40-GTVA-2	Chlorite, Pyrite (A) C/S ? (m) Plagioclase? (tr)	Ankaramitic basalt. May contain a mixed-layer clay mineral as well.
	40-GTVA-3	Pyrite or Marcasite, Halite (A) Chlorite, Smectite, Plagioclase (m-tr)	Mud. As pyrite dominates sample 2, it is probably pyrite here. Pattern incomplete.
41-GTVA Conical SMT	41-GTVA-M	Pyrite or Marcasite (A) Calcite (m) K-Feldspar?, Quartz?, Smectite, Chlorite (tr)	Mud.
	41-GTVA < 2 µm	Chlorite (A) Marcasite (m) Quartz, Plagioclase (m-tr)	Clay-size separate of above sample.
	41-GTVA-1	Pyrite or Marcasite (A) Chlorite, Plagioclase (m) Smectite (tr)	Intensely altered basalt.
	41-GTVA-3	Pyrite or Marcasite, Halite (A) Chlorite (m-tr) Smectite, Plagioclase? (tr)	Basalt.
	41-GTVA-MV	Paragonite (A) Illite/Smectite, Chlorite (tr)	Mineral in vesicle.
43-GTVA horst south of Edison SMT	43-GTVA-BL	Calcite (A) Marcasite, Quartz, Plagioclase (m-tr)	Black mud.
	43-GTVA-BR	Calcite (A) Marcasite, Plagioclase, Quartz (m-tr)	Brown mud.
44-GTVA horst south of Edison SMT	44-GTVA-1??	Calcite (A) Plagioclase, Quartz (m-tr) Kaolinite or Chlorite (tr)	Mud.
51-GTVA Conical SMT	51-GTVA-4	Calcite (A) Plagioclase, K-Feldspar? Pyrite or Marcasite (m-tr)	Mud.
53-GTVA Conical SMT	53-GTVA-1L	Amorphous Marcasite, Plagioclase (m-tr) Smectite? (tr)	Light grey mud.
	53-GTVA-1D	Plagioclase, Pyrite (A) Marcasite (m) Illite/Smectite (tr)	Dark grey mud.
	53-GTVA-3	Calcite (A) Sphalerite (m) Smectite (m-tr)	Mineralized breccia. May also contain marcasite or pyrite.

Station/Area	Sample No.	Mineralogy	Comments
	53-GTVA-3S	Calcite (A) Plagioclase (A-m) K-Feldspar (m-tr) Marcasite/Pyrite, Illite, Smectite (tr)	Scrapings from surface of sample 3.
58-SLS horst structure south of Edison SMT	58-SL 152 cm	Calcite (A) Plagioclase (m-tr) K-Feldspar?, Quartz?, Kaolinite or Chlorite (tr)	Mud.
	58-SL 170L cm	Calcite (A) Plagioclase (tr)	Light grey mud.
	58-SL 170D cm	Calcite (A) Plagioclase, Quartz? (m-tr) Pyrite (tr)	Dark grey mud.
61-GTVA New World SMT	61-GTVA-1	Calcite (A) Aragonite?, Plagioclase, Marcasite (m-tr) K-Feldspar, Quartz? (tr)	Mud
	61-GTVA-1 < 2 µm	Calcite (A) (Plagioclase (m-tr)	Unsuccessful clay-size separation.
	61-GTVA-1IM	Calcite (A) Plagioclase (m) Magnetite?, Analcime? (m-tr) Quartz?, Pyrite? (tr)	Indurated mud.
62-GTVA New World SMT	62-GTVA-1A	Calcite (A) Plagioclase, Analcime? (m-tr) Quartz (tr)	Light grey mud.
	62-GTVA-1B	Calcite (A) Plagioclase (A-m) Magnetite, Smectite?, Analcime? (tr)	Dark grey mud.
72-GTVA seamount SSE of Conical SMT	72-GTVA-1	Calcite (A) Plagioclase, Quartz (m-tr) Illite, Marcasite, Kaolinite or Chlorite (tr)	Mud.
74-GTVA seamount NW of Conical SMT	74-GTVA-1A	Calcite (A) Plagioclase, Quartz (m) Marcasite (m-tr) Smectite (tr)	Buff indurated mud.
	74-GTVA-1B	Calcite (A) Plagioclase, Marcasite (m-tr) Smectite (tr)	Pale green indurated mud.
	74-GTVA-1C	Calcite (A) Plagioclase, Smectite (tr)	Brown rubble.
	74-GTVA-1D	Calcite (A) Marcasite (m-tr) Plagioclase, Smectite, Chlorite? (tr)	Deep green indurated mud.
	74-GTVA-1E	Smectite (A)	Black indurated mud.

Station/Area	Sample No.	Mineralogy	Comments
83-GTVA Conical SMT	83-GTVA-1A	Pyrite (A) Pyroxene, K-Feldspar (m-tr) Calcite, Plagioclase, Chlorite, Smectite, Illite (tr)	Light grey mud.
	83-GTVA-1B	Pyrite (A) K-Feldspar, Plagioclase (m) Pyroxene? (m-tr) Illite, Smectite (tr)	Dark grey mud.
	83-GTVA-1	Pyrite (A) K-Feldspar (m) Calcite (m-tr)	Concentrate of black fines after seiving.
84-GTVA Conical SMT	84-GTVA-1		Mud. Sample not analyzed.

7.3 X-ray Fluorescence Analyses

BY KLAUS BECKER AND MARIO DRISCHEL

7.3.1 Methods

XRF analyses were carried out on a PHILIPS PW1480 sequential spectrometer. The instrument is equipped with a Rh-tube which can be operated up to a maximum voltage of 100 kV at 3kW to enhance sensitivity for heavy trace elements. The samples were ground by hand with an agata mortar. Approximatly 6grams were mixed with 0.6 g of Hoechst Wax C as binder and than pressed into pellets of 40mm diameter backed with boric acid.

Two analytical programs were developed, one for trace elements and one for major elements. Due to a software failure prior to the cruise theorethical alpha factors could not be applied to the major element program, therefore only the most important components of the sulfide ore were determined (Fe, Cu, Zn, S plus SiO_2 and Al_2O_3) using strait line calibrations. For the trace element program the measured net intensities were ratioed against the intensity of the tube's Rh-Compton radiation to achieve matrix correction. Both programs were calibrated with international reference standards.

7.3.2 Results

The results of all analyses performed on EDISON II samples are summarized in Table 7.3.1. Sample descriptions can be found in Chapter 4 of this cruise report. Trace element concentrations are reported in ppm, majors in weight-%, upper and lower limits of analytical accuracy are also given. Note that Cu and Zn were measured with both programs, but only the most reasonable value is given in the table.

Table 7.3.1: XRF shipboard analyses of mineralised samples SO-133.

Ident	Zn	Cu	Fe	S	SiO_2	Al_2O_3	Sb	Te	Sn	In	Cd	Ag	Pb	As	Se	Bi	Ni	Co	Ba
	ppm	ppm	[%]	[%]	[%]	[%]	ppm	ppm	ppm	ppm	ppm	ppm	ppm	ppm	ppm	ppm	ppm	ppm	ppm
lower limit	20	10	0.5	5	2	1	50	30	50	50	70	30	30	100	50	100	10	20	30
upper limit	2000	1000	85	40	90	15	4000	200	15000	500	3000	2000	30000	1000	200	3000	3000	2000	2000
13-DR-9	198	157	82.3	<1.3	14.7	3.2	<50	<30	<50	<50	<70	<30	31	113	<50	<100	118	94	294
14-GTVA-2F	103	194	11.3	6.8	37.5	19.4	<50	<30	<50	<50	<70	<30	31	254	<50	<100	37	50	357
14-GTVA-7/2	82	160	9.8	5.3	39.9	15.2	<50	30	<50	<50	<70	<30	103	143	<50	<100	30	35	284
14-GTVAAu7	91	224	11.1	7.2	32.8	23.8	<50	<30	<50	<50	<70	<30	33	453	<50	<100	35	52	172
14-GTVAAu10	72	185	11.0	6.4	35.3	23.4	<50	<30	<50	<50	<70	<30	28	382	<50	<100	48	68	309
15-GTVA-2F	118	156	15.6	13.6	50.7	6.6	<50	<30	<50	<50	<70	<30	97	<100	<50	<100	28	31	216
15-GTVAAu1	80	212	12.6	9.0	32.8	22.3	<50	<30	<50	<50	<70	<30	262	418	<50	<100	35	45	240
15-GTVAAu2	107	219	14.3	8.6	32.6	20.5	<50	<30	<50	<50	<70	<30	205	442	<50	<100	39	54	241
15-GTVAAu3	103	148	11.8	8.6	50.0	9.1	<50	<30	<50	<50	<70	<30	82	<100	<50	<100	23	27	200
15-GTVAAu4	90	243	12.6	9.1	31.6	19.9	<50	33	<50	<50	<70	<30	36	664	<50	<100	37	53	282
17-DR-4A	5.3%	168	9.4	7.5	46.9	11.9	93	<30	<50	<50	293	21	1023	614	<50	<100	49	37	206
17-DR-4C	5.5%	157	16.8	6.3	47.5	10.7	346	<30	<50	<50	448	36	2220	1465	<50	<100	41	31	106
23-GTVA-1A	2.7%	258	7.7	3.7	42.9	16.1	168	<30	<50	<50	150	25	6200	1686	<50	<100	26	37	30
23-GTVA-2	2.4%	119	12.3	8.6	62.3	9.3	132	<30	<50	<50	133	<30	1672	4757	<50	<100	25	29	196
23-GTVA-5	777	131	19.7	16.8	55.1	4.5	195	<30	<50	<50	<70	<30	964	11241	<50	<100	22	23	135
23-GTVA-6	1.6%	100	11.3	5.1	65.8	9.3	<50	<30	<50	<50	173	<30	1315	3138	<50	<100	25	28	90
25-GTVA-6A	4.3%	1.8%	5.7	3.4	59.5	10.3	1898	<30	<50	<50	183	1017	4500	1294	<50	<100	28	27	242
25-GTVA-6C	1.6%	0.6%	8.5	0.9	50.6	10.4	1950	<30	<50	<50	<70	421	19244	9225	<50	<100	40	38	220
25-GTVA-6C/2	2188	681	7.2	<0.1	46.5	11.3	1097	<30	<50	<50	<70	166	6273	1402	<50	<100	27	31	241
25-GTVA-7	1929	204	4.5	2.0	71.5	7.6	864	<30	<50	<50	<70	64	377	26195	<50	<100	17	13	41
25-GTVA-Sed.	1217	551	10.1	5.3	32.8	16.4	<50	<30	<50	<50	<70	25	1445	1507	<50	<100	37	36	105
28-GTVA-2	85	201	21.5	23.3	30.1	7.1	<50	35	<50	<50	<70	<30	30	1003	<50	<100	51	93	243
28-GTVA-3	629	229	61.5	<1.2	15.9	2.4	<50	<30	<50	<50	<70	<30	127	109	<50	<100	593	184	449
39-GTVA-1	132	136	38.7	39.0	10.2	10.2	<50	<30	<50	<50	<70	<30	315	11457	<50	<100	42	38	105
39-GTVA-2C	182	143	29.7	29.1	21.8	10.0	<50	<30	<50	<50	<70	<30	241	3619	<50	<100	35	35	522
40-GTVA<0.5mm	1528	0.2%	23.7	14.3	23.9	9.4	<50	31	<50	<50	<70	<30	793	848	<50	<100	39	42	824
40-GTVA PyKonz.	326	298	28.3	25.1	21.6	9.9	<50	44	<50	<50	<70	<30	380	4888	<50	<100	53	69	106
53-GTVA-1A	86	127	26.3	23.4	42.0	5.8	<50	<30	<50	<50	<70	<30	120	1349	<50	<100	37	34	58
53-GTVA-3A	2.5%	829	12.2	3.7	55.6	7.4	61	<30	<50	<50	211	50	28803	4029	<50	<100	35	47	63
83-GTVA<0.5mm	1.2%	1034	10.1	7.2	32.2	5.8	81	36	<50	<50	<70	187	3574	240	<50	<100	33	31	275

7.4 Determination of Gold by Anodic Stripping Voltammetry (ASV)

BY BERND HÖPPNER

7.4.1 Method

Anodic stripping voltammetry (ASV) was used for on board analyses of rock and sediment samples for gold. The instrument used for measurements was a portable digital voltammeter (VA-693, Metrohm, Switzerland). The VA-693 was connected to a special computer (VA-694) to run the programs for determination, data acquisition and plotting. Anodic stripping voltametry is an electro-chemical technique were metal ions in solution are reduced and plated onto a working electrode by applying a negative potential. After a pre-selected time the voltage is changed to a positive potential. Gold is reoxidized and stripped back into solution causing a current proportional to the concentration of gold in solution.

Gold has a specific peak position on the voltagram, and concentration levels for gold were determined by peak area. Calibrations were performed by measuring defined synthetic gold standard solutions. The method of standard addition did not yield different results.

Material was decomposed in aqua regia (1h) and evaporated to incipient dryness. The remaining sediment was taken up in 4M HCl. After centrifuging the sample was extracted with ethyl acetate (prewashed with 4M HCl). The yellow to red organic solution was backwashed twice with 10ml of 0.5 M HCl to remove iron (clear solution).

After evaporation to incipient dryness gold was redissolved in 0,5 ml 6M HCl and 1,0ml 8M HNO_3. The solution was transferred to a calibrated test-tube after three hours. De-ionized water was added to make a final volume of 25 ml, which allowed enough solution for repeated analyses. The detection limet for gold on board was 150µg/l Au^{3+} in cell solution. The detection limit for samples during this cruise was 300 ppb for 10 g of sample material. 10 ml sampe solution were pipetted into the cell and 100µl of 1000µg/g Cu-standard were added to ensure excess copper to compensate for interferences (Hall, 1992b) by silver.

A glassy-carbon electrode is used, since the oxidation potential of gold is more anodic than that of mercury. Also a mercury electrode can be used, however, this requires an indirect measuring - technique with sulfide-standard-solution. A plating time of 60 sec. (-600mV) and sweep rate of 240 mV/s in the range 500 mV of 1250 mV were used.

7.4.2 Results

Table 7.4.1 shows the results of samples that are measured on board. Samples "63-GTVA ..." are from Sonne cruise SO-94 and "HS..." are two samples from the "caldera deposit" and were used as reference. The "HS..."-samples showed good aggreement with previously known results of Neutron Activation Analyses (INAA).

Most "GTVA..." samples have high concentrations of sulfur causing severe problems, because no muffle furnace or bunsenbrenner was available. Recovery for these samples was ~30% of the Au-value found by INNA. Boiling with HCl 37% solved the problem for samples with Au concentrations greater then 150µg/l Au.

Table 7.4.1: Comparison of measured Au concentrations with previously analyzed Au concentrations in reference samples.

Lab.No.	Date	Sample	Au (ppb, INAA)	Au (ppb, ASV)
1	21-Jul-98	HS 9	1,900	2,400
2	21-Jul-98	63-GTVA I/K	4,400	1,300
3	22-Jul-98	63-GTVA 5 F	450	< 300
4	22-Jul-98	HS 18	901	930
5	25-Jul-98	63-GTVA I/K	4,400	1,200

The results of the gold determinations of samples from "SO-133/2" are shown in Table 7.4.2. Large problems occurred due to the presence of high sulfur and iron concentrations in these samples (30% and more). Additional acid had to be used (more than 18 ml HCl 37% and 6 ml HNO_3) to disssolve the iron-rich samples. These samples were washed more then twice with 0,5 M HCl to remove iron. This process will probably also remove gold.

The most significant finding are extremely high gold concentrations in sample (25-GTVA-6C) which showed 44 ppm Au for subsample 25-GTVA-6C-1, and 11 ppm Au for subsample 25-GTVA-6C-2 (see Table 7.4.2). However, only five other measurements showed Au concentrations higher than the detection limit of 300 ppb.

Table 7.4.2: Results of ASV measurements during SO-133.

Lab.No.	Date	Sample	Au
1	25-Jul-98	14-GTVA-Au 10	< 300
2	25-Jul-98	14-GTVA-Au 8	< 300
3	26-Jul-98	23-GTVA-1A	3,000
4	26-Jul-98	14-GTVA-7	< 300
5	26-Jul-98	14-GTVA-Au 9	< 300
6	27-Jul-98	23-GTVA-5	< 300
7	27-Jul-98	17-DR-4C	< 300
8	27-Jul-98	17-DR-4A	< 300
9	27-Jul-98	28-GTVA-3	< 300
10	27-Jul-98	23-GTVA-2	< 300
11	27-Jul-98	23-GTVA-crust	400
12	27-Jul-98	28-GTVA-2	< 300
13	28-Jul-98	14-GTVA-2F	< 300
14	28-Jul-98	40-GTVA (pyrite conc.)	< 300
15	28-Jul-98	39-GTVA-I	< 300
16	29-Jul-98	25-GTVA-6C	44,000
17	29-Jul-98	13-DR-Au 1	300
18	29-Jul-98	14-GTVA-7/2	< 300
19	30-Jul-98	41-GTVA (< 0,5 mm)	500
20	30-Jul-98	53-GTVA-4 B	< 300
21	30-Jul-98	15-GTVA-2E	1,000
22	31-Jul-98	25-GTVA-6C/2	11,000
23	31-Jul-98	25-GTVA-6A	not measured
24	31-Jul-98	39-GTVA-2C	< 300

8 Station List, Hydrosweep Profiles and Cruise Statistics

BY SÖNKE NICKELSEN

Abbreviations: DR = dredge, MS = hydrocast, GKG = box corer, GTVA = TV–grab A, OFOS = camera sled, SL = gravity core, SLS = gravity core with trigger weight

Coordinates (differential GPS) are ship position at first bottom contact. For dredges, TV-grabs and OFOS stations the coordinates for the last bottom contact are also given. Depth recorded for dredges is hydrosweep depth at first and last bottom contact. Depth for TV-grabs and OFOS is the actual maximal and minimal cable length. For TV-grabs the actual cable length at the time of sampling is given in brackets. Depth for hydrocast is calculated from CTD pressure sensor. Depth for sediment stations is cable length at bottom contact.

Station	Area	Location	Depth	Objectives	Brief description
01-GKG	NW of Simberi Island	2°07.172' S 151°33.975' E	1716 m	sedimentology, stable isotope stratigraphy	light brown foraminiferal ooze with foraminifera larger than 0.5 mm, Single pebbles on the surface
02-SL	NW of Simberi Island	2°07.152' S 151°34.013' E	1716 m	sedimentology, stable isotope stratigraphy	114 cm gravity core, ash on bottom of core catcher
03-GKG	W of Simberi Island	2°29.950' S 151°33.280' E	1898 m	sedimentology, stable isotope stratigraphy	slightly dark brown foraminiferal ooze, common ash layers of 1-3 cm, "pepper texture"
04-SL	W of Simberi Island	2°29.970' S 151°33.250' E	1897 m	sedimentology, stable isotope stratigraphy	179 cm gravity core
05-MS	Edison SMT	3°18.900' S 152°34.880' E	1460 m	microbiology gas profile (stable isotopes)	24 bottles Methane content up to 125 nl/l
06-DR	Conical SMT SE flank	3°19.040' S 152°39.410' E to 3°18.790' S 152°39.550' E	1416 m to 1125 m	sample southeastern flank of Conical Seamount	dredge empty
07-DR	Conical SMT SE flank	3°19.170' S 152°39.280' E to 3°18.700' S 152.39.610' E	1591 m to 1107 m	repeat 06-DR	200 kg of vesicular pyroxene-rich basalts (ankaramites) with minor olivine phenocrysts
08-GKG	between Lihir and Tabar	3°01.998' S 152°21.015' E	1860 m	Sedimentology Stable isotope stratigraphy	46 cm box core brown foraminiferal ooze
09-SLS	between Lihir and Tabar	3°01.988' S 152°21.007' E	1861 m	Sedimentology Stable isotope stratigraphy	294 cm gravity core

Station	Area	Location	Depth	Objectives	Brief description
10-GTVA	Edison SMT	3°18.995' S 152°34.872' E to 3°18.855' S 152°34.913' E	1429 m to 1479 m (1440 m)	sample hydrothermal material and fauna in the crater of Edison Seamount	10 – 15 kg of basaltic pepperite with numerous small xenoliths; clam shells & barnacles
11-GTVA	Edison SMT	3°19.178' S 152°34.911' E to 3°19.049' S 152°34.887' E	1428 m to 1522 m (1445 m)	sample hydrothermal material and fauna in the crater of Edison Seamount	900 kg of H_2S-rich mud and living as wel as dead clams, barnacles, and worms
12-DR	Conical SMT	3°18.955' S 152°39.552' E to 3°18.691' S 152°39.129' E	1308 m to 1391 m	sample mineralized rocks close to the top of Conical Seamount	60 kg of vesicular pyroxene-rich basalts, some slight alteration
13-DR	Conical SMT	3°18.874' S 152°39.038' E to 3°18.716' S 152°39.391' E	1402 m to 1175 m	sample mineralized rocks close to the top of Conical Seamount	300 kg moderately altered and Fe-oxide coated basalts, lavas are ankaramites to pyroxene-rich, vesicular and lobate, thick Fe-crusts coat surfaces, some sulfide mineralization
14-GTVA	Conical SMT	3°18.795' S 152°39.564' E to 3°18.752' S 152°39.591' E	1034 m to 1119 m (1052 m)	sample mineralized rocks close to the top of Conical Seamount	variably altered and mineralized ankaramites and basaltic breccias
15-GTVA	Conical SMT	3°18.762' S 152°39.584' E to 3°18.751' S 152°39.589' E	1039 m to 1068 m (1064 m)	sample mineralized rocks close to the top of Conical Seamount	mineralized basaltic breccias and altered ankaramites
16-GTVA	Conical SMT	3°18.735' S 152°39.576' E to 3°18.758' S 152°39.582' E	1039 m to 1095 m (1057 m)	sample mineralized rocks close to the top of Conical Seamount	two altered pieces of altered, vesicular basalt
17-DR	Conical SMT	3°18.730' S 152°39.629' E to 3°18.746' S 152°39.707' E	1128 m to 1216 m	sample mineralized rocks close to the top of Conical Seamount	15 kg of altered and mineralized ankaramite, some coated with Fe-oxide, basalts are not as mineralized as on station 15 & 16
18-DR	Conical SMT	3°18.774' S 152°39.432' E to 3°18.695' S 152°39.641' E	1161 m to 1153 m	sample mineralized rocks close to the top of Conical Seamount	3 kg of plates and crusts of Fe-oxide, 1 fragment of ankaramite

Station	Area	Location	Depth	Objectives	Brief description
19-MS	SE of Edison SMT	3°19.505' S 152°35.442' E	1624 m	sample fluids at horst structure SE of Edison Seamount	9000 nl/l methane anomaly near bottom
20-DR	TUBAF SMT	3°14.971' S 152°32.221' E to 3°15.303' S 152°32.543' E	1403 m to 1307 m	sample rocks at TUBAF Seamount	2 small pieces of pyroxene-phlogopite basalt with smalll xenoliths
21-DR	TUBAF SMT	3°14.988' S 152°32.214' E to 3°15.298' S 152°32.546' E	1404 m to 1306 m	sample rocks at TUBAF Seamount	2 small pieces of pyroxene-phlogopite basalt with xenoliths of peridotite and gabbro
22-DR	TUBAF SMT	3°15.234' S 152°31.908' E to 3°15.178' S 152°31.755' E	1453 m to 1447 m	sample rocks at TUBAF Seamount	dredge empty
23-GTVA	Conical SMT	3°18.758' S 152°39.591' E to 3°18.739' S 152°39.581' E	1041 m to 1057 m (1049 m)	sample epithermal mineralization at the top of Conical Seamount	30 kg of highly altered and brecciated basalt, some highly mineralized
24-GTVA	Conical SMT	3°18.732' S 152°39.586' E to 3°18.725' S 152°39.576' E	1026 m to 1062 m (1062 m)	sample epithermal mineralization at the top of Conical Seamount	40 kg vesicular, zonally altered basalt with Fe-oxide crusts
25-GTVA	Conical SMT	3°18.747' S 152°39.565' E to 3°18.728' S 152°39.543' E	1040 m to 1082 m (1082 m)	sample epithermal mineralization at the top of Conical Seamount	75 kg of altered basalt and a variety of intensely altered, pyritic basaltic breccias, large variety of sulfides
26-GTVA	Conical SMT	3°18.731' S 152°39.495' E to 3°18.707' S 152°39.528' E	1068 m to 1102 m (1088 m)	sample epithermal mineralization at the top of Conical Seamount	40 kg, fairly fresh vesicular pyroxene-rich basalt. Weathered and altered basalt with veins and fractures with realgar and orpiment mineralization
27-GTVA	Conical SMT	3°18.749' S 152°39.510' E to 3°18.743' S 152°39.526' E	1072 m to 1097 m (1096 m)	sample epithermal mineralization at the top of Conical Seamount	no sample
28-GTVA	Conical SMT	3°18.702' S 152°39.498' E to 3°18.715' S 152°39.507' E	1075 m to 1130 m (1108 m)	sample epithermal mineralization at the top of Conical Seamount	100 kg of mildly altered ankaramitic basalts, vesicular with thin Fe-oxide coatings, silicious, basaltic breccias

Station	Area	Location	Depth	Objectives	Brief description
29-MS	SW of Conical SMT	3°19.326' S 152°37.225' E	1690 m	sample fluids at the linear feature SW of Conical Seamount	methane anomaly of 450 nl/l at 1620 m (top of the structure)
30-DR	SW of Conical SMT	3°19.376' S 152°37.268' E to 3°19.573' S 152°36.986' E	1691 m to 1595 m	sample rocks at the linear feature SW of Conical Seamount	no bites, dredge empty
31-DR	SE of Edison SMT	3°19.492' S 152°35.372' E to 3°19.072' S 152°35.756' E	1630 m to 1506 m	sample rocks at horst structure SE of Edison Seamount	no rocks, a few clam shells, with Fe-sulfide coatings
32-DR	N of Edison SMT	3°17.729' S 152°34.788' E to 3°17.598' S 152°35.006' E	1550 m to 1452 m	sample rocks at SMT N of Edison seamount	dredge empty
33-GTVA	Edison SMT	3°19.097' S 152°34.864' E to 3°19.041' S 152°34.854' E	1342 m to 1456 m (1446 m)	sample clams and rocks at Edison Seamount	200 kg of mostly clams in a muddy matrix with small xenolith-bearing basalts, rare ultramafic xenoliths
34-GTVA	Edison SMT	3°19.021' S 152°34.849' E to 3°19.051' S 152°34.864' E	1448 m to 1484 m (1448 m)	sample clams and rocks at Edison Seamount	250 kg of mostly biological samples in a muddy matrix that contains sand, pebbles, and cobbles of pyroxene-phlogopite basalt with abundant small xenoliths
35-GTVA	Conical SMT	3°18.748' S 152°39.492' E to 3°18.732' S 152°39.491' E	1084 m to 1114 m (1114 m)	complete sampling survey of Conical Seamount	no sample
36-GTVA	Conical SMT	3°18.759' S 152°39.489' E to 3°18.741' S 152°39.531' E	1081 m to 1154 m (1088 m)	complete sampling survey of Conical Seamount	a 3 kg pyroxene-phyric (ankaramitic) basalt, slightly altered
37-GKG	between Tanga Island and New Ireland	3°37.240' S 152°57.291' E	2516 m	Sedimentology Stable isotope stratigraphy	brown clays with some foraminifera and fine ash layers
38-SLS	between Tanga Island and New Ireland	3°37.281' S 152°57.178' E	2516 m	Sedimentology Stable isotope stratigraphy	360 cm gravity core, clays and tephra, pumice fragments in the core catcher

Station	Area	Location	Depth	Objectives	Brief description
39-GTVA	Conical SMT	3°18.730' S 152°39.561' E to 3°18.714' S 152°39.557' E	1044 m to 1073 m (1059 m)	complete sampling survey of Conical Seamount	75 kg rock and mud, ankaramites, variably altered and mineralized
40-GTVA	Conical SMT	3°18.735' S 152°39.576' E to 3°18.725' S 152°39.563' E	1040 m to 1069 m (1068 m)	complete sampling survey of Conical Seamount	300 kg of altered highly mineralized basalt and mud (clay alteration)
41-GTVA	Conical SMT	3°18.725' S 152°39.565' E to 3°18.731' S 152°39.562' E	1044 m to 1071 m (1059 m)	complete sampling survey of Conical Seamount	150 kg of sulfide-rich altered ankaramite, oxide crusts and less altered basalt
42-GTVA	Conical SMT	3°18.719' S 152°39.620' E to 3°18.724' S 152°39.599' E	1048 m to 1080 m (1051 m)	complete sampling survey of Conical Seamount	10 kg of altered basaltic breccia with trace sulfides, less altered ankaramite, oxide crusts
43-GTVA	horst structure south of Edison SMT	3°19.457' S 152°35.370' E to 3°19.461' S 152°35.370' E	1599 m to 1624 m (1624 m)	survey horst structure south of Edison Seamount	300 kg of hemipelagic mud with polychaete worms
44-GTVA	horst structure south of Edison SMT	3°19.491' S 152°35.370' E to 3°19.352' S 152°35.462' E	1451 m to 1610 m (1598 m)	survey horst structure south of Edison Seamount	50 kg of foraminiferal ooze and biota, mussel clump with carbonate blocks (oxidized methane)
45-GTVA	horst structure south of Edison SMT	3°19.458' S 152°35.409' E to 3°19.340' S 152°35.464' E	1574 m to 1629 m (1606 m)	survey horst structure south of Edison Seamount	a few clams and mud with vestimentiferan worms
46-DR	Conical SMT	3°18.716' S 152°39.468' E to 3°18.748' S 152°39.538' E	1120 m to 1097 m	sample the top 50 m of Conical Seamount for mineralized material	15 kg of slightly altered ankaramite
47-DR	Conical SMT	3°18.715' S 152°39.477' E to 3°18.748' S 152°39.585' E	1118m to 1104 m	sample the top 50 m of Conical Seamount for mineralized material	4 kg, partially altered ankaramites and Fe-oxide crusts, no visible sulfides

Station	Area	Location	Depth	Objectives	Brief description
48-DR	Conical SMT	3°18.755' S 152°39.579' E to 3°18.717' S 152°39.470' E	1098 m to 1099 m	sample the top 50 m of Conical Seamount for mineralized material	dredge empty
49-DR	Conical SMT	3°18.699' S 152°39.573' E to 3°18.761' S 152°39.563' E	1106 m to 1122 m	sample the top 50 m of Conical Seamount for mineralized material	dredge empty
50-DR	Conical SMT	3°18.739' S 152°39.541' E to 3°18.717' S 152°39.656' E	1097 m to 1150 m	sample the top 50 m of Conical Seamount for mineralized material	60 kg of ankaramite, Fe-oxide cemented basaltic breccia, minimal alteration
51-GTVA	Conical SMT	3°18.729' S 152°39.539' E to 3°18.730' S 152°39.553' E	1063 m to 1082 m (1075 m)	complete sampling survey of Conical Seamount	10 kg of mud and indurated mud, some small altered and mineralized basalts
52-GTVA	Conical SMT	3°18.728' S 152°39.539' E to 3°18.730' S 152°39.546' E	1069 m to 1077 m (1075 m)	complete sampling survey of Conical Seamount	large (10 kg) ankaramite, slightly altered and Fe-oxide coated
53-GTVA	Conical SMT	3°18.737' S 152°39.562' E to 3°18.730' S 152°39.565' E	1052 m to 1060 m (1057 m)	complete sampling survey of Conical Seamount	100 kg of sulfide-rich altered basaltic breccia, basalt and oxide crusts with some sphalerite and galena
54-GTVA	TUBAF SMT	3°15.250' S 152°32.500' E to 3°15.135' S 152°32.499' E	1243 m to 1274 m (1263 m)	sample xenoliths at TUBAF Seamount	250 kg of trachybasalt with peridotite, gabbro and sediment xenoliths, pelagic and pebbly mud
55-GTVA	TUBAF SMT	3°15.160' S 152°32.448' E to 3°15.149' S 152°32.447' E	1220 m to 1255 m (1220 m)	sample xenoliths at TUBAF Seamount	75 kg trachybasalt with abundant xenoliths
56-GTVA	TUBAF SMT	3°15.259' S 152°32.455' E to 3°15.140' S 152°32.487' E	1243 m to 1297 m (1258 m)	sample xenoliths at TUBAF Seamount	100 kg of trachybasalt with abundant xenoliths, cinder-like sediment
57-GKG	horst structure south of Edison SMT	3°19.369' S 152°35.312' E	1610 m	sample sediment at base of horst structure	42 cm box core, grey sand, probably degassing of methane

Station	Area	Location	Depth	Objectives	Brief description
58-SLS	horst structure south of Edison SMT	3°19.355' S 152°35.453' E	1574 m	sample sediment at base of horst structure	321 cm gravity core, grey sand, relatively hard sediment
59-GKG	horst structure south of Edison SMT	3°19.341' S 152°35.463' E	1573 m	sample sediment at top of horst structure	box corer empty
60-GKG	horst structure south of Edison SMT	3°19.357' S 152°35.346' E	1625 m	sample sediment at top of horst structure	46 cm box core, 1 cm of a brown oxidized layer above dark grey sand
61-GTVA	New World SMT	2°50.759' S 152°32.697' E to 2°50.719' S 152°32.705' E	1127m to 1134 m (1134 m)	sample New World Seamount	90 kg of mud and indurated hemipelagic mud, some biota
62-GTVA	New World SMT	2°50.762' S 152°32.704' E to 2°50.731' S 152°32.691' E	1126m to 1137 m (1134 m)	sample New World Seamount	carbonate concretions and hemipelagic mud
63-GKG	NE of Lihir	2°23.993' S 152°50.831' E	1813 m	sample sediments on traverse NE of Lihir	40 cm box core, light grey tp brown sand, 2 cm ash layer
64-SLS	NE of Lihir	2°23.947' S 152°50.851' E	1830 m	sample sediments on traverse NE of Lihir	741 cm gravity core, grey sandy clay and very fine sand
65-GKG	NE of Lihir	2°38.964' S 153°01.926' E	2040 m	sample sediments on traverse NE of Lihir	45 cm box core, small pieces of pumice at the top, ash layers
66-SLS	NE of Lihir	2°38.975' S 153°01.898' E	2045 m	sample sediments on traverse NE of Lihir	832 cm gravity core, grey sand
67-OFOS	horst structure south of Edison SMT	3°18.856' S 152°34.901' E to 3°19.902' S 152°35.856' E	1426 m to 1636 m	survey mussel cliff area for gas hydrates and/or methane seeps	282 slides
68-GTVA	horst structure south of Edison SMT	3°18.798' S 152°35.290' E to 3°18.742' S 152°35.731' E	1492 m to 1573 m	sample mussel cliff area for gas hydrates	no sample taken
69-GKG	ENE of Lihir	3°04.597' S 153°04.052' E	2408 m	Sedimentology Stable isotope stratigraphy	box corer almost empty hard sediments
70-SLS	ENE of Lihir	3°06.398' S 152°59.862' E	2387 m	Sedimentology Stable isotope stratigraphy	318 cm gravity core, grey hard sandy clays, brown sand at the top
71-MS	S of horst structure	3°21.456' S 152°37.272' E	1715	sample fluids south of horst structure	methane content up to 65.8 nl/l

Station	Area	Location	Depth	Objectives	Brief description
72-GTVA	seamount SSE of Conical SMT	3°20.423' S 152°40.107' E to 3°20.413' S 152°40.110' E	1639 m to 1679 m (1656 m)	sample seamount SSE of Conical Seamount	no rocks, just foraminiferal mud
73-GTVA	seamount SE of Conical SMT	3°20.113' S 152°40.671' E to 3°20.051' S 152°40.713' E	1625 m to 1650 m	sample seamount SE of Conical Seamount	no sample taken
74-GTVA	seamount NW of Conical SMT	3°17.844' S 152°38.234' E to 3°17.775' S 152°38.208' E	1487 m to 1540 m (1489 m)	sample seamount NW of Conical Seamount	sediment with layered crusts
75-GTVA	seamount N of Edison SMT	3°17.709' S 152°34.907' E to 3°17.643' S 152°34.895' E	1404 m to 1528 m (1493 m)	sample seamount N of Edison Seamount	70 kg of plagioclase-clinopyroxene-phyric basalt, ankaramite, and vesicular ankaramite, in various stages of weathering
76-GTVA	seamount N of Edison SMT	3°17.739' S 152°34.911' E to 3°17.596' S 152°34.948' E	1349 m to 1529 m	sample seamount N of Edison Seamount	no sample taken
77-GTVA	seamount NW of Edison SMT	3°17.375' S 152°33.684' E to 3°17.348' S 152°33.783' E	1415 m to 1521 m	sample seamount NW of Edison Seamount	no sample taken
78-GTVA	seamount SW of Edison SMT	3°20.215' S 152°33.704' E to 3°20.141' S 152°33.774' E	1647m to 1675 m	sample seamount SW of Edison Seamount	no sample taken
79-GTVA	seamount SW of Edison SMT	3°19.563' S 152°34.398' E to 3°19.553' S 152°34.401' E	1552 m to 1590 m	sample seamount SW of Edison Seamount	no sample taken
80-GTVA	Conical SMT	3°18.723' S 152°39.554' E to 3°18.725' S 152°39.569' E	1046m to 1113 m	resample gold-rich material at Conical Seamount	no sample taken

Station	Area	Location	Depth	Objectives	Brief description
81-DR	seamount NW of Edison SMT	3°17.583' S 152°33.488' E to 3°17.266' S 152°33.727' E	1556 m to 1504 m	sample seamount NW of Edison Seamount	dredge empty
82-DR	seamount NW of Edison SMT	3°17.638' S 152°33.691' E to 3°17.302' S 152°33.755' E	1559 m to 1512 m	sample seamount NW of Edison Seamount	sediment and one small (2 cm) piece of pumice
83-GTVA	Conical SMT	3°18.747' S 152°39.542' E to 3°18.725' S 152°39.558' E	1056m to 1078 m (1073 m)	resample arsenic mineralization at Conical Seamount	75 kg of pyrite-mineralized and altered ankaramites, some brecciated
84-GTVA	Conical SMT	3°18.735' S 152°39.546' E to 3°18.719' S 152°39.541' E	1061m to 1073 m (1071 m)	resample arsenic mineralization at Conical Seamount	0.5 kg of pyritized and heavily weathered ankaramite and Fe-oxide crusts
85-GTVA	seamount ESE of Conical SMT	3°20.197' S 152°42.193' E to 3°20.198' S 152°42.198' E	1699 m to 1779 m	sample seamount ESE of Conical Seamount	no sample taken
86-GTVA	Ladolam off-shore	3°20.197' S 152°42.193' E to 3°20.198' S 152°42.198' E	1653 m to 1683 m	sample submarine portion of Ladolam	no sample taken

List of Hydrosweep Profiles

		Start of Profile		End of Profile	
Profile	**Date**	**Position**	**Time [UTC]**	**Position**	**Time [UTC]**
HS 01	21.07.1998	3°17.000' S 152°42.000' E	13:36	3°12.000' S 152°30.000' E	15:15
HS 02	21.07.1998	3°13.100' S 152°30.000' E	15:33	3°18.500' S 152°42.000' E	17:20
HS 03	21.07.1998	3°19.800' S 152°42.000' E	17:36	3°14.300' S 152°30.000' E	19:17
HS 04	21.07.1998	3°15.600' S 152°30.000' E	19:36	3°21.000' S 152°42.000' E	21:27
HS 05	21./22.07. 1998	3°22.600' S 152°42.000' E	21:45	3°17.000' S 152°30.000' E	00:36
HS 06	22.07.1998	3°18.600' S 152°30.000' E	00:59	3°24.200' S 152°42.000' E	02:42
HS 07	30.07.1998	3°20.300' S 152°30.000' E	12:16	3°25.800' S 152°42.000' E	14:04
HS 08	30.07.1998	3°27.700' S 152°42.000' E	14:26	3°22.000' S 152°30.000' E	16:14
HS 09	30.07.1998	3°25.500' S 152°30.000' E	16:35	3°29.600' S 152°42.000' E	18:25
HS 10	30.07.1998	3°31.100' S 152°42.000' E	18:45	3°25.000' S 152°30.000' E	20:30
HS 11	30.07.1998	3°26.300' S 152°30.000' E	20:50	3°32.500' S 152°42.000' E	22:35
HS 12	31.07.1998	3°33.900' S 152°42.000' E	17:35	3°27.600' S 152°30.000' E	19:27
HS 13	31.07.1998	3°28.800' S 152°30.000' E	19:47	3°35.200' S 152°42.000' E	21:35
HS 14	01.08.1998	3°18.800' S 152°42.700' E	10:12	3°36.000' S 152°42.700' E	12:23
HS 15	01.08.1998	3°36.900' S 152°42.000' E	12:44	3°29.800' S 152°29.300' E	14:03
HS 16	01.08.1998	3°29.800' S 152°29.300' E	14:03	3°11.300' S 152°29.300' E	16:55
HS 17	01.08.1998	3°11.300' S 152°28.200' E	17:07	3°30.600' S 152°28.200' E	19:39
HS 18	01.08.1998	3°30.600' S 152°27.000' E	19:52	3°11.300' S 152°27.000' E	22:18

station	date	UTC				type of station								
		begin	on bottom	off bottom	end	GKG	SL / SLS	MS	DR	GTVA	OFOS	HS	other	transit
						duration [days hh:mm]								
	10.07.98	09:12				leaving Manila								4 18:18
	15.07.98	03:30	-	-	06:03	recover moorings							02:33	00:17
01-MS	15.07.98	06:20	-	-	09:20			03:00						19:30
	16.07.98	04:50	-	-	06:35	recover moorings							01:45	00:00
02-MS	16.07.98	06:35	-	-	09:22			02:47						1 12:38
03-MS	17./18.07.1998	22:00	-	-	01:39			03:39						04:21
04-MS	18.07.98	06:00	-	-	08:48			02:48						1 13:48
	19.07.98	22:36				arriving at Kavieng, end of leg 1								05:36
	20.07.98	04:12				leaving Kavieng, begin of leg 2								08:05
01-GKG	20.07.98	12:17	12:55	12:55	13:22	01:05								00:00
02-SL	20.07.98	13:22	14:16	14:16	15:02		01:40							02:34
03-GKG	20.07.98	17:36	18:20	18:20	18:56	01:20								00:04
04-SL	20.07.98	19:00	19:45	19:45	20:24		01:24							07:21
05-MS	21.07.98	03:45	-	-	05:12			01:27						00:57
06-DR	21.07.98	06:09	06:52	08:00	08:12				02:03					00:23
07-DR	21.07.98	08:35	09:37	12:35	12:50				04:15					00:46
HS-01	21.07.98	13:36	-	-	15:15							01:39		00:18
HS-02	21.07.98	15:33	-	-	17:20							01:47		00:16
HS-03	21.07.98	17:36	-	-	19:17							01:41		00:19
HS-04	21.07.98	19:36	-	-	21:27							01:51		00:18
HS-05	21./22.07.1998	21:45	-	-	00:36							02:51		00:23
HS-06	22.07.98	00:59	-	-	02:42							01:43		03:05
08-GKG	22.07.98	05:47	06:28	06:28	07:07	01:20								00:00
09-SLS	22.07.98	07:07	08:04	08:04	08:51		01:44							02:09
10-GTVA	22.07.98	11:00	11:36	12:04	12:44					01:44				00:23
11-GTVA	22.07.98	13:07	13:35	14:42	15:15					02:08				02:19
12-DR	22.07.98	17:34	18:01	19:32	19:55				02:21					00:33
13-DR	22.07.98	20:28	21:05	22:54	23:30				03:02					01:02
14-GTVA	23.07.98	00:32	01:02	02:54	03:28					02:56				00:39
15-GTVA	23.07.98	04:07	04:36	06:20	06:55					02:48				01:35
16-GTVA	23.07.98	08:30	08:55	10:05	10:37					02:07				01:16
17-DR	23.07.98	11:53	12:36	13:01	13:20				01:27					00:14
18-DR	23.07.98	13:34	14:05	14:44	15:11				01:37					00:44
19-MS	23.07.98	15:55	-	-	17:23			01:28						00:56
20-DR	23.07.98	18:19	18:49	19:42	20:35				02:16					00:06
21-DR	23.07.98	20:41	21:12	22:46	23:10				02:29					00:25
22-DR	23./24.07.98	23:35	00:08	02:20	02:39				03:04					01:46
23-GTVA	24.07.98	04:25	04:53	05:03	05:39					01:14				00:00
24-GTVA	24.07.98	05:39	06:01	06:08	06:35					00:56				00:04
25-GTVA	24.07.98	06:39	06:58	07:57	08:32					01:53				00:15
26-GTVA	24.07.98	08:47	09:14	10:35	11:00					02:13				00:13
27-GTVA	24.07.98	11:13	11:41	12:16	12:40					01:27				00:24
28-GTVA	24.07.98	13:04	13:27	14:53	15:25					02:21				01:13
29-MS	24.07.98	16:38	-	-	18:06			01:28						00:25
30-DR	24.07.98	18:31	19:05	19:32	20:14				01:43					00:24
31-DR	24.07.98	20:38	21:07	22:20	22:40				02:02					00:36
32-DR	24./25.07.98	23:16	23:45	00:10	00:31				01:15					01:11
33-GTVA	25.07.98	01:42	02:08	02:18	02:50					01:08				01:04

station	date	UTC				type of station								
		begin	on bottom	off bottom	end	GKG	SL / SLS	MS	DR	GTVA	OFOS	HS	other	transit
						duration [days hh:mm]								
34-GTVA	25.07.98	03:54	04:23	05:45	06:10					02:16				01:45
35-GTVA	25.07.98	07:55	08:17	08:45	10:17					02:22				00:19
36-GTVA	25.07.98	10:36	10:47	11:59	12:22					01:46				03:33
37-GKG	25.07.98	15:55	16:53	16:53	17:55	02:00								00:00
38-SLS	25.07.98	17:55	19:22	19:22	20:20		02:25							02:26
39-GTVA	25./26.07.1998	22:46	23:14	00:21	00:49					02:03				00:23
40-GTVA	26.07.98	01:12	01:36	02:18	02:53					01:41				00:41
41-GTVA	26.07.98	03:34	04:02	04:55	05:29					01:55				00:24
42-GTVA-	26.07.98	05:53	06:15	06:48	07:24					01:31				00:36
43-GTVA	26.07.98	08:00	08:35	08:37	09:25					01:25				00:41
44-GTVA	26.07.98	10:06	10:35	12:25	13:04					02:58				00:17
45-GTVA	26.07.98	13:21	13:52	14:37	15:11					01:50				03:04
46-DR	26.07.98	18:15	18:43	19:10	19:30				01:15					00:08
47-DR	26.07.98	19:38	20:06	20:20	20:40				01:02					00:07
48-DR	26.07.98	20:47	21:11	21:38	21:55				01:08					00:02
49-DR	26.07.98	21:57	22:22	22:41	23:01				01:04					00:12
50-DR	26./27.07.1998	23:13	23:40	23:59	00:16				01:03					00:39
51-GTVA	27.07.98	00:55	01:22	01:38	02:07					01:12				00:12
52-GTVA	27.07.98	02:19	02:39	02:44	03:07					00:48				00:07
53-GTVA	27.07.98	03:14	03:40	03:51	04:34					01:20				00:46
54-GTVA	27.07.98	05:20	05:41	06:09	06:36					01:16				00:38
55-GTVA	27.07.98	07:14	07:34	07:36	08:04					00:50				00:12
56-GTVA	27.07.98	08:16	08:48	10:07	10:36					02:20				01:29
57-GKG	27.07.98	12:05	12:46	12:46	13:15	01:10								00:28
58-SLS	27.07.98	13:43	14:15	14:15	15:04		01:21							01:16
59-GKG	27.07.98	16:20	16:55	16:55	17:28	01:08								00:10
60-GKG	27.07.98	17:38	18:11	18:11	18:38	01:00								06:02
61-GTVA	28.07.98	00:40	01:02	01:24	01:55					01:15				00:30
62-GTVA	28.07.98	02:25	02:45	03:00	03:25					01:00				09:22
63-GKG	28.07.98	12:47	13:24	13:24	14:00	01:13								00:27
64-SLS	28.07.98	14:27	15:11	15:11	16:03		01:36							01:52
65-GKG	28.07.98	17:55	18:35	18:35	19:08	01:13								00:28
66-SLS	28.07.98	19:36	20:22	20:22	21:12		01:36							04:36
67-OFOS	29.07.98	01:48	02:25	05:56	06:31						04:43			00:49
68-GTVA	29.07.98	07:20	07:58	09:50	10:18					02:58				03:14
69-GKG	29.07.98	13:32	14:19	14:19	15:00	01:28								01:27
70-SLS	29.07.98	16:27	17:19	17:19	18:15		01:48							02:21
71-MS	29.07.98	20:36	21:18	21:18	21:56			01:20						00:36
72-GTVA	29./30.07.98	22:32	23:08	23:38	00:12					01:40				00:18
73-GVTA	30.07.98	00:30	01:00	01:30	02:00					01:30				00:38
74-GTVA	30.07.98	02:38	03:02	05:22	05:50					03:12				00:54
75-GTVA	30.07.98	06:44	07:06	07:21	07:54					01:10				00:17
76-GTVA	30.07.98	08:11	08:38	11:05	11:31					03:20				00:45
HS-07	30.07.98	12:16	-	-	14:04							01:48		00:22
HS-08	30.07.98	14:26	-	-	16:14							01:48		00:21
HS-09	30.07.98	16:35	-	-	18:25							01:50		00:20
HS-10	30.07.98	18:45	-	-	20:30							01:45		00:20
HS-11	30.07.98	20:50	-	-	22:35							01:45		01:46

station	date	UTC				type of station								
		begin	on bottom	off bottom	end	GKG	SL / SLS	MS	DR	GTVA	OFOS	HS	other	transit
						duration [days hh:mm]								
77-GTVA	31.07.98	00:21	01:10	02:15	02:50					02:29				00:29
78-GTVA	31.07.98	03:19	03:52	04:03	04:51					01:32				00:09
79-GTVA	31.07.98	05:00	05:32	05:46	06:20					01:20				00:41
80-GTVA	31.07.98	07:01	07:27	09:27	09:52					02:51				00:53
81-DR	31.07.98	10:45	11:12	11:50	12:27				01:42					00:13
82-DR	31.07.98	12:40	13:06	15:39	16:15				03:35					01:20
HS-12	31.07.98	17:35	-	-	19:27							01:52		00:20
HS-13	31.07.98	19:47	-	-	21:35							01:48		01:27
83-GTVA	31.07./01.08.98	23:02	23:26	01:52	02:15					03:13				00:10
84-GTVA	01.08.98	02:25	02:44	03:27	03:58					01:33				00:36
85-GTVA	01.08.98	04:34	05:00	05:21	05:50					01:16				01:31
86-GTVA	01.08.98	07:21	07:47	08:20	08:52					01:31				01:20
HS-14	01.08.98	10:12	-	-	12:23							02:11		00:21
HS-15	01.08.98	12:44	-	-	14:03							01:19		00:00
HS-16	01.08.98	14:03	-	-	16:55							02:52		00:12
HS-17	01.08.98	17:07	-	-	19:39							02:32		00:13
HS-18	01.08.98	19:52	-	-	22:18							02:26		00:00
	01.08.98	22:18				end of scientific operations								23:42
	02.08.98	22:00	(estimated)			arriving at Rabaul, end of leg 2								

total time	12:57	13:34	17:57	1 14:23	3 10:18	04:43	1 11:28	04:18
percentages	6.2	6.5	8.6	18.3	39.3	2.2	16.9	2.1
number of stations	10	8	8	19	44	1	18	2

total ship time	23 days 12 hours 48 minutes
total station time	08 days 17 hours 38 minutes
total transit time	14 days 19 hours 10 minutes